Influence of substrate topography and materials on behaviour of biological cells

Lynn M. Murray

A thesis presented for the degree of Doctor of Philosophy in

Electrical and Computer Engineering, University of Canterbury,

Christchurch, New Zealand.

Summer 2012

Dedicated to my parents, Frank and Barbara,

for their love and support throughout.

Abstract

A cell's interaction with its extracellular environment is critical to tissue structure and function. This work investigates the effect of substrate topography on selective cell adhesion and morphology.

Alterations in cell response to micro- and nanoscale signals and cues can cause changes in downstream functions of proteins and complexes such as invasive and metastatic motility of malignant tumour cells and the differentiation direction of stem cells. Biomaterial surfaces can be modified to provide different chemical and topographical cues and encourage controlled cell-substrate interaction.

Topography of a cell's microenvironment were replicated as a permanent polymer mould by bioimprinting technology, which was developed at University of Canterbury. The resulting high resolution methacrylate polymer samples were used for imaging and analysis, but have not previously been investigated as cell culture substrates. At the protein level, substrates modified with the topography of a template molecule have shown and increased affinity for selective binding of the template molecule antigen or antibody. This work investigates the effect of bioimprinted and photolithographic substrate patterning on cell behaviour in culture.

Optimisation of a methacrylate co-polymer resulted in a 6:3:1 ethylene glycol dimethacrylate: methacrylic acid: photoinitiator polymer mixture cured by 240 seconds of UV exposure. The polymer was used to replicate cell membrane features into a permanent polymer mould [a bioimprint]. The resulting high resolution poly(methacrylate) bioimprints were cleaned and sterilised for use as a secondary cell culture substrate.

Ishikawa endometrial cancer cells were cultured on bioimprinted poly(methacrylate) polymer substrates. Preliminary results showed preferential cell adhesion to bioimprinted areas over flat areas and also showed three dimensional spheroid growth instead of lateral two dimensional monolayer spreading. At higher seeding densities, preferential adhesion was similarly noted as well as peeling artefacts of shear stresses and cell size variation on flat poly(methacrylate) substrate regions. Fluorescent imaging and cell culture stencilling highlighted the association of cells with bioimprint substrate features.

To determine whether preferential cell adhesion effects were due to bioimprint features or general topography modification, cancer cells were cultured on comparable photolithographically-defined, geometrically-patterned substrates. Methods for transferring regular pattern arrays into poly(methacrylate) polymer substrates were developed. No organisation or preferential adhesion effects were observed in association with pillar and hole patterns between 5-30 μm. However, artefact incidence in poly(methacrylate) polymer replication techniques led to development and adaptation of polystyrene patterning techniques.

Experimental analysis of substrate-dependent effects on cell culture adhesion and organisation was extended to a non-cancerous cell line model. C2C12 mouse skeletal muscle cells were chosen for these investigations because of their ability to differentiate further, into myocytes or myofibrils. C2C12 myoblasts seeded on common cell culture substrates showed a notable morphology variation and extent of differentiation between cells grown on tissue culture polystyrene [TCPS] and polydimethylsiloxane [PDMS]. Myoblasts were plated on geometrically-patterned polystyrene and PDMS substrates. Significant alignment to grated pattern features was observed on both substrate types, before and after driven differentiation. Peeling artefacts of confluent tissue-like culture from PDMS surfaces which were observed were unreported previously in literature.

The results reported in this thesis provide a foundation for potential research and commercial application for surface modification methods. The biomimetic topography provided by bioimprinted substrates can be used to identify and investigate cell activities, including for example the mechanisms of cell adhesion and separation in metastatic and invasive cancer research. Altering the material of the bioimprinted substrates may attune substrate topographies as scaffolds to direct specific stem cell differentiation for regenerative tissue engineering applications.

Acknowledgements

This research and thesis is the product of the patience and support of some wonderful people whom I have had the pleasure of meeting and working with throughout my time in New Zealand.

First and foremost, I would like to thank my supervisors: Associate Professor Maan Alkaisi of University of Canterbury and Associate Professor John Evans of University of Otago – Christchurch School of Medicine and Health Sciences. Maan and John, thank you for supporting my research potential and providing a platform for success in the academic environment. I appreciate the level of trust and pursuit of curiosity which I was allowed for the duration of this work. On a personal note, thank you for your help and guidance through the trying and uncertain times following the February 2011 earthquake.

Profound thanks are similarly necessary to Dr. Volker Nock, without whom this project would not have been possible. Thanks to Volker for his input and collaboration, fabrication expertise, and bottomless motivation; similarly, thanks to Volker for forcing me out of the city on occasion and into the beautiful countryside of New Zealand. I could not have asked for a better tour guide through this research or for our conferences and mountain hikes.

I would like to thank Dr. Kenny Chitcholtan for teaching the cell culture techniques necessary to complete this work. His knowledge of cancer cell culture and his willingness to help ensured a high standard of technical execution and provided insightful and entertaining discussion along the way.

Thanks to University of Canterbury School of Biological Sciences [specific thanks to Ms. Nicole Lauren-Manuera and Professor Bill Davidson] with whom we were able to set up the Biological Applications and Technologies Laboratory. Sincere thanks to Dr. John Mitchell of Plant and Food Research in Hamilton, NZ for allowing me to visit and continue my polymer analysis and for his patient support for my chemistry questions and concerns. Similarly, thanks to Dr. Drusilla Mason for temporary use of her lab until the opening of the BAT Lab after the earthquake-related closure of the University of Otago – Christchurch School of Medicine facilities.

I would like to thank the wonderful people within the Department of Electrical and Computer Engineering. Thanks to Helen Devereux for managing the additional product requirements of the BAT Lab and to Gary Turner for supporting and maintaining the Nanofabrication Laboratory. Thanks to Pieter Kirkstra, Mike Shurety and Florin Predan for much needed IT support. Thanks to the University of Canterbury for continued updates and assistance throughout the months lost to the earthquake closure; to University of Otago for providing me with library and journal access; to the MacDiarmid Institute of Advanced Materials and Nanotechnology for funding this wonderful opportunity and for providing a network of scientists and friends throughout New Zealand.

Just as this research and thesis were achieved through collaborative efforts across universities and departments, my personal experiences were influenced by the friends and colleagues I have been fortunate enough to meet throughout this journey. Thanks to both the Nanofabrication Laboratory group and Laboratory for Cell and Protein Recognition group for providing open and welcoming forums for discussion and friendship. Special thanks to my awesome officemates, colleagues, and friends which I have not already mentioned for being supportive, yet appropriately entertaining and distracting, along the way: Andrew Gross, Brad and Rebecca Simons, Clem Roux and Charlotte Delrue, David Anderson, Frankie and Laura Rawson, Janelle Irvine, John Foulkes, Prateek Mehrotra, Robert Heinhold, Salim Elzwawi, Tom Cronje, the Evans family, and the Smart family. I look forward to keeping in touch with all of you.

Lastly, I would like to thank my family for their continued support throughout this past three and a half years. To the Morgan and Pound families, thank you for the effort to keep me in touch and involved, with special thanks to Karla and Harold for travelling to visit. To my sister Leigh, thank you so much for helping me smile when I needed it most. And to my parents, thank you for your unwavering love and support [and a well-timed kick in the pants or two]. I would never have been comfortable travelling to New Zealand for this wonderful opportunity without relying on the strength and encouragement of such an amazing family. I look forward to seeing you soon.

Preface

The work discussed in the following document is the compilation of work completed between 2009 and 2012 with funding provided, primarily, by the MacDiarmid Institute of Advanced Materials and Nanotechnology. Additional funding for this work was provided by Marsden Grant UOC-1006. Cell culture facilities at University of Otago - Christchurch School of Medicine & Health Sciences were used until the Christchurch earthquake on 22 February 2011, at which this point all laboratory work was undertaken within the University of Canterbury Department of Electrical Engineering facilities. Cell culture was completed in the Biological Applications and Technologies Laboratory and substrate fabrication was completed in the Nanofabrication Laboratory, both on the Electrical and Computer Engineering campus of University of Canterbury.

Publications and Presentations

Peer-reviewed articles and proceedings

Murray, L.M., Nock, V., Alkaisi, M.M., Lee, J.J.M. and Woodfield, T.B.F. (2012). Fabrication of polymeric substrates with micro- and nanoscale topography bioimprinted at progressive cell morphologies. Journal of Vacuum Science & Technology B 30 (early access online): 06F902.

Ibrahim, S.N., Murray, L., Nock, V., Evans, J.J. and Alkaisi, M.M. (2012). The quadrupole microelectrode design on a multilayer biochip for dielectrophoretic trapping of single cells. Microelectronic Engineering 97: 369–374.

Nock, V., Murray, L., Samsuri, F., Alkaisi, M.M. and Evans, J.J. (2011). Microfluidic arrays for bioimprint of cancer cells. Microelectronic Engineering 88(8): 1828-1831.

Nock, V., Murray, L., Samsuri, F., Alkaisi, M.M. and Evans, J.J. (2010). Microfluidics-assisted photo nanoimprint lithography for the formation of cellular bioimprints. Journal of Vacuum Science and Technology B 28(6): C6K17-C16K22.

Nock, V., Murray, L.M., Alkaisi, M.M. and Blaikie, R.J. (2010). Patterning of polymer-encapsulated optical oxygen sensors by electron beam lithography. Sydney, Australia: 2010 International Conference On Nanoscience and Nanotechnology (ICONN 2010), 22-26 Feb 2010. In ICONN 2010: 237-240.

Conference presentations

Alkaisi, M.M., Nock, V., Murray, L. and Evans, J.J. (2013). Auckland, New Zealand: 6th International Conference on Advanced Materials and Nanotechnology (AMN-6), 11-15 Feb 2013. (Invited presentation)

Murray, L., Nock, V., Evans, J.J. and Alkaisi, M.M. (2012). Substrate-dependent morphology and differentiation in C2C12 myoblasts. Queenstown, New Zealand: Medical Sciences Congress 2012 (MedSciNZ 2012), 27-29 Aug 2012. (Oral presentation)

Murray, L., Tan, L.H., Alkaisi, M.M. and Evans, J.J. (2012). Living conditions of cancer cells and the neighbourhood. Wellington, New Zealand: New Zealand Society of Oncology Conference (NZSO 2012), 2-4 May 2012. (Poster presentation)

Murray, L., Nock, V., Evans, J.J. and Alkaisi, M.M. (2012). Fabrication of cell-culture substrates with combined regular micro- and bioimprinted nanoscale topographies. Perth, Australia: 2012 International Conference On Nanoscience and Nanotechnology (ICONN 2012), 22-26 Feb 2012. (Oral presentation)

Murray, L., Nock, V., Evans, J.J. and Alkaisi, M.M. (2011). Multifaceted analysis of cell adhesion and growth patterns on Bioimprinted substrates. Queenstown, New Zealand: Medical Sciences Congress 2011 (MedSciNZ 2011), 29-31 Aug 2011. (Oral presentation)

Murray, L., Nock, V., Alkaisi, M.M. and Evans, J.J. (2011). Engineering the cancer microenvironment: the effects of cell-patterned Bioimprint substrates on endometrial cancer morphology and proliferation. Auckland, New Zealand: New Zealand Society of Oncology Conference (NZSO 2011), 12-13 May 2011. (Poster presentation)

Nock, V., Murray, L., Alkaisi, M.M. and Evans, J.J. (2011). Control and measurement of hypoxia in microfluidic cancer assays. Auckland, New Zealand: Benchtop to Bedside - The New Zealand Society of Oncology Conference (NZSO 2011), 12-13 May 2011. (Oral presentation)

Murray, L., Nock, V., Alkaisi, M.M. and Evans, J.J. (2011). Photo nanoimprint lithography of biological samples using microfabricated PDMS stencils. Las Vegas, NV, USA: 55th

International Conference on Electron, Ion, Photon Beam Technology and Nanofabrication (EIPBN), 31 May-3 Jun 2011. (Poster presentation)

Murray, L., Nock, V., Alkaisi, M.M. and Evans, J.J. (2011). Cell Adhesion and Proliferation on Bioimprinted Substrates. Queenstown, New Zealand: 21st Annual Australasian Society for Biomaterials and Tissue Engineering (ASBTE) Conference, 27-29 Apr 2011. (Oral presentation)

Murray, L., Nock, V., Alkaisi, M. and Evans, J. (2011). Bioimprint Surface Patterning and Replication for use as Cell Culture Substrates. Wellington, New Zealand: 5th International Conference on Advanced Materials and Nanotechnology (AMN-5), 7-11 Feb 2011. (Poster presentation)

Nock, V., Murray, L., Samsuri, F., Alkaisi, M.M. and Evans, J.J. (2011). Microfluidic Devices for Cellular Bioimprint. Wellington, New Zealand: 5th International Conference on Advanced Materials and Nanotechnology (AMN-5), 7-11 Feb 2011. (Oral presentation)

Murray, L., Samsuri, F., Nock, V., Alkaisi, M.M. and Evans, J.J. (2010). Bioimprinted polymers as cell-patterned substrates for cell culture. Genoa, Italy: 36th International Conference on Micro & Nano Engineering (MNE), 19-22 Sep 2010. (Poster presentation)

Nock, V., Samsuri, F., Murray, L., Evans, J. and Alkaisi, M. (2010). High Density Microfluidic Arrays for Bioimprint of Cancer Cells. Genoa, Italy: 36th International Conference on Micro & Nano Engineering (MNE), 19-22 Sep 2010. (Oral presentation)

Nock, V., Murray, L., Samsuri, F., Alkaisi, M. and Evans, J. (2010). Microfluidics-assisted Photo Nanoimprint Lithography for the Formation of Cellular Bioimprints. Anchorage, AK, USA: The 54th International Conference on Electron, Ion, and Photon Beam Technology & Nanofabrication (EIPBN), 1-4 Jun 2010. (Poster presentation)

Table of Contents

Table of Figures

1 Introduction

Though the exact mechanisms for the human body's identification and elimination of invasive foreign materials are only recently being understood, human evolution has provided an efficient and complex system for protection against invading materials. By immediate identification and destruction of unwanted pathogens or long-term protection against permanent material threats, the host response protects the body from any of a variety of aggressors. Foreign materials consist of a wide variety of accidental inclusions, such as bacterial or viral pathogens, to incorporated materials, anything from intentionally implanted biomaterials to glass shards or wood splinters.

Due to advancements in modern medicine, implantable devices are becoming increasingly common. In order to maintain the efficacy of implanted devices, biomaterials must be designed to work in cooperation with the body's reaction rather than against it. Materials must be designed to be not only biocompatible, but also bioactive. Rather than just not triggering a negative response, implantable materials should be developed to incur a positive interaction with the local environment.

Requirements for sustaining biomaterials that are introduced as treatments in the body are extreme. Wet, warm, electrolytic, and mobile conditions make biomaterial engineering complicated. In addition to the already stressful environment, the host tissues respond with immediate distrust of their new neighbours. Within seconds after injury or implantation, the surface of the foreign material is covered in adsorbed proteins as the body rallies to identify the intruder. The process of non-specific protein adsorption is spontaneous [1]. Protein adhesion marks the biomaterial surface and allows for defensive cell interaction and adhesion. Once the cells recognise the material as foreign, the reactive responses kick in.

As materials penetrate the dermal barrier, a wound healing cascade consisting of two essential responsive subsets is initiated to minimise damage and begin the healing process. The two familiar parts of this reaction are the immune and inflammatory response cascades. These reactive defence systems immediately detect the presence of an invasive material and react to isolate and destroy the potential threat. For further information regarding the specifics of the components and mechanisms incorporated into the immune and inflammatory responses and the challenges for material engineering, the text Biomaterials Science is recommended [2].

A possible avenue to increasing positive cell interaction with implanted substrate materials is surface modification for increased cell adhesion, thereby improving incorporation into the natural tissue environment. This cell-substrate interaction is the basis for the motivation behind the research constructed into this thesis. Development of cell line-specific models for investigating specific and localised cell adhesion to modified substrate surfaces, while observing the relative morphology and growth characteristics for progressive alteration, is documented using cell lines for two separate cell types. Using adhesion status and relative morphology as indicators of cell health and phenotypic expression, a cancerous cell line and non-cancerous cell line were investigated with different conclusions and implications for clinical applications.

1.1 Background and motivation

In vivo, anchorage-dependent cell types exist with a specific spatial orientation; an 'up-side' and a 'down-side' [3]. Apical cell surfaces contain exposed cell-signalling receptors and constructs while basal cell surfaces are responsible for extracellular matrix [ECM] adhesion and interaction. Adhesion complexes are a critical component of organised and natural cell growth. Modifying the interfacial substrate surface presented for cell culture alters the organisation of the adhesion complexes and affects cell growth and spreading [4]. Ordered, geometric patterning, on both the micro- and nanoscale, has been shown to affect cell morphology and growth distribution, but effects vary for each cell type [5]. Similarly, substrate surfaces containing topographical template protein features have shown cell behaviour modification and demonstrated selective adhesion [6]. Nanoimprint lithography, while originally designed to replicate geometric features[7], has been adapted to replicate cell features in a bioimprinting process [8] developed at University of Canterbury. A portion of the work presented in this thesis discusses cell adhesion and behaviour to these 'bioimprinted' substrates containing multi-scalar replicated cell features. Possible potential applications for biocompatible, intelligent biomaterials in tissue engineering and medical technologies range from laboratory research to clinical use and implantation. This work investigates two researched-based applications for topographically-modified biomaterials.

1.1.1 Cell Culture history and development

Though the first experimental verification that cells could remain viable outside culture were developed around the turn of the 19th century, development of the protocols and procedures still used today began in the mid-1900's [9]. Establishment of the immortal HeLa line by Gey, et.al. in 1952 and the identification of essential nutrients required for culture by Eagle et. al. in 1955 cemented cell culture as a valuable research tool [9]. Since that time, cell culture has been used as extensively as an *ex vivo* model for biological response to experimental stimulus. Cell culture models have been the basis for advances in the stem cell biology, cancer research, and the human genome. Hundreds of cell lines from different human tissues and different animal species have been isolated and used for research purposes. This work uses two such cell lines: Ishikawa endometrial cancer cells and C2C12 murine myoblasts. The details of each of these lines and the protocols used to maintain ongoing subcultures of each are detailed in this chapter.

1.1.2 Substrate surface modification

Among others, three factors contribute to cell adhesion to a given substrate: stress fibres, substrate composition, and focal adhesion proteins [10]. Because F-actin stress fibres and the associated protein complexes are assembled and deconstructed continuously within the cell and focal adhesion complexes are continuously generated and abandoned throughout motile cell movement [1], specific modification of the substrate properties provides the most specific engineering opportunity to encourage or discourage cell adhesion. Molecular biology processes of adhesion and motility, such as stress fibre and adhesion complex construction, are more difficult to modify than alterations to material substrate properties. The growing fields of tissue engineering and regenerative medicine rely and build on fundamental biomaterial integration to provide the desired cues to the local cell population.

Beginning in the late 1990's, modification of substrate surfaces to change cell adhesion properties took off as a popular area of investigation for biomaterial compatibility research. Substrate surface modification has been and continues to be heavily researched because of its promising application in any number of biology-related technical fields. Changing the surface area and roughness and/or the surface chemistry will result in a variation of cell adhesion response [5], with postulated implications for minimization of host response. Instead of replacing the entire bulk material, surface modification techniques were developed to

encourage [or discourage for some applications] cellular interaction with the surface without altering the overall mechanical properties of the bulk [i.e. elastic modulus, yield strength]. An overview of these methods is provided here.

1.1.3 Surface chemistry and dynamic substrates

Altering the physical, chemical, and/or topographical aspects of a substrate material will affect cell adhesion and morphology. The conclusion that cell shape can be controlled [for anchorage dependent cell types] by the adhesiveness of the substrate has been around for several decades [11]. Though this thesis specifically focuses on topographical modification of cell substrate materials, other material modification methods are available.

As expected, the chemical properties of the potential substrate material determine cell adhesion and growth, both in terms of protein specific binding [12] and in terms of preferential functional groups [13]. *In vivo,* cells adhere to the ECM to maintain structural integrity and healthy proliferation [1]. Within the ECM, specific amino acid sequences are expressed for binding with cell receptors, called integrins [14]. At the time of publication in 2004, Kato and Mrksich claim that of 25 known integrin receptors, about one-third bind to the R-G-D amino acid sequence, expressed highly by proteins of the ECM. In addition, the specific surface chemistry of the cell culture substrate has been shown to affect cell adhesion. The hydrophilic nature of hydroxyl groups encourage cell adhesion [13].

Chemical surface modification either directly or indirectly alter the interfacial surface experienced by cells in culture. Microcontact printing and microfluidic patterning are popular methods to pattern ECM proteins on substrate surfaces [15, 16]. ECM adhesion proteins containing the R-G-D sequence [i.e. laminin, fibronectin] are systematically deposited onto polymer substrates using lithographically defined stamps or microfluidic systems. In contrast to chemical patterning, direct substrate treatment can alter the substrates' adhesive properties, but without the localised control. For example, tissue culture polystyrene is distinguishable from untreated polystyrene because of the chemical treatments required for polystyrene to function as an adhesive substrate [17]. Corona discharge or oxygen plasma [18-20] are common substrate modification methods used to increase oxidation at the surface, resulting in increased wettability.

Though the chemical and the physical properties of the bulk substrate material are undoubtedly linked, the physical properties of the substrate show similar influence on cell adhesion and growth. Interfacial free energy affects the level of cell adhesion [21], though contradictory results cause continued debate regarding the ideal hydrophilic/hydrophobic substrate properties for maximum cell adhesion for anchorage-dependent cells [13, 22]. While the relative hydrophobicity of the substrate surface and the corresponding surface energy, are important factors in the prediction of cell adhesion they are not the sole contributing factors [13, 22]. In addition to the substrate surface, the stiffness [23] and porosity [24] of the bulk of the substrate contribute to the strength and consistency of cell adhesion. As material knowledge continues to grow, development of dynamic substrates offers new insights into the mechanisms of cell adhesion. Dynamic substrate surfaces change cell adhesiveness based on imposed stimuli [25]. As discussed by Nakanishi, et. al., materials have been developed to respond to stimuli such as heat, voltage, and light [25].

1.1.4 Topographical modification

Topographical substrate modification refers to imposed treatments or patterning that change the physical roughness and representation at the material surface. Since the publication of the highly cited paper 'Geometric control of cell life and death' by Chen, et. al. in 1997 [26], research investigating the effect of controlled substrate modification has on cell growth has increased significantly. Since then, due mostly to the relative magnitude limitations of instrumentation, substrate patterning has been predominantly limited to microscale features [27]. Due to advances in lithography techniques and nanotechnology, however, physically altering substrate surfaces on the nanoscale is now possible and being heavily investigated for biomedical applications. New patterning methods include electron beam lithography [28] and nanoimprint lithography have been developed [7].

1.1.4.1 Fabricated geometric topographies

Micro-patterning of cell culture substrates has expanded significantly since the late 1990's and, with expansion, a number of different processes have been developed and adapted for increased fabrication resolution and throughput. Photolithography, initially developed for semiconductor

fabrication in micro-electronics industry, has become the leading, standard technology [27]. Soft lithography was developed in combination with photolithography methods, for geometric and microfluidic patterning [29]. Polydimethylsiloxane [PDMS] is poured over a photolithographically defined master and heat cured. When the PDMS is de-moulded, inverse features of the original pattern are permanently included in the substrate surface. Due to its ease and popularity, soft lithography has since branched off into two chemical patterning, sub-categories of its own: micro-contact printing and micro-fluidic patterning [15, 16].

Based on the original findings of Chen, et. al., [26] the cultured bovine endothelial cells were less apoptotic and had higher DNA synthesis when grown on larger island features [50 μm] than for smaller versions of the same features [10 μm]. An extensive review by Flemming, et. al., contains the details of over 50 micropatterning studies, combining data for many different patterning methods, substrate materials, and patterned features and dimensions [5]. [Photolithography was the primary patterning method employed by studies throughout the review.] Interestingly, the conclusions were that cell organisation and alignment to pattern features is dependent on the substrate material and the cell line and for more accurate representation of the basement membrane, the critical component for cell adhesion *in vivo*, is smaller, denser, nanoscale topographical features.

Nanotechnology is a growing field with seemingly limitless application from fundamental science to growing clinical applications in drug delivery and tissue engineering [30]. Nanotechnology is producing exciting new information about the importance of the smallest features on the success of the whole. When focused on substrate patterning, nanoscale topographical patterning takes micropatterning to the next magnitude smaller and more accurately replicates the basement membrane conditions [12]. *In vivo*, cells continuously interact with nanoscale topographical cues, such as proteins and receptors, and respond to the received signals. To determine the extent to which cell morphology and phenotype are influenced by these interactions, nanopatterning has developed into the same general categories as micropatterning: chemical and topographical patterning. A number of methods for geometric patterning at the nanometre scale have been developed to provide high resolution features at nanometre magnitude [31].

Electron beam lithography [EBL] is a common, but expensive, method for producing topographical patterns at the nanoscale. Though resolution is accurate down to 30 nm, expensive equipment and costly time requirements for patterning even millimetre-sized

substrates prevent EBL from being a pervasive nanopatterning tool [32]. Another method for substrate nanopatterning is nanoimprint lithography [NIL]. Since development in 1996 [7], NIL has branched into two further subcategories: UV-NIL and thermoplastic-NIL [31]. However, patterning via NIL reduces throughput and requires expensive, specialised moulds [33]. Hu, et. al. at University of Michigan used NIL to successfully replicate nanoscale pattern features directly into TC-PS substrates [33]. Because of the well-documented success of TC-PS as a cell culture substrate, this process provides a new avenue of exciting applications for manufacturing of nano-topographically modified polymer substrates.

1.1.4.2 Molecularly imprinted polymers [MIPs]

Because viable, anchorage dependent cells are sensitive to nanoscale topographies of the ECM, artificially recreating aspects of the ECM topography in polymer culture substrates would encourage cell interaction and growth [34]. Molecularly imprinted proteins [MIPs] are an older field of research with a new and exciting range of applications for sensor technologies as the scale of imaging and experimental technology move toward the nanometre range [35]. Biologically-active macromolecules, such as enzymes and antibodies, have corresponding receptor molecules which they identify and bind to. For MIP applications, the desired enzyme or antibody 'template' is imprinted into a co-polymer matrix. When the original template molecule is removed a precise replication of the molecular topography remains. Though not with the same efficacy as the original molecule, the resulting MIP surface maintains a percentage of the biological activity [varies based on the specificity of the original molecule] and will selectively bind the corresponding antigen or receptor [36].

MIP-based assays were first published on in 1977 [37] and were re-popularised in 1993 by Vlatakis, et. al. [38]. The technique has shown the highest sensitivity for small molecules, below 1500 kDa [6]. Though applications abound for highly sensitive, molecular-templated polymer substrates, challenges for developing a successful immunoassay without primary antibodies has proved challenging and has gradually slowed over recent years [6, 36].

The objectives of the research detailed in the work of this thesis mirrors the selectively adhesive nature of MIPs. Whereas the earlier works focused on the protein level, the current thesis focuses on imprinting at the cellular level [39]. Verheyen, et. al. specifically identifies imprinting results for "proteins, DNA [40], viruses [41], and bacteria [42] but fails to include

any attempts to imprint and incorporate templated substrates at the cellular level [6]. The basis for much of the work contained in this thesis is a concluding hypothesis from a MIPs paper by Ratner and Shi: "…For example, a cell footprint might 'lock' its template cell adhered into its natural shape and thus maintain its phenotype" [39]. To explore this potential field of applications, MIPs replication techniques were applied to cell cultures and analysed for imaging [8]. The resulting technique, termed 'bioimprint', is described in the following section.

1.1.4.3 Bioimprint

Bioimprint was initially developed in a separate context from its potential applications as a selective cell culture substrate. A precise imaging method was required to validate the hypothesis that cells secreting higher hormone levels would show more exocytotic pore sites on the cell membrane surface. The challenge was how to visualise the topography of the cell surface in order to determine the number of exocytotic pore sites present. Atomic force microscopy [AFM] was used to probe the cell surface and map the topography. Due to the sharp tip in contact with the fragile cell membrane, however, damage to the cell membrane was often incurred [Figure 1.1] and the resulting imaging artefacts were unavoidable [43, 44].

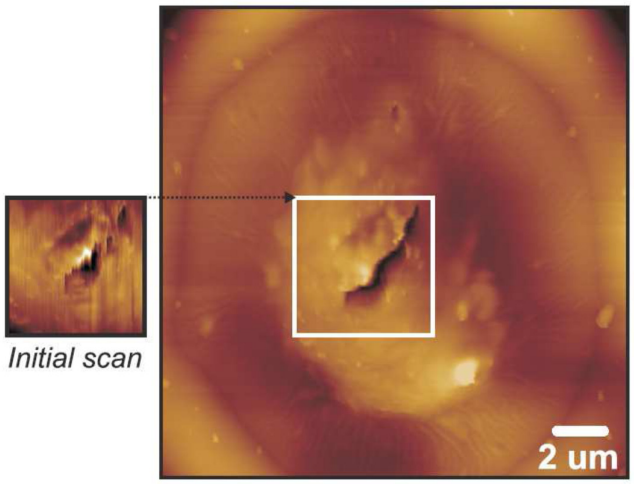

Figure 1.1 - Image from the thesis of Dr. James Muys demonstrating a perforation of a cell membrane by the AFM-tip [44].

To avoid the damaging effect of the AFM tip on live cells with elastic membranes, a replication protocol was developed and patented by the Electrical and Computer Engineering Department at University of Canterbury. The so-termed 'bioimprint' technique replicated cell surface

features into a permanent polymer mould [Figure 1.2] which was then used for AFM imaging [44]. And while the protocol and polymer medium have been changed and optimised for different purposes since the initial development [as detailed, with the complete protocol, in chapter 3], high resolution replication of cell surface features into a polymer template is fundamental to the work discussed in the following chapters.

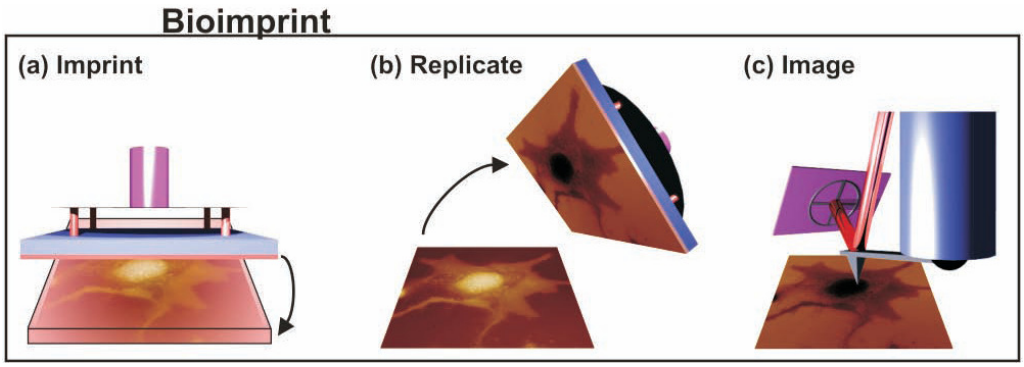

Figure 1.2 - Stages of bioimprinting technique [taken from the thesis of Dr. James Muys [44].

The development evolution of the bioimprint technique represented a significant portion of the doctoral dissertation of Dr. James Muys [44]. Originally the bioimprinting polymer medium was liquid polydimethylsiloxane [PDMS], but the heat curing of the polymer caused the cells to dehydrate and deform before the polymer was completely cured [8]. The next iteration involved a similar polymer with similar mechanical properties once cured. However, curing was initiated by ultraviolet light exposure instead of baking. While the cells did not experience the same denaturation effects, the UV exposure time still was considered too long to accurately replicate cell surface features without artefacts caused during curing. To cut down on curing time a new polymer mixture was adapted for the purpose. A combination of the same methacrylate monomers used to imprint proteins [35, 38] was mixed and the resulting methacrylate co-polymer cured in less than five minutes [45].

Further development and imaging characterization of methacrylate bioimprinting was included in the doctoral dissertation of Dr. Fahmi Samsuri [46]. In collaboration with John Mitchell at Plant and Food Research in Hamilton, the methacrylate co-polymer mixture was optimised for high resolution replication and, as a result, provided excellent AFM images. Dr. Samsuri investigated the effect of different drugs on the physical expression of exocytosis pores on the surface of Ishikawa cancer cells. He was able to distinguish individual pores and compare cell morphology using bioimprinting as the predominant imaging technique [45].

Since the original development of the bioimprinting cell replication technique a few other studies have been published recognising the potential for substrates containing biomimetic cell topography. Zhou, et. al. grew cells on geometrically patterned substrates before applying and curing an optical glue [47, 48]. The cells were intentionally removed from the patterned substrate with the separation of the glue for AFM analysis of the underside of the cell features captured in the optical glue which showed the basal cell membrane conforming to the geometric patterns. This protocol was termed 'reverse cell imprinting'. An additional study used a PDMS-based imprinting technique to replicate neuronal basal lamina into polystyrene for comparable neuron alignment with traditional polystyrene substrates [49]. The study concluded the polystyrene replicas of the neuronal basal lamina were able to guide growing neurite networks.

While extensive work had been done in the Department of Electrical and Computer Engineering and the Department of Obstetrics and Gynaecology to develop the bioimprint as an imaging technique, no one had investigated the effect of the template surface as a cell culture substrate. To this point, there was no work done investigating the biocompatibility and cytotoxicity of the methacrylate co-polymer. Evolution and optimization of the bioimprint as a cell culture substrate will be discussed extensively in chapter 3.

1.2 Objective applications

Based on the mounting evidence concluding that substrate properties influence cell adhesion properties, two experimental models were designed to determine and verify the extent of the influence of substrate topography on relatively understudied areas of application. Cancer cells were used initially to investigate the effects of cell growth on bioimprinted substrates. For comparison purposes, cancer cells were also grown on control tissue culture polystyrene [TCPS] and geometrically patterned methacrylate substrates.

In an attempt to isolate the effects of topography seen by cell cultures on bioimprinted substrates, a non-cancerous cell line, C2C12 myoblasts, was used but required characterisation prior to experimentation. Substrate-dependent characterisation provided results not previously documented in the literature. Continuing investigation drove the myoblast toward differentiation and enabled observation the extent and maturity of differentiated myofibril

development on different substrate materials and topographies. The same experiment was repeated using lithographically patterned geometries to determine the influence of patterned features on directed differentiation.

To support the logic behind the development of these specific application models, supplementary background information is provided in the following two sections detailing the current state of literature for each model separately. The research focuses on the importance of cell adhesion for natural biological function in each case and the importance of cell-substrate interactions in creating a desired microenvironment.

1.2.1 Role of cell adhesion in cancer

As stated in an article in the Economist earlier this year, "The biggest conceptual breakthrough in the war on cancer was the realisation by the 1980s that it is always a genetic disease" [50]. Understanding that, regardless of the manifestation of the disease, cancer is caused by fundamental alterations to the DNA sequence changed the ways we research and treat cancer. Recent hypotheses go so far as to suggest the possibility of de-differentiating cancer cells to, essentially, return the effects of the pathways downstream of the DNA back to correct functions [51, 52]. The extracellular matrix [ECM] and surrounding environmental conditions are proposed to have an important function in the de-differentiation by directing the cell to a specific, presented phenotype. Because phenotype is a physical manifestation of the genetic expression, changes in phenotype can serve as an indicator of genetic expression.

According to a complete and comprehensive review of cancer research there are six so-termed 'hallmarks of cancer' [53]; these six hallmarks are "proliferative signalling, evading growth suppressors, resisting cell death, enabling replicative immortality, inducing angiogenesis, and activating invasion and metastasis". Though all of these hallmarks have been documented for Ishikawa endometrial cancer cell [54], the cell line used for the cancer portion of this presented thesis, the majority of focus will be placed on the adhesive requirements and the implications for cancer invasion and metastasis. Ishikawa endometrial cancer cells are an endothelial cancer cell isolated from the lining of the uterus. As endothelial cells, the potential for induced motility is slightly higher for this cell line in spite of it being a well-differentiated cancer type, a traditionally less aggressive grade of cancer.

Cell dissociation from the basement membrane is an early indication of neoplastic growth and can be caused by the increased binding of required growth factors [10]. Metastasis and invasion, though two different mechanisms for secondary tumour progression, share the initial dissociation transition from the primary tumour site. Induced motility allows cells to break away from the primary tumour site and penetrate the basement membrane. Dissociating cells present an epithelial-mesenchymal transition [10, 55]. While this transition is seen naturally during the wound healing process, an unidentified but inherent shift in the cancer cell enables the epithelial-mesenchymal transition to persist in metastatic cancer cells beyond re-established cell-cell contact. After invasion of the basement membrane tight junctions, invasive cells will relocate to local tissue and grow relatively close to the primary tumour site. Metastatic cells, in contrast, will enter the blood stream after penetration of the basement membrane and will go with the flow until they reach an acceptable ectopic, secondary site to adhere and continue cancerous proliferation. Malignant disease progression is strongly dependent on cancer cell dissociation from the primary tumour and the negative implications of successfully induced motility. This thesis investigates selective, localised adhesion to topographically modified substrates and whether the substrate topography effects the phenotypic expression of adhered cancer cells.

1.2.1.1 Ishikawa endometrial cancer cells

Ishikawa endometrial cancer cells used for the work reported in this thesis were gifted to the University of Otago – Christchurch School of Medicine by Dr. Masato Nishida from Kasumigaura National Hospital, Tsuchiura-shi, Ibaraki-ken, Japan. Ishikawa cells were isolated by Dr. Nishida in 1985 [54]. This is a well-differentiated cancer line, which means tumours formed in three dimensional cell culture develop into tight spheroid morphology with a defined lumen. Additionally, well-differentiated cancers are often less aggressive forms of the disease and are less likely to metastasise *in vivo* than poorly differentiated cancer cell types.

Ishikawa endometrial cancer cells are a type of endothelial cell and, as such, adopt a polygonal, ‘paving stone’ morphology. After confluence, the cells grow above the confluent monolayer and adopt a botryoidal morphology, resembling a bunch of grapes. The ‘control’ morphology of Ishikawa cells grown on glass and tissue culture polystyrene [TCPS] was well characterised in the previous work of Dr. Muys and Dr. Samsuri in their development of the bioimprint

technique. The growth rate does increase at higher passages, but population doubling time remains between 36 and 25 hours.

1.2.2 Directed differentiation of skeletal muscle

Progenitor stem cells develop into a variety of well-defined cell types with specific functions, roles, and phenotypes [56]. An undifferentiated mesenchymal stem cell [MSC], for example, could differentiate into at least eight possible specific cell types, each involved in the structure and function of different tissue and organ systems. Both bulk and surface properties of material substrates have been shown to influence stem cell differentiation. Substrate properties, such as wettability [57], elasticity [58], and porosity [59] have all been found to contribute to the differentiation path chosen by stem cell cultures *in vitro*. Though the mechanism for contact guidance remains unknown [60], the combined effects of surface and substrate chemistry and topography have been shown to affect stem cell differentiation [61].

Unpatterned surface roughness was found to be sufficient to cause cell alignment along the direction of scratch features on PDMS substrates and altered gene expression for MSCs grown on titanium substrates [60, 62]. Micro- and nanostructures reported in literature for investigation of stem cell differentiation have predominantly consisted of lithographically-defined, geometrically-regular basic shapes [63]. Different dimensions of linear patterns and pit and pillar patterns have shown variable success in influencing stem cell differentiation depending on endpoint cell type and the induced phenotype [61, 64-66].

C2C12 mouse skeletal muscle myoblasts have the ability to differentiate into three identifiable cell types and were chosen as the pre-differentiation cell line. This simplified determining the extent and success of differentiation in comparison with mesenchymal stem cell differentiation. C2C12 myoblasts will differentiate, in specific conditions, into myocytes, myofibrils [67] [as illustrated in Figure 1.3], and osteoblasts [68]. Figure 1.3 shows undifferentiated myoblasts on the left driven toward differentiated myocytes and myofibrils [green]. The cells in this illustration are labelled according to their fluorescent emission later in this work. Driven differentiation toward osteoblasts, a progenitor type itself, was not investigated in this work.

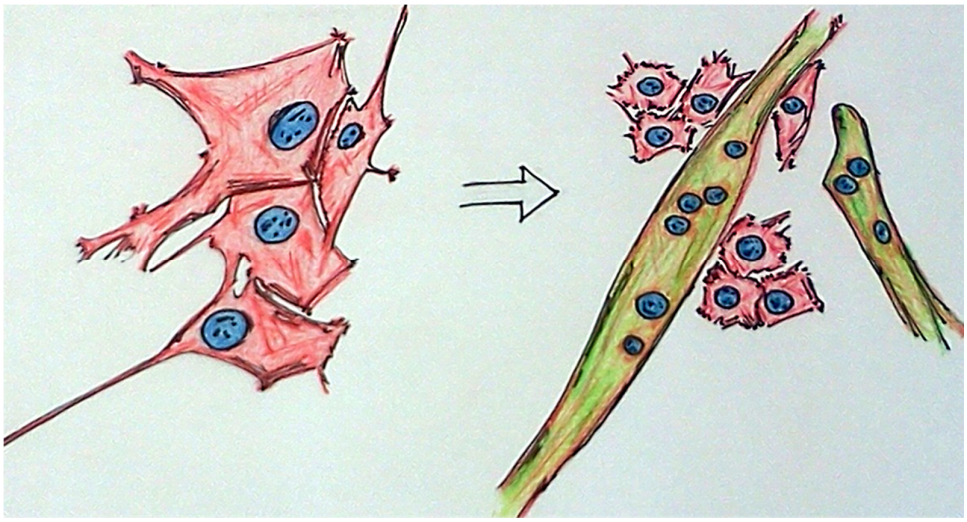

Figure 1.3 - Illustration of myoblast [left] differentiation to fused myofibrils [green on right] and myocytes [red on right]. Cells are represented by the same colour of fluorescent staining in chapters 7 and 8 of this work; the nuclei are labelled blue, actin is labelled red, and myosin II [characteristic of skeletal muscle] is labelled with a green, FITC antibody.

As noted in Shimizu, et. al., literature presents contradictory results regarding the effects of microscale patterning features on C2C12 differentiation [60]. Substrate-dependent phenotype and differentiation were characterised for C2C12 cells on common cell culture substrates. The effects of micropatterning on cell alignment, adhesion, and differentiation was observed and analysed. An additional benefit of this work was a proposed mechanism behind myoblast differentiation and the development of an *in vitro* model for further research on drug delivery and regenerative engineering for skeletal muscle.

1.2.2.1 C2C12 murine myoblasts

C2C12 murine myoblasts were obtained from collaborative partners at Plant and Food Research in Hamilton, New Zealand. The C2C12 cell line was first isolated and published on in 1977 by Yaffe and Saxel [67]. These striated, skeletal muscle cells were isolated from crushed skeletal muscles of C3H mice. In the original 1977 publication, the newly isolated C2 cells were used as a control myoblast population against dystrophic muscle cells. Given sufficient nutrients, the reported generation time for C2C12 cells is 24 hours. C2C12 myoblasts are semi-differentiated from the mesenchymal stem cell precursor; the same precursor which generates fibroblasts, chondrocytes, and osteocytes. Because of the similar differentiation line, myoblasts show what is commonly referred to as a ‘fibroblastic’ morphology.

Arguably the most exciting aspect of this cell line is the differentiation potential of individual myoblasts. In the original publication, Yaffe and Saxel documented the formation of multinucleated fibre networks forming after several days in culture [67]. When grown to confluence and beyond, the long, thin myoblast cells fuse together to form myotubules. These myotubules serve as *in vitro* analogues for functional skeletal muscle fibres [69]. More recent studies document the myoblast's ability to re-differentiate into osteoblasts in the presence of osteogenic growth factors, specifically bone morphogenic protein 2 [BMP-2] [68].

There are two significant differences between the Ishikawa cells and the C2C12 cells. First, the C2C12 myoblasts will differentiate from the initial myoblast state into myocytes and myofibrils. Once they have differentiated into myofibrils, they cannot be broken back into individual myoblasts for continued culture. Second, the C2C12 cell line is not a cancer cell line. This is important because some of the traits considered 'normal' for cancer cells are highly uncharacteristic for undifferentiated C2C12 cells. Most importantly, they should not grow vertically, one on top of the other, prior to confluence. Intercellular connections will cross over neighbouring cells and create networks across the substrate, but the cells will maintain a monolayer until confluence is reached.

1.3 Thesis Outline

The body of the presented thesis describes the experimental development of topographically-modified cell growth models and the resulting conclusions regarding cell adhesion to substrate surfaces.

Chapter 2. Methods used consistently throughout the entire duration of the thesis project are outlined in this chapter. Cell culture maintenance, sub-culture, and seeding techniques along with microscopy and analytical analysis methods are included in this chapter. Predominant fabrication methods, such as photo- and soft lithographies are discussed in detail as well.

Chapter 3. Development and optimization of biocompatible bioimprinted substrates, containing high resolution cell features, are discussed in detail in chapter 3. Characterisation of the physical properties associated with polymer ratio and curing variations is included. Biocompatibility testing and the resulting adjustments to the methacrylate polymer curing

process are discussed. The complete bioimprinting protocol, used for substrate fabrication in the following chapter, is presented and justified.

Chapter 4. Ishikawa cancer cell culture on bioimprinted methacrylate substrates is discussed extensively in this chapter. Variation of the experimental conditions regarding cell culture seeding density, duration in culture, and substrate coverage were altered and analysed. Additionally, methods for determining the relative location of cultured cells growing on top of bioimprinted substrates are described and evaluated.

Chapter 5. Fabrication of patterned polymer substrates is the subject of chapter 5. Defining the topographical features as 'positive' and 'negative' as well as documenting the inversion process is included. The chapter also includes documentation of potential artefacts involved in pattern transfer.

Chapter 6. This chapter investigates Ishikawa cancer cell culture on lithographically patterned substrates for comparison with the results of chapter 4. Cancer cell spreading and orientation are investigated for the effect of microscale geometric features.

Chapter 7. Substrate-dependent growth of muscle cells on common cell culture platforms is documented in chapter 7. Differences in surface chemistries and physical properties were analysed. Muscle cells were seeded on four different polymeric substrates and analysed for morphology and growth. Similarly, myoblast cultures were continued and driven to differentiation and analysed for variation across the same four cell culture substrates.

Chapter 8. In combination with the cell culture results from chapter 7, myoblast culture was completed on lithographically patterned substrates, similar to those discussed in chapter 5. Polystyrene moulding techniques were investigated for the production of consistent, high resolution substrates in an accepted biocompatible polymer. Comparative cell culture of C2C12 myoblasts on patterned substrates was conducted to determine any effects on cell morphology, size, and differentiation.

Chapter 9. Summary remarks regarding the methods and results, theories and conclusions of the previous eight chapters are included in this chapter. Additional potential analysis methods, implications for research and clinical applications, and suggestions for continuing projects and future work are also included. Overall conclusions and contributions close the final chapter.

2 Cell Culture Methods and Analysis

Methods used consistently throughout the work collected within this thesis are discussed in this chapter. Cell culture and pattern fabrication methods are well documented and prevalent within their respective fields. Information and characteristic of control cultures for the cell types used are included, as well as several cell assays and staining protocols used consistently throughout this work to analyse cell adhesion, morphology, and proliferation. This chapter also contains an overview of microscopy techniques used for analysis of stained cell cultures and the programs and processes used for micrograph processing.

2.1 Cell culture protocols and methods

Even though both the Ishikawa and C2C12 cells used in for the experiments described in this thesis applied relatively standard cell culture practices, each line had particular defining requirements and characteristics. The origins of each line and the means by which each were obtained and stored at facilities related to this research were outlined in the previous chapter in sections 1.2.1.1 and 1.2.2.1. Characterization and the specifics surrounding the decisions to use particular cell lines for the experiments will be examined in more detail in the discussion sections for the corresponding experimental results.

The development of more specific and complex cell culture models throughout history highlighted the importance of precise protocols and laboratory techniques. In this work, two different cell culture lines were used to analyse the effects of substrate topography on cell adhesion, proliferation, and morphology. General cell culture methods were similar for each cell type and will be outlined in this section with individualised cell line variations described in parallel with the relevant protocols.

The growth conditions required for supporting cell growth *ex vivo* are not only favourable for cell growth, but also for bacteria, fungi, and mycoplasma growth. Because the experimental work documented in this thesis on the utilised eukaryotic cell culture lines, the presence of bacteria was considered a contamination event. To limit contaminant exposure, sterile techniques throughout the subculture process were critical. Therefore, all sterile work was

completed inside a biological laminar flow cabinet, either at University of Otago – Christchurch School of Medicine or in the Biological Applications and Technologies Laboratory at University of Canterbury.

2.1.1 Subculture and maintenance

Continuous and conscientious monitoring of the incubation conditions was required to maintain optimal cell culture. Gas concentration and internal temperature and humidity were kept constant within the incubator throughout [Forma Steri-Cycle Incubator, Thermo Fisher Scientific, Scoresby, Australia]. Because an external carbon dioxide bottle was used to supply the incubator, consistent monitoring of the supply levels and injection flow rate was required for continuous culture. Internal incubator temperature was regulated automatically by the incubator's own temperature sensors and controls. A small, stainless steel water dish was required within the incubator to maintain humidity levels which prevented cell culture media from evaporating during culture. The dish was placed at the bottom of the incubator and filled with autoclaved deionised water containing 5 mM sodium azide, a cytotoxic preservative added to prevent contamination within the incubator.

Cell culture maintenance consisted of subculture splitting, incremental media aspiration and replacement, and freezing and thawing stock samples. A base level of maintenance was required to keep a consistent living cell population for experimental use. The following protocols are continuations and adaptations of the existing cell culture protocols and methods used within the Laboratory for Cell and Protein Regulation research group.

Subculture splitting techniques were applied to prevent over-confluence and the associated range of consequences. At approximately 80% full confluence, the cell culture media was aspirated from the flasks and replaced with 0.05% trypsin [in PBS] solution. Trypsin is a naturally occurring enzymatic protein which breaks polypeptide sequences at the lysine or arginine amino acid (abbreviated K and R respectively) [1]. Three common amino acid sequences found in integrin proteins responsible for substrate adhesion are RGD, IKVAV, and YIGSR. Short term application of low concentration trypsin disrupts the adhesion bonds of these integrin proteins at the K or R amino acid residues. If the trypsin solution is left in contact with the cells for too long, however, the cell membranes will be disrupted, in addition to the adhesion proteins, causing cell death. Trypsin, initially obtained at 0.5% in solution [Life

Technologies Co., Carlsbad, CA], was diluted by a factor of one in ten for cell sub-culture use. The culture flask, containing 10 mL of 0.05% trypsin/PBS solution, was placed back into the incubator for approximately 20 minutes. When the flask was next removed from the incubator the majority of cells were in suspension. Light agitation was applied by gently knocking on the flask to break any loosely bound cells from the substrate and to encourage cell clumps to disperse as single cells.

The trypsin solution containing dispersed single cells was removed from the flask and transferred into a sterile centrifuge tube. The centrifuge tube containing the cell suspension was tightly sealed before being removed from the hood and placed into the centrifuge. Centrifugation was set at 1500 rpm for 5 minutes. This speed was selected because it is low enough not to damage live cells but high enough to effectively create a compact cell pellet. After centrifugation, the tube was brought back into the cell culture hood, where the supernatant trypsin/PBS solution was removed as completely as possible. A small volume [1 or 2 mL] of fresh media was added to the cell pellet both to prevent cells from dehydrating and for cell counting.

Cell density was counted to determine the cell number and concentration in solution. A small volume [10 – 30 μL] of the media/cell solution was removed and diluted by half with PBS. A 10 μL sample of the diluted suspension was pipetted through a haemocytometer. The number of cells in each of the three diagonal quadrants was tallied and averaged to account for any distribution gradient across the haemocytometer surface. The number of cells per millilitre was calculated from the average cell count by, first, multiplying by two to account for the dilution in PBS and, next, multiplying by 10^4 to expand the cell count to the appropriate cell density per millilitre. From the known cells per millilitre concentration, the volume of cell solution required to reach the desired cell density, designated by the experimental design, could be calculated for a known substrate area. The calculated volume of cell solution was then diluted with media to the total desired volume, pipetted into or onto the desired flask or experimental culture substrate, and placed in the incubator. For a typical 25 cm^2 cell culture flask, cells were kept in 10 mL culture media.

For prolonged culture, beyond 48 hours, replacing the cell culture media was required to replenish the nutrient supply required to support continued cell proliferation and growth. Different media were used for each cell type, but the replacement increments and procedures were consistent across all cultures. With limited exceptions, culture media was replaced every

48 hours. Nutrient-deficient media was aspirated to waste and the fresh working media was added. The time between media aspiration and replacement was minimised to prevent cell dehydration effects. If the phenol red indicator in the media had changed to an orange or yellow colour before 48 hours, the media was changed prior to the two day time point and the cells were closely watched for persisting effects of acidic media.

Continued subculture results in what effectually is a high-speed natural selection process. Cells which grow and divide the fastest will be selected for by subculture techniques and the generation time decreases for high passage cultures. Each subculture event is termed a passage; and as passage numbers increase the relationship of the given cell population to the original, isolated cell set becomes more uncertain. Low passage cell stocks are kept frozen to replace high passage or contaminated cultures. Frozen, low passage stock samples are stored on liquid nitrogen and thawed as required for culture and expansion.

To create frozen cell stocks, cultured cells were dissociated from the culture plates using trypsin, centrifuged, and counted by the same methods used for subculture. The total desired cell number was transferred to an interim centrifuge tube and spun down again. Disposal of the supernatant media left only the cell pellet containing the total desired number of cells. The cell pellet was then re-suspended and dispersed into a solution containing one part of dimethyl sulfoxide [DMSO] [Sigma Aldrich, St. Louis, MO] to four parts foetal bovine serum [FBS] [Life Technologies Co., Carlsbad, CA]. DMSO removed water from the cells, keeping the cell membranes from bursting at below freezing temperatures; and the FBS provides a nutrient-rich environment for the cells during the freezing process [70].

Aliquots of the cells in DMSO/FBS solution at the desired concentration were pipetted into cryotubes capable of withstanding the low temperatures of liquid nitrogen. The filled and sealed cryotubes were placed in an isopropyl alcohol [IPA] bath and the whole bath was placed into a -80°C freezer overnight. The IPA bath allows for a slow, controlled rate of freezing, limiting the stress of freezing water on the cell membranes. The following day, the frozen cryotubes are quickly removed from the freezer and IPA bath and transferred into liquid nitrogen dewers for long term storage.

Starting a fresh culture from frozen cell populations was significantly less time consuming. Cryotubes containing frozen cell aliquots were removed from liquid nitrogen storage dewers and brought up to room temperature as quickly as possible using a 37°C water bath. The thawed

contents of the cryotube vials was then removed to a larger centrifuge tube and spun down to a cell pellet, again at 1500 rpm for 5 minutes. After centrifugation, the DMSO/FBS supernatant was removed to waste and the cell pellet was re-suspended in the cell-specific working media. The entire volume of cell/media solution was added to a 25 cm^2 cell culture flask for growth and expansion. It was important to allow a couple of subculture passages for the cells to 'wake up' and grow at a more typical rate. At this point, a subculture flask was split and aliquoted for freezing to replace the stored supply.

2.1.2 Contamination

The most common complication for working cell culture models is contamination from either environmental or other experimental organisms. Bacterial contamination was particularly prevalent during the early establishment of the PC2 laboratory in electrical engineering at the University of Canterbury. Throughout the course of this research no experiments were conducted on microbial samples; therefore, any bacterial contamination was considered environmental and full lab decontamination was completed for each instance. Decontamination procedures consisted of a heavy dose of bleach to the contaminated sample and re-sterilization of the incubator and fume hoods. Bleach was used in conjunction with 70% ethanol [in water] as the primary sterilizing agents throughout.

Because contamination effects can often not be quantified and are therefore considered experimental endpoints, precautions must be taken to protect against infiltrate particulates. All basal media was filter sterilised before the addition of supplements to create the working solution. PBS and other buffer solutions were autoclaved to maintain sterility when required. Vital stain solutions, stains in which the cells would remain alive and could not afford contamination contact, were filtered with .22 μm filters before use.

2.2 Cell analysis and imaging

The work discussed in the following chapters was designed to locate and identify adhesion and morphology variations across patterned and bioimprinted substrates. Because the analysis was focused on visualizing cell location and adhesion, and less on quantitative molecular methods, cell staining and microscopy methods were utilised heavily. Cells were stained with different dyes and molecular markers specific to the experimental requirements. Commonly used staining protocols are outlined in the section titled Cell staining methods [2.2.1].

The microscopy techniques used to visualise and analyse adhered cells are discussed in the following section, Microscopy [2.2.2]. Atomic force microscopy [AFM] was used to determine the resolution and nanotopographies of the bioimprints and related replications. Fluorescent microscopy was used for cell cytoskeleton and nuclear definition and location. Confocal microscopy advanced the fluorescence microscopy work to provide higher resolution and three dimensional representations of the cells.

2.2.1 Cell staining methods

2.2.1.1 Trypan blue viability assay

Trypan blue staining was used to verify the percentage of living cells within a cell population. The blue colour only permeates the membrane of damaged or dead cells, distinguishing dead cells from the still viable, translucent cells. Trypan blue stock powder [Sigma Aldrich, St. Louis, MO] was dissolved in serum-free PBS at .4% weight to volume. If the cells to be stained and counted were in PBS or media suspension, then ten microlitres of cell solution was removed and isolated to a microcentrifuge tube. Ten microlitres of .4% trypan blue/PBS stain solution was added to the microcentrifuge tube containing the isolated volume of cell suspension, mixed thoroughly, and allowed to stand for one to five minutes. From the combined twenty microlitre volume, ten microlitres was removed and inserted into a haemocytometer to count blue-stained and total cell numbers.

The number of blue cells counted was divided by the number of total cells and multiplied by 100 to determine the percentage of non-viable cells. Subtracting the percentage of blue, dead cells from one hundred equals the percentage of cells present which remain viable. In combination with the cell density information acquired in the counting process, an extrapolation of the viability percentage across the entire cell suspension population gives an estimate for total number of viable cells within the suspension population.

Conducting a trypan blue viability stain on adhered cells was slightly more complicated. Because a representative sample cannot be isolated within a known volume, a representative area was used instead; for the purposes of this research, the area used was the 10x field of vision of the Nikon TS-100 inverted microscope. Within the wells or chambers to be counted, the media was aspirated and replaced with two hundred microlitres of a .2% weight to volume dilution of trypan blue stain in serum-free PBS. The chambers were left for 5 minutes to allow the stain to fully set but without over-staining. The stain solution was removed and replaced with PBS to buffer the cells during counting. By counting the number of total cells and the number of stained blue cells within the 10x field of view and extrapolating across the area of the whole sample size, percentages of viable and nonviable cells were determined.

2.2.1.2 Coomassie brilliant blue assay

Coomassie brilliant blue [CBB] is a general protein stain, which stains dark blue, but can also appear as purple depending on the type of microscopy analysis used. There are two variations of the Coomassie formula consistently used in cell biology: R [red] and G [green], indicating the colour of an underlying tint. For the purposes of this work, all CBB stain protocols were carried out using CBBR-250 [Sigma Aldrich, St. Louis, MO]. The stock CBBR-250 powder was diluted to .2% weight to volume in an aqueous solution containing 10% acetic acid and 40% methanol, both volume to volume quantities. When the cell staining occurred a long time after mixing of the stock solution, the stock solution of dye was filtered with a .22 μm polyethylene filter. Stain setting time was varied across 5-30 minutes based on the desired density of the colour. Beyond 30 minutes, the CBB solution was found to over-stain the cell population and individual cell features were no longer distinguishable.

Because CBBR-250 indicates the total protein quantity present, stained cells could be lysed and the eluted dye quantified via optical adsorption as an indicator of the total number of cells

present. Due to variations in the experimental cell culture environment, however, a standard curve must be completed simultaneously for comparison and valid cell count analysis.

2.2.1.3 Fluorescent staining

Throughout the fluorescent and confocal microscopy conducted in this work, two predominant counter-stains were used: Hoechst 33342 was used to stain DNA and phalloidin-conjugated Atto 590 was used to highlight F-actin.

Hoechst 33342 stains specifically for the adenine-thymine (A-T) regions DNA, which effectively localises and highlights the cell nucleus [71]. Excitation is achieved with UV light at approximately 361 nm. The related emission maximum is 486 nm, and was best observed under the blue/cyan DAPI filter.

Hoechst 33342 powder was obtained from Pierce Biotechnology [Rockford, IL] and used to create a high concentration stock solution. The 20 mM stock solution was kept refrigerated at 4°C before mixing the lower concentration frozen stock solution. For cell staining protocols, the frozen 1 mg/mL stock was diluted 1:100 in 1x PBS solution. The 10 µg/mL Hoechst stain solution was applied to the cell sample for between 20 and 30 minutes at room temperature. Below 20 minutes, nuclear staining was still weak and required long exposure times to pick up with the Nikon fluorescent microscope. Beyond 30 minutes, the cells were at risk of over-staining, increasing the background staining and limiting the usefulness of fluorescent imaging techniques. After 20 minutes, the stain was removed to waste and the samples were washed thoroughly, at least three times for five minutes, in PBS to minimise non-specific background staining.

Importantly, cell fixation was not required for Hoechst staining of cells, meaning that the staining technique would locate and highlight nuclear features in culture without cytotoxic effects. While the membrane permeable nature of the Hoechst stain allowed for vital staining, it was determined that stained cells did not withstand the vital staining procedure due to secondary considerations, like the time out of incubation and UV exposure for fluorescence emission. Therefore, within the context of this thesis, all Hoechst staining was completed on fixed cell samples.

Phalloidin is a naturally occurring phallotoxin, isolated from death cap mushrooms [*Amanita phalloides*], which binds and induces crosslinking of F-actin stress fibres [10]. Actin is a critical component in the cellular cytoskeleton and necessary for cell motility. In muscle cells, featured later in this work, actin-myosin cross-bridging produces the basis for force-generating contractile units. When phalloidin is conjugated to a fluorophore, in this case Atto 590, the assembly works similarly to a secondary antibody system: actin stress fibres are bound by the phalloidin, the location of which is identified and highlighted by the attached fluorophore. The Atto 590 conjugate corresponds to the fluorescent emission of the Texas Red filter spectrum: excitation at 594 nm and emission detection at 624 nm [72].

Stock solutions were created from 20nmol powdered stock of phalloidin-conjugated Atto 590 ordered from Atto-TEC GmBH [Siegen, Germany]. In accordance with specifications, stock solution was created by dissolving the 20 nmol powder into one millilitre of methanol. Stock solution was kept at -20°C, though the methanol content prevented the solution from freezing. Working stain solution was created using a 1:30 dilution from stock in 1xPBS. The working solution was applied to cell samples and allowed to stain for at least 45 minutes in 4°C. Initial actin staining was applied for overnight staining; however, it was observed that no visible difference in staining vibrancy was noticeable for staining times as short as 45 minutes. Therefore, two hours staining time was deemed a consistent medium and was used as the standard protocol throughout this work. After the staining duration was complete, the sample were removed from refrigeration, the working stain solution was removed to waste, and the cell samples were washed at least three times for five minutes, in PBS to minimise non-specific background staining.

In contrast to the Hoechst stain, phalloidin will not permeate a viable cell membrane. Therefore, for phalloidin-conjugated actin staining to be effective, cell samples must be fixed and the membranes permeabilised using either a low grade surfactant solution or, in this case a solvent agent. The Atto 590 was dissolved in 1 mL of methanol, a membrane permeabilising agent, to preclude the requirement of an additional protocol step. For this reason, actin staining was always treated as an ‘endpoint’ process, meaning that cells would be treated as ‘no longer viable’ afterwards.

2.2.1.4 Immunofluorescence

The implementation of immunofluorescent methods, in addition to the fluorescent staining methods already in use, was not required until experimental work done much later in the scope of this thesis; but due to the similarities in reagents and imaging techniques the details are included here. Visualizing and quantifying myoblast differentiation proved incredibly difficult using only the staining protocols outlined above. A consistent contention in C2C12 literature is what constitutes a myofibril and how to quantify differentiation. One paper defines a myofibril as a fused cell with more than 5 nuclei [73]. Another paper uses a normalised experimental standard called a fusion index [69]. Before the quantification issue could be addressed, distinguishing between differentiated cells and the surrounding myocyte background was necessary.

According to the existing literature, using a myosin heavy chain MF20 antibody, immunofluorescence could be used to identify fused cells expressing myosin II [73]. Rather than opting for a more complicated secondary antibody staining method, we used a primary antibody directly conjugated with an Alexa Fluor® 488 [Molecular Probes, Inc.] fluorescent marker [eBiosciences, San Diego, CA]. The FITC green of the Alexa Fluor® 488 allowed for counterstaining with the existing Hoechst and 590-phalloidin protocols, identifying myosin expressing cells, nuclear DNA and F-actin respectively.

For efficient and accurate staining it was critical that antibody interaction was maximised to present the greatest opportunity for fluorescent detection. Cells were fixed with 4% paraformaldehyde for 45 minutes and then permeabilised with 0.1% Triton X-100 for 10 minutes. To prevent non-specific protein binding, cells were subjected to at least an hour treatment with 5% bovine serum albumin [BSA], a non-specific blocking agent. The myosin heavy chain antibody was diluted 1:100 in 2.5% BSA solution and applied to fixed cells to incubate overnight at 4°C. After careful and prodigious washing in PBS, counterstaining protocols, as outlined previously, were applied.

2.2.2 Microscopy

Visual analysis of adhesion locations and cell morphology would have been impossible without combining and contrasting methods of microscopy. Throughout the course of this research, imaging analysis was completed by atomic force microscopy, fluorescent and confocal microscopy, and a variety of optical microscopy methods. Each of these techniques contained inherent advantages and disadvantages and, as a result, were often used in combination. The following sections will briefly introduce each technique and its contribution to the scope of the research undertaken for this thesis.

2.2.2.1 Optical microscopy techniques

Microscopy techniques were used extensively throughout this research to observe and document cell status and, as the most simple and most common type of microscopy; bright field microscopy was the dominant analysis method throughout this thesis work. Variations on traditional upright optical bright field were used in specific circumstances when traditional micrographs lacked the required information. Phase contrast microscopy was used with an inverted bright field microscope to follow cell culture progress [Nikon Co., Tokyo, Japan]. Differential interference contrast was used with the upright Nikon 80i microscope to provide a more detailed depth profile than was available using only bright field [74].

The majority of bright field imaging was done using the Nikon 80i Eclipse microscope located in the Biological Applications and Technologies Laboratory [75]. This microscope also has fluorescent imaging capabilities which will be discussed later in the corresponding section. The microscope has five objectives of increasing magnification: 4x, 10x, 20x, 50x, and 100x. The magnification of each objective was compounded by the 10x magnification provided by the eyepiece, providing a maximum magnification of 1000x. All objectives were attached to a rotating objective mount located above the mechanical microscope stage. The light source was, therefore, located beneath the stage and illuminated the samples from below. A top down light source was additionally available and could be used either in addition to or instead of the underlying light source. The top-down light source was invaluable for transmission microscopy required for opaque substrates, for which the light source from below could not penetrate.

The Nikon 80i also contained polarizing filter options for differential interference contrast [DIC] microscopy. By polarizing the light supplied from the top-down source, DIC micrographs have the appearance of depth. Shadows and highlights created by the angle of incidence of the polarised light created a more accurate sense of the three dimensional aspect of the surface topographies. Filter settings could be altered to optimise the colour and polarization intensity for each image or each substrate. In combination with traditional bright field techniques, DIC provided an excellent verification method for determining the location of bioimprinted regions

However, the top down aspect of the microscope objective set up provided complications when attempting to view cell cultures within a flask or plate because even the lowest magnification objectives had working distance requirements which were less than the height of the flask. Effectively, subcultures of cells growing in flasks or experimental substrates kept in sterile plates were unable to be imaged using a traditional top-down objective arrangement.

In order to monitor the progress of cell subcultures, necessary to determine confluence and watch for bacterial contamination, an inverted cell culture microscope was ordered. The purchased Nikon Eclipse TS100 series inverted phase contrast microscope allowed for easy viewing of continuing cell cultures and fit the Nikon camera previously used with the Nikon 80i. The camera was easily moveable between the two microscopes allowing for a wide range of observation, imaging, and documentation.

2.2.2.2 Atomic force microscopy (AFM)

The bioimprinting technique, which will be discussed extensively in the next chapter and is the central aspect of this research, was initially developed as a high resolution AFM imaging tool. Because of the previous bioimprint analysis done by AFM imaging it seemed logical to begin advanced cell adhesion imaging analysis with a relevant technique [8, 45]. All AFM work discussed throughout this thesis was completed using the Veeco AFM [Digital Instruments (DI) 3100 Nanoscope III AFM, Veeco Instruments Inc., Santa Barbara, CA] located within the Department of Electrical and Computer Engineering at the University of Canterbury. Only a brief overview of AFM mechanics will be explored here; more extensive detail about the AFM and its applications can be found in [76, 77].

Atomic force microscopy was developed by Binning, Quate and Gerber in 1986 as an extension of scanning tunnelling microscopy [78]. The central concept of the AFM focuses on the acquisition of information from a continuous scanning technique. A cantilever is attached to the piezo-actuated AFM head, which is, in turn, linked to the bulk electronics supporting the function of the device. The underside of the attached cantilever contains a sharp tip used to probe the topography of the surface. Based on input settings determined by the user at the computer interface, a step motor lowers the AFM tip into contact with the substrate and begins scanning.

Topography detection works by measuring the deflection of a laser calibrated to correspond with the tip-end of the AFM cantilever [Figure 2.1]. A photodiode and detector are located opposite the laser source at the approximate angle of reflection off the tip. The laser location and detector location are both manually adjusted before scanning. Additionally, a camera is present to verify the tip location on the experimental sample. As the tip is scanned across the surface, the vector deflections of the tip relative to the sample topography are translated into movements of the detected laser reflection. Data processing recreates the deflection data to a digital rendering of the scanned line. Combining lines data across restricted area sizes leads to rendered images of the substrate topography in those areas. The number of lines per image can be altered for speed and/or resolution depending on the immediate requirements.

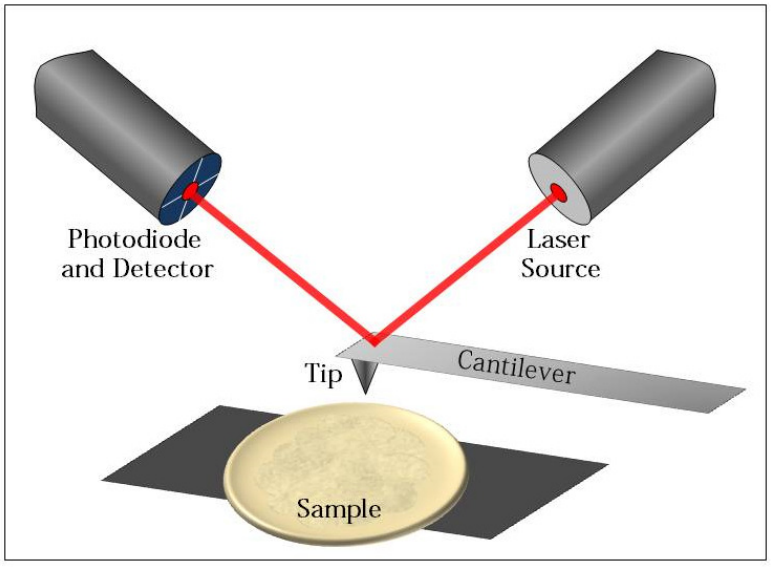

Figure 2.1 - Simplified schematic of the atomic force microscope (AFM). As the cantilever deflects due to contact with topographical surface features, the corresponding movement of the laser reflection is documented by the photodiode and detector.

Two different scanning modes were used in this work: contact and tapping modes. Contact mode required the tip to continuously be in contact with the sample surface. This method offers higher resolution, but is very difficult to use on samples with low elastic modulus. The dragging action of the tip can deform elastic sample and has been shown to puncture cell membranes. Alternatively, tapping mode does not come into contact with the sample and, therefore, is less likely to cause damage to the substrate topography. In tapping mode, the AFM tip is brought close to the surface until a surface-to-tip force interaction is detected. An internal piezo element vibrates the cantilever at a frequency close the resonance frequency of the cantilever. To identify and optimise this frequency an auto-tuning cycle is completed each time the cantilever is replaced. The tip detects the strength of force interactions between the tip and the surface and uses this data to recreate a digital map of the surface topography. Though tapping method is less likely to damage the sample, the resolution is not as high as contact imaging which was used for imaging the polymeric substrates in this work.

2.2.2.3 Fluorescence and confocal microscopy

After realizing the difficulties in locating and evaluating cell growth using only bright field microscopy techniques, fluorescent and confocal microscopy became the most valuable tools for understanding the motility and morphology of adhered cells. Taking both fluorescent and bright field images and overlaying them allowed for visualization of the substrate topography and the cells growing on top of it. The vast majority of the fluorescence microscopy included in this thesis was completed using the Nikon Eclipse 80i with an Osram mercury lamp as the light source [75]. The microscope is located within the Biological Applications and Technologies Laboratory at University of Canterbury.

Fluorescent microscopy works by exciting the sample with light of a specific wavelength band [74]. The fluorophores adsorb the light and, in response, emit light with a slightly longer wavelength which can then be captured and recorded as a micrograph. Keeping in mind that most samples are stained with multiple fluorescent markers, the closer the light source is to monochromatic, the more accurate the specific fluorescence from only the desired fluorophore. Two wavelength limiting filters are used in the Nikon 80i to ensure the quality of the image: one to minimise the excitation wavelength and one to limit the emission wavelength.

The advantages of using fluorescence to document the location and movement of cells was based on the ability to visualise the actin cytoskeleton and estimate the number of cells based on number of nuclei present. Actin stress fibres showed, essentially, the cell membrane borders and cell interactions, as well as providing information about localised adhesion points via lamellipod and microextrusion extensions. The main disadvantage of epi-fluorescent imaging was the lack of depth available in the resulting images. Because all fluorophores responsive to the excitation wavelength will emit a corresponding signal, there was no method for differentiating the depth of the signal. For example, in three dimensional cultures, the fluorescently stained samples are able to show very little and tend to overwhelm the image due to the cumulative nature of the bulk fluorescence. To isolate particular focal planes of interest, confocal microscopy was used.

Confocal microscopy relies on a technique known as optical sectioning to take scanning images at a particular depth of focus while removing background emissions from out-of-focus sample planes [74]. Additionally, the confocal laser scanning microscope relies on a series of lasers to excite the specific fluorophores instead of filtered light from the mercury lamp. User operated control of laser intensity and highly accurate, pinpoint excitation. Image data is gathered one pixel at a time as the laser is scanned across the surface. Similar to the AFM in this respect, user determined settings control the number of lines scanned, which ultimately determines image resolution. Confocal scanning microscopy discussed in this thesis was completed using a Leica TCS series confocal laser scanning microscope [Leica Microsystems, Wetzlar, Germany] located within the University Of Canterbury School Of Biological Sciences.

The confocal microscope contains a sequential scanning method, in which the same area is scanned over separately for each of the desired fluorophore excitations. This means that two relatively similar excitation wavelengths can be isolated from each other by taking two scans with more specific wavelength bands. While sequential scanning does take more time than the single scanning method, the image results are better for samples containing more than two fluorescent markers. In this work, most confocal imaging was done using sequential scanning mode.

Perhaps the greatest benefit of the confocal microscope is the ability to reconstruct as series of optical sections into a three dimensional rendering of the given sample. Optical sections are taken at user defined intervals between upper and lower bounds, also user defined. The

resulting sections provide three dimensional information as to the internal construction of the sample.

Confocal does have some disadvantages and limitations, however. While the resolution is significantly increased, localised bleaching of the fluorophores is increased as well due to the continuous, high intensity laser excitation during exposure and image capture. The best confocal micrographs are obtained in immersion mode, requiring glycerol of oil to be placed across a mounted sample which is not strictly necessary for epi-fluorescent imaging. Confocal techniques in general require much more time and equipment than bulk fluorescent imaging due to the repeated scanning used to ensure high resolution.

2.2.2.4 Image processing

Post-processing of bright field images was rarely required, and when necessary was mostly limited to creating a grey-scale rendering of the initial micrograph. Brightness and contrast of the images were optimised before image capture, but were altered when necessary. Extensive post-capture processing was required for AFM data. The topographical information was present, but was often distorted by bends in the surface or tilted sample surfaces. The NanoScope Analysis [v. 1.2] software provided by Veeco for processing AFM data was used to optimise AFM scans, to analysis surface parameters such as roughness, and to create three dimensional renderings of the recorded topography. Post-processing of fluorescent images was completed using ImageJ software [v. 1.46] [79] while confocal image processing was completed through the Leica confocal software package [LAS AF Lite v. 3.1.0]. Processing for fluorescent images consisted primarily of overlaying the different channels to create one complete image. For the confocal micrographs, processing was predominantly used to maximise contrast, either by altering the channel colours or adjusting the brightness and gains. Maximum contrast was important for all microscopy techniques used throughout this work.

3 Bioimprint substrates

Bioimprinting technology is an imaging technique which was developed in response to a hypothesis that exocytotic events could be visualised, tallied, and used as a measure of cell behaviour. Previous bioimprint work investigated the link between observable membrane pore numbers, secreted levels of VEGF in supernatant media and, cell proliferation rates.

Because of the highly proliferative nature of cancerous cells, increased secretory signalling is necessary to sustain local gradients of hormones and growth factors. In theory, the results of these intracellular exocytotic vesicles merging into the cell membrane would be visible via microscopy and could indicate the metabolic activity of the cells. However, AFM imaging of live cell culture samples proved extremely difficult [76]. High resolution microscopy of biological samples has several innate complications which prevent accurate pore analysis on living cell cultures. Predominantly, keeping cells alive throughout imaging requires maintaining environmental culture conditions. Regulating temperature, humidity, and carbon dioxide concentration often requires specific microscope modifications. The properties of the cells themselves provide additional obstacles. The elasticity of the cell membrane can cause dragging of the AFM tip or full puncture of the membrane, damaging the cell without providing accurate images. Also, depending on the cell type and specific AFM capabilities, the z-range from substrate to full cell height may exceed the working AFM z-range causing the tip to retract.

To overcome the trials of imaging live cells, bioimprinting was developed. Essentially this technology replicates the cell's surface features and monolayer growth organization into a permanent, more robust polymer material for further analysis. Initial trials at bioimprinting were attempted with PDMS [Dow Corning, Midland, MI] [44]. Though PDMS will cure at room temperature in about twenty four hours, curing was accomplished in this case by heating the samples to 80°C for 2 hours. While the replication resolution was about 20-50 nm, the bioimprint samples showed artefacts, predominantly surrounding the nuclear membrane, due to cell dehydration during curing.

To eliminate the heating requirement of the curing process, a UV-curable version of PDMS was used. RMS 033 [ABCR GmbH, Karlsruhe, Germany] had similar elastic properties as heat-cured PDMS, but curing was induced by UV exposure. The resolution of this polymer was

similar to that of regular PDMS, but the UV exposure-based curing time remained too long. To minimise the curing time, and cell exposure to UV, a new polymer solution, a methacrylate co-polymer, was developed in collaboration with Dr. John Mitchell of Plant and Food Research Centre, Hamilton, New Zealand. Previously used to imprint proteins for MIPs devices [36, 38], the methacrylate co-polymer showed very high resolution, 5-20 nm, with curing times of less than a minute, a great improvement in both resolution and curing time. In the work described in this thesis, the high resolution polymethacrylate [poly(MA)] samples were characterised and optimised as a platform for cell growth in culture instead of solely for imaging purposes. Cells were grown, imprinted, and then a second culture of cells performed on the polymer imprint. Thus, we provided a substrate with physical features of the same order as the growing cells.

3.1 Methods and protocols

3.1.1 Methacrylate polymer recipe

Throughout the evolution of the methacrylate co-polymer, a liquid mixture of ethylene glycol dimethacrylate [EGDMA] and methacrylic acid [MAA] monomer solutions [both Sigma Aldrich, St. Louis, MO] provided the reactant groups of the liquid precursor for the cured polymer [Figure 3.1]. The ratio between the two predominant reactants was optimised by curing samples at a range of monomer concentrations and observing the change in the physical properties. To induce the radical curing mechanism, a photoinitiating compound, IRGAcure 2022 [CIBA Specialty Chemicals, Basel, Switzerland] was included. Because the liquid co-polymer was spin-coated onto the template substrate for curing, triethylene glycol dimethyl ether [triglyme] [Sigma Aldrich, St. Louis, MO] was added to the polymer mixture as a thickening agent. The initial combination ratio for these liquid ingredients was as follows: 1200 µL triglyme; 425 µL EGDMA; 43 µL MAA; 20 µL IRGAcure. Liquid pre-polymer was mixed with a vortex mixer for at least 30 seconds before use to ensure the solution was as homogeneous as possible.

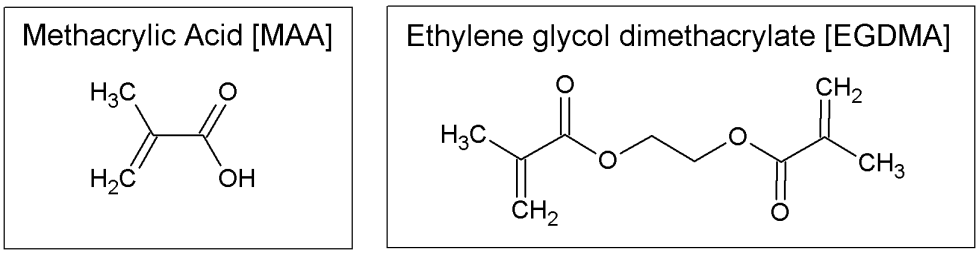

Figure 3.1 - Molecular diagrams of methacrylate-based reactants, methacrylic acid (MAA) and ethylene glycol dimethacrylate (EGDMA), which polymerized to form the poly(MA) substrate.

Changing the ratio of MAA to EGDMA monomers changed polymer surface chemistry and noticeably altered the cured polymer's physical properties. Contact angle measurements were taken using an Edmund Scientific camera with video capture software and analysed using the 'drop analysis' plugin for ImageJ [v. 1.46]. Polymer recipes were altered across two different variables: with or without triglyme, and reactant ratio variation. Two water droplets were placed on each of the samples and still images were captured from the camera feed.

To prevent premature and undesired curing, the uncured methacrylate liquid was mixed either in the Nanofabrication Laboratory clean room or, at University of Otago School of Medicine, in a dark room with UV filtered yellow light. For disposal, vials containing unused liquid polymer were left on the bench top in full natural light to cure overnight and then thrown out.

3.1.2 Bioimprint protocol

In the version of the bioimprint protocol existing at the outset of this work, initial cell cultures were grown on glass cover slips immersed in media [46]. After 10 days, the cover slips were removed from media and washed in PBS to remove non-adhered cell debris. Cover slips were then mounted cell-side up on a spin-coater [Laurell Technologies, North Wales, PA]. Liquid methacrylate pre-polymer was mixed using the ratio mentioned in the previous section, 1200 µL triglyme; 425 µL EGDMA; 43 µL MAA; 20 µL IRGAcure, and 125-500 µL was pipetted onto the centre of the cover slip. Spinning at 50 rpm for 10 seconds spread the polymer evenly across the cells. Continuous UV-irradiation was applied using flood exposure for 15 minutes to fully cure the polymethacrylate [poly(MA)] substrate. The bioimprint sample was separated from the glass microscope slide and cleaned before imaging analysis.

3.1.3 Biocompatibility

Biocompatibility encompasses a range of implications and assumptions regarding the substrate material's effect on the surrounding biological environment. Biocompatibility of bioimprinted methacrylate substrates for cell culture applications consisted of three phases, each addressing specific concerns: chemical stability in aqueous medium solution, cytotoxicity, and removal of all cellular debris from the substrate surface.

3.1.3.1 Poly(methacrylate) chemical stability

Cured methacrylate samples were placed in 16 wells, 8 with triglyme and 8 without triglyme added, of a 24-well plate while the remaining 8 wells were left as control tissue culture polystyrene [TCPS] substrates. α-MEM containing a phenol red pH indicator was used to determine the relative pH effects of polymer inclusion on aqueous medium acidity [Figure 3.2]. Two wells from each substrate condition were subjected to each of the experimental conditions: water wash before medium application, medium application without treatment, and sodium hydroxide [NaOH] treatment before medium application. Water and NaOH treatments were simple wash and agitation steps and were not allowed to soak. Observations were recorded after one hour. After 24 hours, medium was replaced and pH response was observed again.

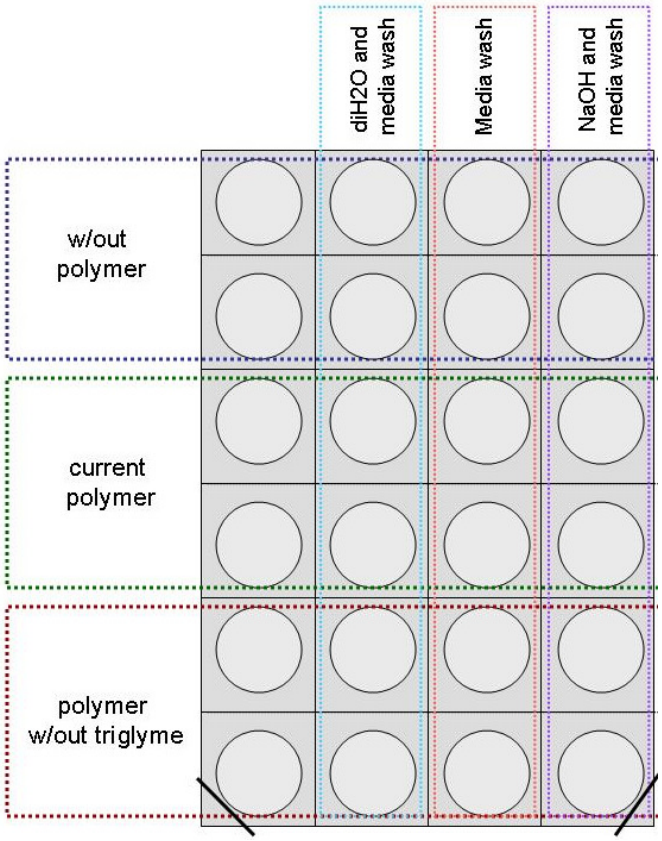

Figure 3.2 - Schematic outline of the chemical stability experimental setup. Current polymer refers to the methacrylate mixture with triglyme included.

3.1.3.2 Cytotoxicity

To determine the cytotoxicity of poly(MA) cell culture surfaces, 5.0 x 10^4 cells/cm^2 Ishikawa endometrial cancer cells, which will be discussed in greater detail in later chapters, were cultured *in vitro* on cured poly(MA) samples within 6-well TCPS wells. Experiments were carried out with simultaneous, corresponding polystyrene controls seeded with the same cell density.

3.1.3.3 Substrate cleaning

After curing, the bioimprint samples were placed directly into a water bath and agitated to remove loosely attached cell debris. Samples were then transferred to a cell lysing solution of 10% [w/v] sodium dodecyl sulphate [SDS] in .01M hydrochloric acid and placed in an

ultrasonic bath. Substrates were then subjected to a .05% trypsin soak for at least 20 minutes. When removed from the trypsin solution, methacrylate samples were transferred to a de-ionised water soak for at least 24 hours. Before use [less than 48 hours after soaking to minimise contamination], substrates were sterilised with ethanol [70%] or an ultraviolet sterile cycle.

3.2 Results

While the bioimprint had been extensively developed and optimised for high resolution imaging, no experimental work had investigated its suitability as a cell culture substrate. Optimisation of the methacrylate ingredient ratios and curing protocols were required. Biocompatibility testing was completed to determine the practicality of the methacrylate co-polymer as a cell culture substrate.

3.2.1 Poly(methacrylate) optimisation

Methacrylate co-polymer ingredient ratios and curing properties were evaluated, altered, and analysed. Under the supervision of Dr. John Mitchell, physical analysis of varied ratio samples was conducted at Plant and Food Research in Hamilton, NZ.

3.2.1.1 Adhesive substrate interactions

A critical observation during optimisation phase of the methacrylate co-polymer curing process was the inability to separate cured poly(MA) sample from polystyrene substrates. Liquid methacrylate co-polymer was poured over non-confluent cell cultures that were adhered to polystyrene substrates and cured using the existing bioimprint protocol. After curing, however, the cured methacrylate sample was inseparable from the underlying polystyrene substrate. Similarly, when combining the liquid methacrylate mixture in a polystyrene test tube, the test tube began deteriorating. From this point all liquid methacrylate pre-polymers were combined in polypropylene microcentrifuge tubes.

To circumvent poly(MA)-polystyrene adhesion interactions but still using commercially-available cell culture substrates for consistency, Nunc LabTek II slides [Thermo Fisher

Scientific, Scoresby, Australia], consisting of Permanox cell culture surfaces defined by polystyrene borders, were used for the pre-imprint cell culture. The commercially available LabTek slides included a rectangular polystyrene barrier which provided bioimprint substrates with reproducible dimensions. However, even the small amount of polystyrene in contact with the cured poly(methacrylate) would not release without scoring and force, which often resulted in broken samples.

Because the polystyrene defined chambers were no longer a practical option, new avenues were investigated for defining the available cell culture region. In order to control the cell culture area, rectangular areas matching the dimensions of the LabTek II slides were cut from PDMS slabs which were then sealed to the sterile glass substrates. While this method was less expensive and allowed freedom in defining the culture area, the chamber borders were cut manually with a scalpel. As a result, no two PDMS-defined rectangular borders, and thus their resulting bioimprints, were exactly equivalent. Consistency of bioimprint size was important because the bioimprint substrate was press fit into a second PDMS chamber for the second cell culture step. If the original imprint sample did not fit exactly into the secondary PDMS chamber, the added cell and media suspension leaked under the poly(MA) substrate altering the actual cell seeding density on the bioimprint surface and making washing and staining steps more difficult. This consistency was later addressed by using a cork borer to create highly regular circular cut-outs in the PDMS sheets attached to glass microscope slides.

3.2.1.2 Curing and ratio optimisation

Alterations of to the polymer ingredient ratios and concentrations changed the physical appearance and properties of cured samples. Increasing the quantity of IRGAcure, for example, led to a neon yellow tint to the translucency of the cured methacrylate polymer substrate. Removing triglyme from the polymer increased the relevance of the chemical interactions between the other substituent groups. Changing the ratio of ethylene glycol dimethacrylate to methacrylic acid caused changes in the optical translucency and the elasticity of the cured polymer substrate.

Observable insufficiencies with the properties of triglyme-inclusive, 10:1 EGDMA:MAA initial methacrylate monomer ratio suggested further optimization was necessary. Due to the thinness and the brittle nature of the cured polymer, removal of the bioimprint from the

template often resulted in cracking of the delicate methacrylate samples. Especially when liquid polymer managed to round over the edges of the template coverslip, careful separation of sample and substrate was required and still resulted in delicate samples.

In its original formulation, the bulk of the liquid polymer mixture consisted of the thickening agent, triglyme, and not reactant monomers. The minimal thickness of the liquid polymer, as assured by spin-coating, lead to an unknown distribution of monomer groups and a variable, heterogeneous surface chemistry for the cured product. Because of its non-curing contribution to the bulk and the resulting effect on biocompatibility, triglyme was quickly eliminated as a polymer requirement.

Notably, IRGAcure 2022 has a very low viscosity, which complicated pipetting techniques, especially at low volumes such as the 20 μL required. The yellow liquid dripped continuously from the pipet and made accurate volume measurement difficult. To ensure accurate quantities of IRGAcure were used in polymer curing, IRGAcure was weighed by volume prior to the addition of the other liquid ingredients. IRGAcure 2022 was weighed and volume calculated using the 1.1 g/mL density provided in the product specifications sheet [80].

To evaluate the chemical effect of the ingredient ratio on surface chemistry and wettability, contact angle testing was conducted on two different polymer mixtures. Additionally, each mixture was tested with and without triglyme incorporated in order to isolate the effects of the thickening agent. Contact angle analysis showed no significant wettability difference in any of the samples, even in the lower ratio poly(MA) samples. Incorporation of triglyme had no effect on the contact angle measurement. Across all substrate samples the maximum difference between angle measurements was less than ten degrees.

After the elimination of triglyme and the increased consistency for IRGAcure inclusion, new methacrylate monomer ratios were tested and characterised for optimum use in bioimprinting. Initially, three different polymer ratios, all excluding triglyme, were examined. Each of the resulting samples showed different physical characteristics as documented in Figure 3.3. The ratios represented in this figure are from left to right 6:6:1, 6:4:1, and 6:3:1 EGDMA:MAA:IRGAcure. [NOTE: all ratios given from here on will be given as ratios of EGDMA to MAA to IRGAcure]. As visible in the figure, the equivalency ratio, 6:6:1, cures opaque white and varies quite strongly from the other two. The high ratio 6:3:1 samples cure perfectly translucent, but the middle sample shrivelled and burned as a result to high

crosslinking under intense UV. The 6:4:1 sample appeared to be the most consistent curing. However, cloudiness was detectable in the central regions of the imprint suggesting that a lower ratio would be still more efficient for imaging purposes.

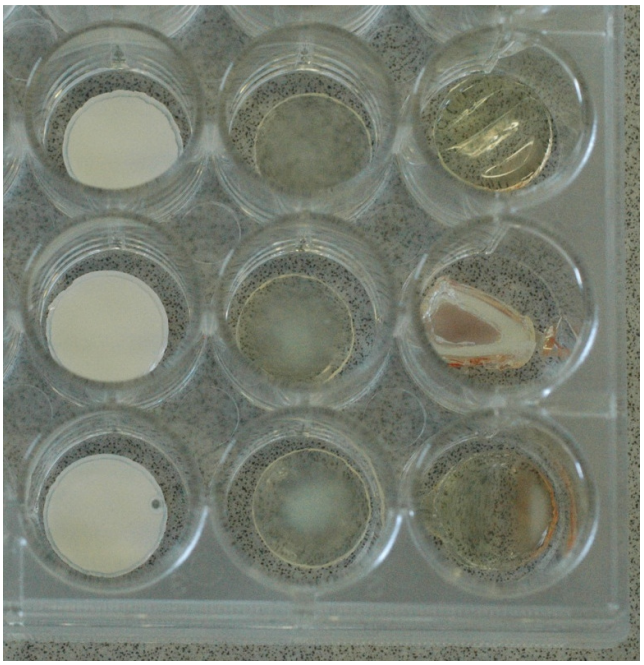

Figure 3.3 – Methacrylate monomer ratio testing showing the difference in physical characteristics for samples with differing reactant ratios. Ratios, from left to right, are 6:6:1, 6:4:1, and 6:3:1. Completed at Plant and Food Research in Hamilton, NZ.

To expand on the results of the initial trials, repeat experiments were performed for comparison, together with the inclusion of 6:2:1 and its inverse 2:6:1. The obvious variation of physical appearance across ratio recipes can be seen in Figure 3.4. As expected, the samples with relatively high concentrations of methacrylic acid [MAA], the 2:6:1 and 6:6:1 samples in Figure 3.4, cured opaque, with curing initiating, unexpectedly, from the bottom up. The newly included 6:2:1 ratio [Figure 3.4] showed the highest and most desirable optical translucency, but lasted only 30 seconds into the UV curing cycle before audible polymer cracking occurred. Based on the slight cloudiness in the central regions of the 6:4:1 samples, 6:3:1 was determined to be consistently the most reliable ratio, though some non-fatal cracking did occur in one of these samples as well.

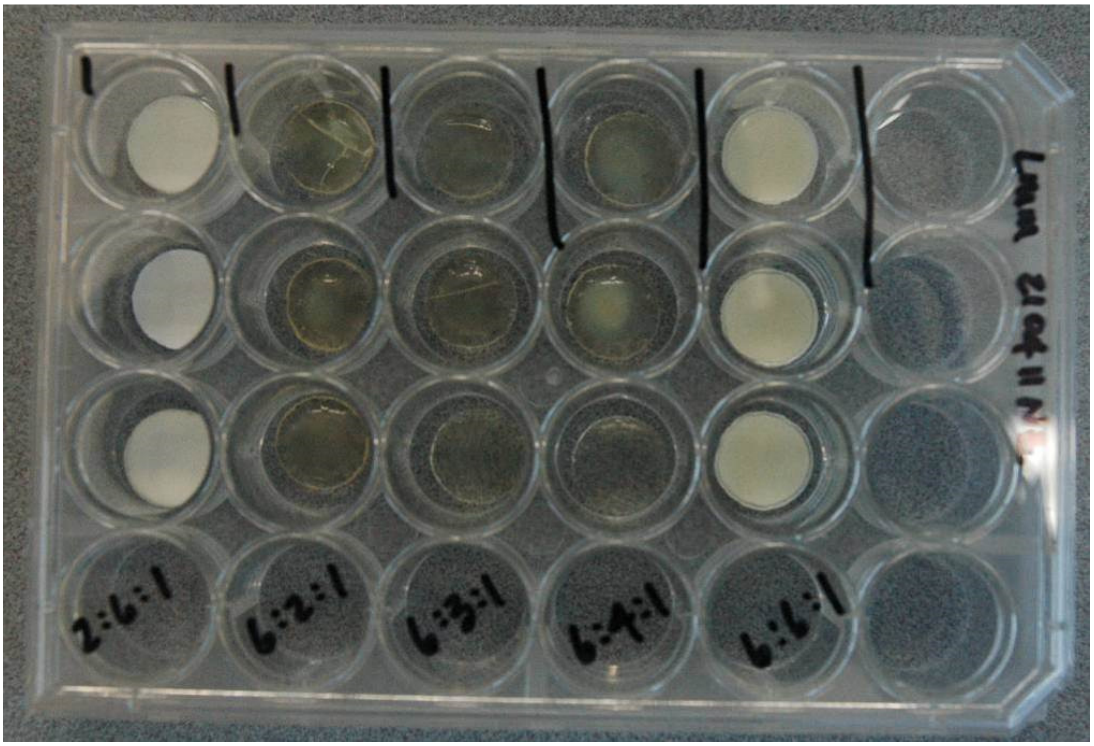

Figure 3.4 – Cured poly(methacrylate) samples showing the variation in physical appearance dependent on EGDMA:MAA:IRGAcure liquid polymer ratio. Monomer ratio is shown in black over across the bottom row. Completed at Plant and Food Research in Hamilton, NZ.

Bioimprints fabricated after polymer optimisation experiments compared the most consistently translucent ratios, 6:2:1 and 6:3:1, and showed not only the consistent fatal cracking of the higher ratio samples, but highlighted the importance of mixing the polymer freshly for each sample set. In Figure 3.5, six samples were obtained from each millilitre of mixed liquid methacrylate pre-polymer. Though six samples could be poured consecutively, only one microscope slide, consisting of three samples, could be cured at a time. The resulting trend, consistent across all four sets regardless of ratio, showed an increasing cloudiness in curing for the second slide of the same polymer mixture.

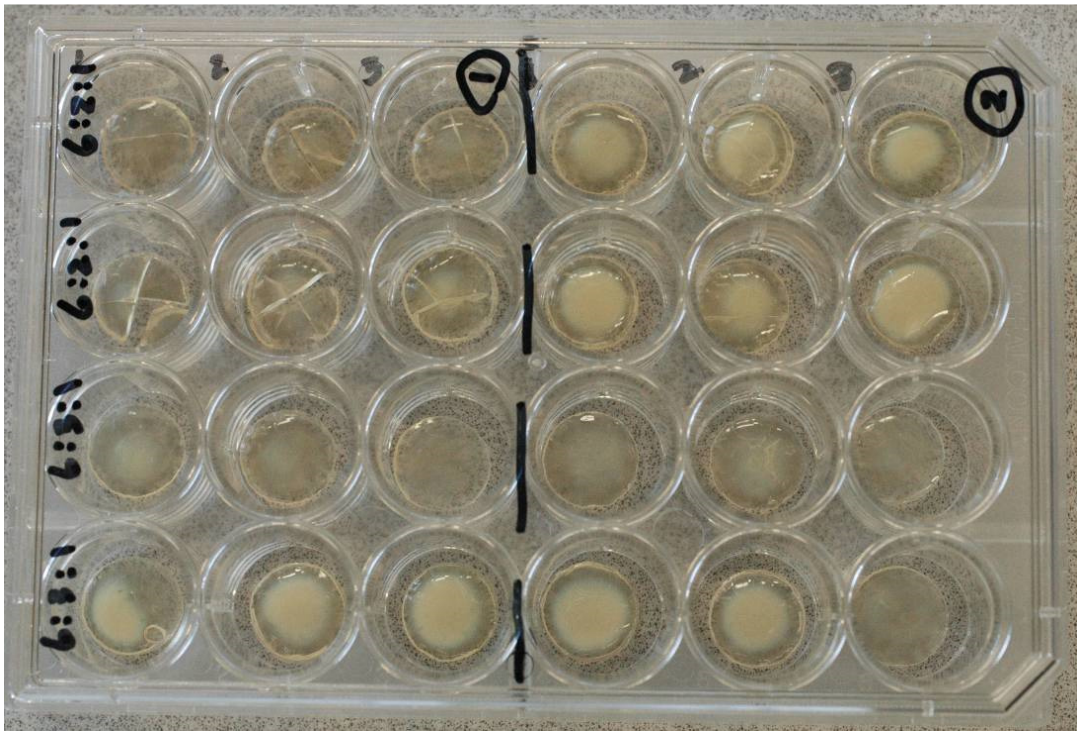

Figure 3.5 - Cured poly(MA) samples showing the importance of mixing the liquid pre-polymer immediately before curing. For each polymer mixture [labelled at left] the first row was cured first and the second was cured within 10 minutes. Each row representing secondary curing shows increased cloudiness and lower optical transparency. Completed at Plant and Food Research in Hamilton, NZ.

3.2.1.3 Physical properties

Thin samples were difficult to manipulate without cracking. To make the samples more robust and easier to handle thicker samples were poured, but the geometry was found to be very important. While the poly(MA) cured more quickly than PDMS bioimprints, the fast curing process induced stress within the cured bulk of the poly(MA) that affected its usefulness as a cell culture substrate.

In the opaque samples cured from polymer mixtures containing high ratios of MAA, gradients of curing were seen along the vertical axis, with the opaque white layer actually occurring at the polymer-substrate interface. Observable 'layered' curing of the liquid methacrylate mixture resulted in polymer variation along the vertical axis. Additionally, an uncured liquid layer often remained along the top surface. Sometimes the thin liquid layer responded to a second curing cycle, but more often was removed during the biocompatibility washing phases.

As previously mentioned, to circumvent the adhesive response of the liquid methacrylate in contact with any polystyrene surface area, PDMS borders were used to define cell culture chambers on glass substrates. Rectangular chambers were defined in large PDMS sheets to the same dimensions as the Nunc LabTek II borders and cut out with a scalpel. The geometry of the chamber walls was found to be critical in curing thicker samples. Square and rectangular geometries were easiest to produce, but were not highly reproducible and showed an induced stress in the cured polymer substrates at the corner regions. Though the stress deformation effects were not on the bioimprint-face, the meniscus formed meant samples were unlikely to sit flat for secondary cell culture and imaging steps. Uneven samples were difficult to image and more likely to leak when used as cell culture substrates.

To force the poly(MA) to cure flat on both sides, PDMS borders were sandwiched between two glass slides during polymer curing; one slide was slightly offset to allow for pipetting of the liquid methacrylate mixture into the vacancy. The assembly was placed under the Omnicure UV light source and methacrylate pre-polymer was added in. While the sandwich assembly did impose even curing on both sample faces, the liquid polymer was so thin that it tended to leak between the PDMS-glass conformal seal. This had minimal impact on the resulting bioimprints, but the liquid disruption allowed the slides to float and shift too easily.

The PDMS chamber design was altered to prevent points of increased stress by using circular cut-outs instead of rectangles or squares. Chambers were punched in PDMS sheets using a size 7 cork borer [14 mm diameter]. The circular hole punch method had the added benefit of ensuring that all chambers were reliably produced with cylindrical chambers of the exact same diameter, ensuring press-fit samples for secondary cell culture were more likely to seal to the next set of PDMS chamber borders. The PDMS sheets with circular cut-outs were conformally sealed to a glass microscope slide. The PDMS-defined cell culture chambers that were adhered to glass microscope slide substrates were used for the greater portion of the experimental work presented in the following chapters [Figure 3.6].

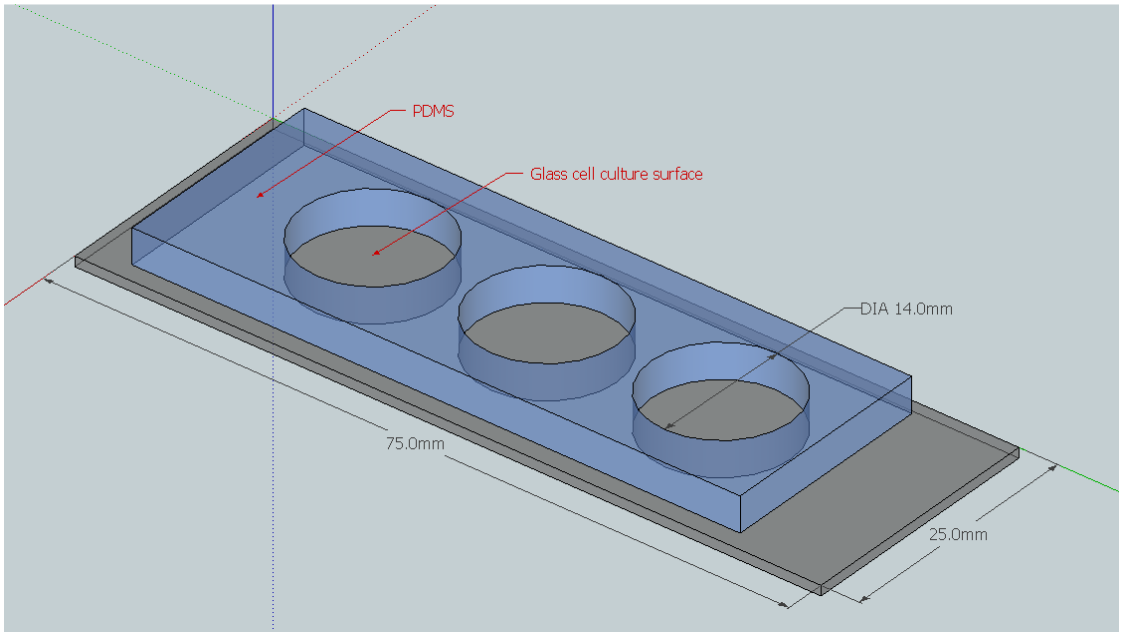

Figure 3.6 - PDMS with circular cut-outs conformally sealed to a glass microscope slide for use in cell culture and bioimprinting protocols

The circular chambers effectively distributed the stress away from any particular point locations. However, the new stress distribution was also problematic. Instead of the polymer pulling to the corners during the cross-linking stages of curing, the liquid polymer now pulled into the middle and up from the template substrate. The resulting bioimprinted sample was noticeably concave, as shown in Figure 3.7. Because the curing at the surface was reliably fast, the separation rarely affected the quality or resolution of the bioimprint, but occasionally produced artefacts which rendered the samples undesirable as cell culture substrates, discussed in detail in chapter 6. As expected, the cross-linking stress was greater for higher ratio polymers. EGDMA's two terminating alkene bonds encourage cross-linking to a greater extent than MAA, leading to greater internal stresses for polymer mixtures containing higher proportions of EGDMA.

Figure 3.7 - Cured circular poly(MA) sample, bioimprint-face up, showing the concavity and stress across the surface. Completed at Plant and Food Research in Hamilton, NZ.

3.2.2 Bioimprint protocol

Three modifications were made to the existing bioimprint protocol. Firstly, the substrate samples were no longer spin-coated onto the template cultures. The thin, delicate samples were difficult to handle and likely would not last though experimental cell culture protocols requiring press-fitting. Second, the curing cycle was changed to 240 seconds [4 minutes]. Previous protocols consisted of 15 minute curing cycles. Lastly, cells were fixed prior to bioimprinting.

For spin-coated samples, the cured poly(MA) layers were often difficult to separate from the template substrate. A scalpel was required to tease the edge of the polymer away from the template substrate and slowly drive release between the sample and substrate. Insertion of the scalpel between layers was extremely difficult if any liquid polymer had cured over the edges of the slide or coverslip. The brittleness of the highly cross-linked polymer contributed to cracking of samples. On the other hand, incomplete or heterogeneous curing also contributed to sample deformation and, possibly, destruction.

Additional protocol modifications were made regarding the curing time and procedure. Other curing variables, such as iris opening and vertical distance between UV source and sample were identified and fixed. Repetitive curing experiments showed the majority of curing occurred within 30 seconds of high-intensity UV-curing; approximately no additional curing was observed beyond the initial 150 seconds. When curing was interrupted within a cycle, no

additional curing was seen beyond that point even after the re-initiation of UV exposure. For consistency, UV exposure was set beyond the 150 second requirement at 240 seconds at 40% aperture opening for the UV light guide which was fixed at 15 cm above the substrate surface.

Changes to the cell culture aspect of the bioimprinting protocol included the addition of a fixation step prior to polymer coating and curing. Cell fixing used 4% paraformaldehyde in PBS solution to crosslink the structural scaffolds within the cell and allow for more time between the initial cell culture steps and the bioimprinting process. The addition of the fixation step was important when the cell culture templates were being transferred between facilities prior to imprinting [for example, between the cell culture laboratories at University of Otago School of Medicine to the Nanofabrication Laboratory at University of Canterbury]. Protein denaturation and cell dehydration were prevented by cell fixation, though fixation in itself produced minor imaging artefacts from solute salts from the fixative and/or PBS.

3.2.3 Biocompatibility

3.2.3.1 Poly(methacrylate) chemical stability

The high resolution properties of the poly(methacrylate) samples allowed for an intricately detailed biomimetic substrate, but there were several assumptions about the bioimprint's biocompatibility in transition from imaging tool to cell culture substrate and scaffold. Cell culture must be maintained in media solution, so the stability of the polymer chemistry in solution for extended periods was critical. In order to determine the short- and medium-term effects of poly(MA) substrates on cell culture medium conditions, and vice versa, cured polymer samples were treated with different pre-culture washes before being placed in cell culture medium for 48 hours. The αMEM media used for the biocompatibility experiments contained a phenol red pH indicator to ensure the solution pH was maintained within a physiologically acceptable range.

Almost immediately upon immersion of the poly(MA) sample, the media changed from a dark red to a translucent yellow, indicating a highly acidic shift in the media pH. The columns containing samples washed before immersion in media altered the pH of the surrounding solution less than the untreated samples. Samples treated in basic solution were less acidic

toward the medium solution than any other sample set. Sample rows containing samples with triglyme incorporated within the cured polymer sample increased the acidity of the immersion solution enough beyond the buffer region that the medium turned yellow [Figure 3.8]. The media was changed for all samples at 24 hours. When the plates were observed again at 48 hours, no difference was noticeable between the sample sets. The polystyrene control wells showed no change over the 48 hours.

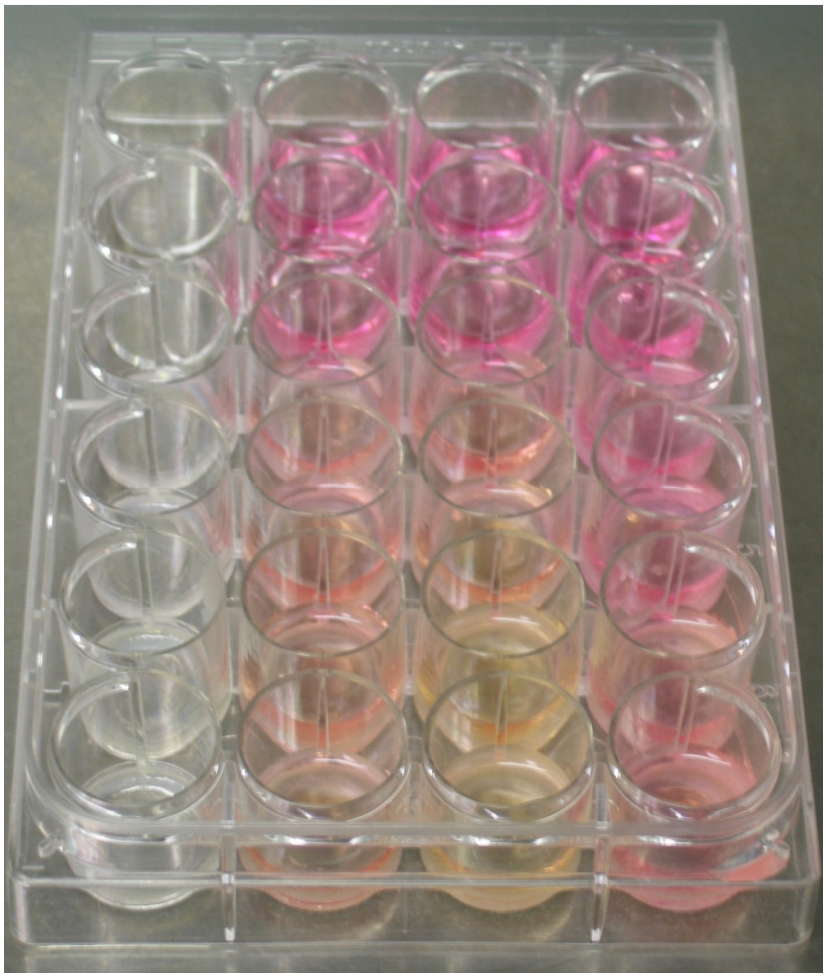

Figure 3.8 - Experimental plate for testing chemical stability in aqueous conditions. Each two set of two rows contains, from top to bottom, control TCPC [top], methacrylate polymer with triglyme [middle], and methacrylate polymer without triglyme [bottom]. The first column was left blank for reference; the remaining columns contain, from left to right, water wash prior to addition of medium, no treatment before addition of medium, and sodium hydroxide treatment before addition of medium.

3.2.3.2 Cytotoxicity

To determine the whether the cured poly(MA) would provide a practical cell culture substrate or would inadvertently cause cell death, samples were incubated in 6-well plates with Ishikawa cancer cells in 6-well plates. Poly(MA) substrates were placed within the wells and fifty thousand cells were seeded in each well. Polystyrene control wells showed normal adhesion and spreading. Cell adhesion to the poly(MA) substrates was significantly lower and, rather than large surface expanses of adhered cells, Ishikawa cells existed mostly in suspension or loosely tethered to the poly(MA) surface. Whether the cells in suspension remained viable was unknown.

3.2.3.3 Substrate cleaning

The addition of substrate cleaning techniques to the preparation of bioimprinted polymer samples was adopted much later in the course of the work discussed in this thesis, but led to tighter control of the substrate chemistry. The results of the chemical stability testing showed that pre-treatment decreased the effects of the poly(MA) susbtrates on media pH. The cleaning treatments, consisting of a water wash, an SDS/HCl bath, a trypsin soak, and an overnight water bath, lowered the pH response of the medium while also removing any remaining cell debris and/or protein material from the substrate before use as a cell culture substrate.

3.3 Discussion and working protocol

3.3.1 Poly(methacrylate) optimisation

Following the inherited bioimprint protocol, the methacrylate co-polymer was mixed and cured using spin-coating for even polymer application. UV curing after spin coating resulted in very thin bioimprints, which, while practical for AFM purposes, were too fragile as a secondary substrate. Separation and handling of the thin bioimprint was slow and unpredictable. The most relevant contributor to the non-reproducibility of spin-coated bioimprint substrates was the polymer thickness, both as a liquid pre-polymer and post-curing. The tenuousness of sample-substrate separation led to protocol alterations for producing thicker bioimprint substrates for secondary cell culture.

The physical appearance and properties of the cured poly(MA) substrates were found to depend heavily on the ratio of EGDMA to MAA. Because ethylene glycol dimethacrylate monomers have two terminating alkene groups, it acts as a crosslinker between polymer chains. In comparison, methacrylic acid monomers have only one available polymerization site which results in more ordered polymerization and greater flexibility within cured polymer. Radical polymerization was initiated by the reaction of IRGAcure 2022 [phenylbis (2,4,6-trimethylbenzoyl)-phosphine oxide] and UV light. The alkene bonds of the reactant monomers were split into their corresponding radicals, which then bonded to radical groups of the surrounding monomers. Changing the ratio of monomers and the relative concentrations of the other polymer ingredients changes the chemistry and physical properties of the resulting sample

An equivalent or lower ratio of EGDMA to MAA [higher concentration of MAA] will result in a more flexible cured polymer which is easier to separate from the substrate. However, at this ratio the cured polymer is no longer translucent. Instead of a yellow-tinted, transparent block, methacrylate mixtures containing high ratios of MAA separate into stratified layers of opaque white and cloudy yellow upon UV-irradiation.

The curing striations are likely due to the curing progress through the liquid polymer; upon UV-exposure, the curing progresses from the substrate interface upward toward the light

source. This produces fast curing at the imprinting interface, thus significantly lower curing times and high resolution bioimprint features, but can leave uncured liquid polymer across the top surface. Secondary curing cycles show limited effect on curing the remaining liquid layer. This suggests that once curing has been initiated, the UV must remain continuous for complete curing. If UV curing was interrupted, the poly(MA) substrate is unlikely to recover to complete curing. Similarly, the clouding over of the central areas of the curing areas is linked to both the polymer ratio and the 'freshness' of the polymer mixture. We propose that some self-crystallization occurs if the liquid methacrylate mixture is left too long before curing and this prevents completely translucent curing beyond that time point.

Increased yellowing of the cured methacrylate samples was also seen if an unusually high percentage of IRGAcure was incorporated. Because IRGAcure 2022 has an extremely low viscosity pipetting accurate volumes was difficult. In the initial polymer formulation, because of the relatively low concentration of IRGAcure, precise volume measurement was necessary. The Ciba specifications for IRGAcure 2022 suggest use at 1-3% by volume. The 20μL volume required in the initial polymer recipe comprised only 1.2% of total volume and, therefore, careful measurement was important. Due to the low viscosity and inconsistency in pipetting volumes, the volume was measured by weight using the 1.1 g/cm^3 density. Precautions were taken to ensure this was done in limited or filtered light to prevent undesired polymerization action. In later formulations of the liquid pre-polymer the exactness of the IRGAcure measurement was less critical as it represented a higher percentage of the bulk mixture.

Triglyme, which was initially included in the poly(MA) formulation as a viscosity agent, accounted for over 70% of the liquid pre-polymerised bulk. Triglyme monomers, however, do not polymerise into the polymer bulk. Therefore, to prevent potential, undesired leaching into cell culture media, triglyme was eliminated as a polymer ingredient for cell culture substrates. No noticeable physical variations occurred at the omission of triglyme. The removal of triglyme showed no effect on the contact angle measurements of surface wettability. While undocumented, triglyme may have had a porogenic effect within the cured bulk as well. In theory, areas occupied by triglyme monomers were left vacant after the monomers were removed during washing, theoretically changing the porosity and density of the cured poly(MA). This hypothesis, however, remains untested due to the early elimination of triglyme as a polymer ingredient.

Polystyrene exists almost ubiquitously in cell culture biology and is the most common expansion culture substrate. Eliminating tissue culture treated polystyrene [TCPS] as an acceptable imprinting template greatly limited the employment of commercially available products. With the acuity of hindsight, the inseparable substrate-surface interaction was likely due to a solvent-like incorporation of styrene monomers into the liquid methacrylate pre-polymer, thus permanently fusing the two together upon poly(MA) curing. The adhesive strength associated with the poly(MA)-polystyrene interaction does not occur between the poly(MA) and glass. While glass substrates are less pervasive than TCPS in biological applications, glass still has a high cell adhesion rate and has the additional benefit of being autoclavable for sterilisation.

PDMS cell culture chambers were cut from larger PDMS sheets and conformally sealed to the glass microscope slides for use as cell culture assemblies. The PDMS-bounded cell culture borders have been shown to have no effect on the quality of cell culture in previous works [81]. Initial designs mimicked the size of the rectangular LabTek II assemblies. The physical properties of the cured poly(MA) depended greatly on the volume and geometry of the poured, liquid polymer.

The higher surface tension at the corners of rectangular PDMS chambers pulled uneven quantities of liquid polymer to these regions, which noticeably affected the curing. Because of the uneven polymer distribution circular cut-outs were punched with a 14 mm cork borer. This method provided consistent size for the cell culture area and was more effective at sealing in preparation for secondary cell culture. In spite of the stress-related complications, the resulting disk-like poly(MA) samples were used for the remaining duration of the project. Incorporating the new slide design into the bioimprinting protocol was simple enough as PDMS conformally seals to glass, which is widely accepted as a viable cell culture substrate.

The bioimprint protocol was modified for controlled and reproducible curing of bioimprint substrates. Height and aperture opening were fixed to 15 cm and 40% respectively. Cell cultures were fixed prior to bioimprinting to prevent denaturing of structural proteins and cell dehydration before imprinting could be done. Artefacts caused by both the paraformaldehyde fixative and dissolute PBS salts were observed and identified by comparison with Moloney, et. al. [82]. An additional water washing step was added after cell fixation in order to remove any remnants from the fixation step.

An immediate question regarding the imprint surface was whether or not any cell material was being accidentally incorporated into the substrate. Small scale trans-membrane molecules surrounded by the liquid polymer may be trapped in the cured polymer and pulled from the bulk cell material. If the biological molecules attached to the surface provide some cues for cell growth, there would be no way to distinguish the hypothesised effect of the bioimprint from the effect of the biomolecules present. Adhesion proteins such as fibronectin, poly-D-lysine, and laminin are known to encourage cell adhesion and have been used for chemical substrate modification [15, 16]. Ensuring that any membrane remnants were inactive was critical to the culture results analysis. Without knowing the exact chemical composition of the poly(MA) surface, isolating a technical method for identifying any biological contaminants was difficult. Therefore, to circumvent any potential effects of cell debris on the substrate, extensive cleaning and sterilization steps were undertaken before the samples were used as cell culture substrates.

The unknown nature of any biological remains within the bioimprint features required several contingencies to reasonably ensure removal or, at least, denaturation of bioactive molecules. Protein structure is described by four hierarchical levels, each increasing in complexity [1]. [The primary structure is defined by the amino acid sequence; this sequence will remain unchanged for attached debris with or without treatment. Secondary protein structure explains the folding characteristics of the amino acid chain based on binding affinities and internal forces. Hydrogen and thiol bonding, Van der Waals forces, and steric hindrance determine the helical or sheet conformation of amino acid stretches. How these folded stretches combine to form the working protein is covered in the tertiary structure. Quaternary structure considers structure changes required for the interactions of proteins with receptors and complexes.]

Sodium dodecyl sulphate [SDS] is an organic surfactant commonly used to disrupt higher order protein folding. SDS identifies and attacks the non-covalent bonding determining the secondary, tertiary, and quaternary properties of the protein structure. The resulting peptide chain will consist of the same amino acid sequence, but without the recognizable ‘lock and key’ binding regions, thus inactivating the protein through the conformation denaturation. The ultrasonic bath provided agitation of the sample in the SDS suspension which removed any loosely bound cell material and biological debris. In the case of the bioimprinted substrates, it was important to minimise the amount of biological material remaining and ensure that any debris remaining was incomplete and/or inactive.

In addition to the SDS wash, the samples were subjected to a 30 minute trypsin soak. Soaking in the trypsin solution for at least 30 minutes allowed the enzyme time to recognise and cleave the lysine- and arginine-based protein sequences which may have been later recognised by attaching cells as binding domains. Additionally, albeit unintentionally at first, the SDS and trypsin washes aided in the removal of unreacted monomers remaining in the bioimprint samples.

The intent of the final water soaking step was more to remove unreacted MAA monomers than to attempt to remove any remaining deactivated and cleaved protein material. Because methacrylic acid is water soluble the samples were allowed to soak for at least 24 hours [up to 48 hours] in sterilised water. The water dissolved any unreacted monomers leaching from the bioimprint sample into solution. In media, the pH variation caused by MAA monomer leaching exceeded the buffer range and was shown to have a cytotoxic effect on cell cultures. The overnight water soak pulled the unreacted MAA monomers from the cured polymer bulk and into solution.

Because the curing of the poly(MA) substrates and several of the soaking steps were conducted outside of sterile conditions the samples were sterilised with ethanol [70%], rinsed thoroughly in PBS, and further sterilised by a cycle under UV in the laminar flow hood. In later bioimprint experiments, the bioimprint samples were immersed in media before cells were added as a precaution against any pH altering agents which may remain on the surface, predominantly MAA monomers or ethanol. This additional soaking step was incorporated entirely as a precaution against pH variation effects.

In the 6-well plates used to compare methacrylate biocompatibility with control tissue culture polystyrene cultures a high percentage of cells were found not adhered to the substrate, but were instead rounded up in solution. There are two possible explanations for the high cell numbers in suspension. One, the cells were dead and are no longer able to adhere. Or two, the substrate was non-adhesive and the cells remained viable as microtumour aggregates in suspension. The latter explanation is only a reasonable hypothesis because the experimental cells were cancer cells. Whether the cells remained viable or not was unknown. Ishikawa cancer cells, which were used for the cytotoxicity testing, will grow in three dimensional, non-adhesive cultures and, therefore, could remain viable either loosely tethered or not adhered to the methacrylate substrate. Based on literature for related methacrylate-based polymers [83]

and the cytotoxicity investigations here, the methacrylate co-polymer was identified as a non-adhesive substrate.

3.3.2 Optimised working protocol

The result of the work throughout this chapter was the development of a modified bioimprint protocol which produced biocompatible substrates that still contained the high resolution template features of the original cell cultures. The modified bioimprint protocol used for the majority of this work, except where noted otherwise, was executed as follows. Initial cell culture was carried out in circular, PDMS-defined chambers conformally sealed to glass microscope slides. PDMS/glass slide assemblies were sterilised either by autoclave or UV sterile cycle prior to initial cell culture. Cells were seeded according to the selected experimental parameters and immersed in cell culture medium corresponding to the cell type-specific nutrient requirements. At the desired time or confluence of cell culture, media was removed to waste and the cells were washed once with PBS before fixation. Adhered cells were fixed in a 4% paraformaldehyde solution [Life Technologies, Carlsbad, CA] for at least 30 minutes. At completion, the fixative solution was removed to waste and the cells were washed in PBS. [Later in the bioimprint evolution a water wash was added after the PBS as several imprint samples inadvertently replicated lingering PBS salts.] Cells were kept at 4°C for 2 hours for drying while maintaining the crosslinking effect of the fixative. Immediately before imprinting, the samples were transferred to a dark room, under UV-filtered yellow light if at University of Otago – Christchurch School of Medicine or the yellow room in the Nanofabrication Laboratory at University of Canterbury.

Liquid methacrylate pre-polymer, extensively discussed in section 3.2.1, was mixed while fixed cells were allowed to adjust to room temperature. Freshly mixed 6:3:1 pre-polymer was the most consistent for imaging and considered the optimal choice for bioimprint substrate fabrication. Once thoroughly mixed by vortex mixer for 30 seconds, the pre-polymer liquid was applied to the cell-covered surfaces still contained within PDMS borders. The liquid was left to settle for 10-20 seconds to allow for the liquid methacrylate to seep into the smaller scale cell features. Slides containing the poured polymer precursor were placed below the light guide for the UV light source and subsequently exposed for 4 minutes [240 seconds]. When further curing was necessary, an additional repetition of the UV curing step was included.

After curing, the PDMS borders were removed and the methacrylate substrates were separated from the cell material and the glass substrate. Methacrylate substrates were turned bioimprint-face upward into a water wash and manually agitated to remove large cell debris still adhered to the bioimprint features. Substrates were then transferred to a 10% SDS in .01M hydrochloric acid solution and placed in an ultrasonic bath for several minutes. Bioimprinted substrates were then removed and transferred to a trypsin soak [.05% trypsin in PBS] for at least 30 minutes. From the trypsin soak, substrates were placed into a water bath overnight in order to remove any remaining water-soluble methacrylic acid monomers. Bioimprinted substrates were sterilised with either ethanol or a 30 minute UV sterile cycle before press-fitting into the secondary cell culture PDMS chambers. Secondary cell culture results are discussed extensively in the next chapter.

4 Bioimprint influences cancer cell morphology and adhesion

As discussed in the introductory chapter of this thesis, disruptions to the adhesive complexes of anchorage-dependent cell types play a critical role in the progression of metastatic and invasive cancers. The work discussed in this chapter aims to determine the effect of a bioimprinted cell culture substrate on the growth characteristics and the adhesive status of Ishikawa endometrial cancer cells, a representative cancerous endothelial cell line.

Bioimprint samples were employed after being fabricated as described in chapter 3. Subsequently, a second culture of Ishikawa cells was grown on the bioimprints. The culture used to create bioimprinted substrates in this section is referred to throughout as the 'initial' cell culture in order to distinguish it from the conventional cell biology concept of 'primary cell culture', which refers specifically to cells explanted from live tissues, most commonly by tissue biopsy. Thence, 'secondary' cell culture, in the context of the following work, refers to the addition of a second set of sub-cultured Ishikawa cells to bioimprinted substrates.

Adjustments and amendments to existing imaging techniques were necessary to extract information regarding the adhesion location and relative cell morphology of the Ishikawa cells growing across bioimprinted substrates. Complete mapping of each substrate before and after secondary cell culture was done to compare the cells' adhesion locations relative to the bioimprint features. A development whereby fluorescein was incorporated into the uncured liquid methacrylate mixture, which resulted in a fluorescent background emission upon bioimprint curing, was a more elegant solution to identifying the interactions of secondary cells with topographical features. The addition of stencils within the cell culture platform provided accurate, reproducible patterned bioimprint substrates and furthered the progress of differentiating bioimprint topographies from secondary cell features.

4.1 Methods

4.1.1 Cell culture

Ishikawa endometrial cancer cells were selected for this work due to their previous validation and characterisation in the doctoral dissertation of Dr. Fahmi Samsuri. He had undertaken extensive bioimprinting and atomic force imaging. As to be expected with cancerous cell lines, the adhered, spreading cell morphology can vary greatly but the Ishikawa endometrial endothelial cells tend to adapt a polygonal, 'paving stone' morphology with well-defined cell borders [Figure 4.1]. Initial adhesion occurs almost completely within an hour of cell plating.

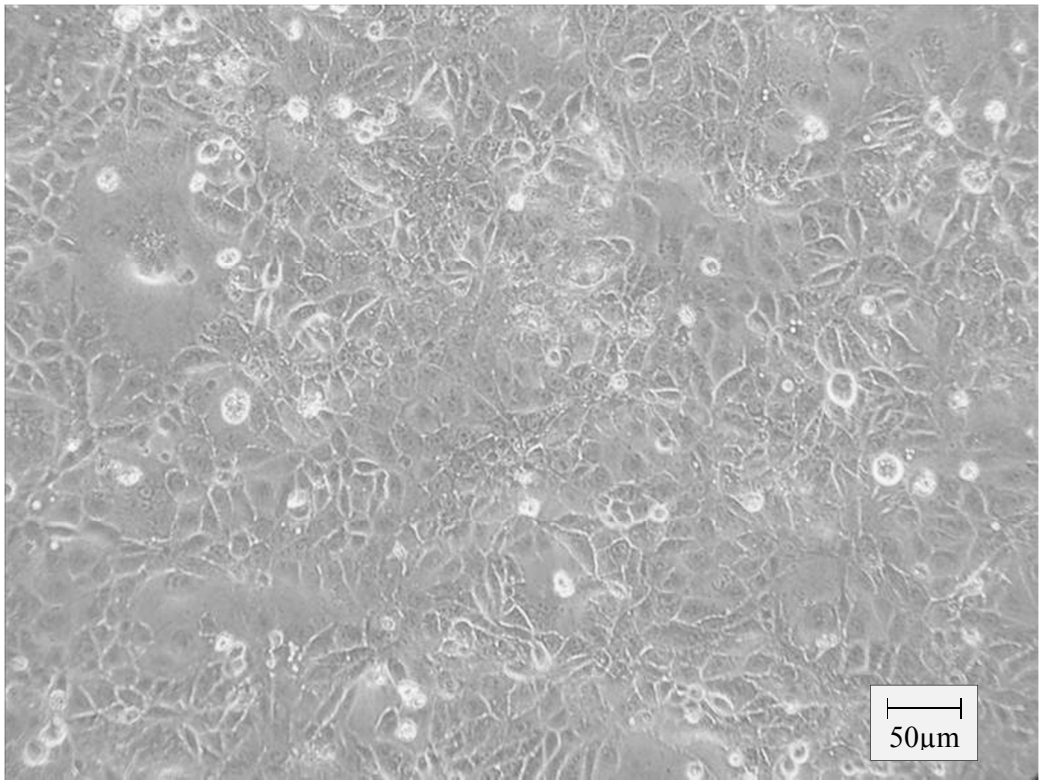

Figure 4.1 - Control culture of Ishikawa endometrial cancer cells grown to confluence (at 100x magnification).

Cell culture work for these experiments was completed in two culture passages: [i] an initial culture for bioimprinting and [ii] a secondary culture on the bioimprint substrate to investigate in this study of adhesion. Many aspects of the protocols were similar in both stages. Experiments took place at the University of Otago – Christchurch School of Medicine. Ishikawa endometrial cancer cells were sub-cultured and maintained in supplemented α –

minimum essential medium [α-MEM] culture medium in 25cm^2 tissue culture grade polystyrene flasks. When cell growth reached approximately 80% surface coverage after approximately 48 hours, the cells were trypsinised, counted, and diluted for either experimental use or re-plating for continued subculture. Re-plated cells were seeded at a density of 1.0 x 10^5 cells/cm^2 in sterile 25cm^2 tissue culture polystyrene flasks. Cells diluted for experimental culture were designated as either initial cell cultures, which would be sacrificial template cells for the creation of the bioimprint substrate, or secondary cells, which would be monitored for their response to the particular substrate surface on which they were cultured.

4.1.1.1 Initial cell culture

Ishikawa cells plated for bioimprinting were cultured following the same counting and plating protocols designed for subculture, discussed in chapter 2. Trypsinised cells were counted and diluted to the desired cell density before seeding. Cells of a known density, as calculated from haemocytometer counting, were seeded onto glass slides with PDMS-defined chambers. The PDMS borders were cut from larger PDMS sheets using a 14 mm cork borer as a hole punch. The cut PDMS was then carefully placed and sealed to the glass slides [as shown previously in Figure 3.6. PDMS-glass slide assemblies were sterilised or autoclaved. Each chamber allowed for approximately 200μL media. Cells were predominantly seeded at 5.0 x 10^4 cells/cm^2, but this was varied on occasion to observe prolonged growth periods or increase cell density for whole-chamber bioimprints.

Culture duration varied according to the parameters determined for each experimental design. After the allotted amount of time, cells were removed from culture and fixed with 4% paraformaldehyde [in PBS solution] for at least 30 minutes. After fixation, the fixative was removed and the cells were carefully rinsed with sterile water in order to remove any traces of fixative or precipitate PBS salts. Immediately prior to bioimprinting, fixed cells were placed in the refrigerator at 4°C for drying. Two hours were allowed for drying, at which point the cells were transferred to either the Nanofabrication Laboratory at University of Canterbury or a re-purposed dark room at University of Otago – Christchurch School of Medicine for bioimprinting.

4.1.1.2 Secondary cell culture

For secondary cell culture, trypsinised cells were counted and diluted to the desired suspension density, in the same manner as for initial cell culture. Approximately 150 µL of the cell suspension was pipetted over the bioimprinted face of the substrates. Less media volume per chamber was used than for initial cell culture because of the presence of the bioimprint substrate within the chamber. In the preliminary experiment, Ishikawa cells were plated at 5.0 x 10^4 cells/chamber onto bioimprinted samples press-fitted into rectangular PDMS barriers. Cells were grown in supplemented αMEM. Media was changed every 24 hours when required, shorter than the usual time between aspirations due to the lower media volume. At the desired culture duration, cells and substrate assemblies were removed from incubation. Medium was aspirated, same as for initial cultures, but two PBS washes were added before fixation to remove residual media which may have leaked between the PDMS and bioimprint interface. Fixation was completed with 4% paraformaldehyde [in PBS solution] and cells were washed with water before staining. After fixation, cells were stained with either eosin or CBB stains. Staining was allowed to set for 10 minutes before being thoroughly washed away with PBS. Experiments were independently repeated four times and all samples were imaged [though the number of images per sample varied by microscopy analysis method].

4.1.2 Bioimprint substrate fabrication and preparation

Fabrication of bioimprint substrates followed the protocol resulting from extensive optimization, documented in chapter 3. The implemented bioimprinting protocol, which is also outlined in the conclusion section of the previous chapter, produced one bioimprint sample for each initial culture chamber. Briefly, Ishikawa cancer cells were cultured on glass and then a mould, called a 'bioimprint', was produced using an ethylene glycol-dimethacrylate [EGDMA] and methacrylic acid [MAA] copolymer cured by brief exposure to UV. After initial Ishikawa cell cultures were fixed and rinsed, approximately 250 µL of freshly mixed methacrylate polymer was poured into each PDMS chamber on the slide. One or two slides of samples were cured simultaneously [each slide containing three circular samples]; more than two slides were never cured in each UV exposure cycle to ensure similar UV exposure across all samples. Curing consisted of four minutes of UV exposure at 40% intensity. Post-curing, bioimprint

substrates were subjected to the series of wash steps required to increase biocompatibility and minimise biological contamination.

Upon completion of the washing steps, the bioimprints were placed 'imprint-side up' into a new PDMS border sheet bound to a glass slide. The bioimprints were carefully pressed into the PDMS borders, which had been cut with the same instrument used to create the initial PDMS containment features for initial cell culture prior to the bioimprinting. Because the initial PDMS borders defined the shape of the cured bioimprint sample, the bioimprinted substrates fitted tightly into the secondary border set and required careful manipulation for maximum throughput.

4.1.3 'Biomaps'

To determine a relative reference position for the bioimprint features and the position of secondary cell adhesion, additional characterization was required. The most direct method for characterizing cell adhesion location was termed a 'biomap' because it provided an accurate, high resolution representation of the entire bioimprint surface. 'Biomaps' were created by taking sequential micrographs across the entirety of the bioimprint surface and digitally reconstructing the overall surface as a single panoramic image using Autopano Giga 2 [v. 2.6, Kolor SARL, www.kolor.com]. Each biomap consisted of 50 to 90 high resolution images. Repeating the imaging after the secondary cell culture and staining produced a second biomap; this could be placed over the 'initial' biomap for the same sample and aligned to show areas of cell adhesion relative to the bioimprint.

4.1.4 Fluorescein incorporation

In order to isolate the bioimprinted cell features from the cell features of secondary cells grown on the bioimprinted surface, a fluorescent agent was incorporated into the liquid methacrylate mixture. Before addition of the liquid polymer ingredients, 30 mg of fluorescein was weighed and added to a 2 mL micro-centrifuge tube. The polymer ingredients were added to the tube, totalling 1 mL in volume. The tube was closed and thoroughly mixed using a vortex mixer to dissolve the fluorescein into the liquid. This 30 mg/mL stock solution was kept away from UV exposure and used for all subsequent liquid methacrylate mixtures occurring within 24 hours.

For bioimprinting with fluorescence incorporated, 10 µL of the stock solution was added to 1 mL of a non-fluorescent polymer mixture. The resulting working dilution of fluorescein was 30 µg/mL in liquid pre-polymer mixture. The working solution was pipetted into the PDMS chambers containing fixed cell cultures for imprinting and poly(MA) curing was carried out according to the existing bioimprinting protocol.

4.1.5 Elastomeric stencils

Polymer stencils were fabricated from PDMS and used to define areas in which initial Ishikawa cell culture would be performed. Previous methods had been developed by other groups [84, 85]; however, cell culture growth confined to selected areas had not been used in association with substrate fabrication. Stencils were fabricated in thin PDMS sheets by an exclusion moulding method. Exclusion moulding was achieved after the production of an SU-8 silicon master pattern containing the desired stencil patterns [Figure 4.2 [A]]. The thickness of the SU-8 photoresist layer was determined according to the MicroChem SU-8 2005 [86] specifications for spin speed and verified with Dektak [Veeco Instruments Inc., Santa Barbara, CA]. Master patterns were produced with pattern height as close to 100µm thickness as possible.

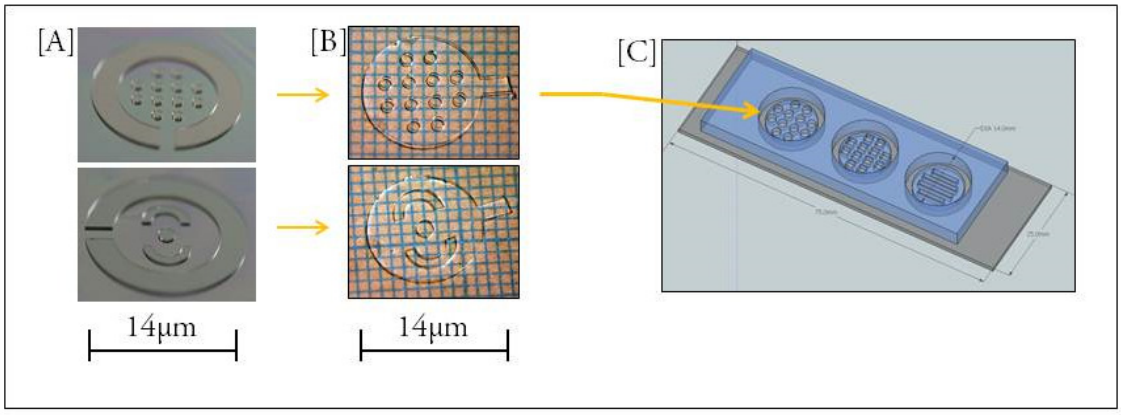

Figure 4.2 - Fabrication phases for culture assemblies containing elastomeric stencils. [A] Developed patterns defined in SU-8 on silicon. [B] PDMS stencils produced by soft lithography. [C] Schematic of entire culture assembly with PDMS stencils sealed to the glass microscope slide within the borders of the larger PDMS chamber borders.

The exclusion moulding protocol is a variation of the soft lithography protocol which will be discussed in more detail in chapter 5. The lithographically-defined silicon master mould was

first treated with TMCS vapour to prevent any PDMS adherence. Then a small volume, approximately 5 g, of liquid 10:1 PDMS was mixed, desiccated, and poured in the centre of the silicon master wafer. A polyethylene transparency was carefully applied on top of the liquid PDMS as a backing for the cured mould. The transparency was applied at one end and pulled across the PDMS to spread the polymer but prevent bubbles from forming. The wafer was then transferred to a hotplate where a 5 kg weight was carefully placed over the transparency. The PDMS was allowed to cure for 2 hours at 80°C. After complete curing and cooling, the PDMS and wafer were carefully separated. The thinness and flexible elastomeric nature of the cured PMDS sometimes was associated with sticking and tearing at removal, especially at locations of SU-8 features where the PDMS had been excluded by the added weight.

Upon successful removal, another polyethylene transparency was placed on the other side to keep the stencils clean. The polyethylene-protected stencil patterns were then re-placed on the hotplate for a second curing cycle. Because the stencils were intended for cell culture purposes and not just replica moulding, a second baking step was used to ensure complete PDMS curing. The resulting PDMS sheet contained through-hole impressions of the master-defined geometric features. Stencils were cut down from the larger PDMS sheet with an 11mm cork borer [Figure 4.2 [B]] and then conformally sealed to the glass microscope slide concentrically within the larger 14mm cut outs of the thicker PDMS chamber borders [Figure 4.2 [C]]. A thirty second oxygen plasma treatment was found to aid in wetting effects of the stencilled glass areas. Additional agitation of cell culture medium via pipet was also found to aid wetting of the stencil features. Complete and sealed stencil chambers were sterilised either by UV and/or autoclave before use as a cell culture substrate.

4.2 Results

Sub-cultured Ishikawa cells were added to bioimprinted substrates in order to determine what effects the template features would have on cell organization and growth. Initial and secondary cell culture durations were varied according to the experimental design. The incomplete optical transparency of stained secondary cells presented a serious hindrance to data collection because the position of cells relative to the substrate features could not be directly determined. Methods, such as biomapping, fluorescence incorporation, and cell culture stencilling, were employed to simultaneously identify bioimprint features and secondary cells. Combined results indicated an

inconsistent but identifiable preference toward localised adhesion to bioimprint features, as well as a noticeable morphological variation in cells that was dependent on the topography of the adhered location.

4.2.1 Cell culture on bioimprinted substrates

Bioimprinted substrates were successfully fabricated using the previously developed protocol, outlined in chapter 3. High resolution substrates, accurate to the nanoscale, were cured and cleaned for either imaging analysis or for additional cell culture experiments. Bioimprinted substrates moulded the exact organisation of the Ishikawa cells in culture [Figure 4.3]. Therefore, the distribution of cell features across the substrate face depended on the adhesion location of the cells in initial culture. Higher cell adhesion and growth in the central region of the initial culture substrate was consistently noted across all substrate shapes and chemistries. Higher confluence in the centre of initial cultures led to increased incidence of bioimprinted cell features in central regions.

Figure 4.3 - DIC micrograph of bioimprinted Ishikawa cell features. The bioimprint successfully replicated cell features and organisation to nanoscale resolution.

As noted during biocompatibility testing, the observer encountered the immediate obstacle of being unable to distinguish cells cultured on bioimprinted substrates from the bioimprint features themselves. The transparent secondary cells appeared extremely similar to the

replicated cell features present in the polymer substrate. As a testament to the accuracy of the replication resolution, the bioimprinted cells were only identifiable from secondary Ishikawa cells using DIC microscopy. Even with the polarizing filter of DIC the similarity between secondary cells and bioimprinted cells was only visible at higher magnifications. Therefore, in order to accurately and consistently differentiate between the template and the secondary Ishikawa cells, cell staining was required.

For the first experimental iteration, secondary Ishikawa cells were plated and incubated on bioimprinted substrates for the same duration as the initial cells were cultured before imprinting. Initial cultures of 3.0×10^5 Ishikawa cells were plated on glass substrates within rectangular PDMS cut-outs. The cells were fixed after 24 hours in culture and bioimprints were successfully taken. After soaking and sterilization, bioimprint substrates were press-fit into PDMS borders of the exact measurements of the initial culture chambers. Secondary Ishikawa cells were plated on the bioimprinted substrates at a density of 1.0×10^5 cells/chamber and allowed to adhere and spread for 24 hours in incubation before being fixed and stained.

Eosin successfully stained the secondary cell cytoplasm light red or pink [Figure 4.4]. The bioimprint features appear as shadows [in Figure 4.4] or refractive outlines [in Figure 4.5] depending on whether the bright field image capture was done using a top-down or inverted microscope, respectively. Using the top-down imaging system, the bioimprint features are obscured by the cell clusters adhered to and spreading across them. Individual cell boundaries were indeterminate and Ishikawas could only be identified by stain density. While areas of bioimprinted cells are visible without secondary cells in Figure 4.4, few cells clusters were identified as growing independently from bioimprinted regions.

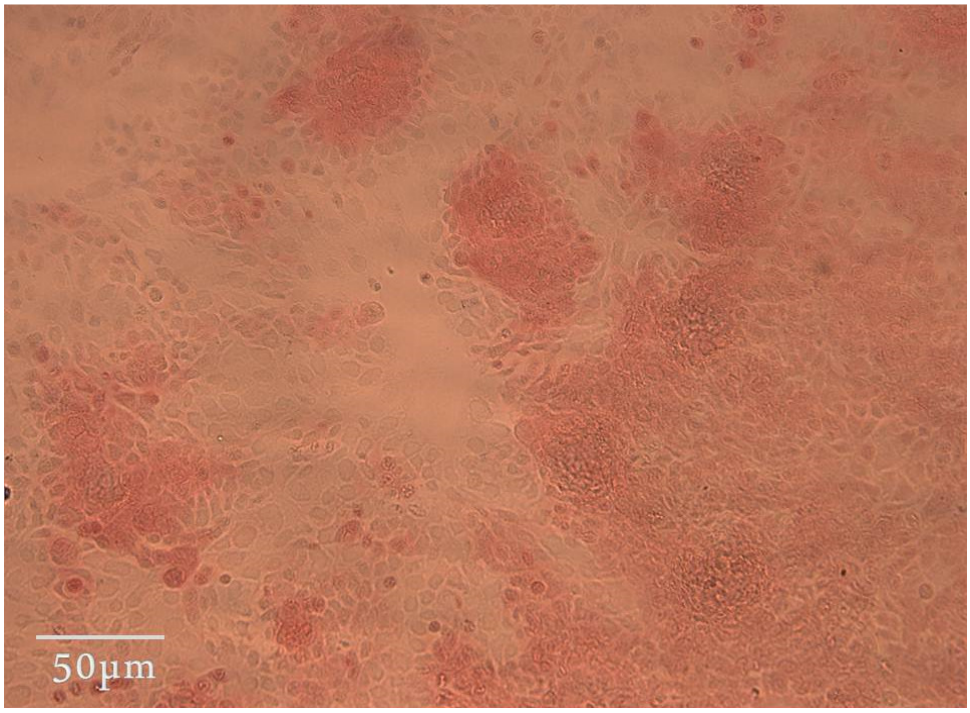

Figure 4.4 – Eosin stained Ishikawa cells grown on bioimprinted poly(MA) substrates. Notably the pink stained regions are difficult to distinguish from the bioimprinted cell features.

In Figure 4.5, eosin-stained Ishikawa cells were captured using an inverted microscope setting. Inverted microscopy provided a refraction of the light shining from underneath the sample and provided a more three dimensional capture of the cells relative to the bioimprinted surface. Bioimprinted features were visible across the substrate by the apparent texturing due to the light refraction and local variation in focal plane (red arrows below). Secondary cell clusters were still primarily visible by high density stain adsorption, indicated by yellow arrows in Figure 4.5. Shifting the focal plane slightly changed the working focus from the bioimprint features to the stained cells. The focal plane of the bioimprint never had high resolution, however, due to the refraction associated with inverted imaging. Using this rough imaging method, cell growth appeared to be almost exclusively localised to bioimprinted regions. Localised instances of Ishikawa cell growth beyond bioimprinted cells were also documented, indicated below by green arrows.

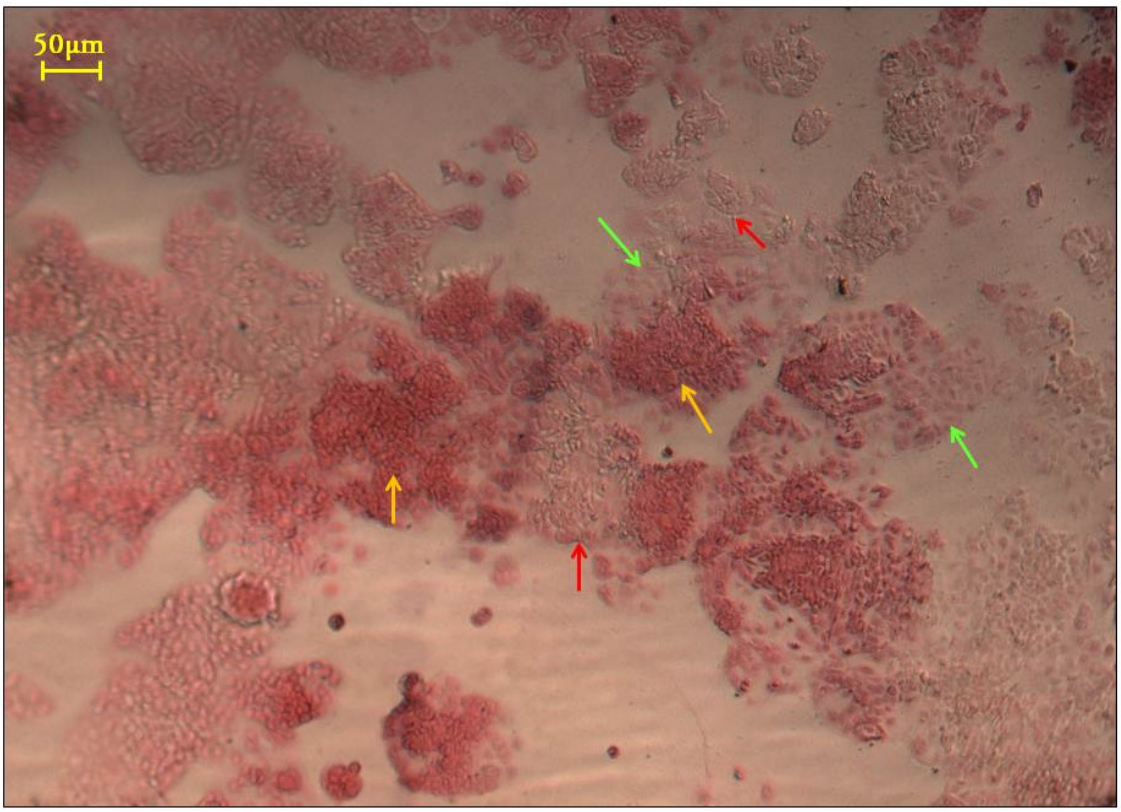

Figure 4.5 - Eosin stained Ishikawa cells grown for 24 hours on bioimprinted substrates taken at 24 hours of initial culture (shown at 50x magnification). Arrows indicate areas of high density cell growth (yellow), cell growth away from bioimprinted regions (green), and identifiable bioimprint regions (red).

Staining, however, revealed a major obstacle in itself that continued to complicate results interpretation until new methods were introduced to circumvent it. When the cells were grown on bioimprint substrates, distinguishing between bioimprinted negative cells shapes and the actual cells, translucent without staining, was extremely difficult. Eosin staining was determined to be too light to provide much information beyond cell cluster location. Individual cells, especially in areas of low monolayer confluence, stained pink with eosin were still stained too lightly to be differentiated from bioimprint features.

The experiment was repeated with slight modifications to the cell seeding density and the incubation time. Bioimprints for the experimental set were taken after 1.0×10^5 cells were incubated in rectangular chambers for 48 hours [in comparison with the 24 hour substrate samples of the previous set]. Instead of press-fitting the cells into PDMS chambers for the secondary culture, however, the bioimprinted substrates were placed in the bottom of the wells of a 6-well plate. Due to the larger area, 5.0×10^5 secondary cells were plated in each well.

To increase the intensity of staining, a combination stain referred to as the 'dollop stain', previously used for rat smear histology, was used. The combination of low concentration [0.6% v/v for all three stains] eosin, light green, and brilliant blue produced a deep purple cell staining. Unfortunately, higher background staining accompanied the new staining protocol and individual cell features were difficult to identify without high magnification. Cells were stained for ten minutes with a one to one dilution of dollop stain in PBS before washing with PBS to remove excess to waste before imaging.

The agitation inherent to the rinsing and washing steps of the stain removal procedures provided an interesting insight into the adhesion locations of the Ishikawa cells. Inadvertently, the dollop-stained cell monolayers were peeled away from the substrates at the edges of the adhered regions unintentionally revealing the bioimprinted area underneath. Comparison of the areas of doubled-over cell material to the revealed bioimprint area shows remarkable alignment between the two, outlined in Figure 4.6 and Figure 4.7. Additionally, areas which did not peel away from the bioimprint edges showed growth exactly along the edge of the bioimprint features, as indicated but the magenta arrows in Figure 4.7.

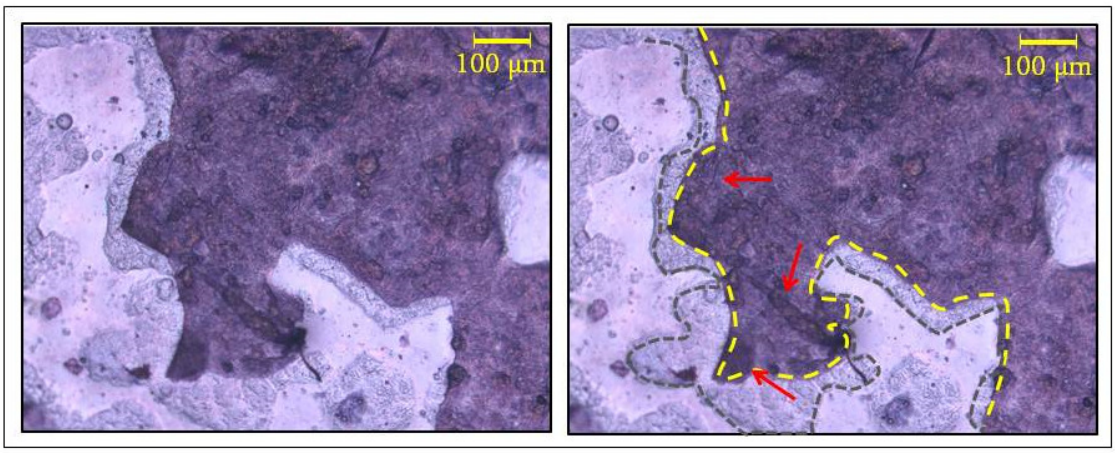

Figure 4.6 - Side by side copies of the same image of CBB stained Ishikawa cells grown on bioimprinted substrates for 48 hours. The right image contains additional outlines highlighting the bioimprint feature outline (grey), the cell growth outline at staining (yellow), and arrows (red) noting high density staining regions indicative of peeling and folding over of the Ishikawa monolayer.

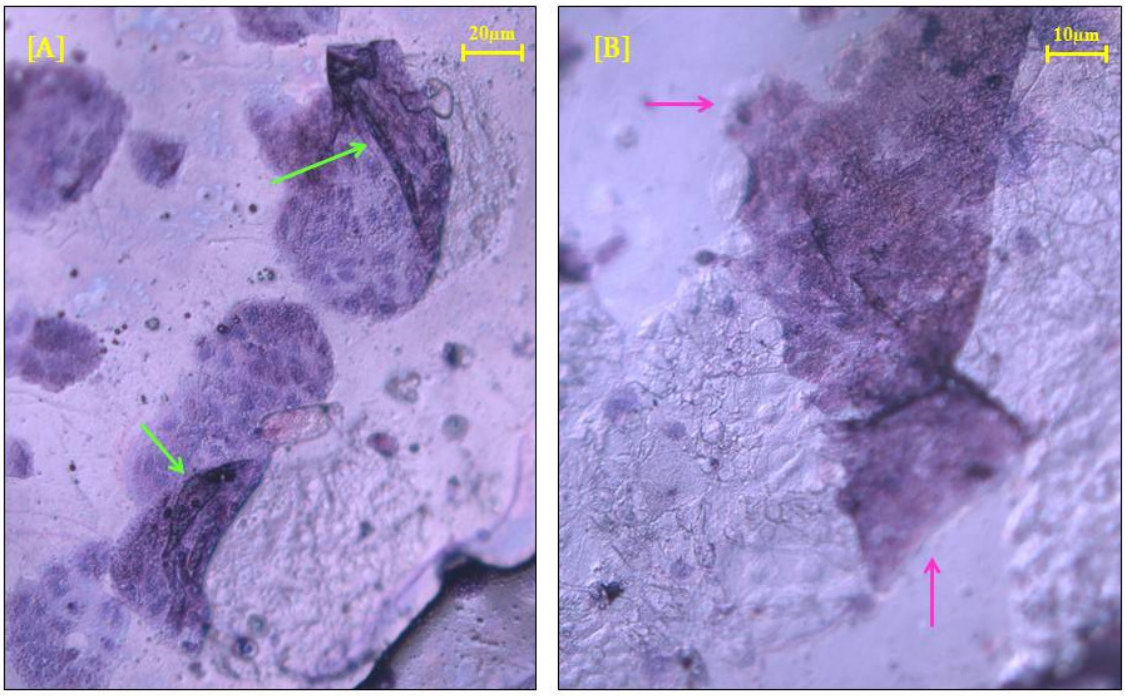

Figure 4.7 - Stained Ishikawa cells grown on bioimprinted substrates showing peeling effects (green in [A]) and organization to the bioimprint features (magenta in [B]).

While the difficulty prior to dollop staining was determining which cell-shapes were living cells and which were imprint features, after dollop staining it was impossible to 'see through' the cells to determine whether they were growing on top of imprinted features or not [Figure 4.7].

In a follow up experiment, secondary cells were plated at lower densities and were allowed to grow for 48 hours before fixation and staining. Initial cell cultures of 1.0×10^5 cells were plated on glass and incubated for 24 hours, at which point cells were fixed in paraformaldehyde and bioimprinted. For this experimental set the additional detergent wash and trypsin soak were added to further remove and/or denature any cell material remaining on the bioimprinted substrate surface. Secondary cells were plated at a density of 5.0×10^4 cells/chamber and incubated for 48 hours before removal. After incubation, secondary cells were fixed and stained for 5-10 minutes in CBB R-250 using the protocol detailed in chapter 2. After thorough washing to remove any remaining stain solution, the substrates were dried before imaging.

Two different microscopy modes were used for imaging the CBB stained samples. Using differential interference contrast, the exposed bioimprinted regions were imaged in much greater detail but the stained cells appeared as a blue or purple mass with no intracellular detail

[Figure 4.8], the nuclear features of the bioimprint on the right and the apparent nuclear features of the cells on the left are the same approximate size and shape. In higher magnification images, the nucleus can be distinguished. It is difficult to definitively say, however, if the nuclear features observed in these images are that of the actual cells or a moulded replication of the bioimprint observed through the cell monolayer. In general, however, DIC imaging methods showed the stained cell monolayers as complete entities and could not recognise individual cell borders.

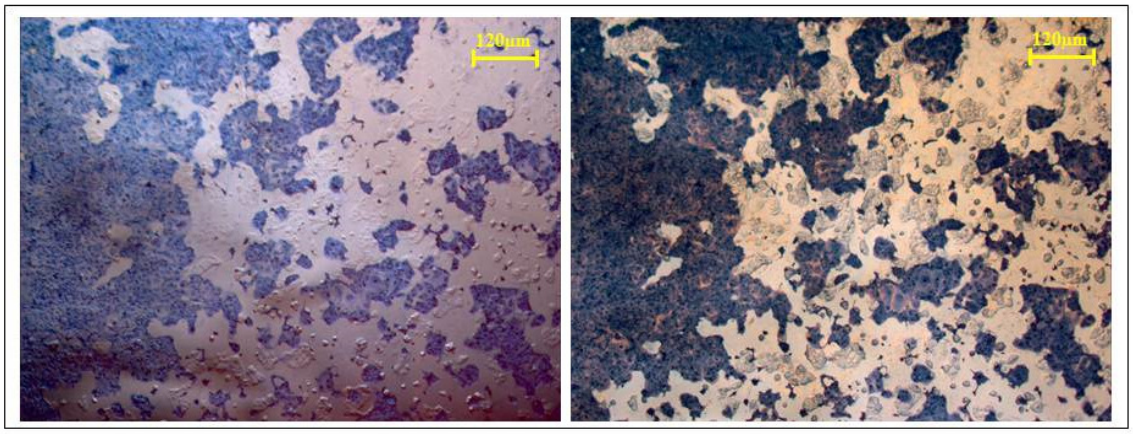

Figure 4.8 – Bright field (left) and differential interference contrast [DIC] (right) image captures of Coomassie brilliant blue stained Ishikawa cells grown on bioimprinted poly(MA). Bright field shows more detailed cell features, while DIC shadowing emphasises the bioimprint feature location.

Bright field imaging showed the cell features in more useful detail, but the bioimprinted regions were less distinguishable from the adjacent flat areas. The cell nuclei and nucleoli were identifiable in bright field images of cells stained with CBB. Similarly, a peri-nuclear mass which consistently stained darker than the cytoplasm surrounding it was observed [Figure 4.9]. Anatomical pathologist Dr. Gavin Harris [Canterbury Health Laboratories] suggested these were protein aggregates contained within the cell. As CBBR-250 is a general protein stain, this seems to be a valid hypothesis.

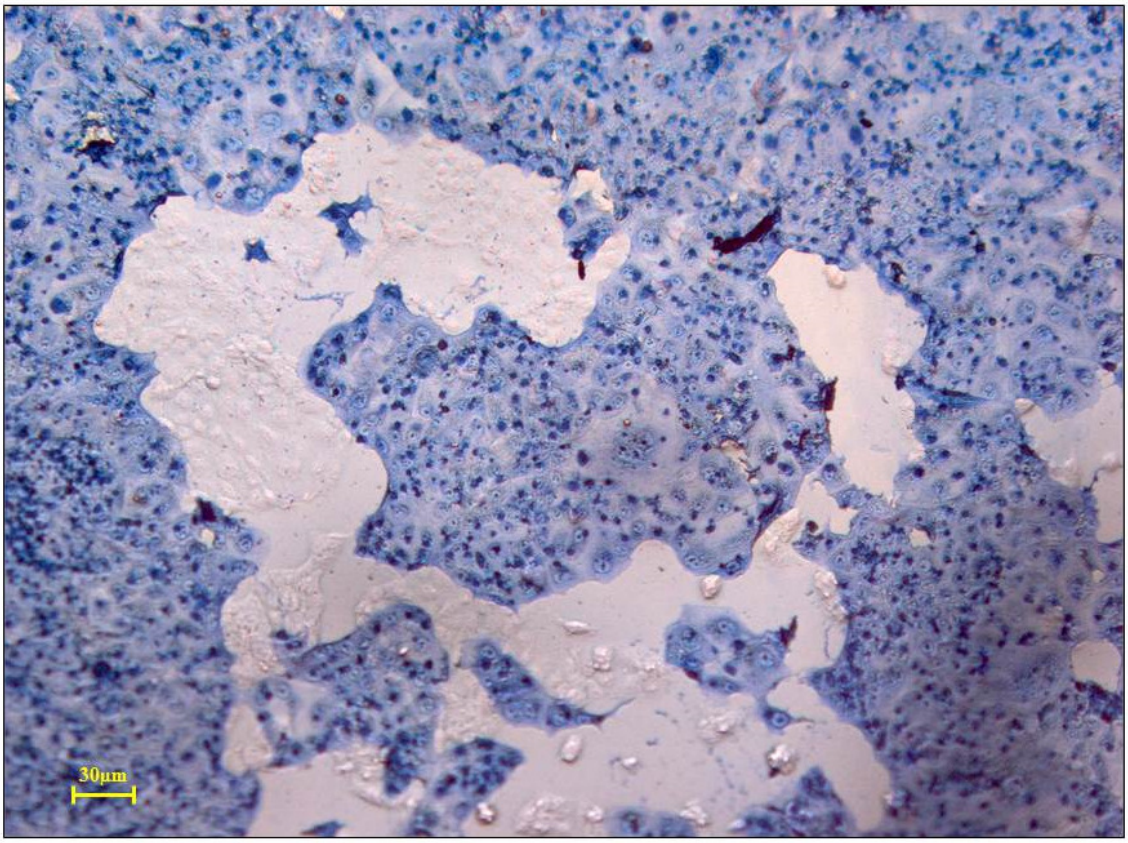

Figure 4.9 - Bright field micrograph of CBB stained Ishikawa cells grown on bioimprinted poly(MA). Bioimprinted cell features can be seen in the clear, white sections [shown at 200x magnification]. Note the dark peri-nuclear staining spots.

Individual cell membrane boundaries were difficult to determine on bright field image captures of CBB stained cells. Substrate areas covered by stained cytoplasm all appeared as light blue and precluded conclusions about relative cell size at low magnification. As seen in the top left and central regions of Figure 4.9 and indicated by green arrows in Figure 4.10, extreme cell size variation was visible off bioimprinted regions. Cells in excess of 40 µm were discernable and had a 'stretched' appearance of the membrane. The thinner membrane stained lighter than the smaller, 'rounded up' cells, in which the density of protein was higher.

Some bioimprint features were visible through thin, lighter blue cell membrane regions. These features, indicated by yellow arrows in Figure 4.10 below, and the cells grown on top show no active alignment interaction. On the other hand, some bioimprint features which were visible because of the lack of cells grown over them induced an alignment effect at the feature interface between the flat areas and the bioimprint features. Adhesion was observed on the flat poly(MA) regions [red arrows in Figure 4.10] as well as assumed bioimprinted regions [yellow arrows in

Figure 4.10]. These areas were prone to peeling and containing debris. However, there was a lower general adhesion to the un-templated poly(MA) substrate and cells were more likely to peel up than at bioimprinted sites.

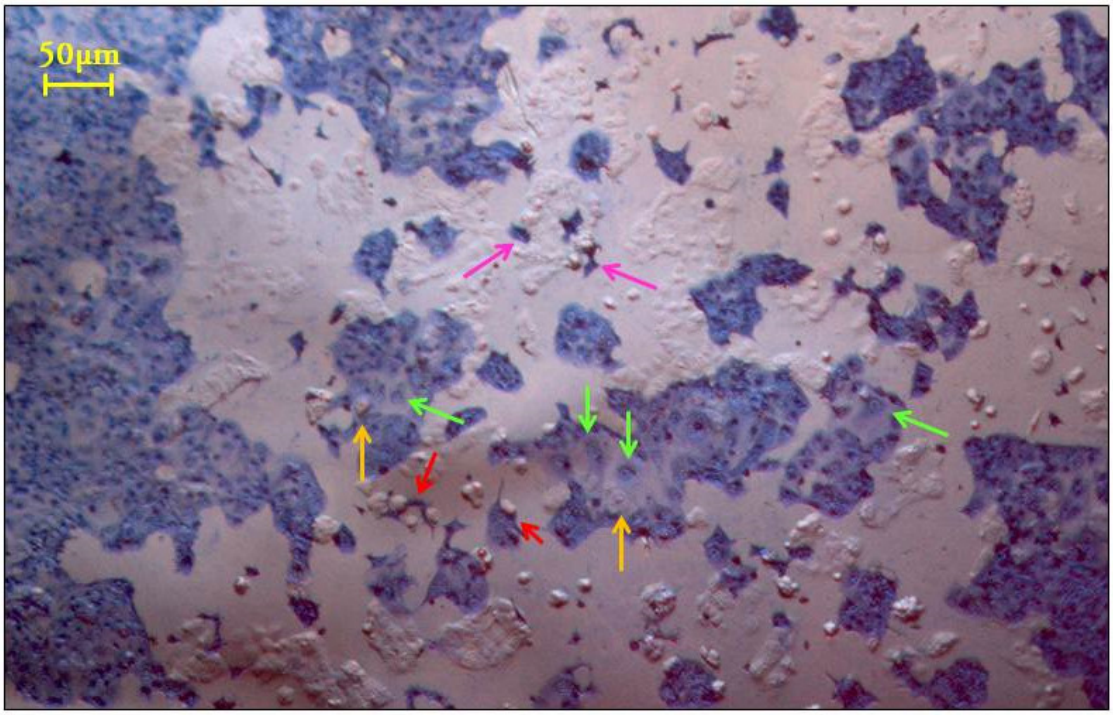

Figure 4.10 - Bright field micrograph of CBB-stained Ishikawa cells cultured on a bioimprinted substrate. This representative micrograph identifies several effects of the bioimprint on secondary cell culture, as identified by the coloured arrows.

This cell size variation was documented in previous experiments [Figure 4.11], even when bioimprint overgrowth was not an intentional variable. Cell spreading across the substrate consisted of areas of noticeably larger cell growth, as indicated by the green arrows in Figure 4.11. At lower magnifications, determining the exact substrate underlying these regions was impossible, but the organisation of cell clusters, and the obvious monolayer structure in the areas indicated, suggests these are flat rather than bioimprinted areas. There was no significant difference in secondary cell adhesion distribution across the whole culture area of the substrate, though the central area was most easily imaged and analysed. As in the previous experiments, cell debris was found scattered across the substrate, presumably due to the detachment during washing agitation and redistribution upon drying [magenta arrows in Figure 4.10].

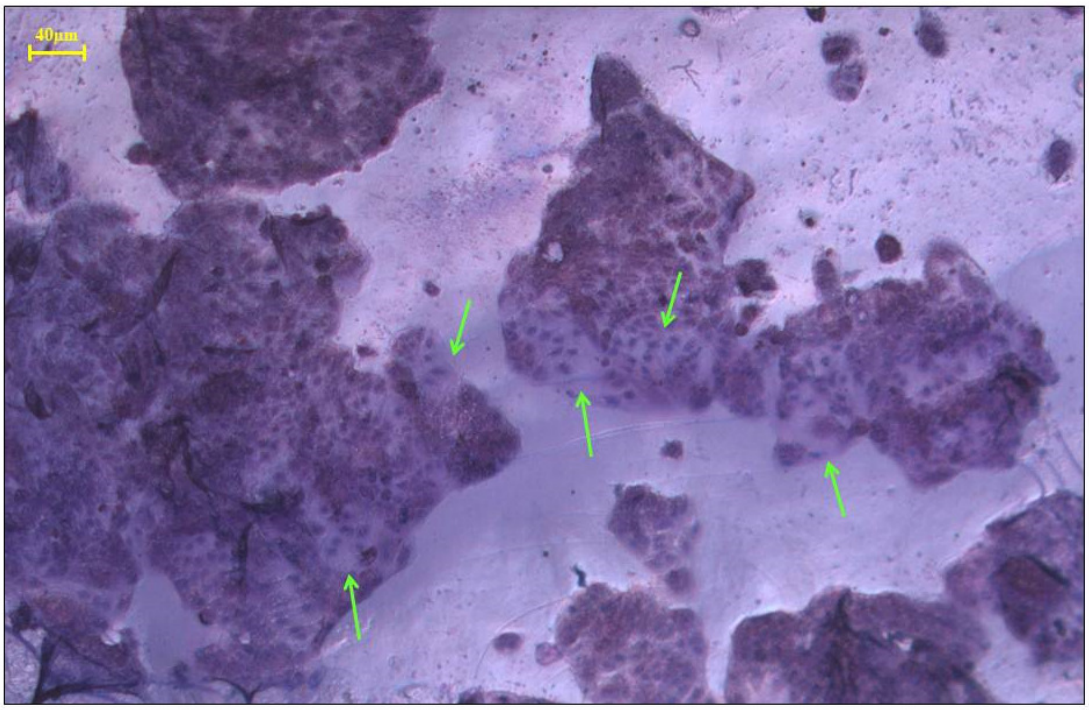

Figure 4.11 - DIC micrograph of stained Ishikawa cells grown over bioimprint features. Arrows indicate areas of oversized cell growth, up to 40-50 µm per cell.

Differential interference images showed cells spreading specifically across bioimprint substrate. This could only be investigated at the borders of cell growth due to the 'see through' problem, but clearly showed the cells producing and projecting lamellipodia across the imprinted regions [Figure 4.12].

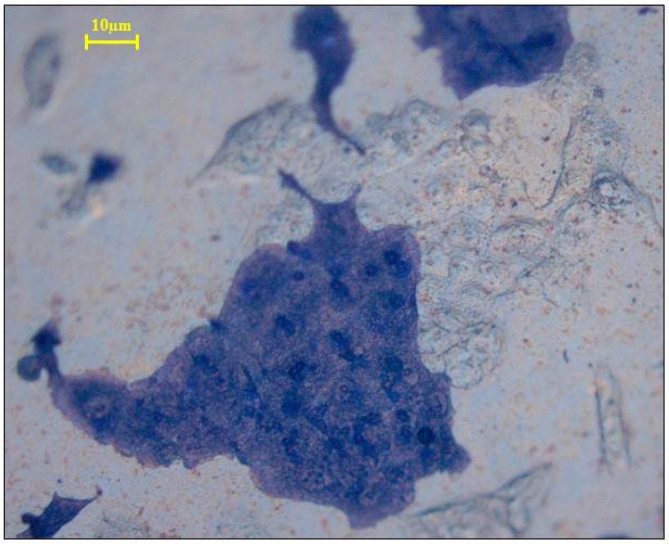

Figure 4.12 - DIC capture of CBB stained Ishikawa cells spreading across bioimprinted features.

Again the uncertainty of the bioimprint location beneath the superimposed cell culture prevented the absolute conclusion that the bioimprint and adjacent flat areas were the cause of this drastic morphology variation. Little evidence could be gleaned from repeat experiments without being able to identify bioimprinted regions both 'before and after' secondary cell culture and staining. Before any definitive conclusions could be made about the localised adhesive influence of bioimprinted topographies, a method for simultaneously identifying the bioimprint features and the secondary cells on the substrate surface was required.

4.2.2 'Biomaps'

Biomap images were compiled from individual images taken across the substrate surface [Figure 4.13]. Up to 90 images were taken across the entire bioimprinted face and digitally stitched together to produce a single image rendering the bioimprint face of the entire sample. In Figure 4.13, for example, 57 images of the substrate surface were taken and combined using Autopano Giga 2. The resulting collage combined the high resolution of the smaller individual images with the overall size and perspective of the entire substrate. Though acquiring the images was tedious and repetitive, the resulting biomap accurately documented the positions of bioimprinted features across the substrate.

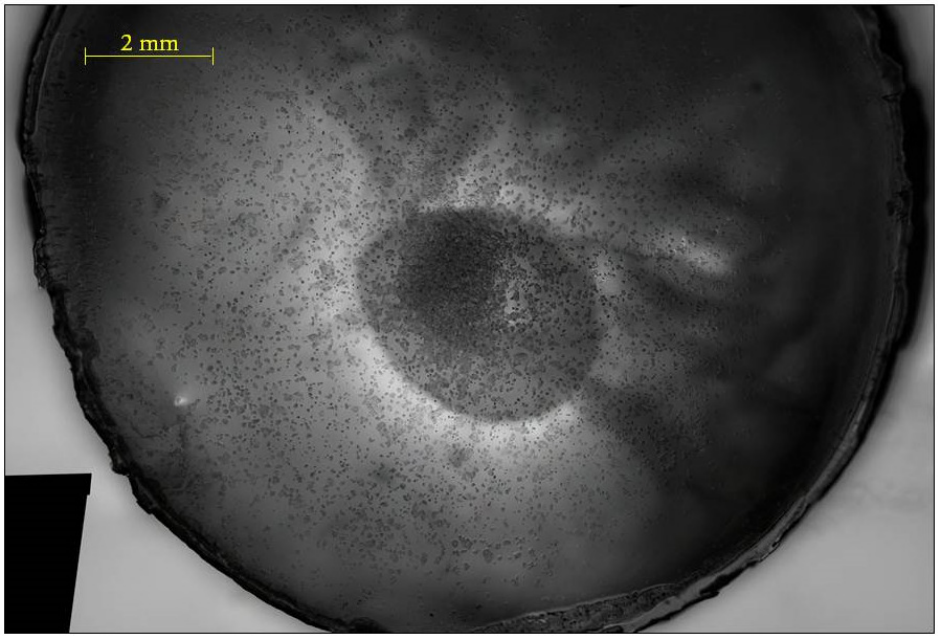

Figure 4.13 - Biomap of bioimprinted Ishikawas before secondary cell culture.

Optimal stitching of biomap images depended on acquired images containing overlapping area in the images taken both before and after cell plating. Rendering time for each biomap depended greatly on the number of images to be compiled, but was on the order of a few minutes per sample. Changes in focal plane across the substrate surface were documented in the rendering of the final biomap. When taking the individual images which were to be compiled for the map, either the focus was changed for each image to keep the entire biomap in focus or the focus remained the same for all images and only a portion of the substrate was in focus. Changing the focus provided images with higher resolution and thus more accurate information of the surface, but also complicated the stitching procedures. A feature appearing in focus in the first of several sequential images was not necessarily in focus after the focal distance was adjusted and the stage was moved for the next image. More images were required to keep the whole substrate in focus as opposed to a general, single plane mapping method.

After secondary cell cultures were grown, fixed, and stained, a complementary second biomap was taken of each sample for comparison [Figure 4.14]. The most useful secondary biomaps were taken with DIC imaging. Though detailed information about specific cell features was lost using this method instead of bright field, primary importance was placed on locating bioimprinted features for overlaying the images. Bioimprinted features were easily visualised with DIC capture. Isolating and overlaying two complementary individual images from biomaps compiled before and after the secondary cell culture was difficult due to several complications inherent in the size and nature of this imaging system.

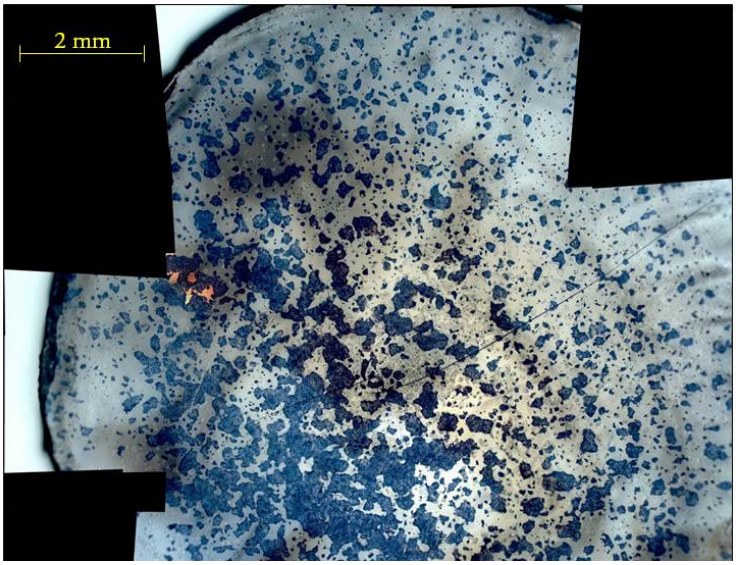

Figure 4.14 - CBB stained secondary Ishikawa cell culture on bioimprinted substrates.

When using circular bioimprint samples, rotational symmetry provided significant difficulties in alignment. Identifying unique bioimprint features present on both biomap images was necessary to ensure both rotational and translational alignment of features on before and after maps. Because the Ishikawas in the initial cell culture and resulting bioimprint were not constricted in their growth, meaning there was no imposed organization to their growth patterns, no two imprints ever contained the same bioimprint features in the same locations. Additionally, bioimprint topography varied as confluence varied from the centre toward the edges. Isolating a unique grouping of cells required tedious analysis of each individual image, keeping in mind the bioimprinted feature may be located in any of the 50-90 compilation images, may be rotated in any orientation around the centre, and may or may not be covered by stained secondary cells.

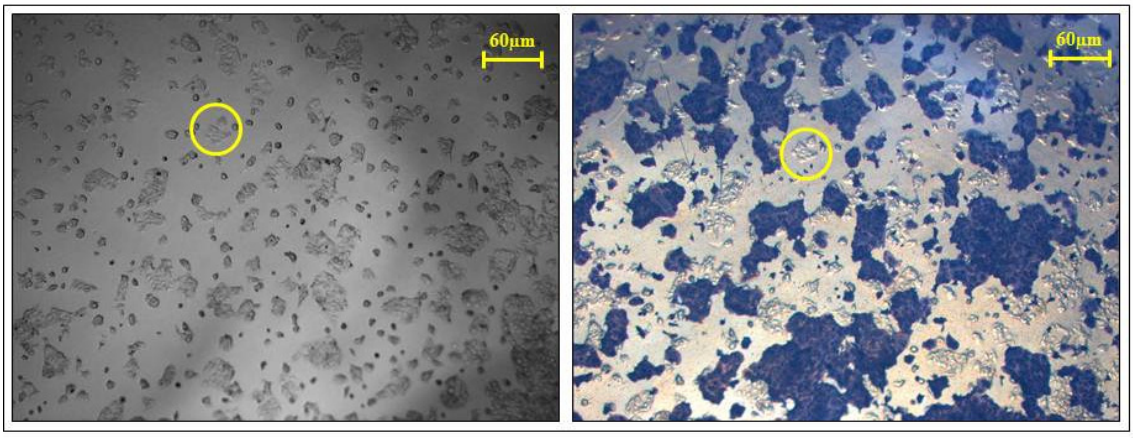

Figure 4.15 - DIC captures images isolated from biomap sets before (left) and after (right) secondary cell culture of Ishikawa cells. The yellow circle highlights a unique feature which was used to identify the corresponding images out of the sets.

When bioimprint topographies could be identified and the before and after images aligned, the biomap functioned as intended and highlighted the areas of cell growth relative to the bioimprint regions. As seen in Figure 4.15, circled in yellow, the same bioimprinted cell cluster was identified in corresponding before and after biomap sets. The two images were imported to Microsoft PowerPoint, the transparency was set to allow for visual overlap, and image rotation was applied by increasing degrees until the bioimprint features of the overlapping images were exactly aligned. The resulting overlay image was converted to a .jpg and exported for analysis.

Overlay images showed surprisingly little correlation between the bioimprinted areas and patches of cell adhesion away from the central regions [Figure 4.16]. While most stained cell clusters overlap some bioimprint features, there does not seem to be any exact alignment to the features as suggested by previous results. Cells appear to spread around the edges of bioimprinted features, almost as if using them as an anchor for extension. In highly confluent bioimprint regions, secondary cell confluence was high as well. Whether higher secondary cell confluence in central locations was due to the confluence of the underlying bioimprint features or was a natural result of the circular cell culture was unclear. Larger regions of cell growth, however, appear happy to adhere and spread across relatively large, flat substrate regions. High quantities of stained cell debris were documented across the cell surface supporting the cell peeling results also seen in previous results.

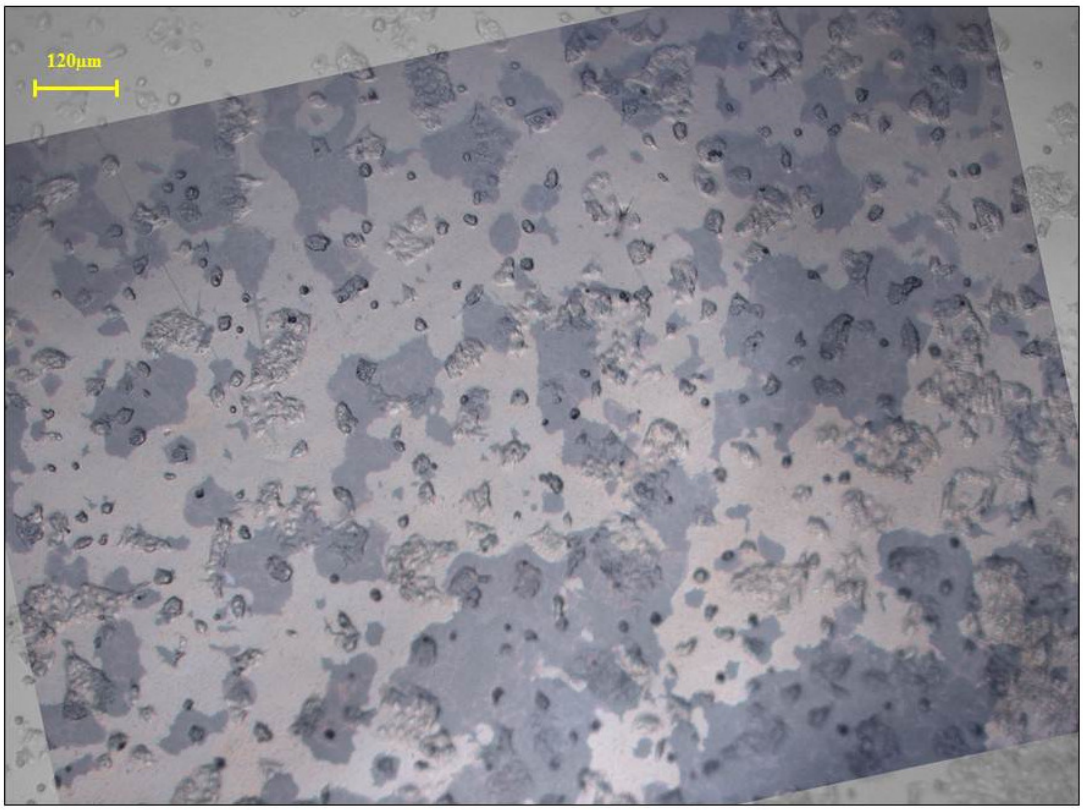

Figure 4.16 – Individual images isolated from pre- and post-secondary cell culture biomaps showing CBB stained Ishikawa cells grown on bioimprinted substrates. Note the rotation required to align the images.

Slightly offset from the centre, however, where the cells were at approximately 70% confluence, the cells showed no particular preference for the bioimprinted regions or the flat regions [Figure 4.16]. While in some areas the imprint seems to provide an anchoring point,

across the majority of the substrate cells seem to distribute as randomly during secondary culture as the initial culture. However, there was a notable amount of cell debris present indicative of cell peeling and dissociation. Whether the cells predominantly peel from bioimprinted regions was undetermined; however, the strong cell-to-cell interactions associated with the edges peeling back in previous experiments might suggest the bioimprinted areas are more prone to losing entire areas of cell growth whereas the surrounding regions may lose only single cells during the agitation of staining. Images of the cultured cells were taken after the staining and washing process so only well adhered cells remain in place. Imaging before washing would be ideal but has its own complications.

The biomap method did not actually solve the 'see through' problem directly, but managed to circumvent it by having a comparison available. If exact features could not be correlated on both the before and after biomap images, the images were only as valuable as the previously obtained bright field images, providing interesting inferences but offering little evidence toward a robust conclusion.

4.2.3 Fluorescein incorporation

Cured poly(MA) was analysed for naturally occurring background fluorescence of before any recipe alterations were considered. Inherent background fluorescence is not uncommon for polymers and was thus a reasonable possibility for cured poly(MA) samples. Two different ratios of poly(MA) were tested: one a translucent, high crosslinking mixture; and the other an equivalent monomer ratio which resulted in an opaque white sample face. Both samples were tested with three different fluorescence filters, each of which selectively filtered for specific 30-50nm regions of the visible spectrum. No reliable background fluorescence was detected for either poly(MA) sample for any of the three filters. The B-3A filter showed some promising illumination, but was too dim to be effective without extreme exposure times.

Due to the lack of inherent poly(MA) fluorescence, a fluorescent additive was required within the poly(MA) background. Fluorescein was chosen as the fluorescent additive because its powder form was soluble in the liquid polymer mixture and emits in the green spectrum when excited. Green fluorescence allowed for the counterstaining to remain constant; red and blue channels continued to capture actin and DNA emission as previously described in chapter 2.

Because fluorescein is water soluble, pre-experimental testing was done to determine the stability of the incorporated polymer chemistry and whether it would leach from the cured bulk into solution. Cured poly(MA) samples, containing serial dilutions of fluorescein concentration, were allowed to soak in water in 24-well plates for up to 7 days on the laboratory benchtop. Ongoing observation and evaluation showed no fluorescein leaching into the water, even in the polymers containing higher concentrations. Benchtop storage was designed to expose the samples to potential photobleaching, though no significant bleaching was noted over the 7 day trial.

Optimizing the fluorescein concentration was done by creating a stock solution and then adding known volumes to different polymer ratio mixtures. For testing, the stock solution consisted of 2.2 mg fluorescein mixed into 1 mL of methacrylate pre-polymer [always 600 µL EGDMA: 300 µL MAA: 100 µL IRGAcure for stock solution]. An initial estimate suggested 50 µg/mL would be a good working concentration. Therefore, for the initial experimental dilutions, 10 µL and 20 µL of the stock solution were diluted into the same 6:3:1 polymer ratio, giving fluorescein concentration at 22 µg/mL and 44 µg/mL respectively. In the equivalent ratio polymer, 6:6:1, the 10 µL and 20 µL accounted for 17 µg/mL and 34 µg/mL respectively.

After curing, the samples were transferred to the BAT Lab for fluorescent microscopy. Not surprisingly, the dilutions with twice as much fluorescein added were brighter than the others, though the difference was less noticeable for the significantly brighter 6:6:1 opaque poly(MA) samples. The B-3A filter showed much brighter results for all concentrations, but often overpowered the camera, even at low exposure times. Therefore, a fluorescein concentration of 30-50µg/mL was selected for use with the FITC filter for fluorescent bioimprint imaging.

Bioimprint samples were analysed for the resolution of the fluorescent feature imaging. Initial imaging attempts using the Nikon 80i upright fluorescent microscope in the BAT lab were not able to identify any surface features beyond the bulk fluorescence of the poly(MA). The bioimprint features were quite clearly present in bright field and DIC imaging, but unable to be resolved on the transition to fluorescence microscopy.

The same samples were successfully imaged using the Zeiss epifluorescent microscope at the University Of Otago School Of Medicine at Christchurch Hospital. Differential interference imaging was used to find and focus on the bioimprint features before switching to fluorescent filters. Using the FITC filter, the bioimprint features were visible through the fluorescent

background [Figure 4.17]. Exposure time was found to be very important for the FITC fluorescence because of the tendency for the fluorescence to overwhelm the capture and drown out the substrate features. The image planes were slightly offset between the DIC and FITC images as a consequence of the automated filter switching. Imaging was limited to 20x and 40x objectives because the concavity of the poly(MA) prevented immersion imaging.

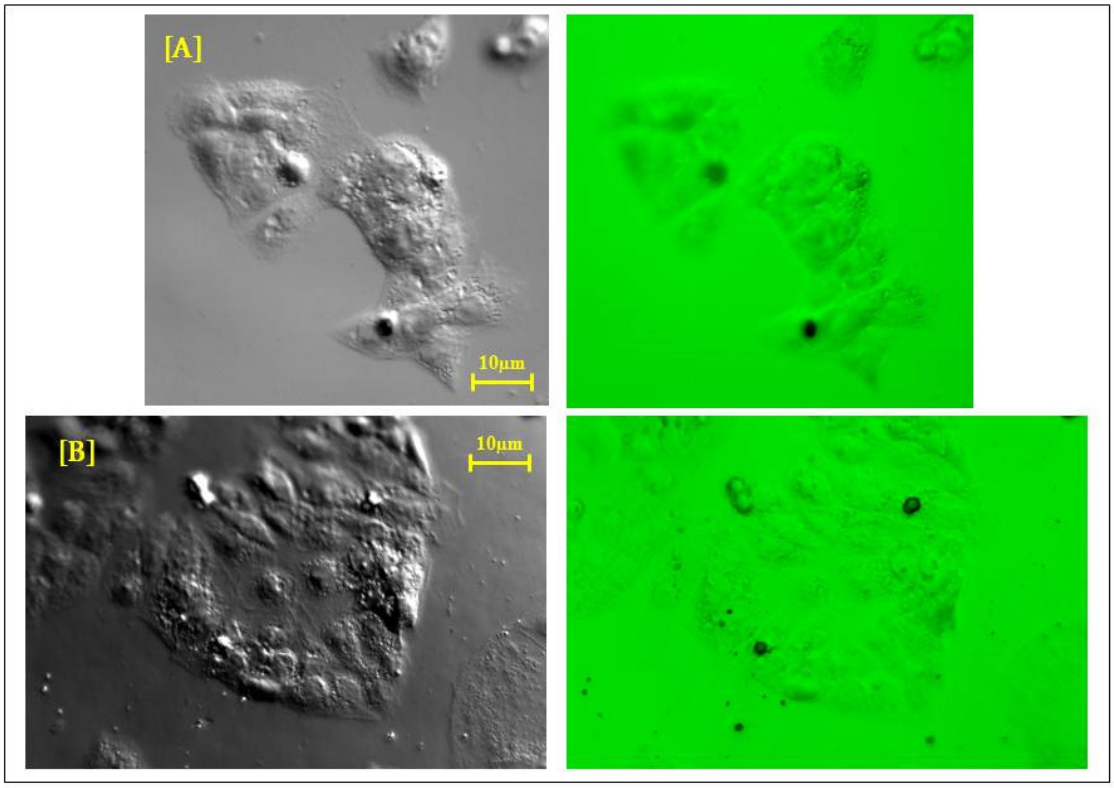

Figure 4.17 - Two examples, [A] and [B], of bioimprint features viewed with DIC and FITC fluorescence. The slight focal plane offset was caused by the slight differences in working distance between the DIC and fluorescent microscope settings.

When the same images were imaged using the Leica TCS SP5 confocal microscope at the University of Canterbury School of Biological Sciences, the same features were not visible. The bioimprint features could be identified with bright field, but the bioimprint concavity prevented a single, uniform focal plane across the surface. For confocal microscopy, this meant that only a narrow band of the substrate was in focus, and therefore at the desired exposure. The situation made bioimprint features nearly impossible to view with laser scanning fluorescence.

For analysis regarding the adhesion location of Ishikawa cells on bioimprinted substrates, the cells themselves required fluorescent counter-staining. The cell nucleus was stained with Hoechst 33342, which stains DNA. UV-excited Hoechst was isolated using the DAPI-range fluorescence filter. Cells were stained in accordance with the methods detailed in chapter 2 using in a 1:100 dilution of Hoechst stock solution [in PBS] for 20 minutes at room temperature. To identify directionality of motility and relative intensity of adhesion, a phalloidin-conjugated Atto 594 rhodamine dye was used to label the actin filaments throughout the cell. As detailed in chapter 2, the stock solution consists of the supplied 20 nM powder which was dissolved in 1 mL of methanol. The working solution was a 1:30 dilution of the stock solution in PBS. Rigorous washing minimised background staining.

Results and analysis of cell cultures grown on fluorescent bioimprinted substrates showed more significant aligning effects than seen on overlapping biomap images. Bioimprint features could be accurately documented using the fluorescein emission on the FITC channel. Counterstaining for F-actin and DNA highlighted the cell location on top of the bioimprinted features. Figure 4.18 provides an example of the four channel output of the Zeiss epifluorescent microscope: three separate filter channels and an overlay image.

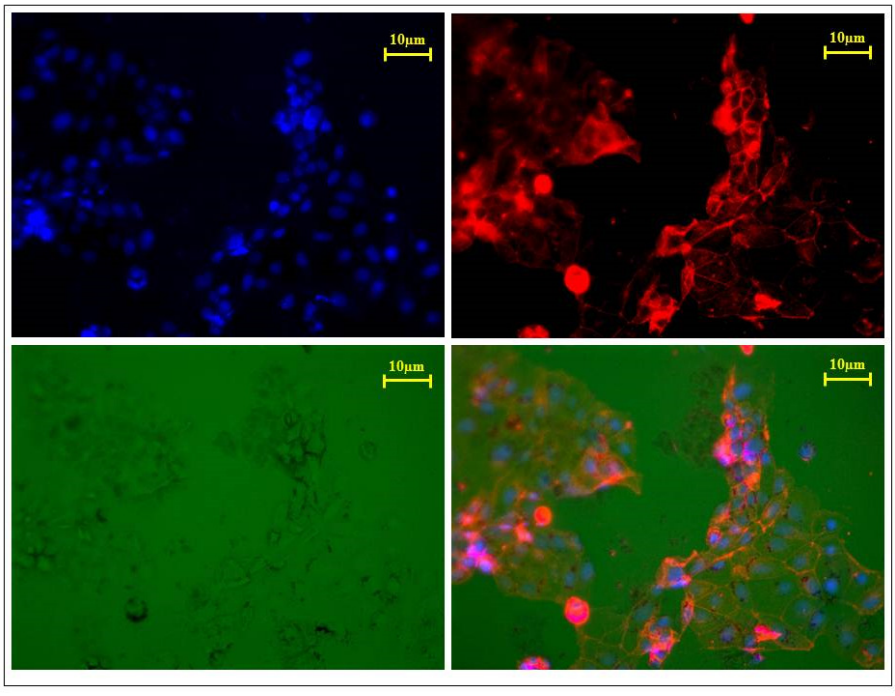

Figure 4.18 - Split channels and overlay of counterstained Ishikawa cells grown on bioimprinted substrates. Top images show Hoechst (blue) and Atto 594 phalloidin (red) counterstaining. Bottom images show the topography features of the bioimprint with fluorescein (green) and the overlay image of the three channels combined.

As seen on the FITC channel in Figure 4.18, the bioimprinted topography was outlined by the fluorescein incorporation to make it visible even underneath areas where counterstained cells had grown on top. Counterstained cells grown on the cell-shaped bioimprint features seen on the FITC channel appear to align perfectly to the bioimprint. The actin cytoskeleton appears to track exactly with the outer borders of cell features on the bioimprint. The location of nuclear features were less predictable, but also appeared closely associated with the template bioimprint. While some areas of the bioimprint appeared clearly without locally confluent cells adhered, all secondary counterstained cells appeared co-located with the bioimprint features. Few instances of cells grown on the available flat poly(MA) regions were documented.

The epifluorescent microscope operates in bulk fluorescence mode unless specifically switched to a separate mode for confocal-like scanning z-slices. This means that the fluorescence for the counterstaining images were summed over the vertical focal planes and appeared slightly out of focus when the working focus was set at the bioimprint topography. Though the nuclear locations and cell membrane boundaries are visible, significant information about the exact location of adhesion contact points was unattainable using only this method.

4.2.4 Elastomeric stencils

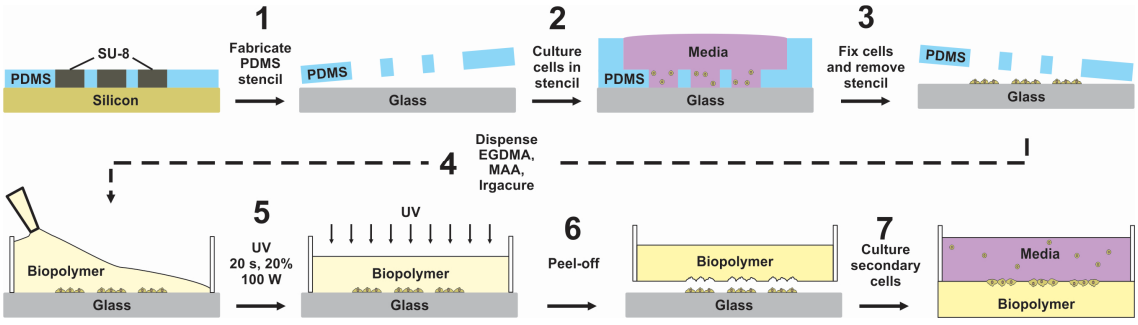

Figure 4.19 - Schematic outline of the PDMS fabrication and cell culture protocols. Photolithography and exclusion moulding [1] are used to produce stencils which are then used in initial cell culture [2]. The stencilled Ishikawa cells are fixed and imprinted [3-6]. The resulting bioimprint, containing cell features only in the stencilled locations, are sterilised and used for secondary culture [7]. Image by Dr. Volker Nock.

Stencils were successfully fabricated from PDMS using the exclusion moulding method previously outlined in section 4.1.5. SU-8 master moulds were fabricated to 100 µm thickness, therefore limiting the height of the exclusion moulded stencils to 100 µm as well. The PDMS sheet required extremely careful removal due to the thinness of the fragile moulded layer.

Adhesion stress at the PDMS-photoresist interface was the most likely place to experience tearing of the stencil pattern. In spite of careful removal, the most common defect of the moulded PDMS was incomplete exclusion. This occurred when the photoresist patterns on the master mould did not displace all of the liquid PDMS, which led to a thin layer of cured PDMS. The PDMS membrane, which covered the intended stencil region, prevented cell culture medium and initial cell cultures from contacting the underlying glass substrate. In fortunate cases this layer could be easily removed with a carefully applied scalpel. In cases of extensive inclusion the stencils were not viable for cell patterning.

Stencils were cut from the larger, wafer-sized PDMS sheet into 11 mm circles, concentric around the stencil features. The smaller 11 mm PDMS outlines were placed concentrically within the larger 14 mm PDMS chambers and conformally sealed to the underlying glass substrate. Assemblies were then sterilised either by autoclave or with UV irradiation. First trials used 70% ethanol for sterilisation, but high cell death in culture suggested ethanol or remnants thereof persisted. Autoclave sterilisation was practical, but increased rigidity and permanent adhesion of the PDMS chambers to glass substrates was noted and, therefore, UV sterilisation was utilised more frequently. When completely cured, PDMS stencils showed no cytotoxic effects on Ishikawa cell growth [60].

One concern regarding stencil patterning was the effect stencil removal would have on the cells located at the glass/stencil interface. Cells growing toward the edge of the available glass substrate could continue to grow and adhere to the side-walls of the PDMS stencils, and upon stencil removal, these cells would experience massive forces at the side wall adhesion sites. Previous studies coated the PDMS stencils with low percentage bovine serum albumin solution, a non-specific blocking agent, to prevent adherence to the PDMS stencils and minimise resulting cell membrane damage [81]. For this work, membrane damage for the initial cell culture was not critical as the initial cell culture was sacrificed at the bioimprinting stage anyway.

Ishikawa cells grew to confluence more slowly when grown within PDMS stencils, but were maintained until confluence rather than a pre-determined time point [Figure 4.20]. Confluent cell monolayers within the exposed substrate regions of the stencil were necessary to define the complete area as bioimprinted. At less than confluence, analysis of secondary cell growth analysis produced the same difficulties as encountered before, negating any beneficial effects of pre-patterning cell growth within defined stencil areas. At confluence, the PDMS stencils

were carefully removed and the Ishikawa cells were fixed. After washing, bioimprints were taken. The resulting bioimprint substrate contained geometrically-defined areas of bioimprint features immediately adjacent to flat, un-patterned topography [Figure 4.20]. As long as secondary cell cultures were less than confluent the bioimprint/stencil pattern was visible and could be used for localised adhesion analysis.

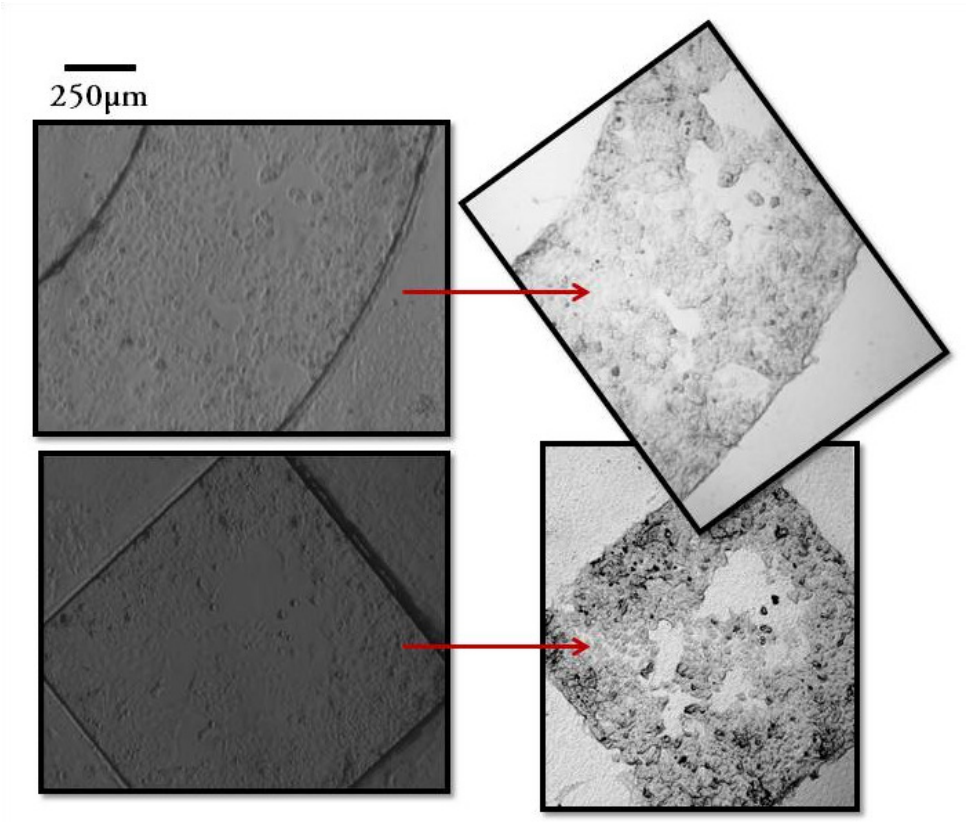

Figure 4.20 - Microscope images documenting the transfer resolution of Ishikawa feature in culture (left) into stencilled bioimprint substrates (right).

Bioimprinted substrates without stenciled cell culture organization allowed for random cell growth and clustering [Figure 4.21]. The importance of cell location relative to a central confluent region was eliminated by requiring the initial culture to grow to confluence within the stenciled regions. Stencils provided the same bioimprint features, but in easily located and well documented regions [Figure 4.22]. Stenciling the bioimprint features simultaneously increased the relative reproducibility of the substrate surface. Constraining the bioimprint features to a designated region allowed for mapping of the substrate; and even if the exact features were not consistent from one substrate to the next, the areas containing the cell imprints were the same.

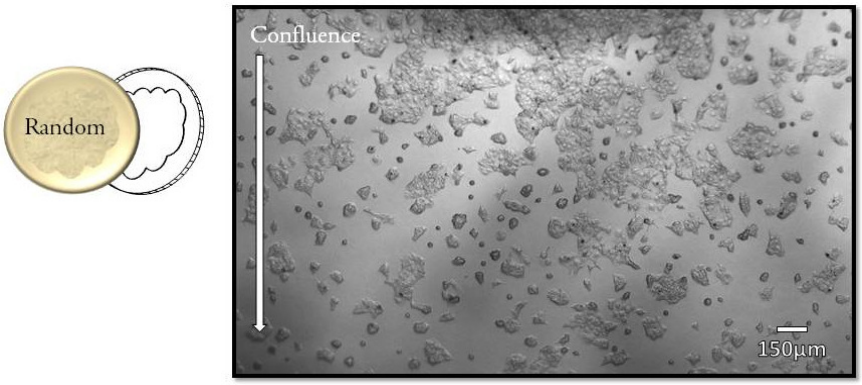

Figure 4.21 - Bioimprinted Ishikawa features without conditioned initial growth. The decreasing confluence across the substrate is evident from top to bottom of the micrograph capture.

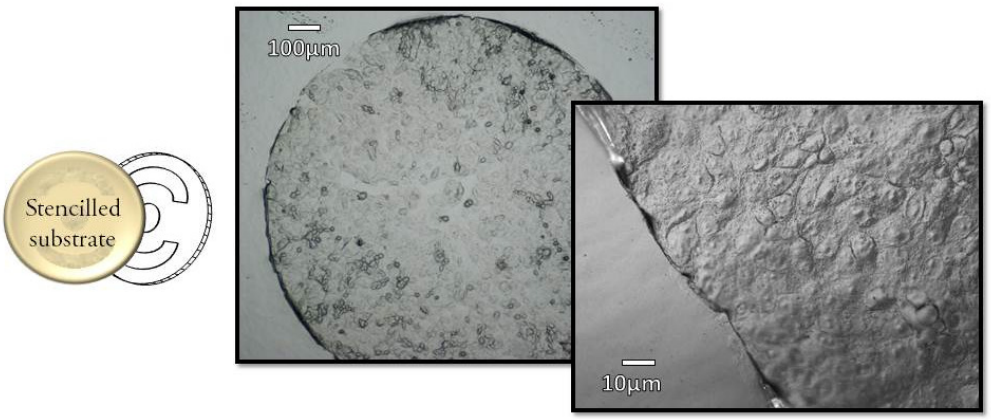

Figure 4.22 - Stencilled Ishikawa bioimprints showing designated regions of bioimprint features. Higher magnification shows the high resolution obtained by bioimprinting. [The circular feature of the stencil pattern on the schematic sample on the left is shown in the images on the right.]

Secondary cells cultured on stenciled bioimprinted substrates did not show any increase in adhesion, but did show distinctly different adhesive cell morphology on and off adjacent patterned and un-patterned regions [Figure 4.23]. Cells grown on the bioimprint grew closer to each other, generally smaller, and to higher confluence than cells grown on flat poly(MA) regions. Fluorescent staining highlighted the cell membrane boundaries of the cells adhered to the stenciled bioimprint substrates. Confocal imaging provided the best results using the bright field as the background channel instead of the fluorescein background; however, using the confocal only allowed for a single focal plane without including stacks and image summation so the cell features are not as well-defined as on control images with black backgrounds.

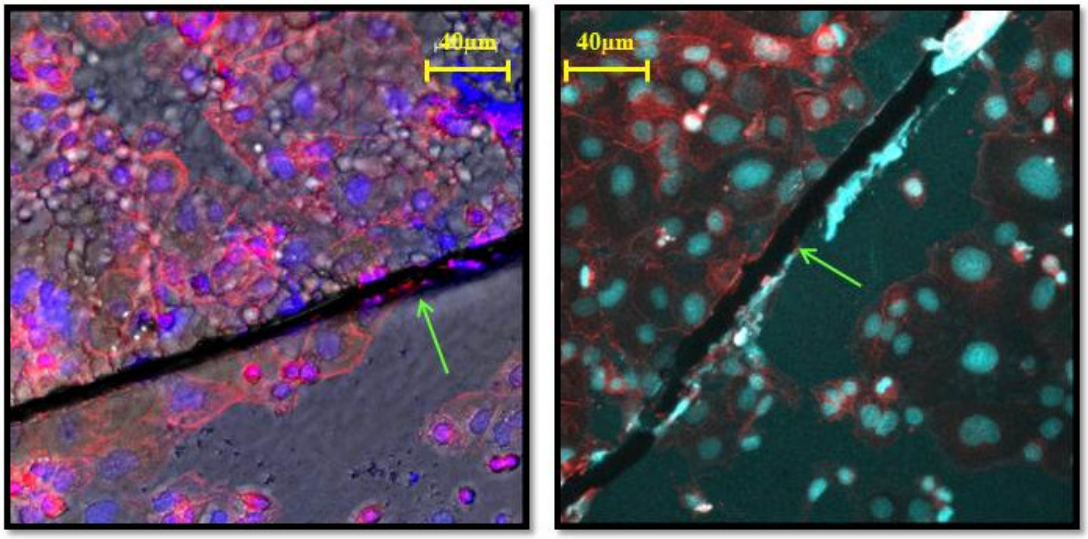

Figure 4.23 - Confocal captures of counterstained Ishikawa cells growing on stencilled bioimprint substrates. Green arrows indicate the border between the flat and bioimprinted areas, with the bioimprinted area on the upper half.

As seen in the example figures shown in Figure 4.23, the higher number of blue nuclear features in the image on the left indicates increased cell numbers in the bioimprinted region. Cell size was taken to be a function of the distance between nuclei. Notably, only one cell within the bioimprinted region grew to more than 40 µm. Based on the density and location of nuclear features in the image on the right, cell size was more consistent on the bioimprinted regions than on the flat areas. Cells grown on the flat regions show wide size variation: small cells clumped together in clusters [near the interface between bioimprint and flat] and others were large cells, over 40 µm.

4.3 Discussion

4.3.1 Cell culture on bioimprints

'Preferential adhesion' was defined in this work as an active, intentional cell adhesion which directs anchorage-based cells to interact with higher affinity to specific substrate regions of varying chemistry or topography. Although cells growing on bioimprinted substrates showed indications of preferential localised adhesion to both the bioimprinted areas and the interface with the relative flat poly(MA) regions, the balance of the evidence supports the hypothesis that cells will initially adhere to bioimprinted regions and spread from there. This conclusion incorporates the results showing cells adhered to the flat regions, but tangentially contacting bioimprint interface features, as seen in the 'overgrowth' experiments. Experimental results where fewer cells seeded on the imprint than were used to create the imprint substrate showed distinct clustering of adhered cells strictly limited to bioimprinted regions. Images showing high density staining on refracted bioimprint patterns indicated a preferential relationship.

The less adhesive, three dimensional growths documented in eosin-stained micrographs more closely represent *in vivo* cancerous tumours. Traditional monolayer subculture growth has been used extensively in cancer research to model tissue behaviour. More and more this traditional two dimensional model is being replaced by more biologically accurate three dimensional spheroid and microtumour models [87]. One method for spheroid formation specifically relies on the anti-fouling, non-adherent properties of poly-hydroxyethylmethacrylate [pHEMA] [2, 88]; and though not too much emphasis should be placed on the relative similarities of the methacrylate chemistries between pHEMA and the cured poly(MA), it does suggest why the cells may not be as adhesive as on control TCPS and glass substrates.

Cells appeared to adhere almost in two phases. Initial cell adhesion was primarily isolated to bioimprinted features, while cells adhering later were more likely to search out already adhered cells instead of adhering to the polymer substrate at all, as shown in Figure 4.4 Figure 4.5. Though the poly(MA) substrate did not appear to be a favourable substrate for the cells, it appeared cells adhere to bioimprinted areas containing topographical features which they can 'grab on to'. As these cells on the surface begin to spread and grow, other cells from suspension

interact with the adhered cell instead of adhering independently. This was seen most extremely in the first cell experiments, which did not contain denaturing detergent washes. The lack of detergent wash and trypsin soak is significant in that any biological debris remaining from the bioimprinting protocol was likely to still be present [though sterilised] at the time of secondary cell plating.

As the cells attach laterally to the adhered cells and the adhered cells grow and proliferate, a monolayer is formed. The general adhesion strength of this monolayer, however, is lower than that of more 'friendly' substrates. Therefore, when the agitating motion of the washes was applied, the intercellular forces are stronger than the cell-substrate adhesion forces, and so the cells pull away from the substrate but do not dissociate from each other. Unintentionally, the cell sheets revealed the bioimprint borders highly associated with the corresponding peeled region. These images furthered the hypothesis that the cells were adhering specifically to the bioimprinted areas and expanding from there until they reached the border region, at which point they would either grow 'up' above the monolayer to a three dimensional culture or would become quiescent and the culture would grow in another direction.

A consistent effect documented in cell cultures grown on bioimprinted poly(MA) substrates was the peeling up of cells during staining protocols. Staining was necessary to visualise the cell locations across the substrate. However, the wash steps required to minimise background staining, which was found to be particularly high for the methacrylate polymer, caused a repetitive shear stress on the cells. The repetitive application of stress across the locally confluent cell cultures caused peeling up of the monolayer, as shown in Figure 4.6 and Figure 4.7. The peeling monolayers often detached from local interfaces of bioimprinted topographies and flat regions. Fortuitously, the peeling confluent layers revealed an alignment to the bioimprinted features which would have otherwise been difficult to verify using only bright field microscopy.

In both the initial and secondary Ishikawa cultures, cells showed a significantly higher confluence in the central regions of any confining geometry. As a result, it was impossible to determine if the higher density of secondary cells adhering in the central regions were related to the higher concentration of bioimprint features or if this was as naturally occurring as the same phenomenon in the initial cell culture. Therefore, for the experiments where the initial cell culture was allowed to adhere and spread at random, the central region was excluded from analysis.

To validate the relationship between preferential cell adhesion and bioimprinted features further experiments were done with secondary cells cultured in 6-well polystyrene culture plates instead of wells of PDMS, which has been reported to be mildly cytotoxic [89] [although no cytotoxicity was observed using the exclusion moulded stencils in the current cell culture studies]. No difference was seen in the health of the cells though accurate growth and proliferation rates were not determined. PDMS was later found to have an effect on cell morphology, but this finding will be discussed in greater detail in chapters 7 and 8.

Bright field images of the overgrowth experiment showed a variation in cell size in cells which were likely to be growing off the imprint features [Figure 4.10]. Morphology changes for Ishikawa cancer cells grown across the bioimprint are difficult to define due to the variation and robustness inherent in cancer cells. And while the overall effect was difficult to quantify, several notable observations could be made. Anatomical pathologist Dr. Gavin Harris of Canterbury Health Laboratories analysed images and described the overall morphology as 'less cancerous' than control Ishikawa cultures. Identifying the relative 'cancerousness' of adjacent cells in culture is well beyond the scope of this work, but the observation validates the investigation of the cell-substrate interaction and its involvement in the development and proliferation of cancers. Due to the uncontrolled nature of cancerous growth, it is not impossible to see morphology variations even in control cell cultures, but the frequency and consistency of extreme cell size increases at overgrown regions suggests a notable correlation.

Thus, it may be suggested that cells growing on bioimprint topographies would grow within a smaller morphology than cells proliferating across the adjacent flat regions. The signals provided by the underlying topography relating to cell size are yet to be defined. Ishikawa cells grown in control cultures on TCPS and on flat methacrylate polymer substrates rarely grew to the sizes seen in these experiments, suggesting the bioimprint topography was affecting the cell size.

4.3.2 'Biomaps'

The greatest advantage of the biomap was the highly detailed nature of the information regarding the bioimprint and related cell growth provided by full size microscope images being stitched together. Individual images containing bioimprint feature locations were taken before and after secondary cell culture and could be aligned and overlaid to show the exact location of the cell culture monolayers in relation to the bioimprinted cell features. The results from this method highlighted the amount of information that was being hidden under confluent cell culture layers. In contradiction to control cell cultures and previous experimental results, Ishikawas spread across the entirety of the substrate. While the graded confluence does not affect the quality of experimental results, the even distribution of cell adhesion across bioimprinted substrates, which contain imprint features of graded confluence of initial cell culture chambers, implied that bioimprint features were not absolutely a requirement for cell adhesion and spreading. Bioimprint features might however have indirect effects, such as by cell-to-cell communications, which extend beyond the physical boundaries of the imprinted topology. These results and speculations hint at still unidentified complexities in ways the microenvironment controls cell function.

Several impracticalities inhibited the usefulness of the biomap. Predominantly, taking and stitching together 50 to 90 images per sample required minute, accurate stage movements and large amounts of time. Notably, the cells would not persist outside of cell culture for this amount of time to take the pictures without consequence, so live culture comparisons were never obtained by this method. Keeping the images in focus across the entire substrate proved difficult and led to errors in stitching. With so many image manipulations required to obtain successfully overlaid comparisons, biomapping every substrate surface proved an impractical task.

4.3.3 Fluorescein incorporation

Instead of mapping the substrate surface after the bioimprint was already fabricated, as required by biomapping methods, fluorescein incorporation into the cured poly(MA) was implemented in order to identify the bioimprint features on the polymer surface using a separate fluorescence filter block. Including a fluorescent ingredient into the poly(MA) itself provided an alternative

method for identifying the substrate topography in spite of staining of the secondary cells. Background fluorescence of the poly(MA) substrate was intended to highlight bioimprinted features upon excitation and allow for differentiation between bioimprinted cell topographies and secondary cell features. Combining the three fluorescent channels, green, blue, and red, with the bright field gave a detailed picture of exactly where cells were adhering.

Low inherent background fluorescence was insufficient to provide a useful image, and hence an additive was required to obtain the desired background levels. The easiest addition step was to include a fluorescent marker within the liquid polymer mixture to provide fluorescent information about the bioimprinted regions. Fluorescein was chosen because it was readily available within the lab, emissions were detected on a filter different from those already used in counterstaining protocols, and it required no additional chemical synthesis for incorporation within the poly(MA) mixture. Fluorescein was included in the liquid polymer mixture. As with the previous iterations of poly(MA), the mixing and curing phases were carried out in a light-filtered, clean room to prevent photobleaching of the fluorescein.

The effectiveness of the fluorescein emission in highlighting bioimprint features varied greatly depending on which microscope type was used for excitation and detection. Optimal results were obtained using the Zeiss epifluorescent microscope located at the University of Otago - School of Medicine at Christchurch Hospital. Therefore, stained secondary cell culture samples were imaged with the same microscope.

Exposure time was determined to be a critical variable in the efficiency of the fluorescence method. Over exposure of the fluorescein resulted in an overwhelming green channel capture which overrode any contribution from the red and blue channels in the capture overlay. Under exposure led to dark green images which did not provide enough contrast to distinguish bioimprinted cell topographies.

Inclusion of the fluorescein fluorophore within the liquid polymer and resulting bioimprint provided, perhaps, the most convincing evidence in support of the hypothesis that Ishikawa cells selectively adhered to bioimprinted features. Bioimprint cell features were easily identifiable on the FITC channel, while the corresponding counterstain channels showed the arrangement of secondary cell features around the region in question. The exact alignment of the secondary Ishikawa features to the underlying bioimprint topography contributes to the

balance of evidence gathered by the previous results supporting a preferential adhesion to bioimprinted topographies.

4.3.4 Elastomeric stencils

Stencils were used to restrict areas of Ishikawa initial culture prior to bioimprinting. While PDMS stencils have been documented previously in literature [84, 85], the stencilled cell cultures were always used as an endpoint and not as an intermediate for further substrate modification. When used as an intermediate step for bioimprint substrate fabrication, PDMS-defined areas that cell culture translated to specific areas of bioimprint within surrounding flat areas. Bioimprinted regions now exactly corresponded to a CAD-defined master pattern. The master design was used as a map of the bioimprinted regions and for comparison after secondary Ishikawa cultures. The thickness of the SU-8 layer was critical in the production of stencil inserts as it directly translated into the end thickness of the PDMS stencils. Thin stencils took up less available volume within the larger PDMS borders, but were also fragile and difficult to handle without tearing.

Though cells adhered to and grew on the top surface of the PDMS stencils, these cells were removed and discarded with the stencil prior to bioimprinting. Confluence was required within the open glass regions in order to fully define the bioimprinted areas. This conflicted with the time point analysis methods previously used to characterise bioimprint features. Previously, bioimprint substrates were defined by the time initial cells were in culture prior to removal for fixation and bioimprinting. When using stencils, the time to confluence varied for each culture based on the cell seeding density, random adhesion locations of cells, and speed of growth to confluence. Therefore maintaining specific time course deadlines, such as the 24 and 48 hour time points of non-stencilled initial cell cultures, was impractical before confluence.

Changing of cell seeding density was a controlled experimental; however, adhesion location was often negatively influenced by the natural hydrophobicity of PDMS. Chemical properties of the PDMS surface cause water-based liquids to bubble up and prevent full wetting of the substrate surface [90]. In the case of the stencil surfaces, the 1 mm holes were often too small to overcome this natural chemical response and the bulging media did not actually permeate below the upper PDMS bounds into contact with the underlying glass substrate. A short Corona plasma treatment was found to aid in wetting effects of the stencilled glass areas.

The only negative aspect of pre-patterning the bioimprint with stencil was the decreased throughput. Bioimprinted substrate fabrication was limited by the production of exclusion moulded stencil patterns, which decreased sample production for imaging and secondary cell culture. Additional pattern replication methods were investigated in order to eliminate the one to one cell culture to bioimprint requirement imposed by the technique, but complicated by the addition of stencil patterning.

Methacrylate-based polymers have been shown to have low cell adhesion [91, 92] and cytotoxic monomer chemistries [83]. Therefore, the observed cell adhesion and spreading of Ishikawa cancer cells on bioimprinted methacrylate substrates occurs in the presence of the intentionally anti-fouling characteristics of methacrylate polymers. Implications of the increased cell-substrate interaction between the cells and the bioimprinted methacrylate-based polymer, an expected non-adhesive substrate, suggest the preferential adhesion effects would translate to more adhesive substrates, but would not be as influential due to the naturally adhesive chemistry of control cell culture substrates. The bioimprint represents negative substrate topography, effectively simplified as pits in the substrate surface. The next two chapters investigate the fabrication of lithographically-defined, geometrically-simplified patterned substrates and secondary cell culture results in order to isolate the effects of general substrate topography from the effects specific to bioimprinted topography. Unavoidable outside influences, such as gravity and Brownian motion, will be accounted for by comparison. We look to address whether cells are intentionally drawn toward bioimprint features based on biomimetic features or are directed into the negative topographies by gravity.

5 Patterned substrate fabrication

In order to compare the effects of bioimprint features on cell distribution with patterned methacrylate polymer substrates, reliable and consistent methods for producing positive and negative patterned polymer substrates were necessary. The protocols and methods used to define and develop regular, geometric pattern features on the surface of methacrylate co-polymer substrates are discussed in this chapter. Additional methods were required for an additional inversion step which was necessary to produce a comparable substrate with inverted geometry.

Photolithography has been used extensively in literature for surface modification applications [5]. The traditional substrate produced by photolithographic patterning techniques is polymeric photoresist features adhered to silicon substrates. One popular method for transferring the photoresist patterns into other polymer substrates has been soft lithography [29], which replicates the lithographically-defined structures into PDMS moulds. From PDMS moulds, the pattern features can be replicated into a variety of polymeric substrates.

As detailed in the Introduction chapter of this thesis, cells have been shown to adhere and grow differently on substrates with different chemical and mechanical properties. While chemical substrate variation influences adhesion and spreading based on the exposed surface functional groups, mechanical substrate differences change the physical surface the cells are exposed to at plating. Properties such as substrate elasticity, surface roughness, and porosity are important considerations when designing biomaterials and analysing cell and tissue response. In addition to the physical and chemical properties of the material, altering the surface topography has been shown to influence cell adhesion. Including intentional, periodic geometric features on the substrate surface has been shown to alter cell behaviour for several different cell lines.

The organization effects of cells grown on bioimprint substrates may simply be effects of the gravity and the negative topography of the substrate. In other words, the localization effect discussed in the conclusion of chapter 4 could be interpreted as an effect of bioimprinted pits in the surface. What if the selective adhesion seen was simply a result of cells getting stuck in the micro-sized holes created by the bioimprint? To verify the observed localization effects of Ishikawa cell organization and growth on bioimprinted substrates is due to the topography of

the bioimprint, it is necessary to compare the observations with those correspondingly sized patterned substrates.

In order to compare Ishikawa cell growth for patterns and bioimprinted substrates, photolithography protocols were used to define a variety of pattern features across a range of sizes. Pattern size was initially quite large in accordance with the observations of Chen, et. al. which showed that cells prefer pattern arrangements on the same magnitude as the overall cell size [26]. Smaller patterns were added to investigate any potential 'gripping' effects of the cells, where the cells would grab onto the patterned regions and use them as anchors for continued spreading.

Several methods were then used to transfer the photolithography-defined patterns into substrate materials with different physical and chemical properties. Most commonly, PDMS-based soft lithography was used to transfer the master pattern from the silicon wafer into a flexible PDMS mould. Due to the undesirable aspects of the poly(MA) several other substrate materials were investigated. Throughout the replication process the polarity of the pattern (pillars vs. holes) changes several times. Therefore it was important to define each substrate and track the number of pattern inversions to accurately describe the positive or negative surface topography and describe the corresponding cell reactions.

5.1 Photo- and soft lithography

5.1.1 Photolithography

Photolithography has developed as a standard microelectronic fabrication method. Used widely in the production of semiconductors and transistors, the protocols are now being used by burgeoning nanotechnology industries and interdisciplinary materials projects. Based on lithographic printing procedures dating back hundreds of years [93], photolithography uses photochemical crosslinking properties of polymers to define features according to binary design masks. The lower end resolution limits of photolithography are defined by molecular chemistry of the photoresist, collimation of the light source, and diffraction at the binary transition boundaries. These resolution limits are a significant hindrance to the semiconductor industry, but were not greatly challenged by the work described here. The smallest designed

features were 1-3 μm and, while they showed some defects in the development stages, were sufficient for testing the cell 'grabbing' hypothesis.

5.1.1.1 Chrome on glass mask patterning

Binary pattern masks containing the desired feature information can be created using one of several CAD programs. Mask designs for this work were done in L-edit [v. 14.1, Tanner EDA]. High resolution inkjet printers printing on transparency films can provide enough resolution for larger scale projects. The resolution of the product depends greatly on the printed resolution of the mask, however. Therefore, patterns requiring small scale features are difficult to print without specialised equipment. Mask exposure for this work was done using a μPG101 laser mask writer [Heidelberg Instruments Mikrotechnik GmbH, Heidelberg, Germany] which allowed for design precision down to between 3-5μm.

Masks were printed on soda-lime glass which was coated on one face with chrome and photoresist. The mask writer translated the CAD-defined pattern to laser exposure on the photoresist face of the inserted mask plate. Upon completion, the mask plate was removed and unexposed photoresist was removed in a short development step. The remaining photoresist contained the inverse of the desired pattern features. To remove the photoresist and the chrome in the desired areas, the exposed mask plate was developed for 60 seconds in AZ MIF326, thoroughly rinsed in deionised water, and blow-dried with nitrogen gas, before being placed in a chrome wet etching solution for 60 seconds. The photoresist and the non-protected chrome were removed from the plate leaving the desired pattern in a permanent, reproducible, and reusable chrome/glass mask.

5.1.1.2 Silicon wafer master fabrication

Concurrently with mask design and fabrication, silicon wafers were prepared. While the underlying substrate material was not limited, due to widespread use in microelectronics, silicon wafers are the most commonly used substrate for photolithography and the only substrate used for this work as a master stamp. Pre-processing required wafers be kept overnight in the 185°C oven to remove as much ambient moisture as possible for increased photoresist adhesion. Due to the photoresist's susceptibility to UV light, fabrication steps must

be carried out in a filtered yellow light clean room; for the purposes of this work, within the Nanofabrication Laboratory at University of Canterbury. Plasma ashing and wet etching steps were the only exceptions only because these needed to be carried out in an appropriate fume hood.

The photoresist chosen for the majority of this work was SU-8 2100 [MicroChem, Newton, MA]. Though a variety of different resists are available, the relatively large pattern features for this work required a deeper photoresist layer than would be feasible in thinner SU-8 versions. For photoresist deposition, wafers were removed from the oven, cleaned with blown N_2 to remove any dust, and placed on the central chuck of the spin-coater. Vacuum was applied to keep the wafer from spinning off the chuck at high rotation speeds. A large drop of SU-8 2100 was poured onto the middle of the wafer and allowed to settle slightly before running the pre-entered spinning program. Continuous pouring while avoiding air incorporation was critical to the outcome quality of the finished master. SU-8 thickness was determined by the spin time and maximum speed reached during the program set. For master wafers to be used for exclusion moulding, thickness was targeted at 100μm. After spinning, the wafers were transferred to a 65°C hot plate, allowed to pre-heat at 65°C for 20 minutes and then ramped to 95°C for another 90 minutes.

When the coated wafer cooled to room temperature, the wafer was UV-exposed through the previously developed chrome and glass mask using the Karl Suss MA-6 mask aligner [Suss MicroTec, Garching, Germany]. Ultraviolet intensity measurements were taken before exposure to determine the correct exposure time for the photoresist thickness. The mask aligner brought the mask and wafer into contact to limit undesirable diffraction effects and increase overall exposure resolution. Once in contact, a 365 nm UV source with 9 mW/cm^2 intensity was applied. The areas of the mask not covered by chrome transmitted the UV light through to the photoresist layer, crosslinking the photoresist in these regions and causing it to adhere to the wafer surface.

After exposure, the wafer was baked again by pre-heating at 65°C but ramping quickly to 95°C. Baking times were in accordance with the MicroChem SU-8 specifications sheet and based on the estimated photoresist thickness. Post-exposure baking encourages any remaining solvent out of the photoresist layer and increases crosslinking bond strength. Post- baking also allows for reflow of minor dimple defects in the photoresist layer. Cooling back to room temperature

was done at a controlled ramp of 15°C/hour to avoid inducing mechanical stress and warping in the photoresist layer.

Once the wafer had completely cooled it was removed from the hotplate for pattern development. Developing the exposure consisted of a timed bath in PGMEA solvent, which removes non-crosslinked photoresist quickly but will also dissolve the crosslinked areas if left for too long in developing solution. The wafer was removed from the bath after the required time, rinsed with fresh PGMEA solution, and then rinsed thoroughly with isopropyl alcohol to clean and identify any remaining undeveloped areas. Completed master wafers were blown dry with nitrogen and stored until required [Figure 5.1].

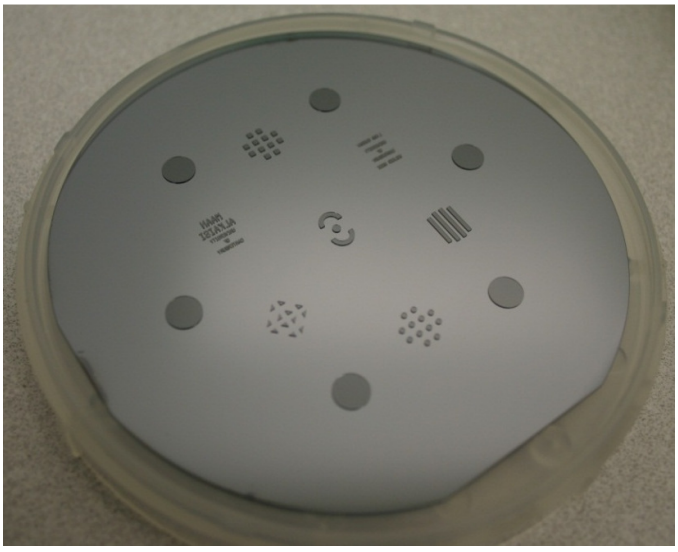

Figure 5.1 - Fully developed master wafer patterned with features of 100 µm height for continued soft lithography and exclusion moulding. The full wafer is four inches in diameter.

5.1.2 Soft lithography

Developed at Harvard University, soft lithography has become a staple protocol for fabrication of microfluidic devices, a growing field in and of itself with a broad range of applications [29, 94]. In the seminal soft lithography paper, Whitesides et. al. introduced polydimethylsiloxane [PDMS] as an elastomeric moulding medium for replicating well defined features from photolithographic master patterns. PDMS is a heat cured polymer consisting of an elastomer and a curing agent. When combined and cured, the viscous PDMS liquid crosslinks and becomes a highly gas-permeable, elastic solid.

For soft lithography replications in this work, PDMS was combined at a 10:1 elastomer to crosslinker ratio, mixed thoroughly, and desiccated for at least 20 minutes to remove air from within the liquid pre-polymer. Concurrently, the master wafer to be moulded from was treated for several hours with vapour from trimethylchlorosilane [TMCS] [Sigma Adlrich, St. Louis, MO]. The TMCS coating discouraged adhesive interactions between the curing PDMS and the underlying silicon master wafer. Uncured PDMS, which occurred most often when the crosslinker and elastomer components were incompletely mixed, left a residue on the silicon wafer preventing further replication from the master pattern. Because TMCS is highly corrosive, the treatment protocol was completed within a fume hood within the Nanofabrication Laboratory yellow room.

The TMCS-treated SU-8/silicon master wafer was removed from the fume cabinet with wafer forceps and placed in a wafer holder to prevent incidental contact with the corrosive TMCS surface. A metal bounding ring, with a diameter just smaller than the 4" diameter wafer, was placed at the wafer's edge and was used to confine the outside flow boundaries of poured, liquid PDMS. Desiccated PDMS was poured within the bounding metal ring and a weight was applied over the ring, but not in contact with the curing polymer, to seal the ring to the wafer and prevent PDMS from leaking underneath. The entire assembly was transferred to the hotplate where it was baked for 2 hours at 80°C. After curing, the master and PDMS were carefully separated [Figure 5.2] and stored until future use.

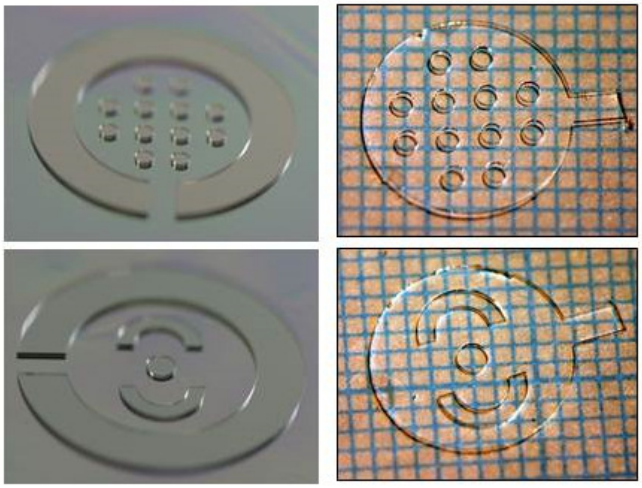

Figure 5.2 - Pattern features on both the developed silicon master wafer [left] and the resulting PDMS stencils after exclusion moulding [right]. [Blue boxes in the right image indicate mm^2 to show pattern feature size.]

Exclusion moulding, as discussed in chapter 4, is a modification of soft lithography techniques which produced through holes in PDMS casts. Exclusion moulding was used to produce stencils which were used to define the cell culture substrate for initial cell cultures.

5.2 Positive and negative topographies

Before analysing the effects different pattern topographies have on cell growth it was necessary to differentiate and define the polarity of the substrate features created by inversion of the mould. Inversion of replicated features caused two possible topographies produced from the same binary mask, from here on referred to as the 'positive' and 'negative' variations. At this point, it was unknown whether or not cells grown on an inversion of the same pattern topography would alter their response, so the opposing topographies needed to be determined and tracked through the replication process.

Substrates expressing a 'negative' topography were defined by the apparent removal of material below the flat of the surrounding polymer material. As shown in Figure 5.3 [A] and Figure 5.4, the negative substrate appears as series of holes instead of positive columns, pits instead of pillars. Conversely, a 'positive' topography was defined as the apparent build-up of material from the flat [Figure 5.3 B].

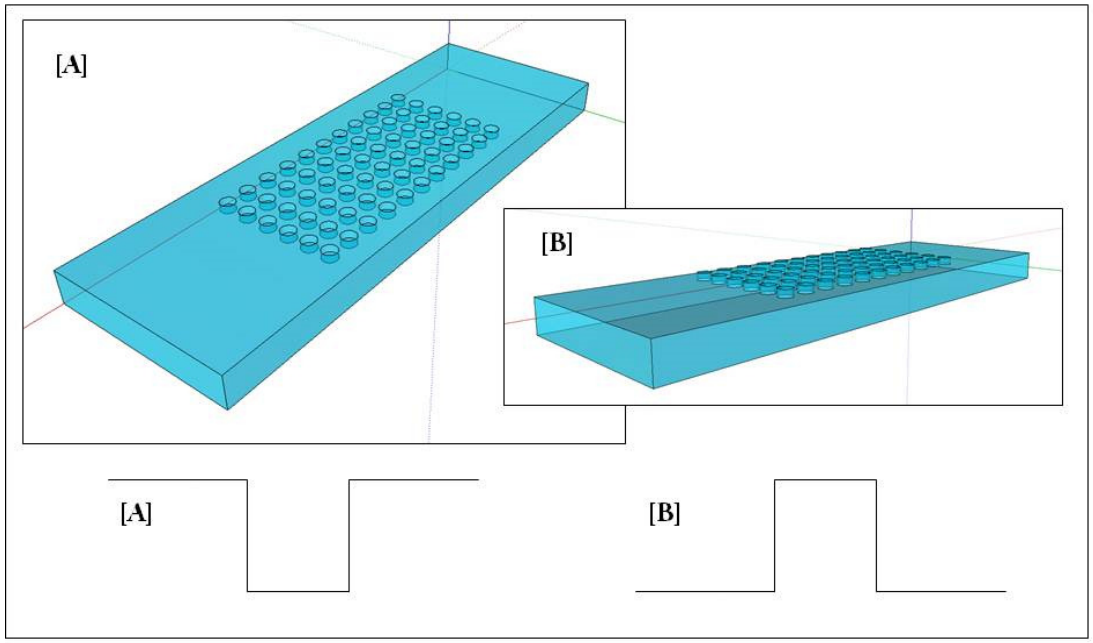

Figure 5.3 - Schematic repetitions of comparable PDMS moulds with [A] negative topography and [B] positive topography. The trace of each (shown with the same labelling just below each representation) shows the initial pattern direction from the surrounding flat areas and demonstrates the effect of the pattern inversion.

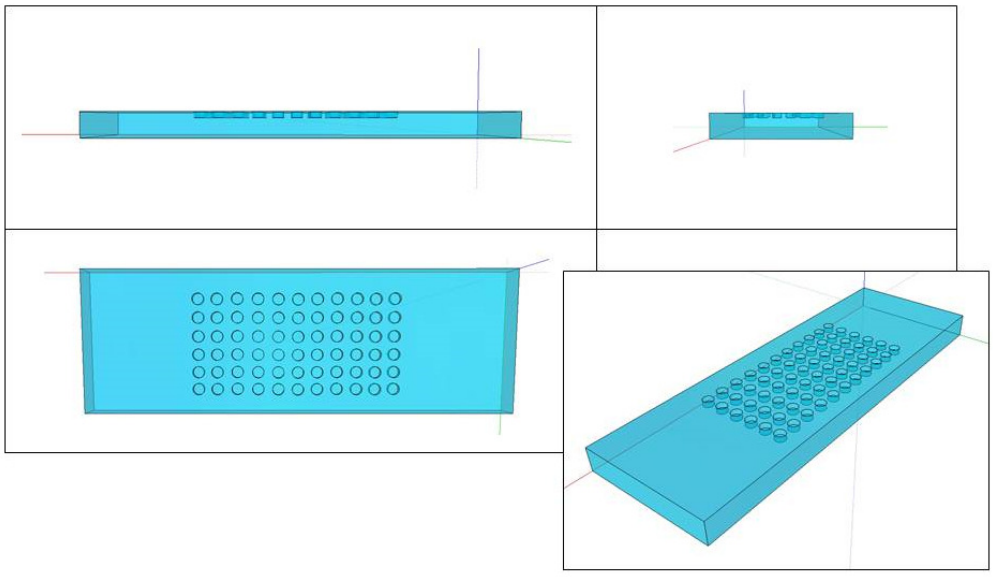

Figure 5.4 - Engineering drawing of negative pattern topography in PDMS. The features appear as holes instead of pillars, material removed from the flat surface rather than built up from the flat.

The bioimprint protocol results in an inherently negative primary replication. The template cells impress into the curing polymer, which results in indented features below the defined flat. The area occupied by the template cells can be thought of as, effectively, removed material from the bulk. Further replications lead to inversion of the bioimprinted features and a recreation of the initial cell culture organization built up from the material bulk. Positive replication of bioimprinted features will be discussed in greater detail in chapter 8.

Though the binary definition was defined by the orientation of the first replicated feature from the surrounding flat area, pattern features could be interpreted by the cells as either relatively positive or negative independent of the overall polarity of the pattern. Particularly for large area samples, the topography of the pattern becomes relative to the cell's local position rather than the flat substrate area, which could be several hundred microns away.

5.3 Replication methods

In order to directly compare the effects of cells growing on bioimprinted substrates with cells grown on patterns, it was important that the same polymer was used as the substrate in both experiments. By keeping the polymer surface chemistry constant, any difference seen in the effects of cell proliferation and growth were increasingly likely to be due to the topography of the substrate. Therefore, because the bioimprinting medium was the poly(MA), replication methods transferring the patterns were necessary.

Because of the unknown effects of the pattern polarity on the cell growth and distribution, it was important to not only identify the topography but also to be able to fabricate its opposite for comparison. Methods for replicating pattern features directly from the SU-8 were investigated. Continued replication protocols were adopted to create substrates with inverted substrate pattern features in the desired polymer chemistry. While PDMS was extremely useful as an elastomeric mould, it was not used directly as a cell substrate due to suggestions of cytotoxicity in literature [89]. Therefore, methods for transferring the pattern from the soft lithography, PDMS mould were extensively investigated. Several different polymer chemistries were used as transfer moulds to determine the optimal protocol for maintaining high resolution.

5.3.1 Primary replication from SU-8

While PDMS soft lithography methods detailed previously are well known for their use for microfabrication, it remained to be seen if this method would produce the highest resolution replication. And because PDMS was not used as an immediate substrate, further replication steps were required to produce a useable cell culture substrate. The resolution loss for the final output substrate was likely to be higher due to the multiple moulding steps. Therefore, poly(MA) curing directly to the SU-8 pattern was examined as a direct template method.

The fabrication of poly(MA) samples, cured directly from the SU-8 master wafer was based on the same curing protocol used for bioimprinting. The liquid methacrylate pre-polymer was freshly mixed immediately before use at the desired monomer ratio and then pipetted over the area to be replicated. Initial trials did not contain border material to define the outside boundary of the liquid polymer, so the liquid polymer was allowed to expand beyond the lithographically defined boundary. The wafer containing the immersed pattern was exposed to UV for four minutes using the Omnicure source and light guide. After exposure was complete, the wafer, with the poly(MA) sample attached, was set aside to cool completely from any heat transfer during curing. When both the wafer and the poly(MA) sample had cooled to room temperature, careful pressure was applied to the surface interface with a scalpel to encourage release between the two rigid materials, SU-8 and polymethacrylate.

As shown in Figure 5.5, once successfully removed from the wafer, the poly(MA) substrate showed resolution of features at least down to 5 μm, which approached the resolution limitations of the photolithography equipment used at the University of Canterbury and, therefore, was the smallest available pattern size in SU-8. Direct replication in poly(MA) was one of the cleanest methods identified in this body of work.

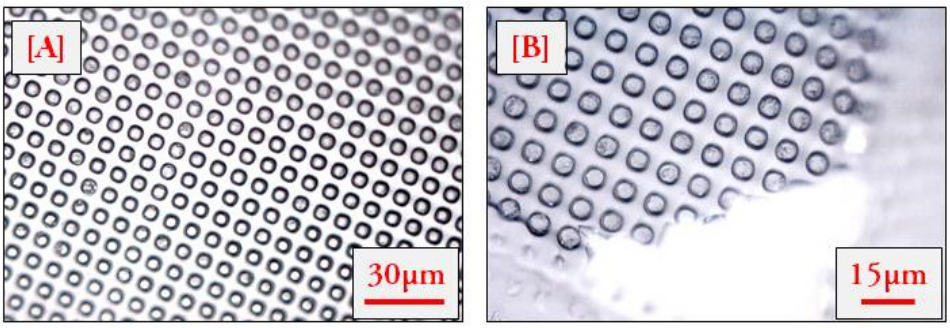

Figure 5.5 - Negative poly(MA) substrates patterned directly from the SU-8 master. While the majority of the pattern shows a clean replication and high resolution features [A], at the pattern edges the poly(MA) removes the SU-8 from the master and incorporates it into the pattern creating a relative flat region as shown in the bottom of image [B].

Direct replication from the SU-8 master wafer into cured poly(MA) was discontinued as a substrate fabrication method for one main reason: with each substrate separation some of the SU-8 was incorporated into and removed with the cured poly(MA) sample. Because of this, the master wafer was destroyed after only two or three replications. Photolithography of an SU-8 master wafer takes several days and was, therefore, not practical to repeat on the scale necessary for continuous production of patterned poly(MA) substrates. While secondary replication methods would contain a loss of resolution due to an additional step, intermediate moulds could be used to increase throughput.

5.3.2 PDMS to poly(methacrylate)

Due to the desire to keep the substrate surface chemistry consistent, the first method investigated for patterning from a soft lithography mould was transferring into poly(MA). The poly(MA) topography resulting from replication from PDMS was the same polarity as the original patterns developed in SU-8.

PDMS borders were placed around the feature area to define the outer boundary of the resulting substrate. The PDMS boundaries conformally adhered to the underlying PDMS mould. Liquid methacrylate was mixed and approximately 100 µL was pipetted into the PDMS-defined boundaries. The PDMS assembly filled with liquid methacrylate was allowed to sit for 30 seconds to allow the liquid polymer to completely coat the pattern features before it was exposed to UV for 4 minutes at 40% iris opening.

While replication from PDMS into cured poly(MA) was an extremely useful method of patterned substrate fabrication, it was also the most difficult. PDMS is naturally hydrophobic, preventing the liquid methacrylate mixture from pervading the micro- and nanoscale features to be replicated. Therefore, even when cured completely to the surface, the poly(MA) samples often contained only minimal traces of the pattern after separation. Additionally, separation of the cured poly(MA) and the PDMS mould became difficult and led to delaminating defects on the poly(MA) substrate surface [Figure 5.6]. While these de-wetting defects often intersected patterned areas, they showed some interesting properties in the cell culture stages which will be discussed in the next section. Poly(MA) curing from PDMS also caused a stress-related 'double-vision' artefact, which will be discussed in more detail later, but often produced undesirable substrates.

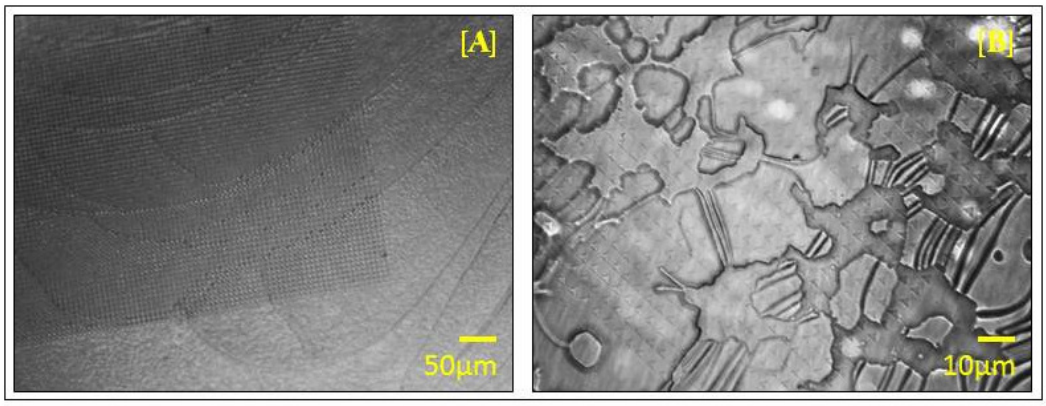

Figure 5.6 - Micrographs documenting the dewetting artefacts of cured poly(MA) at removal from PDMS. The dewetting features depended on the completeness of poly(MA) curing. More thoroughly cured samples showed regular, linear features [A] while more liquid layers caused larger, random features. [Shown at [A] 100x and [B] 500x magnification].

To combat the hydrophobicity of the PDMS surface, a short Corona plasma treatment was applied. [Corona plasma treatment is atmospheric plasma which imparts a charge on the normally inert polymer surface. Corona plasma treatment was used instead of related oxygen plasma treatment methods because no vacuum was required for surface treatment.] By increasing the wettability of the PDMS surface, the liquid methacrylate mixture was able to seep around all of the pattern features and more faithfully replicate them into the cured substrate. Optimization of this protocol determined that 45 seconds was the optimal treatment time. Plasma treatments shorter than 45 seconds showed no noticeable effect and developed the same disfiguring artefacts in the curing process. Treatments beyond 45 seconds led to strong

adhesive interactions between the PDMS mould and the cured poly(MA). These interactions could be so strong that the intended separation of the two permanently damaged the PDMS mould. Poly(MA) substrates cured to patterns treated with 45 second Corona plasma showed fewer de-wetting effects and high resolution pattern transfer [Figure 5.7].

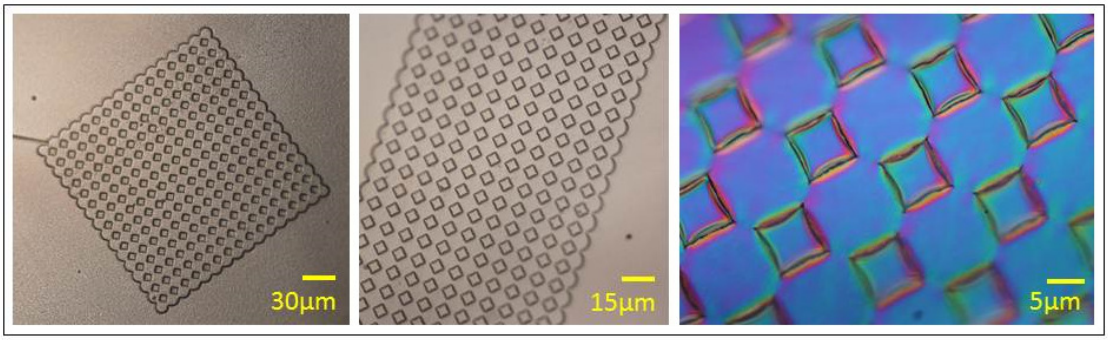

Figure 5.7 - High resolution replication of positive diamond patterns in poly(MA) from PDMS moulds subjected to a 45 second Corona plasma treatment. [Shown from left to right at 100x, 200x, and 500x DIC.]

5.3.3 PDMS to Smooth-Cast

Because of the substantial de-wetting effects of transferring patterns directly from PDMS into poly(MA), an intermediate polyurethane mould was made to aid in the pattern transfer, with the additional benefit of inverting the pattern polarity again. Smooth-Cast 322 [Smooth-On, Easton, PA] was used to create a more rigid, but well-defined polymeric master from PDMS, which allowed patterns to be replicated into poly(MA) [95]. Smooth-Cast comes as two separate parts which cure only when mixed together. To create the moulds, equal parts of the polyurethane elastomers A and B were measured and desiccated prior to mixing. After mixing, complete curing took less than 3 minutes. Therefore, efficient mixing and quick pouring were required to ensure a uniform polymer block and complete curing throughout.

Moulding from the PDMS mould allowed for the same mould to be recreated several times without defect. Pattern transfer was simple, accurate, and reproducible [Figure 5.8]. The most difficult aspect of Smooth-Cast resin patterning was microscopy. Because the polyurethane output was an opaque mould, however, microscope imaging of the small scale features was usually very difficult. With careful microscopy, grated patterns on the order of 375 nm were resolved.

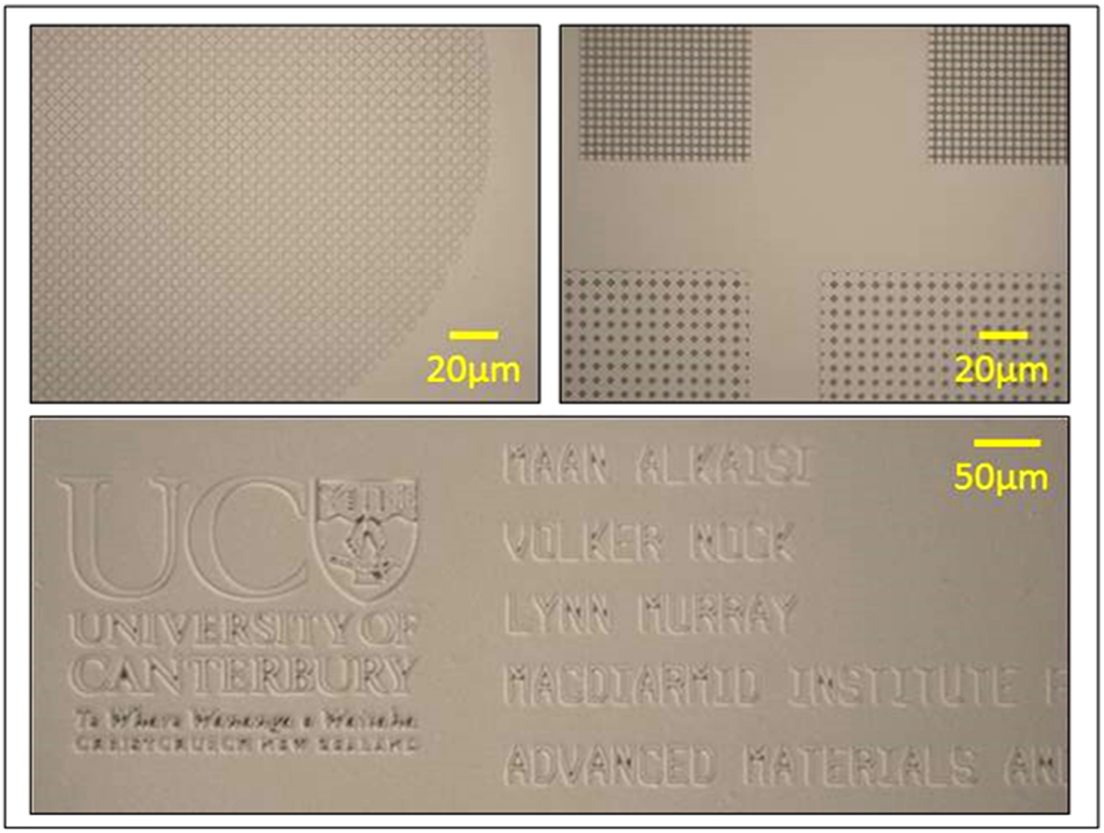

Figure 5.8 - Patterns in Smoot-Cast 322 replicated from PDMS mould. While never used directly as a cell culture substrate, the polyurethane mould provided a high resolution intermediate between PDMS and poly(MA).

The inversion of the pattern features in the Smooth-Cast transfer mould was an additional benefit. While duplicating patterns in poly(MA) from PDMS was difficult, protocol optimization provided consistently usable cell culture substrates. If a protocol could be developed for patterning poly(MA) substrates from the polyurethane intermediate, positive and negative inversions of the same design features would be available for direct comparison as cell culture substrates.

5.3.4 Smooth-Cast to poly(methacrylate)

Transferring patterns from the Smooth-Cast master to poly(MA), however, turned out to be more of a challenge than anticipated. The basic protocol mirrored previously used poly(MA) curing procedures. PDMS borders were attached around the feature area and approximately 100 µL freshly mixed liquid polymer was pipetted over the patterns. UV was applied for 4

minutes and the samples were allowed to cool to room temperature before sample separation was attempted.

The adhesion between the PDMS borders, which were necessary in order to limit the flow of the liquid polymer and defined the size of the cured poly(MA), and the Smooth-Cast mould depended on conformal contact between the two. Therefore, because the adhesive bond was not very strong, it was prone to leaking. Plasma treatment of the Smooth-Cast substrate increased the adhesion bond strength, but led to permanent bonding of the two and prevented reuse of the master. Though new masters could be reproduced relatively quickly in Smooth-Cast, the one to one replication for transfer mould production was an undesirably low throughput. In spite of the curing deformations and low throughput, the Smooth-Cast to poly(MA) replication protocol was able to successfully transfer patterns down to at least 375 nm [Figure 5.9]. The 375 nm pattern features were produced by interferometric lithography by Dr. Trey Holzworth and used as a calibration sample for the limits of pattern resolution.

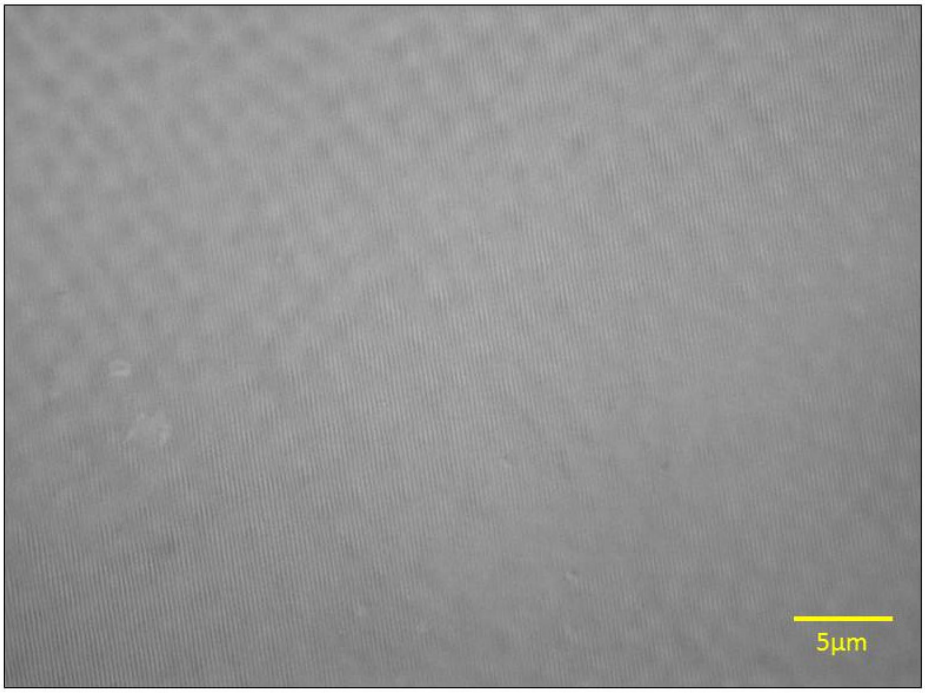

Figure 5.9 - Poly(MA) replica of 375 nm vertically oriented grating patterns transeferred from a Smooth-Cast resin master. The patterned features are difficult to distinguish even with 1000x magnification and DIC (as shown).

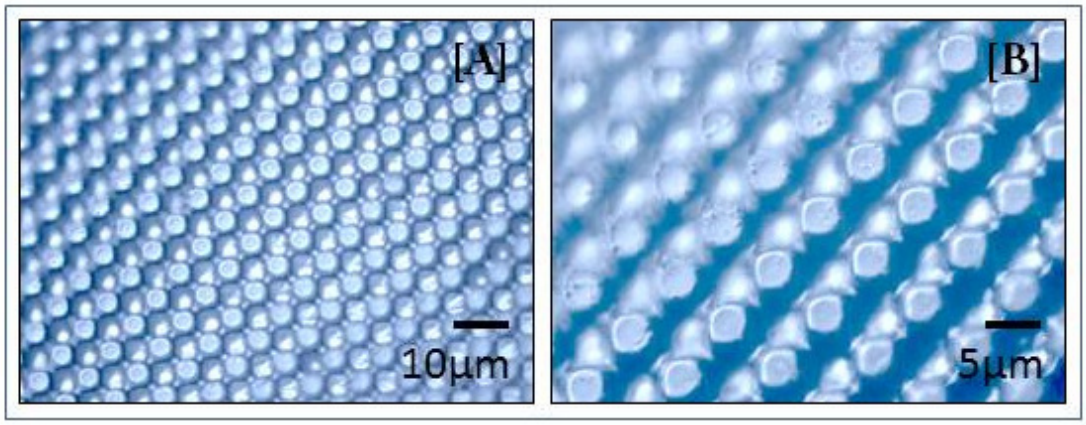

Figure 5.10 - Differential interference micrographs of patterned poly(MA) substrates replicated from a Smooth-Cast master. Though pattern resolution satisfactory, some bubbles are incorporated into the cured features [B]. (Shown at [A] 500x and [B] 1000x magnification).

An additional complication of curing poly(MA) to the Smooth-Cast resin was deformation due to the thermal effects caused by the prolonged, intense UV exposure. As discussed late in chapter 6, the crosslinking reactions involved in poly(MA) curing induce stress across the face in contact with the mould which causes the curing polymer to want to pull away from the mould surface. When curing from a polymer with a high glass transition temperature or a rigid substrate with a high melting point the heat produced by the UV is not enough to deform the original mould. For Smooth-Cast master moulds, however, the combination of heat induction and stress-related withdrawal of the curing poly(MA) led to deformation of the Smooth-Cast master itself. The poly(MA) face in contact with the Smooth-Cast patterns did deform due to the crosslinking stress as expected. Rather than simply pulling away from the central region of the curing interface as seen with glass and PDMS moulds, the adhesive interface between the Smooth-Cast and the poly(MA) remained intact and, due to the heat present from the high intensity UV exposure, the Smooth-Cast was remodelled to contain the convex deformation corresponding to the deflection caused by the poly(MA) crosslinking.

While the adhesion strength at the interface between the polyurethane resin and the poly(MA) substrate ensured a higher resolution replication, the strong bond also made separation of the two materials more difficult. Careful upward pressure was applied with a scalpel carefully inserted between the two material layers. Slowly lifting upward with the scalpel allowed the poly(MA) to peel itself away from the Smooth-Cast mould, limiting cracking and breaking of the resulting substrates. The deformation of the Smooth-Cast also made separating the two materials more difficult and, sometimes, impossible. In most cases, even if the cured poly(MA)

completely released from the Smooth-Cast, the mould was not reusable and, subsequently, discarded. Due to the complications of this protocol without the benefits of a more permanent master mould, the protocol was eventually dismissed.

5.3.5 PDMS to PDMS

As noted earlier in this chapter, it was critical to follow substrate inversion throughout the replication processed to determine the polarity of the resulting features. Because of its widespread usefulness as a mould and a substrate, PDMS was a desirable medium for pattern transfer. However, PDMS has a 'self-healing' property, in that if liquid PDMS is allowed to cure in contact with cured PDMS, the two will combine into a single solid block. Advantages of this property were exploited in other protocols of this thesis, but were decidedly negative when trying to replicate pattern features.

A method for successfully replicating features from PDMS into PDMS without the annexation of the additional liquid elastomer to a solid bulk was accomplished by Gitlin, et. al. [96]. A ten minute surface treatment of the PDMS mould in 10% [w/v] hydroxypropylmethylcellulose [HPMC] dissolved in PBS allowed PDMS to be moulded from lithographically patterned PDMS. After treatment the substrate is washed extensively with water and dried before pouring liquid PDMS over the feature area. The HPMC layer creates a barrier between the PDMS master mould and the liquid PDMS being cured. Separation of the PMDS layers required careful manipulation, but was generally simple. This protocol was ideal for inverting soft lithography and bioimprint patterns originally moulded into PDMS. The resolution, however, was lower and of the order of 3-5μm.

5.4 Bioimprint replication

To test the resolution of each moulding step on cell features and determine the feasibility of creating a positive bioimprint substrate, the replication chain outlined above was duplicated using an original bioimprinted substrate. In order to accomplish this, the first requirement was to determine a protocol for creating a template mould from the bioimprinted poly(MA) sample. PDMS was the best material to transfer into due to its elastic properties, which would make sample separation easier than replicating with a rigid polymer, and multiple options for replication paths.

5.4.1 Poly(methacrylate) to PDMS

Bioimprint samples were placed feature-face up in a polystyrene dish. Desiccated, 10:1 liquid PDMS was carefully poured to completely cover the entire sample. The sample was left on the bench to cure overnight at room temperature.

Just as transferring patterns from PDMS into poly(MA) required careful optimization and contained some inherent variability with each repetition, copying bioimprinted cell features from the cured poly(MA) into PDMS was similarly complicated. In the first attempt, incomplete PDMS curing, even after being left several days beyond the usual 24 hour curing time, produced an inaccurate mould and prevented use of the original bioimprint for any imaging or other replication techniques. Local curing allowed for parts of cured PDMS to be removed, but the low resolution illustrated disruptive effects at the interface [Figure 5.11]. The general outline of cell features could be recognised, but the smaller scale cell features, characteristic to bioimprint substrates, were not distinguishable.

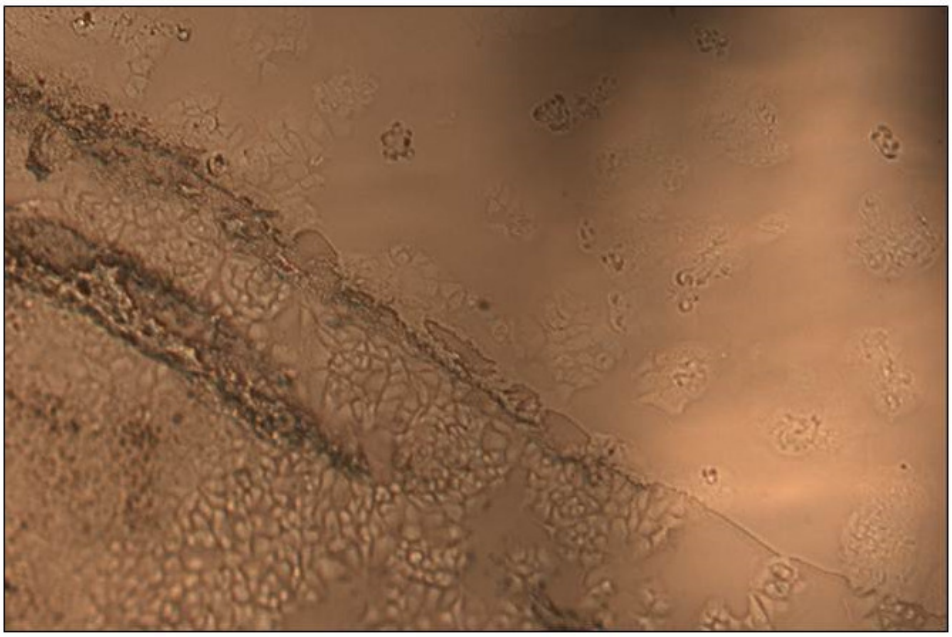

Figure 5.11 - Micrograph documenting the low resolution resulting from incomplete curing of PDMS in contact with the poly(MA) template. The cell outlines are visible, but no cell features are distinguishable. Similarly the image is diagonally divided by a dewetting artefact created during mould separation. [Shown at 100x magnification].

The responding hypothesis was that monomers leaching from the poly(MA) or the presence of an uncured, liquid layer were preventing the PDMS curing. PDMS is known to remain in the viscous liquid state, instead of curing, when in contact with solvent films [97]. The assumption, therefore, was that there was an uncured poly(MA) layer across the surface of the bioimprint which presented the same solvent-like properties of the liquid poly(MA) mixture which caused the degradation of polystyrene plastics in chapter 3 and prevented complete PDMS curing. In response, a 24 hour water soak, which showed great success in increasing the biocompatibility of the poly(MA), was implemented to remove any leaching methacrylic acid monomers.

Upon duplicating the experiment, this time incorporating the water bath for at least 24 hours before moulding, the results showed significantly higher replication resolution [Figure 5.12]. Cell membrane outlines and individual nuclei were identifiable. Some artefacts were seen, however, at the small scale nuclear features [Figure 5.12 red arrow] and at the locations of three dimensional adhesions [Figure 5.12 yellow arrows]. The small scale features of the cell membrane covering the nucleus induced bubbles in the PDMS and show as small black dots restricted to the nuclear regions of the secondarily moulded features. The artefacts caused by the three dimensional growth was considered to be more disruptive to additional replication

procedures, however. In these regions, the secondary PDMS imprint showed little to no resolution and, instead, appeared as dark circles obstructing clear view of any successfully replicated underlying features.

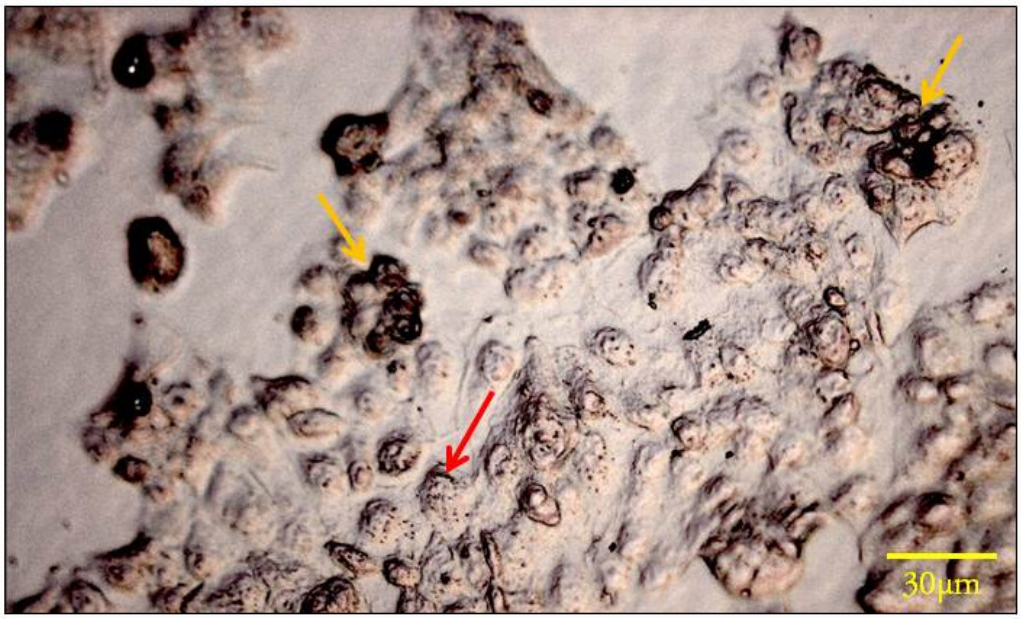

Figure 5.12 - Replication of Ishikawa cancer cells in PDMS taken from an original poly(MA) bioimprint. Yellow arrows indicate lower resolution areas due to 3D cancer cell growth and the red arrow indicates bubbles which appear as little black spots mostly on and around the nucleus.

In any case, the resolution of cells expanding in a monolayer was high enough to warrant further production of PDMS bioimprint moulds. Bioimprinted substrate fabrication was improved significantly as the substrates could now be produced from an existing mould using the PDMS to poly(MA) transfer method and would not require a new cell culture and bioimprint each time a new substrate was required.

5.4.2 Bioimprint replication

To verify the resolution for the replication chain documented in section 5.3, the series of mould transfers was repeated using a bioimprinted sample and the creation of a PDMS master mould using the method just described [Figure 5.13].

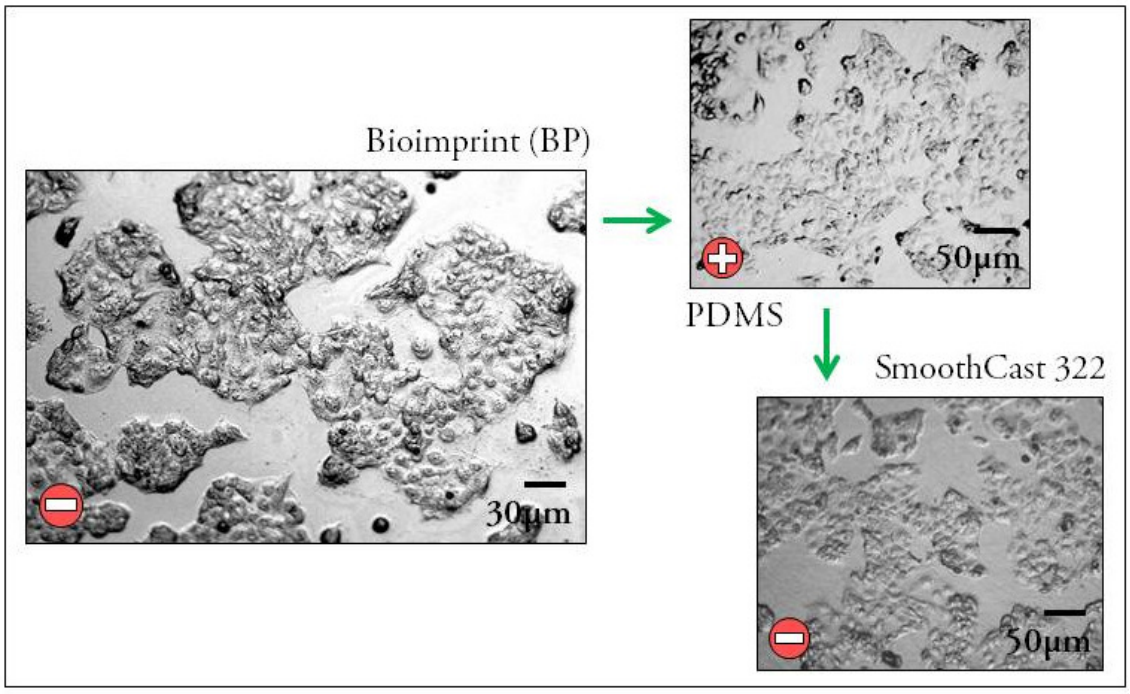

Figure 5.13 - Micrographs taken at each step across the replication chain: Bioimprint in poly(MA), PDMS, and SmoothCast 322 resin. Positive or negative was designated and shown in the bottom left corners of each image.

Because high magnification microscopy was difficult on PDMS samples due to the substrate thickness and optical effects and AFM imaging was very challenging due to the associated elastic modulus of the material, documentation of successful pattern transfer was recorded by AFM imaging of the further replicated Smooth-Cast resin [Figure 5.14]. Similarly, optical imaging of Smooth-Cast masters was difficult due to the opacity of the materials, also making AFM a more effective analysis method for resolution verification. Atomic force images show high resolution replication in the Smooth-Cast resin, three replication steps beyond the initial cell culture. Cell membrane boundaries and the nuclear and nucleoli features are easily distinguishable. The relatively large scale (100 µm) of the images only hints at the actual resolution limit, but based on the nucleoli, the resolution limit is lower than 2 µm.

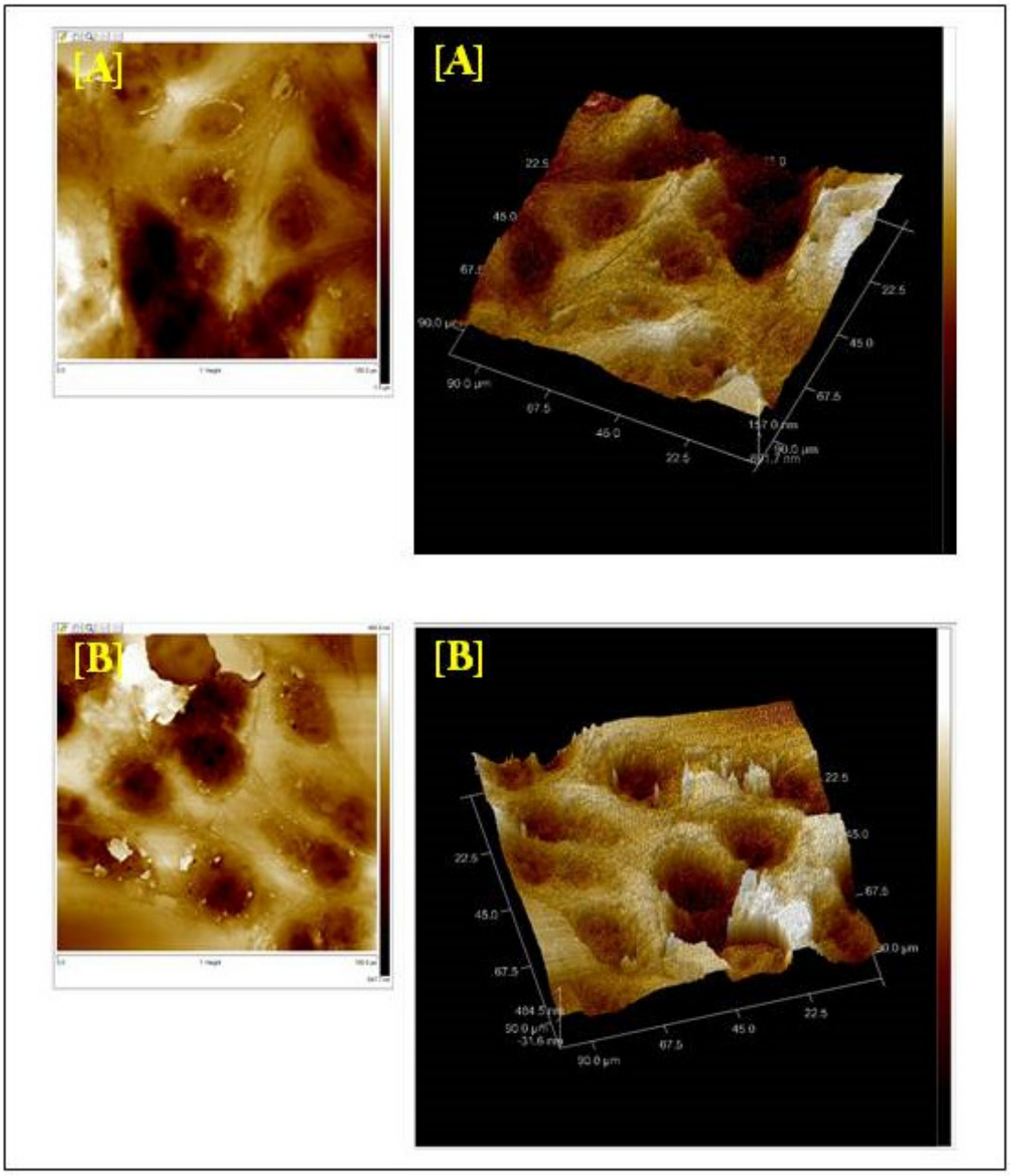

Figure 5.14 - AFM images and 3D renderings of Ishikawa cells replicated in Smooth-Cast 322. Some artefacts of material removal remain [top left of AFM height image [B]].

Disturbingly, some artefacts were seen when imaged with AFM that were not found with optical microscopy. The apparent flat found in the top left corner of Figure 5.14 [B] was mostly likely created by material which was removed along with the Smooth-Cast during separation from the PDMS mould; though isolating the exact replication stage in which the artefact was produced was unlikely. The difficulty verifying the surface accuracy was found to be the

greatest drawback of the bioimprint replication chain using the previously outlined method. Time and resources were taken to process bioimprints and resulting moulds with unknown resolution and artefacts, only to be determined by post-processing imaging.

5.5 Discussion

Patterned substrate fabrication was necessary to isolate the effects of generally patterned topographies from the effects of bioimprinted topographies on the cell growth and organization of cancer cells in culture. Experimental results from chapter 4 for cells growing on bioimprinted surfaces showed some interesting localised adhesion effects, but we were unable to strictly isolate those effects to bioimprinted regions. Controlling the pattern sizes and regions using photolithography allowed for detailed, well-documented surface features in designated regions corresponding to the designed mask.

Soft lithography was used to produce reusable PDMS moulds from the SU-8 photoresist master patterns. PDMS mould production increased throughput for patterned samples in several ways. No longer subject to direct curing and removal of the poly(MA), the SU-8 masters lasted longer and were able to produce several PDMS moulds. In turn, the PDMS moulds were able to produce more substrates per single mould than was possible with direct fabrication of patterned substrates from the master wafer.

To accurately identify the effects of lithographic patterns on cell culture growth it was first necessary to identify whether the cells would ‘see’ the patterns as a series of holes or as a series of pillars. By defining the topography as either positive or negative based on whether material was added above or removed from below the relative flat, we were able to create a reference terminology which would describe the topographic nature of all substrates, including those containing bioimprint features. The importance of the pattern polarity was unknown at this point and, therefore, was carefully documented through the replication phases.

To keep the surface chemistry consistent, poly(MA) substrates containing the desired pattern topography needed to be fabricated. With several attempts at optimization, a protocol was developed for producing poly(MA) substrates containing the pattern features with enough resolution for use as cell culture substrates. While the Corona plasma treatment was necessary for any pattern production, inherent variability of the plasma produced could provide only an

approximate time for the most consistent positive results. Corona plasma was distributed across the surface using a linear torch and was, therefore, unable to cover the entire surface at once. Because the torch had to be constantly moved across the substrate to ensure approximately equivalent plasma coverage across the substrate it was impossible to determine the actual treatment time for any given region of the substrates.

Similarly, there was no method to determine the length of time the PDMS surface remained 'activated' after the plasma treatment. The purpose of the plasma treatment was to remove the hydrogen atoms attached to oxygen groups on polymer surfaces; however, hydrogen from the air will attach and negate the plasma effect. No investigations were made into the time-dependent effect of the plasma treatment on PDMS due to the assumed variation in the plasma treatment itself. A short plasma treatment with a plasma asher, available at University of Canterbury, would have provided a consistent plasma treatment across the surface, but would have required removing the samples from the controlled environments of either the nanofabrication laboratory or biological applications and technologies laboratory.

Continued replication from the PDMS mould into Smooth-Cast 322 resin allowed for another inversion of the pattern features before replication into poly(MA). When poly(MA) substrates were patterned from the Smooth-Cast moulds they contained the inverse of the topography produced by poly(MA) replication from PDMS. Though the resolution was not necessarily the same, both the positive and negative substrates were used for cell culture, the results of which are discussed in the next chapter.

6 Cancer cell growth on patterned substrates

Ishikawa cancer cells ultimately showed some organisation when grown on bioimprinted substrates as discussed in chapter 4. There was no direct evidence, however, to determine whether the cells were actually identifying imprinted proteins and cell structures rather than simply responding to areas of modified topography. Because of the vast literature available on patterning topographies for cell adhesion as discussed in chapter 1, experimental investigations were necessary to separate the effects of patterned topography from specifically bioimprinted topography.

6.1 Experimental methods

Two specific experimental conditions were investigated: comparison of growth on patterns across the entirety of the substrate and comparison of cell adhesion and morphology on patterned regions of the substrate directly adjacent to flat, un-patterned regions. Completely patterned substrates were designed to determine any morphology variation and/or overall cell spreading, while local patterned areas were designed to identify any selective adhesion and organization.

6.1.1 Patterned substrate fabrication

Patterned substrates used in this work consisted of regular geometric arrays of pillar or hole patterns, mostly 5-15 μm side length or diameter, and were initially fabricated in SU-8 photoresist on silicon wafers using the photolithography processes outlined in chapter 5. Spin speeds, baking temperatures and times, and UV exposure doses were all adjusted based on the recommendations of the MicroChem SU-8 2100 specifications sheet [86]. After successful master pattern fabrication, inverse PDMS moulds were made using soft lithography replications as follows. The silicon master was transferred to a hot plate and a four inch metal ring was placed around the borders to contain the liquid PDMS during curing. A 10:1 ratio of

elastomer to crosslinker was mixed and desiccated for 20 minutes before being poured over the SU-8 pattern within the bounds of the outer metal ring. A weight was placed over the top of the ring in order to effectively seal the ring to the wafer and prevent PDMS from leaking. The hot plate was then turned to 80°C for 2 hours. After curing the moulds were carefully separated and the PDMS was used for further replication into methacrylate polymer.

To fabricate patterned poly(MA) substrates for cell culture, an additional replication phase was required. Following the method discussed in chapter 5, poly(MA) substrates were created from the PDMS moulds and contained the same topographical polarity as the initial SU-8 features. PDMS chambers for cell culture confinement were cut from larger PDMS sheets and conformally sealed around the patterned areas to confine the outer bounds of the liquid methacrylate mixture before curing. The methacrylate liquid was mixed at the desired ratio immediately before curing. Fresh methacrylate polymer was mixed for each curing iteration. The thoroughly mixed liquid polymer precursor was pipetted over the patterned surfaces within the PDMS-defined regions. Curing consisted of four minutes of continuous UV exposure using the light guide of the Omnicure source at 40% iris opening. Cured samples were carefully separated from the PDMS mould. After separation, the cured, patterned samples were imaged and analysed for defects using bright field microscopy techniques. Usable samples were placed in a sterile water bath for at least 24 hours to increase biocompatibility before UV sterilization and cell culture.

To directly compare the effects of geometrically patterned lithography with those of the bioimprint, different patterned substrates were fabricated, corresponding to either the full-chamber or stencil-patterned bioimprint substrates used in chapter 4. The bioimprinted area was lower for stencilled substrates due to the surrounding flat areas. Therefore, patterned substrates were created to mimic the stencilled area as well. For overall adhesion analysis, full chamber sections were patterned or bioimprinted to eliminate overlapping effects of patterned and flat areas within the same samples. Comparison was focused on overall adhesion to polystyrene, flat poly(MA), bioimprint, and patterned.

On the other hand, localised adhesion was also investigated. For these experiments, lithographic masks were designed with patterned areas corresponding to the exposed elastomeric stencils used for the bioimprint. After replication into the final substrate polymer, as discussed in chapter 5, the patterned area corresponded to the bioimprinted area in substrates created from stencilled cultures [approximately 1mm^2 depending on the stencil shape]. After

Ishikawa cell culture on both of these substrate types, comparing cell growth locations determined any notable preference for bioimprinted regions over topographically modified substrates.

To construct a working assembly for cell culture, PDMS sheets were cut to the approximate size of a microscope slide and holes matching the exact geometry of the PDMS borders used for poly(MA) curing were cut into the PDMS. The PDMS, containing cut-outs of the exact size and shape of the cured poly(MA) substrates, were sealed to glass microscope slides. The assembly was either UV sterilized or autoclaved. Sterile poly(MA) substrates were then press-fit, pattern side up, into the PDMS borders.

6.1.2 Cell culture

Ishikawa endometrial cancer cells were removed from continuous subculture for experimental use. Culture medium was aspirated and replaced with a 0.05% trypsin-EDTA [in PBS] solution. Cells were incubated in trypsin solution for 20 minutes or until large cell conglomerates were no longer visible in solution. The trypsin solution, containing the detached Ishikawa cells, was aspirated from the culture flask and placed into a centrifuge tube. The test tube was sealed and transferred to the Eppendorf centrifuge where it was spun against a balance for 5 minutes at 1500 rpm. After spinning, the trypsin-containing supernatant was removed and replaced with 2 mL of culture media for cell counting. Counting was completed using a haemocytometer. A suspension containing the desired cell density was created by diluting the initial cell concentration with culture media. The cell/media suspension containing cells at the desired density was pipetted into the PDMS-defined chambers containing the patterned poly(MA) substrates. Experimental assemblies containing seeded cells were incubated until the desired endpoint. A suspension containing 5.0×10^5 cells was added to a 25 cm^2 flask for continued subculture and re-placed in the incubator.

6.2 Results

On substrates containing patterns across the entire area, cell groups were not identified as growing together based on any given influence of the substrate. Patterns consisted of 15 μm negative hole features separated with 5 μm diamond pillar features. Cell seeding density was 5.0×10^4 cells/chamber and cultures were maintained in incubation for 24 hours. CBB staining easily identified areas containing cellular material from the background topography. Large areas of cell adhesion and spreading appeared across the entirety of the patterned substrate. Low magnification bright field imaging showed groups of cells clustered across the substrate, but with no more inherent organization or outline than was found in the corresponding unpatterned control culture surfaces.

Interestingly, cells adhered and proliferated prominently at the boundary regions at the edges of the patterning close to the borders of the substrate [Figure 6.1]. High cell adhesion in this area was unexpected as the contribution of 'graded confluence', where the cells grow more densely and confluent in the centre of the substrate prior to outward growth, suggested higher confluence in the central regions would occur before growth at the boundaries. Figure 6.1 shows relatively sparse cell growth in the patterned area immediately to the right of the border as well as similarly thin cell growth beyond the dewetting effects to the left of the pattern border.

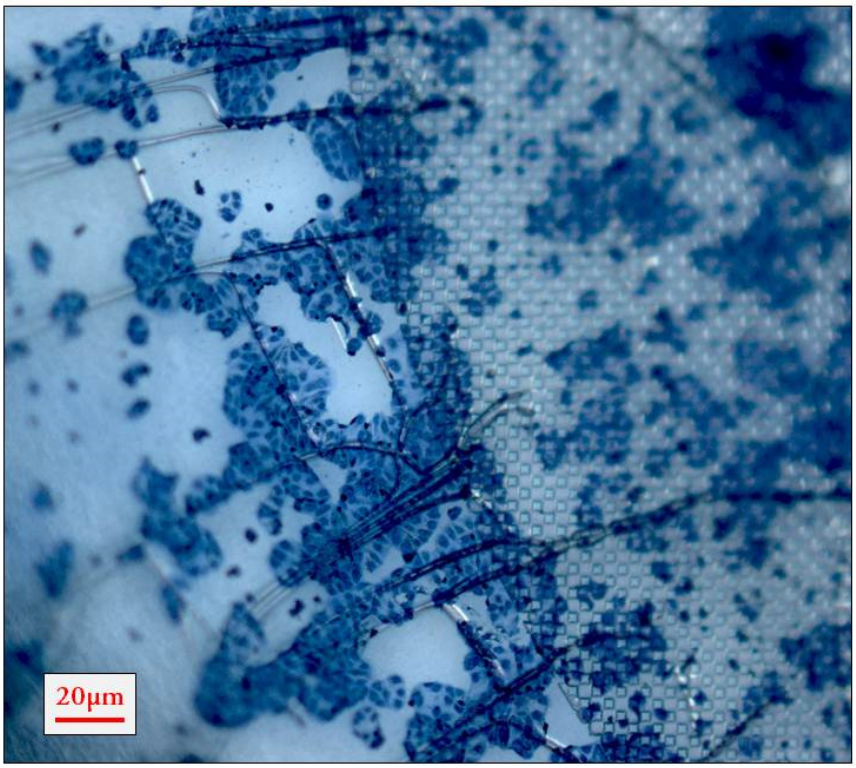

Figure 6.1 - Micrograph showing the Ishikawa cells, stained blue with Coomassie brilliant blue, organizing along the dewetting artefacts present across the patterned surface. Local organization effects were most obvious in the flat region adjacent to the patterned areas.

The cellular organization along the dewetting defects on the substrate surface, even within the pattern borders, provided the only observable effects of the patterned substrate. Growth along and around the linear branching features does not indicate any alignment to the features, but does serve as the central feature for local cell spreading. While the dewetting lines did not appear to dictate cell direction or limit cell spreading in any specific direction, the increased growth along and around these linear defects in comparison with the adjacent flat areas shows some preferential cell organisation to the artefacts.

The patterned variation in topography caused no observable variation in morphology, however. Ishikawa cells maintained the loosely polygonal membrane structure expected of an endothelial cell line. Because the size and shape of Ishikawa cells varies even in control cultures based on confluence and growth density, observations regarding morphology shifts across the multiple focal planes of the patterned substrates was difficult to document and interpret. While no cell morphology variation was noted, features of single cells were difficult to determine using the CBB stain, masking more subtle morphology and organisation effects. The nucleus and the boundaries of individual cell membranes were determinable, but the general protein stain

overwhelmed any more specific information. The experiment was repeated with phalloidin-conjugated actin fluorescence to increase contrast at the cell membrane boundaries.

Fluorescently stained cell cultures revealed a greater influence of the underlying topography than could be attributed using only bright field staining. Patterned substrates used in the repeat experiment consisted of 5 µm pillar features in regular arrays across the entire substrate. Fifty thousand cells were seeded in 300 µL of media per sample and cultured for 24 hours before fixation and staining. Cells were only stained for actin, not DNA, because the location and identification of the nucleus was conclusive with the previously analysed CBB stained experiments. Fluorescent imaging, however, highlighted the relationship of the actin cytoskeleton to the underlying pattern.

Generally, the Ishikawa growth appeared to have no relationship to the patterned surface, as seen with the previous CBB stained experimental results. As shown in Figure 6.2, however, instances of the cytoskeleton both specifically circumventing and enveloping the topographical pattern features, indicated by the yellow arrows, suggest some imposition on the natural organization of Ishikawa cell growth.

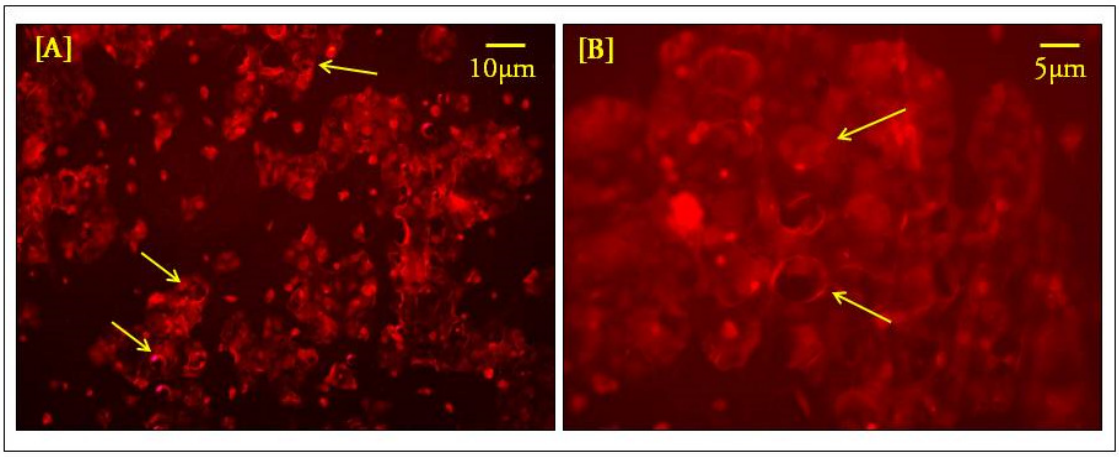

Figure 6.2 - Fluorescent images of actin-stained Ishikawa cells cultured on patterned substrates. Arrows identify example of incidences where the actin cytoskeleton has evaded or enveloped the underlying pattern topography.

High quantities of actin are visible surrounding the pattern features in the instances of evasion; whereas actin levels at the envelopment events are consistent with background cellular levels, suggesting the cells climbing over the patterns are more similar to control cell behaviour than the cells growing around the pattern impositions. Consistent with the bioimprint fluorescent staining, the poly(MA) was found to have a high absorbance of the fluorescent stains and thus

produced a high background, obstructing analysis of specific lamellipod extensions and adhesion points. While the inability to document particular adhesion locations was unfortunate, an unforeseen advantage to the high background fluorescence was that the pattern was often visible without overlaying images from a bright field channel.

Locally patterned substrates were also investigated in order to directly compare cell adhesion and morphology on patterned regions to the adjacent, relative 'flat' regions. Patterns varied in size, but were easily identifiable based on the corresponding CAD-designed mask information used to fabricate the master wafer. Cell seeding density was 5.0 x 10^4 cells/chamber, in approximately 250 µL of cell culture media, and cultures were maintained in incubation for 24 hours before fixation. Cell adhesion appeared to be greatly dependent on the location of the pattern on the substrate. Substrates containing regional pattern features more often exhibited decreasing confluence at the edges. As seen in the control cultures and on the bioimprinted substrates, cells seemed to grow most quickly in the centre of the chamber region, regardless of whether the central area contained the micro-scale patterning or not. Patterned areas from the outside toward the confluent centre are depicted in Figure 6.3, showed varied cell numbers ranging from practically no cells present on outer patterns to pattern overgrowth in the centre of the same substrate sample. Patterns in Figure 6.4 and Figure 6.3 consist of 15 µm negative hole features separated with 5 µm diamond pillar features within a triangular region.

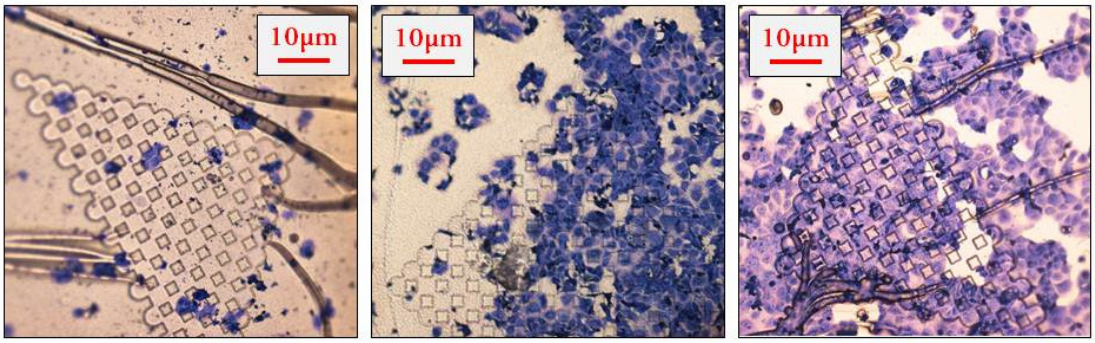

Figure 6.3 - DIC micrographs of CBB stained Ishikawa cells grown on patterned regions of poly(MA) substrates. Note the variation in growth density across the three sample regions, all taken from the same substrate sample; from left to right: edge of the substrate [left] to the centre of the substrate [right].

Bright field imaging at higher magnification confirmed the cell's limited acknowledgement of the underlying pattern surface. No difference in cell size was noted between the cells growing over the diamond pillars and the cells growing beyond the borders of the patterned regions [Figure 6.4]. The only consistent observation across all substrates was that the cell nucleus

rarely resides on the top of the diamond pattern features. The nuclei of spreading Ishikawa cells were consistently located in the negative, circular hole patterned portions of the local patterns. Similar deductions were difficult in the adhered, non-spreading regions due to the local optical absorbance density of the CBB staining. Areas of darker CBB staining were commonly visible across the substrate surface. Darker stained regions within a locally confluent organization were attributed to areas of denser protein population, possibly due to peeling up of lamellipodia or intracellular features containing higher protein content. Isolated points of darkly stained material were designated as cell debris caused by either the forced separation of cells previously adhered at that location or the random settling of cell debris at that location.

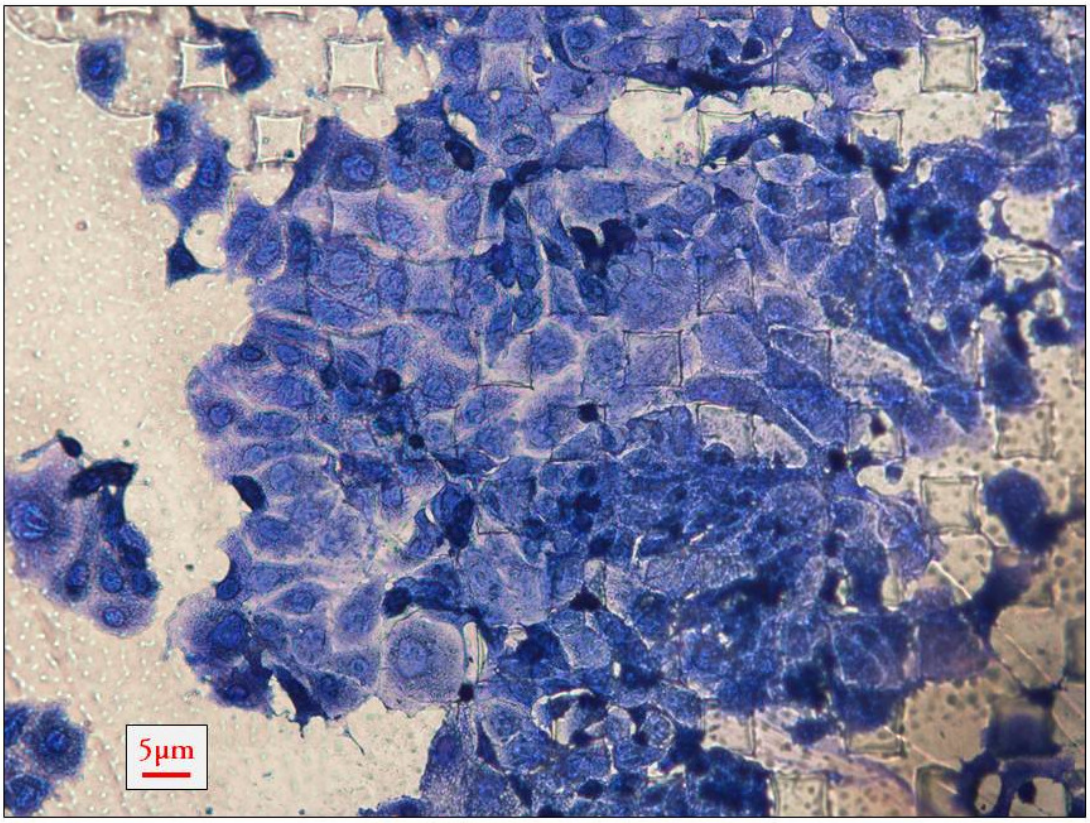

Figure 6.4 – DIC micrograph of CBB stained Ishikawa cancer cells grown on a patterned poly(MA) substrate.

The CBB staining method was only useful, in combination with DIC imaging, up to and including 20x magnification. Beyond 20x, the subtle differences in shadow depth produced by DIC only served to confuse the image. The membrane borders of individual Ishikawa cells were no longer discernable from random refraction noise. Therefore, the experiment was repeated and the resulting cells were fixed and fluorescently stained for analysis.

The supplemental information obtained by repeating the experiment with fluorescent staining provided different insights into the reactions of the Ishikawa cancer cells to patterned substrates. The experimental variables for the repeat experiment were similar to the original for cell seeding density, media volume, and duration of incubation. Fluorescent imaging proved to be complicated by the multiple focal planes represented by the tops of the diamond patterns and the bottoms of the negative hole features. For this reason, basic fluorescence microscopy was found to be preferable to confocal microscopy. Epifluorescence provided sum fluorescence from all of the fluorophores, whereas confocal images only recorded fluorophores on a specified focal plane. Bulk fluorescence allowed for observations to be made based on the presence of emission even when exact features were indistinguishable. Ultimately, fluorescent analysis confirmed several observations of the previous results and provided additional semi-quantitative information on actin density and more accurate identification of cell nuclei.

Ishikawa cancer cells seeded on the patterned poly(MA) substrates were documented adhering and growing to both the patterned and un-patterned regions of the poly(MA) substrate samples. Cell spreading, as in the previous iteration of the experiment, showed no hesitation in crossing the pattern boundaries; whether the initial cells adhered to the patterns and spread to the neighbouring flat areas, or vice versa, was indiscernible by the time of staining. Slightly contrary to the previous findings, however, cells growing within the whole feature patterns seem to spread to a larger size than the cells growing on the flat regions. The variation in cell size was most prominent on the patterned side of the pattern-flat interface, but returned to normal morphology within approximately 50 μm. Based on the Hoechst nuclear staining and the phalloidin actin staining [Figure 6.5 [A] and [B] respectively], the distribution of nuclei across the field of vision backed by a consistent layer of actin confirms the slight variation in Ishikawa cell size.

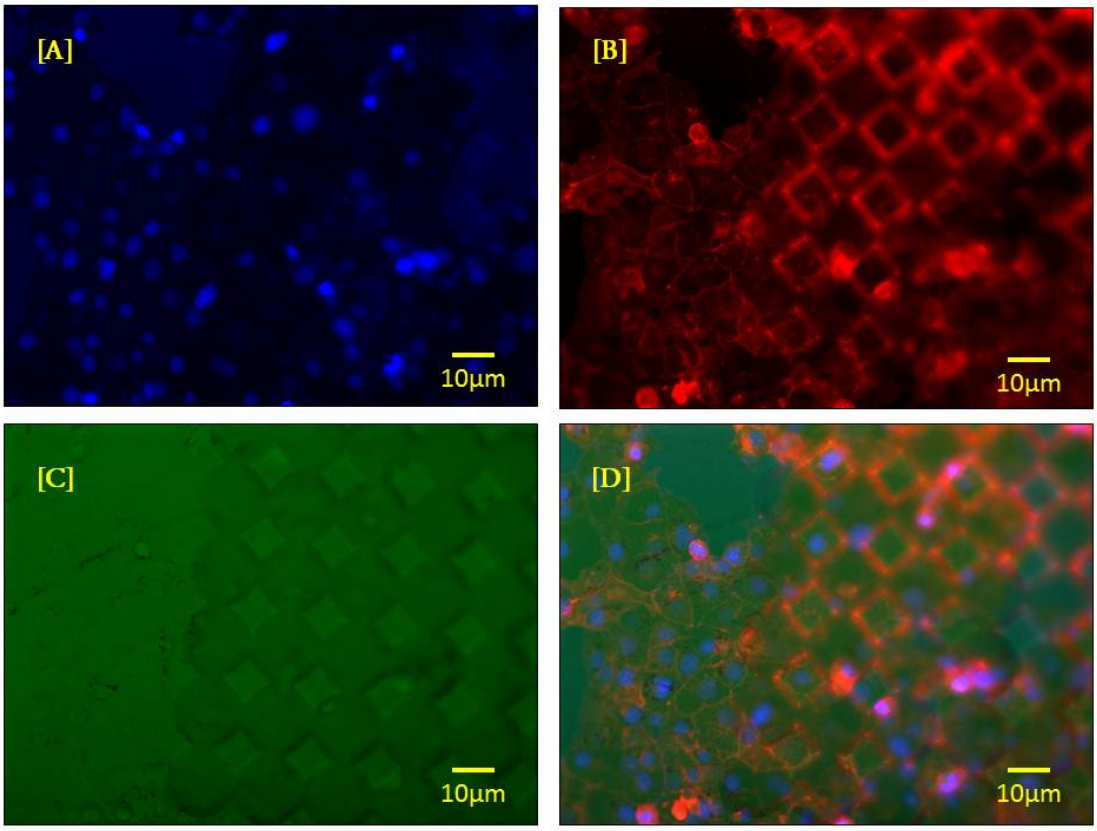

Figure 6.5 - Epifluorescent images of the [A] Hoechst-stained nucleus, [B] phalloidin-conjugated actin filitiments, [C] fluorescein poly(MA), and [D] channel overlay. The increased intensity of actin staining around the diamond pillar features is possibly due to some combination of two effects: the vertical summation of fluorescent emission during image capture and/or increased actin presence at the vertical walls of the pattern features.

Using only CBB staining techniques, determining the exact location of each cell nucleus was inaccurate. Using fluorescent imaging overlay [Figure 6.5 [D]]; however, the exact nuclear location could be accurately isolated. The new fluorescent overlay data showed some cell nuclei located on the top of the diamond pillar features [Figure 6.5 [D]], which was not evident in previous experimental iterations with general protein staining.

6.3 Discussion

6.3.1 Patterning effects

Pattern sizes in this work were relatively large compared to most current work in topographical substrate modification. There were two important reasons why 5-30 μm pattern features were chosen for this work. First, the initial publication on substrate topography patterning, from Chen, et.al. in 1997 and an extensive review on patterning done by Flemming, et. al. conclude that patterns on the same order of magnitude as the cells themselves have the most observable impact as substrate features [5, 26]. None of the previously published work had been completed using Ishikawa cancer cells. Ishikawa endometrial cancer cells tend to grow larger than other cell types and can reach up to 50 μm when fully adhered and spread. Therefore, larger patterns were used to in order to affect the cell spreading response. The second reason for the large pattern features was to isolate the effects of the nanotopography of the bioimprint from a cumulative topographical effect. Determining the effects of the micro-scale patterns allowed us to separate observations of cell growth on micro-patterned, fabricated substrates from bioimprinted substrates, full of biomimetic, nano-scale topographical features.

When the pattern features continued over the entirety of the fabricated substrate, the pattern showed little effect on the overall culture organization and growth. Cell clusters were visible across the diameter of the substrate. Interesting growth effects occurred, however, at the boundaries of the patterned regions near the edge of the substrate and along the dewetting defects created during fabrication. In the control cultures, few cells were seen as far from the central confluence region as the distance corresponding to where the pattern-flat interface was located on experimental samples. This suggests that the transition between the patterned and flat regions is more attractive for cell adhesion and/or proliferation than the patterned region itself. Additionally, cell organization around the de-wetting artefacts, particularly prevalent beyond the borders of the patterned area, was not linear enough to be deemed an ‘alignment’ per se; but the increased localised adhesion near and stemming from the linear de-wetting lines certainly shows an effective increase in cell population compared to completely flat poly(MA) regions.

The interface region between local patterns and adjacent flat regions, similarly, provided the most variable results for analysis. Cells were observed to grow larger just inside the patterned region, especially in the fluorescent iteration of the experiment, but also visible in the CBB micrographs in hindsight, cells grow larger just inside the patterned region. The exact size relation is impossible to quantify due to the limits of the microscopy methods, but sizes up to 50 μm can be seen on the pattern side of the feature interface in Figure 6.4 and Figure 6.5. These findings were verified by the location and relative distance between cell nuclei seen with Hoechst staining on the blue channel [Figure 6.5 [A]]. Cell nuclei are spaced further apart in the first 50 μm of the pattern features. Beyond the first 50 μm, the cells maintain a 'normal' cell morphology, but obviously react to the pattern by growing either over or around it.

The cell debris and peeling effects of locally confluent cells were not observed to the same extent on fluorescently stained substrate samples, in both full substrate and partially patterned fluorescent experiments. This is likely due to the increased washing requirements for limiting the non-specific background staining.

As seen by actin staining for both the full and partially patterned substrates, the patterns are visible even without a bright field or fluorescein channel solely based on actin wrapping around the pattern features. Whether the more actin that is present at the vertical walls of the pillar features of the brighter fluorescence is a visual effect of cumulative fluorescence, as viewed and captured from a top-down microscope, is unknown. As mentioned in the results section, some nuclear features were located on top of the pillar pattern features. Though it is unlikely that so many cells landed and adhered squarely on the pillar features, it is possible. More realistically, this suggests that the cells were capable of extending vertical lamellipodia to climb the 5 μm pillars. The vertical extension of the actin cytoskeleton would explain the higher fluorescence seen at the vertical borders of the pattern features.

Figure 6.5 above, corresponding to the epifluorescent results of Ishikawa cell growth on bioimprinted substrates Figure 4.18 in Chapter 4, cast doubt on the most promising of the preferential adhesion results discussed in chapter 4. The definition of the lithographic pattern features was certainly evident in the green, substrate-only, fluorescein channel [Figure 6.5 [C]]. In addition to the pattern features, however, indistinct cell-shaped shadows occur outside the pattern area. These areas are co-located with high-fluorescent regions of Atto 594 shown on the red channel. Fluorophore emissions from rhodamine dyes, such as Atto 594, and fluorescein have been known to produce some overlap in their emission spectra [98]. In effect, this means

the argon laser exciting the fluorescein at 488 nm wavelength will initiate some excitation in the Atto 594 rhodamine as well. To determine the plausibility of this rationalization, stained samples were examined under the B-3A filter of the Nikon 80i. Both the Atto 594 and the background fluorescein could be detected using the B-3A filter, suggesting that the cell artefacts off the pattern region were at least partially consisting of Atto 594 emissions captured at the high end of the fluorescein spectrum.

Overall, it can be said that the pattern features exerted limited influence of on Ishikawa cell organization. A possible hypothesis to explain the modest effects is founded on the use of cancer cells instead of a non-cancerous cell line. Though Ishikawas are a well-differentiated cancer line, which means they usually lead to less aggressive tumours and only moderately invasive disease [54], the cancerous nature could lead to enhanced adhesive properties. Metastatic cancer cells, cells already separated from the primary tumour and travelling through the circulatory system, require the property of being able to be extracted out of the blood flow and adhere and proliferate at an ectopic site. The on and off adhesion systems of cancer cells provides interesting areas of research for treatment and material interactions, but may also simultaneously complicate extrapolations from the results to applications for non-cancerous cells. Similarly, cell proliferation would expectedly be higher for any cancer, producing a larger population and a higher probability for successful adhesion and continued proliferation.

6.3.2 Poly(methacrylate) obstacles

Though the replication resolution of the poly(MA) imprinting was unarguably superior to any other method previously investigated, several inherent effects contributed to it eventually being discarded as a cell culture substrate. Induced stress, caused by the crosslinking reaction during UV curing, caused a concavity of the surface that was, in some cases, larger than the working distance of the microscope objectives. Surface artefacts were seen on both bioimprint and patterned substrate samples when replicating into poly(MA). And, even when the replication and surface features were perfectly in order, the seal between the poly(MA) substrate and the PDMS culture border for the second cell culture step was rarely water-tight.

6.3.2.2 Imaging concave substrates

There were two major implications of the concave substrates. First, and most importantly, several imaging complications arose from the variation of focal planes across the breadth of the substrate. Second, there was no way of imaging the secondary cell cultures.

Imaging complications ranged from 'mildly frustrating' to 'dead-end road blocks'. The majority of imaging for this work was done using the Nikon Eclipse 80i upright fluorescent microscope located in the Biological Applications and Technologies Laboratory at University of Canterbury. Bright field, differential interference contrast [DIC], and fluorescent imaging modes all experienced troubles imaging across the diameter of the substrate due to the concavity of the cured poly(MA). For any given field of vision there was the possibility of incorporating more than one focal plane. The resulting image then consisted of three general regions: above the focal distance, the in focus plane, and below the focal distance. This effect was greatly compounded at higher magnifications to the point that the x100 objective required extensive photo stitching to be useful. One possible method of circumventing this imaging obstacle was to take sequential pictures, varying the focus across the field of vision, and digitally stitching them together after the fact. Though similar to the biomaps technique used to document the topography across the entirety of the substrate surface, in this case, though the focal plane was changed the substrate stage was not moved. Several images of the same field of vision were taken at different focal planes in order to stitch together the equivalent of one field of vision image as taken from a flat substrate.

Confocal imaging methods also experienced complications due to the concavity of the poly(MA) substrates. The field of vision issues, which were merely complications in bright field microscopy, were incapacitating with confocal microscopy. Confocal microscopy relies on laser surface penetration, which varied extensively across the uneven bioimprint substrates. Figure 6.6 shows a gain image from the Leica TCS SP5 microscope in the School of Biological Sciences at University of Canterbury. The blue indicates the over-exposed, in focus region while the surrounding dark red regions are under-exposed and will show no detail in fluorescence. The thin, circular, gold band is the only region of the resulting image which would be in focus.

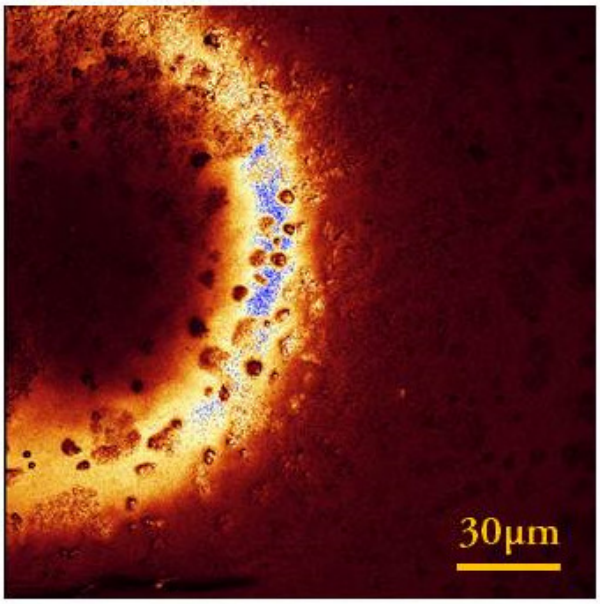

Figure 6.6 - Capture of the gain image of a bioimprinted sample using the confocal microscope. Darker areas represent underexposure while blue areas indicate overexposure. Only the bright, circular outline will be in focus when exposed.

The fastest solution to overcoming the concavity imaging obstacle was to consistently image the central region where the sloping gradient was least. Imaging the central region, however, provided its own complications. Due to the relatively small size of the poly(MA) discs, they were placed on microscope slides for imaging, as in the right schematic of Figure 6.7. When using inverted imaging methods, such as the confocal microscope, the polymer discs were placed with the bioimprint side down. As a result, the centre region of the poly(MA) disc was displaced above the glass slide by the depth of concavity. For the confocal objectives, the z-offset due to the concavity was greater than the working distance of the objectives, the largest of which is 290µm. In effect, no matter how flat the central region was, it would never be in focus.

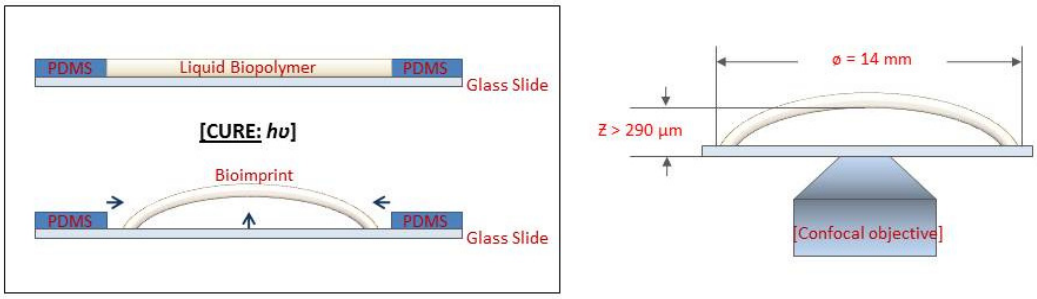

Figure 6.7 - Schematic representation of the central stress induced by the poly(MA) crosslinking during curing and the resulting height range beyond the 290 µm range of the lowest confocal scanning objective.

Stack slices could be taken to cumulatively counteract the out of focus issues cause by the concavity of each sample. The more slices necessary, however, the longer the laser scanning would take, the higher the photobleaching, and, while the maximum summation would contain the fluorescent information from all slices, the out-of-focus slices were still included in the summation. Therefore, the ideal solution was to focus on fabrication methods which would produce or retain a flat background surface after bioimprinting or patterning.

6.3.2.3 Identifying artefacts

While cross-linking stress was the predominant cause of artefacts, other cell culture variables also caused variation in the replicated surface. Poured poly(MA) was allowed to settle for several seconds before imprinting to incorporate all distinguishable surface features. In some cases, however, the only obvious cell features are the semi-spherical nucleus and the cell outline. Artefacts caused by stress, on the other hand, show high resolution cell features, but with additional noise. Two curing-related artefacts were commonly observed: a 'double-vision' artefact and a bubble imprinting artefact.

'Double vision' refers to an imprinting defect in which the features are replicated twice at a slight translational offset [Figure 6.8]. The offset between double-patterned features was due to the stress-induced movement of the curing polymer. Partial poly(MA) curing prior to significant crosslinking causes a partial feature imprint which was then re-replicated as the poly(MA) reaches mechanical stress equilibrium. This artefact was observed in both geometric replicas and bioimprints; and ranged from a 'dragging feature' appearance to two complete but offset feature replications.

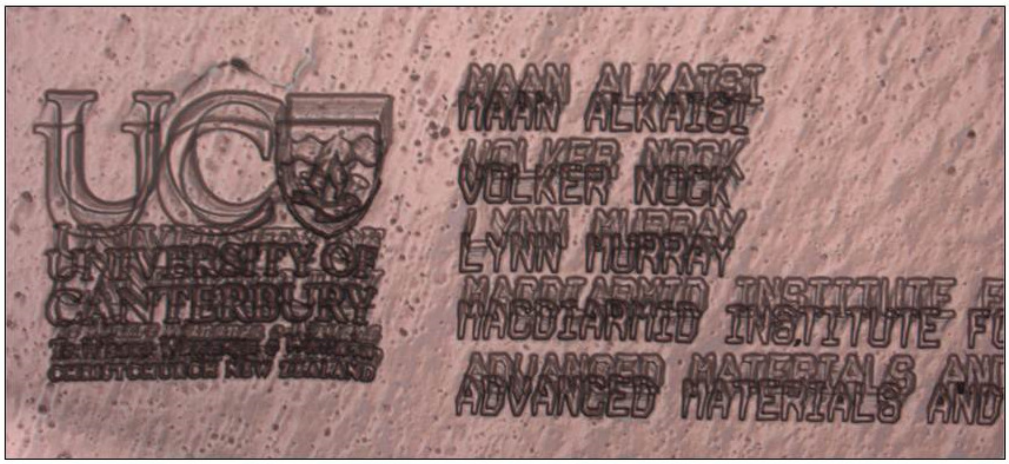

Figure 6.8 - DIC micrograph of the 'double vision' artefact.

The second commonly observed artefact of poly(MA) curing was the accidental imprinting of bubbles at the polymer-mould interface. Bubble formation at the surface was caused by the water vapour present after refrigerated condensation was heated by the UV light source during the imprinting process. The heat associated with the high intensity UV curing used for the poly(MA) caused the condensation to vaporise and bubble at the cell-polymer interface. The artefact [Figure 6.9] shows bubbles attempting to escape from the cell culture substrate and accidentally incorporated into the bioimprint. Fixed cells, ready to be imprinted, were refrigerated to prevent the denaturation of the fixed cytoskeletal crosslinks. [This denaturation effect had been previously observed by fluorescent staining of the actin filaments in control samples left to dry at room temperature.]

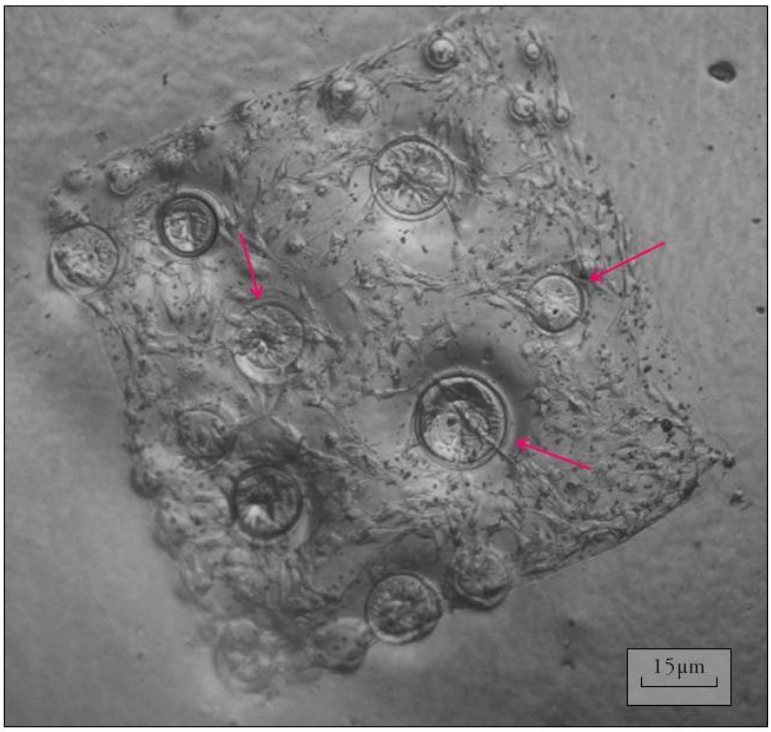

Figure 6.9 - DIC micrograph capture of bioimprinted bubble artefacts, indicated by pink arrows. Bubble artefacts are caused by the evaporation of condensation caused by the heat generated during UV curing of the methacrylate co-polymer.

To minimise the occurrence of this artefact feature, fixed template cell cultures were brought up to room temperature before being exposed to UV. While this alteration decreased the incidence of bubbling artefacts, some occurrence was still seen due to the thin condensation layer even at room temperature. Bubble formation was only seen in bioimprint samples as the polymer templates used for pattern fabrication were easily stored and maintained at room temperature. Atmospheric humidity conditions did not contribute sufficient condensation at the template mould surface to cause bubbling at the interface.

6.3.2.4 Secondary culture press-fit complications

Secondary cell culture on cured poly(MA) substrates, bioimprinted or patterned, was reliant on the fact that cells would only see the poly(MA). If the cell culture substrate was used as an island substrate sitting in a well of 24 well plate, the medium was easier to change and experiments could be carried out more efficiently, but any cells in suspension that happened to 'fall off' the top polymer surface had no hopes of ever getting back, thus skewing the adherent cell count numbers from the beginning.

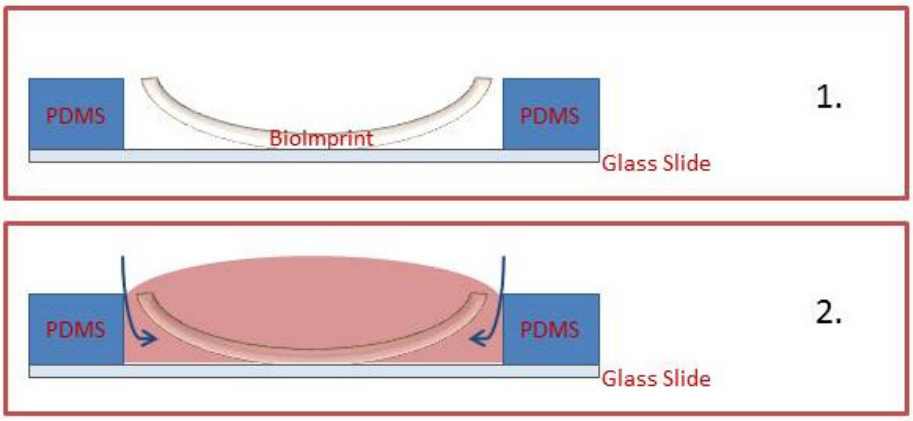

Figure 6.10 - Schematic representation of the bioimprint or poly(MA) substrates being press-fit, pattern-side up, into PDMS chambers of the same exact geometry [1] for secondary cell culture [2]. When cells, dispersed in media solution, are pipetted into the chambers, leaking underneath commonly occurred.

As a way to combat this gravitational side effect, cured and cleaned polymer substrates were press-fit into PDMS chambers cut with the same cork borer as those of the initial culture. Ideally, the substrates fit to the PDMS edges well enough to seal and not allow media and cell underneath. In practice, this often resulted in media leaking underneath the polymer sample [Figure 6.10]. And while this method was still likely to contribute more accurate adhesion and proliferation data than culture in a 24-well chamber, samples sometimes experienced unintended complications such as drying out or contamination.

6.3.2.5 Resolution

In spite of the time-consuming optimisation and characterisation, the poly(MA) curing process introduced some complications, which could not be expediently resolved. Due to the combined inefficiencies of the poly(MA) substrate fabrication and the inherent variation of mixing new polymers for each sample, the poly(MA) mixture was substituted as an experimental substrate. Throughout the remaining work, the poly(MA) continued as a highly valuable imprinting medium. The fabrication of patterned substrates and the replication of bioimprint features into polystyrene substrates are discussed extensively in the next chapter.

Because the cancer cells adhered to the traditionally non-adhesive methacrylate polymer substrates and proliferated in patterned and un-patterned locations with only minimal difference in morphology and organisation, perhaps non-cancerous cells would react differently to the topographical modification. Is the increased proliferation, a fundamental hallmark of cancer cells, enough to override and obscure any relationship at the cell-substrate interface? In order to determine whether topographical influences may be stronger for non-cancerous tissue cells, the project moved from Ishikawa cancer cells and began investigating muscle cells. The tissue engineering and regenerative medicine applications for were additional driving mechanisms behind the shift of focus.

7 Muscle cells on substrates

The decision to switch to a non-cancerous cell line was designed to eliminate effects of over-proliferation, a trademark characteristic of cancer cells. C2C12 myoblasts were decided upon for the continuation of this work due to previous success as a bioimprint template cell [46] and their ability to differentiate further to myofibrils or osteoblasts. Similarly, C2C12 myoblasts have been well documented in relation to patterned substrate research, highly relevant to the research undertaken in the following chapter.

Cell growth and morphology of C2C12 mouse skeletal muscle cells were characterised to determine basal experimental conditions. Time to differentiation and the importance of confluence for differentiation were determined separately. Complete differentiation was achieved in a few days after confluence in low-serum differentiation medium. [The equivalent experiments were never carried out for Ishikawa cells due to the existing knowledge available within the Laboratory for Cell and Protein Regulation group regarding growth, morphology, and behaviour of the Ishikawa endometrial cancer cell line.]

Due to discontent with the non-adhesive properties of poly(MA) substrates, other substrate materials were used to employ more desirable surface properties regarding substrate wettability and roughness. Tissue culture polystyrene [TCPS], glass microscope slides, Permanox® polymer slides, and polydimethylsiloxane [PDMS] substrates were prepared and investigated as cell culture substrates. Cell morphology was documented and analysed. Differences in substrate-dependent morphology and differentiation were observed and analysed.

7.1 Methods

The majority of methods used for the continuous sub-culture and analysis of C2C12 myoblasts were carried out identically to the methodology used for Ishikawa cancer cell culture and analysis in previous chapters. Sub-culture and splitting techniques, trypsinising and cell counting, fixing and staining protocols all translated across cell lines and were effective methods for C2C12 cells as well. Details regarding the specifics of these methods and protocols are located in chapter 2 for further reference. Methods specific to the experimental design discussed in this chapter and not previously included in other work are organised below.

7.1.1 Cell culture methods

The cell culture methods used for C2C12 culture were extremely similar to the methods used for the culture of Ishikawa cells. All C2C12 work was completed within the biological laminar flow cabinet in the BAT Lab at University of Canterbury. C2C12 stock cells were frozen down and kept in a liquid nitrogen dewer within the BAT Lab until use. Low passage replacement cells required after a contamination event were graciously provided by Plant and Food Research in Hamilton, NZ.

Two different media types were used to maintain the C2C12 cultures, depending on whether differentiation induction was desirable or not. High glucose Dubelcco's modified eagle's medium [DMEM] powder was used to create the basal medium for both working media types and was supplemented as required. One packet of DMEM powder was added per one litre of autoclaved, sterile water. Sodium bicarbonate was added [2.2-2.4 g/L] to buffer the basal media. The pH was adjusted to between 7.2 and 7.4 to ensure cell health and viability. Thoroughly mixed basal media was then vacuum-filter sterilised and stored at 4°C until use.

For general culture, sub-culture, and experimental work when differentiation was undesirable, basal DMEM was supplemented with 10% FBS, 1% GlutaMAX®, and 1% pen/strep [referred to from here on as DMEM-GM (growth media)]. In the opposite instance, to encourage differentiation, a different working medium was used. The same basal DMEM was instead supplemented with 2% horse serum [HS] and 1% pen/strep [referred to from here on as DMEM-DM [differentiation media]]. Both media were consistent with literature and showed no negative effects in culture.

Sub-cultured cells were maintained below confluence to prevent accidental and irreversible differentiation to myotubules and three dimensional growths [87]. At 70-80% confluence, cells were trypsinised and re-plated; in effect, this requires subculture splitting every two to three days for 5.0×10^3 cells/cm^2 initial seeding density. Experiments were designed to use cells as soon as possible to ensure relatively low passage numbers for experimental results. Sub-culture protocols used for splitting and re-plating were the same as those outlined in chapter 2.

7.1.2 Characterisation of differentiation

To determine the importance of confluence on the extent of and time to differentiation, C2C12 cells were cultured in DMEM growth media [GM] in polystyrene flasks and on Permanox slides. The polystyrene flask was maintained as the ultimate control for comparison with the smaller chambers, which were more easily accessed and isolated for experimental conditions. One 25 cm^2 [T25] and two LabTek II Permanox slides were plated with C2C12 cells, at 5.0 x 10^3 cells/cm^2. Each LabTek II Permanox assembly allowed for a quadruplicate experimental sample due to its four chamber divisions. All cultures were maintained at 5% CO_2 and 37°C.

After 3 days [72 hours] in incubation, the growth medium was aspirated and replaced with either FBS-supplemented growth media [GM] or differentiation media [DM]. Medium from one of the LabTek II Permanox slides was aspirated and replaced with fresh DMEM-GM. The metabolised media from the polystyrene T25 flask and the second LabTek II Permanox slide were aspirated and replaced with DMEM-DM. At 5 days [120 hours], the various media within the experimental cultures were aspirated and, at this point, all media were replaced with differentiation media and the experimental vessels were maintained in incubation. Cells were permanently removed from culture for fixing and immunofluorescent analysis after 11 days. The quantification of myofibril differentiation was based on the current definitions in literature [69, 73], identifying myofibrils by fusion of myoblast cell membranes. 'Mature' myofibrils were defined to contain five or more nuclei, indicating an advanced stage of myoblast fusion. Similarly, myofibrils were distinguished by immunofluorescent staining of myosin heavy chain [MHC], the majority component of myosin II, as previously demonstrated in literature [73, 99]. These experiments were repeated twice for validation, but were not repeated in triplicate due to the relatively long time required in culture.

7.1.3 Immunofluorescence

As discussed in chapter 2, immunofluorescence methods were used to detect the tag and detect presence of myosin heavy chain [MHC] in differentiated myofibrils. Primary antibody MF20 was used to bind to the location of MHC, a significant component of myosin II dimers responsible for the binding and contracting mechanisms of the actin-myosin cross-bridge structure critical for skeletal muscle contraction.

Cells were fixed with 4% paraformaldehyde for at least 30 minutes. Fixed cells were washed and then permeabilised with a 0.1% Triton X-100 solution in PBS for 10 minutes. Non-specific binding of the MF20 antibody was minimised by treatment with 5% bovine serum albumin [BSA] for at least an hour at room temperature. The myosin heavy chain antibody, containing a pre-conjugated Alexa Fluor® 488 fluorescent marker, was diluted 1:100 in 2.5% BSA solution and applied to fixed cells to incubate overnight at 4°C. After careful and prodigious washing in PBS, counterstaining protocols, as outlined previously, were applied.

7.1.4 Substrate characterisation

Identification of the differences in substrate chemistries and topographies were necessary to accurately interpret cell culture results. Atomic force microscopy was used to determine the surface roughness for TCPS and glass. AFM scans of 100 μm x 100 μm sample areas were captured and analysed using NanoScope Analysis software. Average [R_a] and RMS [R_q] roughness values were obtained for several scans. Comparable values for Permanox and PDMS were obtained from literature. Similarly, approximate surface chemistries were determined from product information and literature, except for Permanox for which exact chemical information remains patent-protected.

7.1.5 Substrate preparation

To identify the substrate-dependent effects on C2C12 growth and differentiation, control cultures were grown on tissue culture polystyrene [TCPS], glass, Permanox®, and PDMS. TCPS and glass are well documented control substrates within biological applications. Six-

well TCPS plates were used directly as the cell culture substrate for the TCPS experimental set. The glass experimental sets were cultured in petri dishes which had a portion of the bottom removed and replaced with a glass coverslip. The dishes were available commercially and were provided as a sample product by MatTek [MatTek Corporation, Ashland, MA]. They also provided an immediate comparison between the TCPS and glass at the interface between the two substrate materials.

PDMS is a common substrate for microfluidic applications and diagnostic tests due to its compatibility with soft lithography processing protocols [94]. For the PDMS substrates, liquid 10:1 PDMS was poured into three of the six wells in TCPS plates, desiccated, and then allowed to cure overnight in the desiccator. The plate was then baked at 80°C for 2 hours. Plates were re-sterilised with UV before cell culture use. No aging or solvent extraction methods were used to alter the PDMS substrate surface.

Permanox is a commercially available polyolefin cell culture substrate produced by Nunc-Nalgene [Thermo Fisher Scientific, Scoresby, Australia]. Permanox slides were used 'as purchased' with no additional modification or treatments. The slides were received as part of the LabTek II culture assembly which consists of the Permanox substrate with a polystyrene border structure adhered to define the cell culture region.

7.1.6 Substrate-dependent morphology and differentiation

Cells were seeded at 5.0 x 10^3 cells/cm^2 across all substrates defined in the previous section. Media volume was specific for each vessel type, but cell seeding density was consistent and normalised to the surface area of the substrate. Cells were grown in DMEM-GM for 120 hours [5 days] to ensure confluence across all substrates before differentiation. Medium was aspirated and replaced every 48 hours. Phase contrast micrographs were taken at approximately 24 hour intervals across the pre-confluent duration in order to document cell morphology across each substrate.

After 120 hours [5 days], cells had reached confluence across all experimental substrates. Rather than concluding the morphology experiments and restarting the exact set for differentiation experiments, the same experiments were continued beyond confluence to differentiation. To encourage differentiation, the media were changed after 5 days in DMEM-

GM to differentiation media. The differentiation medium [DMEM-DM] was consistent with relevant literature [73, 99, 100]. Media aspiration and exchange was scheduled and maintained every 48 hours with DMEM-DM as well. Differentiation progress was monitored by phase contrast microscopy.

Six days [144 hours] after the change to DMEM-DM [11 days total in culture], medium was aspirated and cells were fixed for immunofluorescent endpoint staining. All four substrates were stained in the same manner: immunofluorescent staining for myosin heavy chain and counterstained with Texas Red phalloidin and Hoechst 33342. Though different analysis methods were investigated for determining and quantifying the extent of differentiation, they turned out to be unnecessary and therefore will not be discussed any further.

7.2 Results

7.2.1 C2C12 culture and characterisation

C2C12 myoblasts tended toward a delineated, fibroblastic morphology when grown on tissue culture polystyrene substrates in control growth medium. Long and thin, these cells typically extended lamellipodia in one or opposite directions to network with adjacent cells. This bilateral extension ranged in distance, but individual cells reached 30 µm in length while barely exceeding the width of the nucleus, approximately 5 µm, in width [Figure 7.1].

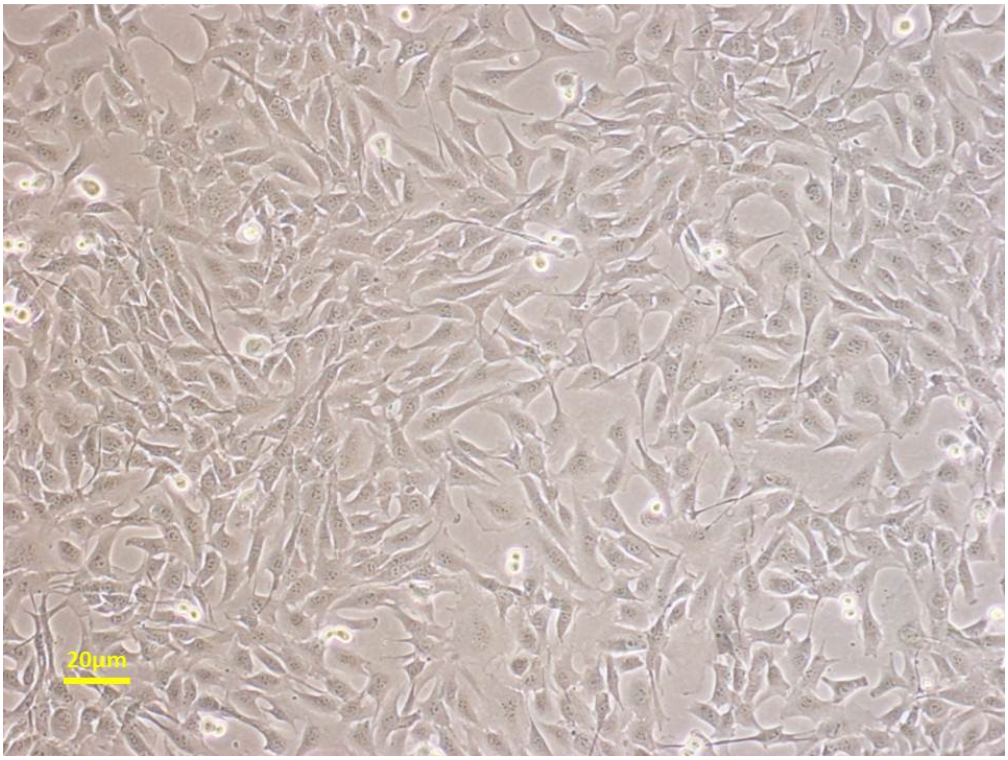

Figure 7.1 - C2C12 cells showing bilateral extension morphology in subculture just before sub-culture splitting (shown at 100 x magnification).

Cell proliferation and membrane interactions imposed an organised alignment of nuclei of adjacent cells. While this effect was difficult to quantify, a specific conformation was observed repeatedly in control cultures. The nuclei aligned in a curved line orthogonal to the directionality of the actin fibres and the lamellipodia extensions [Figure 7.2]. Even in low confluent circumstances, adjacent cells tended toward likewise orientation, creating a

brickwork-like, stacking effect. Neighbouring cell lengthening along a designated axis corresponded to the nuclear organisation [Figure 7.3].

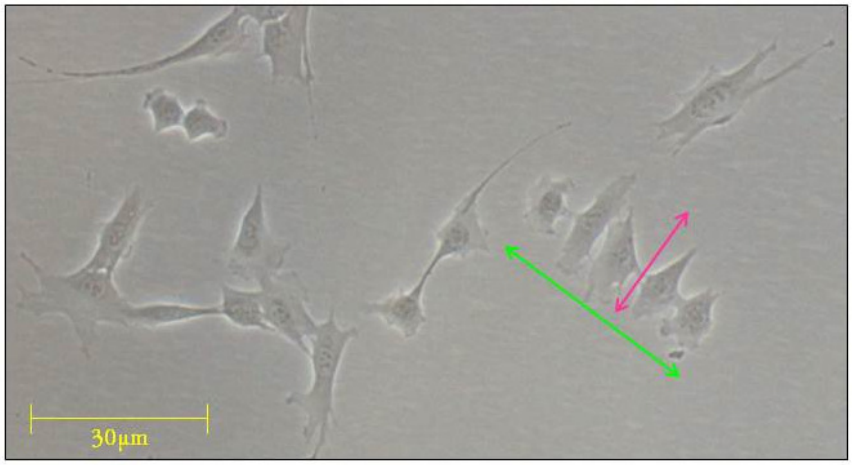

Figure 7.2 - Phase contrast image capture showing nuclear alignment of adjacent cells even in low confluence conditions. Nuclear alignment direction [green arrows] is perpendicular to the axial extension direction of local lamellipodia [magenta arrows].

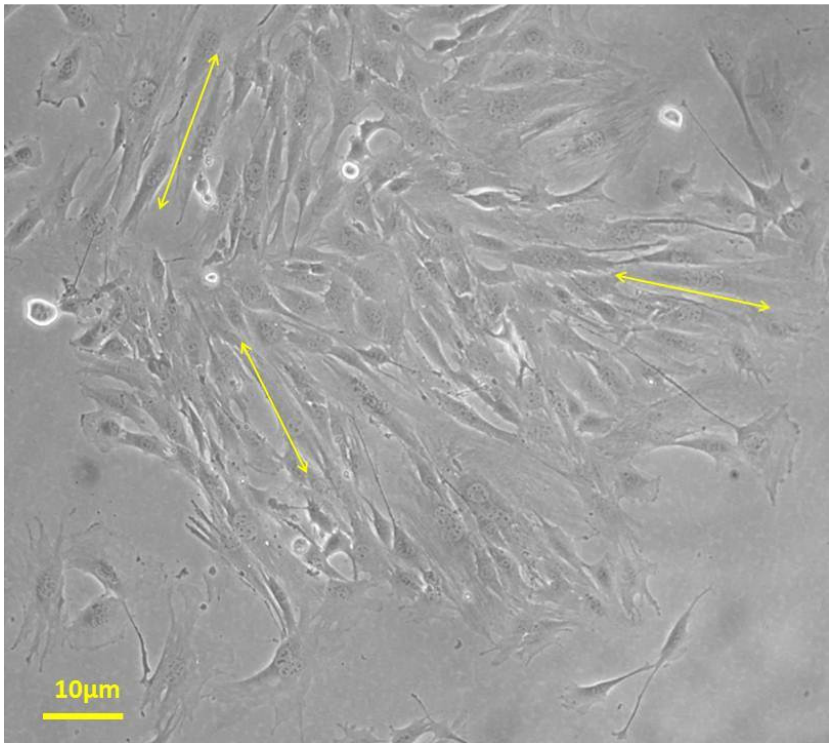

Figure 7.3 - C2C12 cells as grown in subculture. Arrows correspond to a generalised local orientation of cell elongation (shown at 200x magnification).

To investigate the effect the 'stacking' mechanism and local confluence imposed on differentiation alignment, three different experimental conditions were tested for confluence and extent of differentiation. A TCPS sub-culture flask was kept as the control across all time points. Two LabTek II 4-chamber slides were used as experimental cultures carried out in quadruplicate. Cells were plated at 0 hour and monitored for the duration.

At 72 hours [3 days] in DMEM-GM, the cells in the T25 polystyrene flask had reached confluence while the cells plated on Permanox were approximately 80% confluent. Importantly, minimal visible differentiation was noted in the confluent flask. The TCPS flask and one LabTek II 4-chamber slide were switched to DMEM-DM while the remaining LabTek II assembly was refilled with DMEM-GM. All cultures were re-placed into incubation for further observation.

While the experimental slide kept in DMEM-GM grew to confluence after 5 days in culture, no visible differentiation was seen. Cells seeded on the slide with substituted DMEM-DM grew more slowly and barely reached confluence even at 5 days also with no visible differentiation. No increase in differentiation percentage [remaining at < 10% differentiated] was observed before day 5 between cells switched to DMEM-DM prior to confluence and cells given two extra days in DMEM-GM [Figure 7.4].

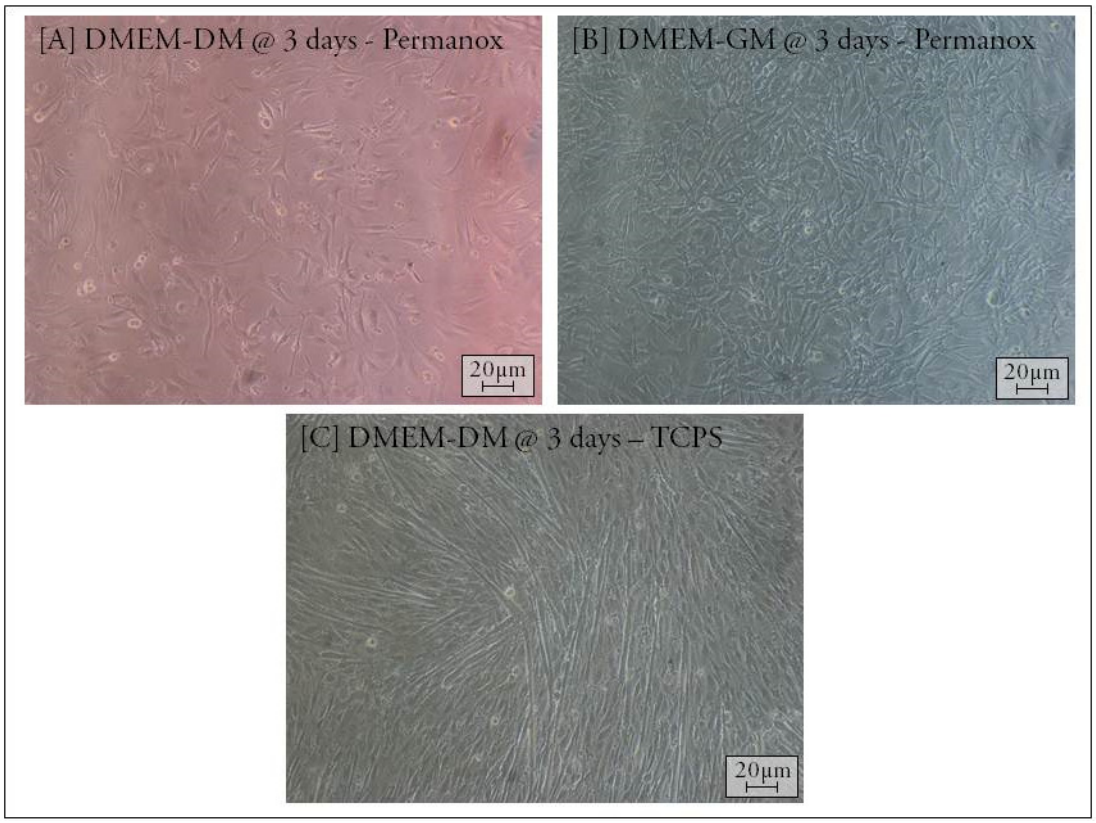

Figure 7.4 - Phase contrast micrographs, taken after 5 days in culture, showing the importance of confluence and media supplementation for C2C12 differentiation. [A] Cells switched in spite of incomplete confluence at day 3. [B] Cells with replaced growth medium at 3 day replacement now at approximate confluence. [C] TCPS culture flask control which was confluent at 3 days and shows notable differentiation at 5 days.

TCPS showed consistent differentiation across the substrate, but was difficult to image at high magnification due to the height of the flask. Low magnification images show local directionality of myofibrils, but inconsistent alignment across the substrate [Figure 7.5]. Notable differences in the extent of myofibril differentiation between the two LabTek slides occurred beyond 5 days, at which point the confluent slide had been changed to DMEM-DM [Figure 7.4]. The slide which was allowed to remain in growth medium until the cells reached confluence differentiated, though not to the same extent as the TCPS control flask. The slide which was switched to DMEM-DM before the muscle cells had reached confluence showed incomplete confluence and approximately no differentiation to myofibrils.

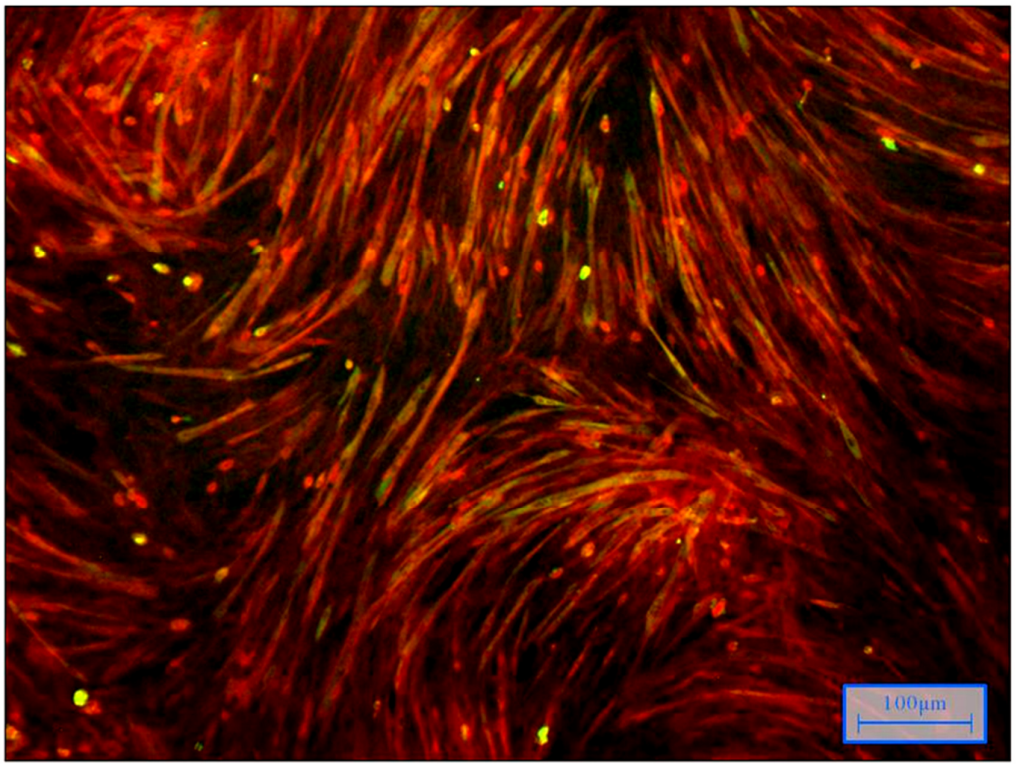

Figure 7.5 - Differentiated myofibrils grown beyond confluence within a T25 TCPS flask for 3 days in DMEM-DM. Shown orange/yellow due to the overlap and co-localization of actin [red] and myosin II [green], myofibres keep swirling alignment shown in locally confluent cultures, but show no continual alignment across the entirety of the field of view.

Use of the 50x lens [500x magnification total] provided the highest quality imaging as the variation across focal planes was overemphasised in 100x objective imaging. Hoechst staining was found to be overwhelming to the image and not necessary beneficial to overall analysis due to the cumulative nature of bulk fluorescence microscopy [Figure 7.6]. Any stained nuclear features present were detected by the bulk fluorescence, which often highlighted background and overlapping nuclei not directly relevant to the differentiation analysis. Differentiation was consistent but not continuous across the substrate. In areas where differentiation was minimal the confluent background network was visible. The only difference between Figure 7.6 and Figure 7.7 is the location on the substrate. Figure 7.6 shows the differentiated myofibrils whereas Figure 7.7 shows an area of confluent cell network where no myofibril differentiation occurred.

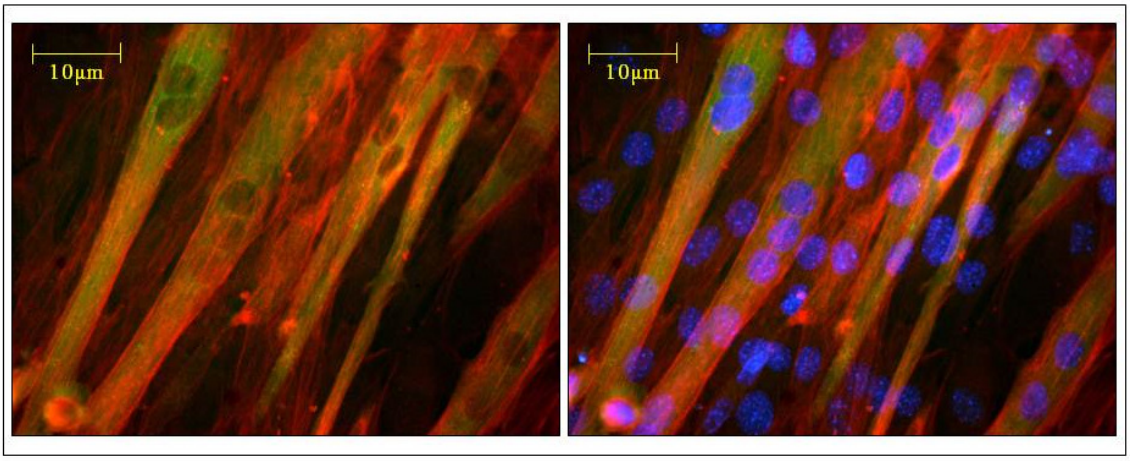

Figure 7.6 - Fluorescent micrographs of differentiated myofibrils grown on Permanox within LabTek II assemblies for 3 days after confluence in differentiation medium before immunofluorescent staining for myosin II [MHC] expression. The left image omits the Hoechst 33342 staining information whereas the image on the right contains the stained DNA fluorescence.

Interestingly, in all instances, the confluent background contained highly regular cells forming a support network [Figure 7.7]. As seen in Figure 7.6, nuclear features indicate the presence of the background monolayer even around areas of high differentiation.

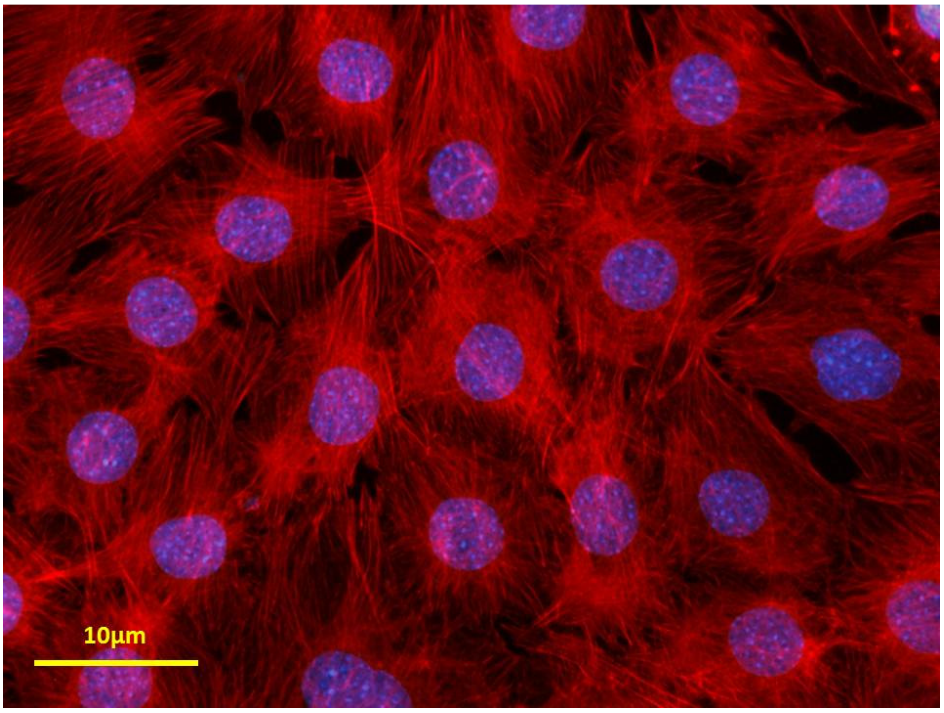

Figure 7.7 - Fluorescent micrograph of confluent C2C12 myoblasts grown on Permanox for 6 days total. The cells show no evidence of myosin II and in spite of being grown at confluence in differentiation medium.

7.2.2 Substrate-dependent morphology and differentiation

AFM analysis produced surface roughness values for TCPS were RMS roughness [R_q] = 10.1 nm and average [R_a] = 8.65 nm. Values for glass were R_q = 17.7nm and R_a = 5.4nm. Literature values for Permanox surface roughness show an R_a = 50nm ± 10nm [101]. Values on PDMS were difficult to determine with the AFM due to repeated tip retraction because of the elastic nature of PDMS. Similarly, roughness values in literature vary greatly due to common surface treatments and modifications. Reported by [102], PDMS surface roughness was R_a = 5.7nm ± 1.2nm.

Differences in cell morphology on different cell culture substrates were noticeable in the first micrographs taken at 24 hours. The most drastic differences were between the control substrates [TCPS and glass] and PDMS. Cells expressed the 'normal' spreading morphology of the C2C12 cells on both TCPS and glass substrates as expected. On Permanox, cells grew slowly, but still maintained the traditional phenotype shape. This corroborates the longer time to confluence observed in the characterization experiments.

On PDMS, however, cells presented a markedly different morphology. While there was no indication the cells were adhering more or less than on the TCPS substrates, the cell body showed very little spreading on PDMS and rarely grew larger than the size of the nucleus. Additionally, the extrusion fibres protruding from the cells were noticeably thinner and 'stringier' than the corresponding intercellular connections on TCPS. Due to the presentation of an altered morphology, focus was shifted to the differences between cells grown on control TCPS and PDMS substrates

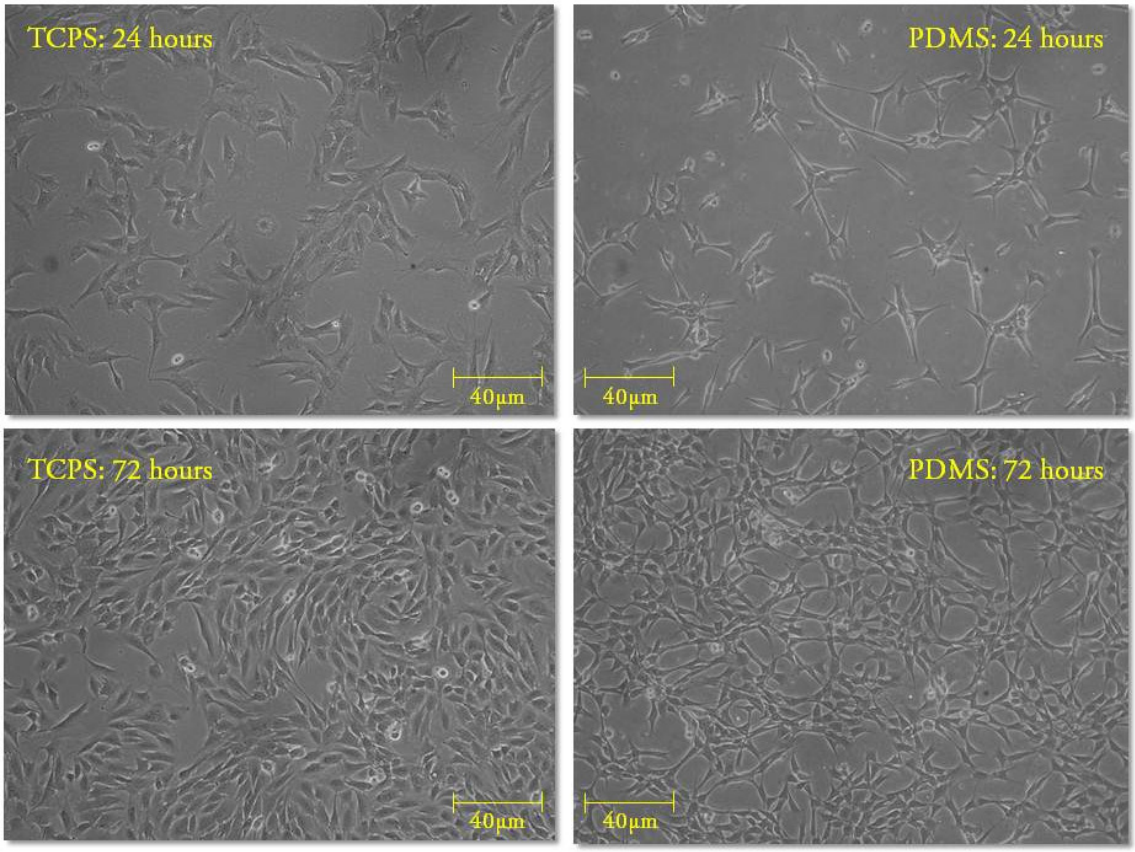

Figure 7.8 - Morphology comparison for TCPS and PDMS substrates at 24 (top) and 72 (bottom) hours. Note the swirl organisation on TCPS at 72 hours, not present in the network organisation on PDMS at the same timepoint.

The relative 'stringiness' of the cell lamellipodia was quantified by comparing the length to width ratio [aspect ratio] of single cells. The aspect ratio [A.R.] for each cell was determined in micrographs taken at 24 hours, before confluence, using ImageJ. By manually placing a four point boundary around each cell in and including the A.R. selection in the measurement tab, the relative pixel area of each cell and the aspect ratio were tabulated and exported to Excel for analysis. Figure 7.9 shows screenshots of the TCPS [A] and PDMS [B] micrographs with the four-point cell outlines highlighted in yellow. Results are summarised in Table 7.1.

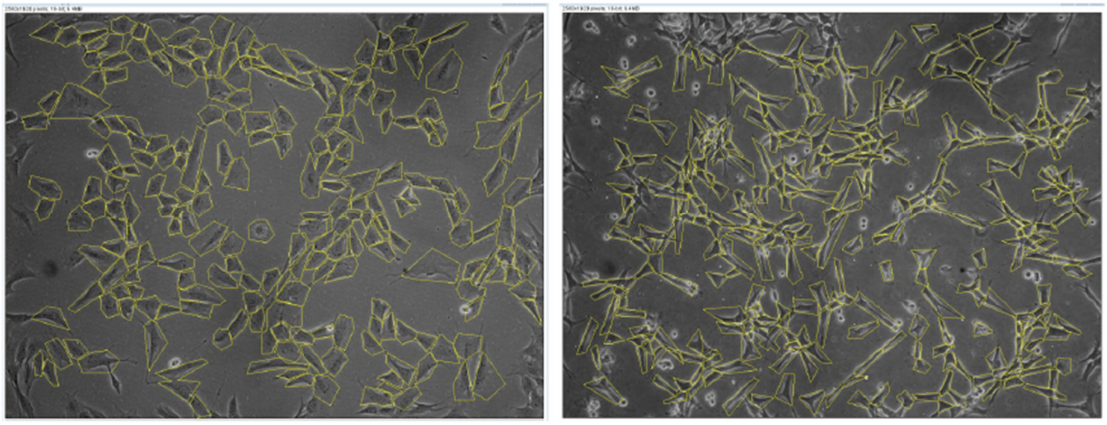

Figure 7.9 - ImageJ screenshots showing cells grown on TCPS (left) and PDMS (right) after 24 hours, each highlighted with a four-point boundary in yellow. Each cell boundary was measured for aspect ratio and area (in pixels). The exported data was processed in Excel to determine the average aspect ratio and area (pixels) per cell.

Substrate (24 hours)	TCPS	PDMS
Avg. Aspect Ratio	2.56	1.55
Avg. Area	17.3%	12.7%

Table 7.1 – Comparative values of average aspect ratio and average cell area for single cells grown and mapped on either TCPS or PDMS for 24 hours. Area percentages represent single cell area relative to the total image area.

Unexpectedly, the aspect ratio results show a smaller mean ratio for individual cells grown on the PDMS, which were observed to be 'stringier' and generally longer. This can be attributed to the lack of spreading by the cell bodies growing on the PDMS; meaning that even though the extrusion fibres produced by the cells on PDMS were longer and thinner, the cell bodies were still generally smaller and squarer than those found on TCPS. Some cells are barely adhered and maintain a 'rounded-up' phenotype. Because all cells were included in the analysis, the smaller central cells were weighted the same as the longer, spreading cells at the edges.

The higher degree of cell spreading on TCPS was reflected in the average cell area analysis. The exported data contained the bounded area for each cell in pixels; the single cell data was summed and averaged. Rather than converting the pixel areas to square microns, the pixel areas were compared to the total pixel count for the image size and determined as a percentage. In

the area analysis, higher cell spreading on the TCPS sample shows any given cell was seen to be about 5% larger than a corresponding cell on PDMS.

While this technique has a high error associated with it due to the manual and tedious nature of the outlining process, a broad analysis was enough to document the morphology variation in this instance. General trends in cell size and spreading were notable even based on the possibility of extreme user error. The objective of the four-point generalization analysis was to more clearly explicate the morphology variation observed between TCPS and PDMS substrates. Precise quantification would require repetition across several fields of vision on each substrate.

Continuing the experiment on to differentiation, the results showed an interesting phenomenon regarding the mechanism of C2C12 differentiation and how different substrates influence the effectiveness of this mechanism.

Only 24 hours after switching to differentiation media, myoblasts on TCPS showed general, random alignment and began to adhere on top of the confluent monolayer. Cells growing upward were identified by their relative brightness and comparatively rounded morphology. This three dimensional growth effect was even more predominant on glass substrates [as seen in Figure 7.10]. In both cases, areas displaying three dimensional developments were the areas in which differentiation initiated and extended from.

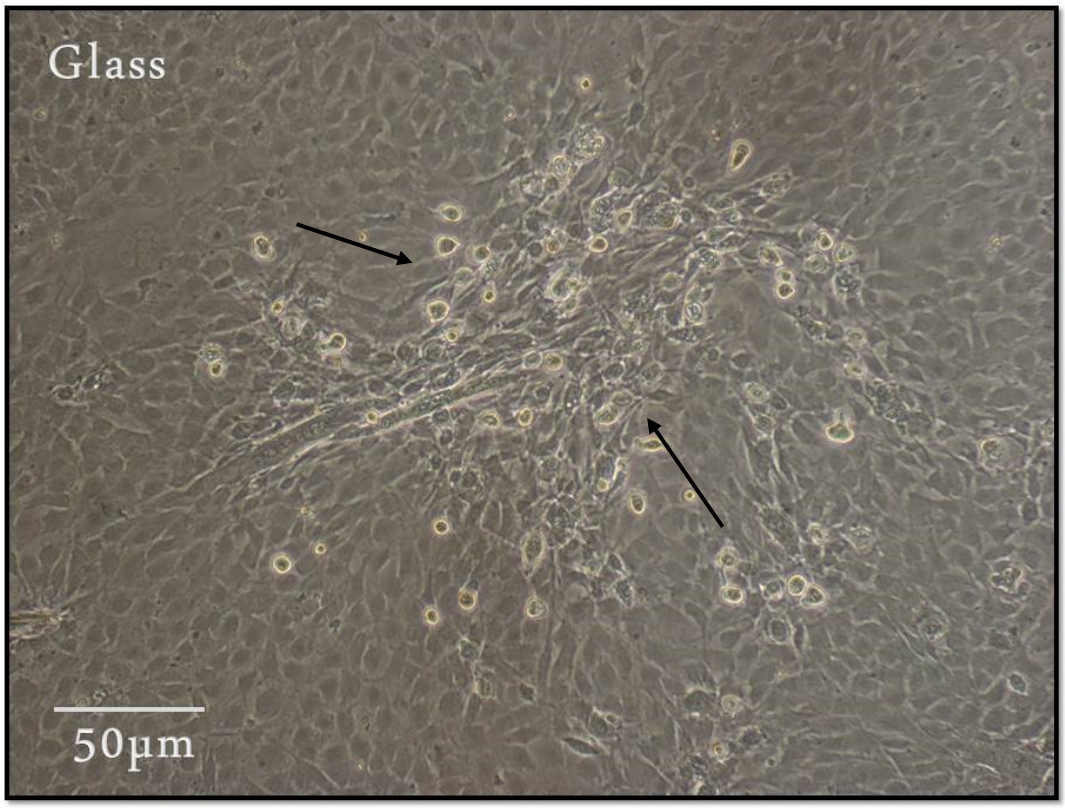

Figure 7.10 - C2C12 differentiation on glass 24 hours after changing to DMEM-DM. The micrograph shows the three dimensional nature of the continuous cell growth [indicated by the black arrows] and shows the beginnings of mature myofibrils forming.

Both polystyrene and glass substrates were predominantly covered in mature myofibrils by the end of day 6 [after 11 days in culture total]. Permanox showed some differentiation, but mostly cells pulled together to form three dimensional clusters above the confluent monolayer. Similar grouping was seen at the early stages of differentiation on TCPS, leading to the hypothesis that these cells would differentiate to mature myofibrils given enough time to develop. Cells grown on PDMS similarly pulled into three dimensional clusters, however, an apparent adhesion disparity led to the disruption of the underlying confluent monolayer [shown by the difference between the areas indicated by the blue and magenta arrows in Figure 7.11].

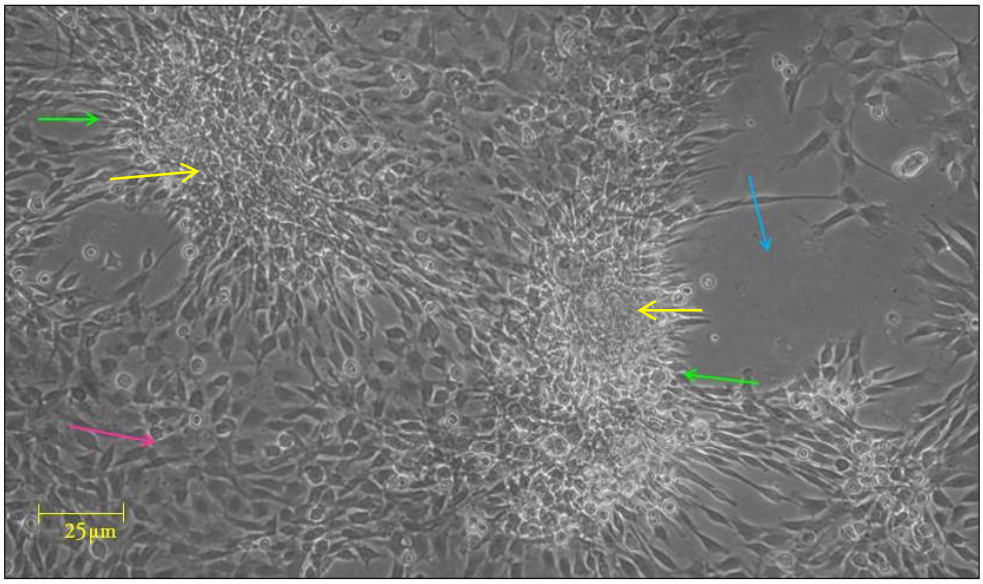

Figure 7.11 - Phase contrast capture of C2C12 cells growing on a PDMS substrate after 10 days [5 days in DMEM-DM]. Cells appeared to pull (green arrows) into the aggregating three dimensional clusters (yellow arrows) and leave open, non-confluent areas of the substrate (blue arrow) where a confluent background network should be present (magenta arrow).

Permanox and PDMS exhibited three dimensional grouping [Figure 7.11] similar to that seen in early differentiation, but as a result of decreased cell-substrate adhesion properties the end effect was drastically different. Instead of initiating differentiating, cells from the confluent monolayer appeared to be pulled from their adhesion locations on the substrate and into 3D aggregates. Many high density clusters formed on PDMS were accidentally removed to solution during media changes and staining washes. Trypan blue staining, conducted as outlined in chapter 2, was unable to penetrate the exterior of the cluster suggesting that at least the outer regions of the 3D aggregates remained viable in suspension

Differentiation on TCPS and glass proceeded as expected and after 6 days the only difference between TCPS and glass was the number of mature myofibrils. Mature myofibrils were defined [consistent with literature; [73, 99]] as myofibrils containing five or more nuclei. TCPS showed more complete differentiation and a higher number of mature myofibrils. As seen in Figure 7.12, the myofibrils on TCPS have a more developed length and all obviously meet the criteria for maturity as compared to the glass myofibrils which, while obviously differentiated remain thinner and shorter with only the central four qualifying for mature status.

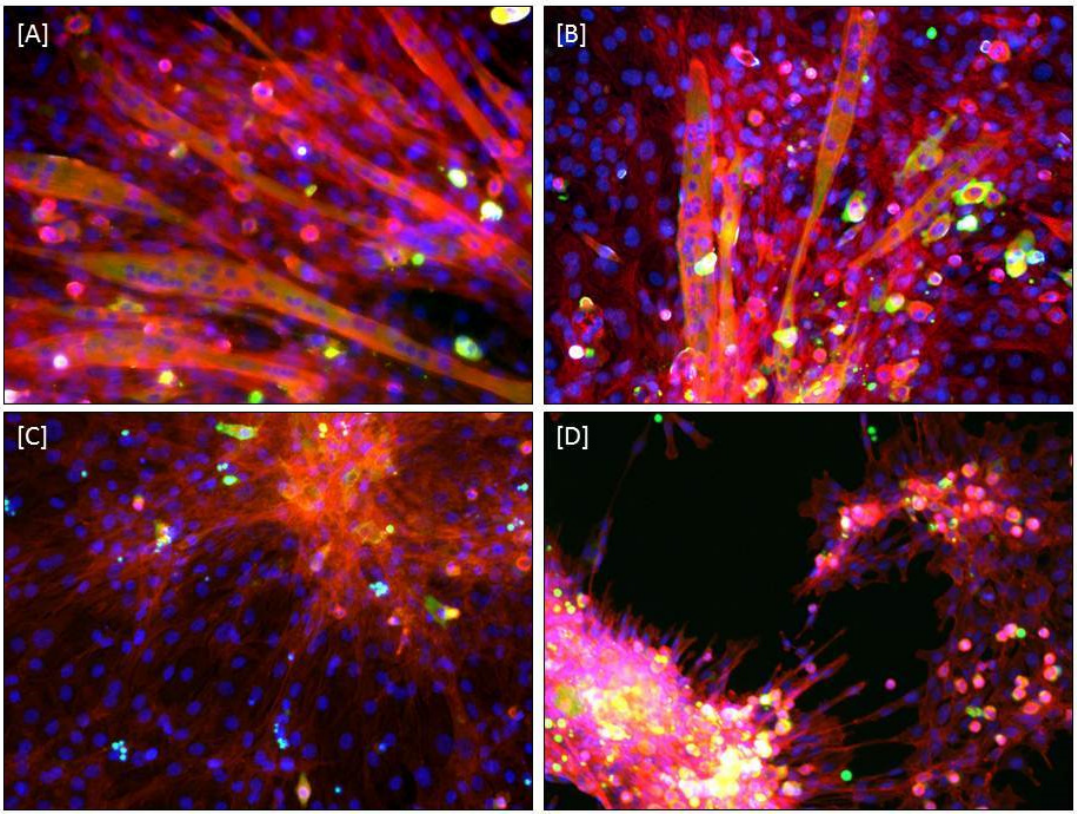

Figure 7.12 - Fluorescent micrographs of differentiated myofibrils on flat TCPS [A], glass [B], Permanox [C], and PDMS [D] substrates. Results show distinct myofibril formation on TCPS and glass substrates while cells tend to pull into 3D clusters on Permanox and PDMS substrates.

The consistent differentiation observed on TCPS and glass culture substrates was in contrast to the minimal differentiation on Permanox and PDMS substrates. Permanox substrates showed cells forming well defined, central clusters, which were seen as a precursor to differentiation on the control substrates, and maintenance of the confluent background network. Previous experimental work showed differentiation on Permanox substrates, though still well below the coverage and consistency seen on TCPS substrates.

PDMS substrates, however, continued to display the pulling aggregation seen prior to endpoint staining. No differentiation was seen in the clusters formed. While the green fluorescent channel was not blank, the stained features could not be identified as cells, like the green dot seen in the PDMS image in the bottom right of Figure 7.12. Lack of co-localization and identifiable cell features led to the suspicion that any MF20 staining observed within large cell clusters on PDMS substrates was due to non-specific antibody binding and cell debris staining.

7.3 Discussion

The results obtained from characterization of C2C12 growth and subsequent differentiation on different substrates with different chemistries and surface properties indicated an intentional organization and alignment not seen in Ishikawa cancer cell cultures. As opposed to the Ishikawa endometrial cancer cells used in the previous chapter, the C2C12 myoblasts developed to a more consistent size. Organization from the initial adhesion and nuclear alignment at low confluence persists through to complete monolayer confluence. C2C12 cells, especially before confluence and without differentiation media, grew in monolayers and were less likely to expand upward. Possibly, the early nuclear alignment may have required less cell movement during the cell fusion phase of differentiation and provided the underlying alignment cues for future differentiation.

Differentiation characterisation prior to the comparative substrate analysis allowed for method validation and provided an approximate timeline for differentiation. Two conclusions were drawn from the characterisation experiments. First, confluence, in and of itself, is not enough to drive substantial differentiation. Second, differentiation is not stimulated or enhanced when the differentiation medium is added prior to cell confluence. In fact, substitution with differentiation medium delayed confluence beyond the control set. Therefore, it can be concluded that for maximum differentiation opportunity, C2C12 cells should be grown to confluence in FBS-supplemented DMEM-GM before being switched to low serum DMEM-DM.

Substrate characterisation prior to cell seeding showed interesting similarities and differences across the four different substrate surfaces. All four experimental substrates are widely used in biological testing; TCPS is the gold standard for cell culture work, while PDMS is predominantly used for bioengineering and surface modification applications [103]. The exact nature of the surface modification treatment to convert moulded polystyrene into Corning® tissue culture grade polystyrene [TCPS] was not provided by the product specifications. Similarly, minimizing the chemistry of ‘glass’ to silicon dioxide implies a purity which is not necessarily accurate for all ‘glass’ samples and types. Permanox® is categorised by the product specification sheet as a polyolefin, meaning that its fundamental polymerisation unit is an alkene bond. While the exact nature of the side chains remains unknown, it is likely to have a hydrocarbon backbone more similar to polystyrene than to the silicon structures of glass and

PDMS. The predominantly hydrocarbon TCPS and Permanox substrates showed higher surface roughness, though in the case of TCPS, by only 5-10 nm.

In literature, substrate wettability is suggested to more greatly influence cell adhesion and proliferation than chemistry or topography [104]. Untreated PDMS was reported to have a surface contact angle measurement of 110° [105]. The hydrophobicity of the surface associated with such a high contact angle likely caused the increase in cell protrusions and lamellipodia seen from cells growing on PDMS substrates. Results of the aspect ratio and relative cell area analysis were counterintuitive but illustrated the difference between the cell morphology differences on TCPS and PDMS substrates. The 'stringy' morphology associated with C2C12 cells on PDMS likely reflects reduced forces of adherence and therefore the cells require increased number and length of lamellipodia, both for adherence and to overcome the distance to contact neighbouring cells. When these extrusion fibres break or cells grow locally confluent, the aspect ratio of the cell drastically shifts toward equivalence. An additional hypothesis suggests that the white outline of cells adhered to the PDMS [as seen in PDMS: 24 hours in Figure 7.8] is the refraction effects of the cell's adhesion forces on the elastic PDMS substrate. Importantly, all other substrate materials have high elastic moduli. A contributing condition to the altered morphology on PDMS could be due to the cell's ability to push and pull the substrate to some extent.

Comparison of the differentiation results across the four cell culture substrates showed that the TCPS and glass both produced consistent, mature myofibrils whereas the Permanox and PDMS substrates were less reliable. C2C12 differentiation was difficult to image within the TCPS flask, but at low magnification showed the highly organised local myofibril alignment. Glass and Permanox both grew to confluence more slowly than cells grown on TCPS. Due to lower confluence at the time of differentiation, cells cultured on glass never reached the same extent of differentiation witnessed on TCPS. Permanox substrates showed more variability than any other substrate. Areas of high confluence produced mature myofibrils comparable to the fully differentiated myofibrils seen on other substrates. Particularly in central regions, however, little to no differentiation was visible. Inconsistencies across the diameter of the surface could be due to the stress at the adhesion interface between the polystyrene chamber barriers and the polymer substrate. No other variable is inconsistent across the cell culture face.

After confluence and during differentiation, a background of myocytes was visible. In the suggested mechanism for differentiation supported by the results of this work, C2C12 cells

grow to confluence first. At confluence, the cells no longer have space to maintain proliferation within the two dimensional monolayer. 'Nucleation' sites for instigation of myoblast differentiation appear to be closely related to the instances of cells proliferating up above the confluent monolayer. The differentiating myofibrils generate from a central region, while maintaining an approximately parallel fibre alignment. This progression is most pronounced on TCPS and glass substrates. However, the maintenance of a complete confluent background network on Permanox indicates that, if this suggested mechanism is accurate and given enough time, complete differentiation would occur.

Differentiation experiments completed on PDMS substrates produced results that were consistent with the mechanism. The background network, which, though consisting of cells with a non-traditional morphology, did grow to confluence, was pulled away from the less adhesive substrate surface and into large, three dimensional cell aggregates. Cells growing up above the confluent layer with the intention of initiating differentiation may be the initiation points for these three dimensional clusters. As the cells are annexed into the loosely adhered cell clusters, the background monolayer is disrupted. No identifiable differentiation was visible within the cell aggregates, though trypan blue staining suggested that at least the outer layer of cells remained viable beyond monolayer growth. This further indicates the importance of an adhered underlying monolayer structure as a requirement of myoblast fusion and mature myofibril differentiation.

The organization of C2C12 cells across the culture area shows local alignment for both cell growth and continued differentiation. Extending this effect across the entirety of a desired region and to an exact patterned region would allow extensive myofibril networks to be created *in vitro* and tailored to individual, experimental needs. In the following chapter, the substrate-dependent results discussed in this chapter are taken a step further and analysed on substrates containing photolithographic patterns and bioimprinted C2C12 features.

8 Muscle cell growth on patterned substrates

This chapter expands upon the substrate-dependent morphology results included in the previous chapter to investigate the effect of patterning the substrates has on the variable morphology of adhered C2C12 myoblasts. Due to the suggested cytotoxic properties of PDMS [89] and the pervasiveness of polystyrene within biological research, opportunities to replicate from PDMS into PS were investigated and used to produce the substrates used in this work. Two categorical methods were used, solvent casting and hot embossing, and are described here in detail. Cell culture methods for growth and differentiation were carried over from previous experimental work.

Based on the observation and literature that grated patterns greatly increase directionality in C2C12 growth [106, 107], grated patterns of various periodic feature designs were included on the photomask for fabrication. An increase in differentiation alignment on these grated regions in comparison with the adjacent flat areas was posited. Similarly, it was hypothesised that using a patterned PDMS surface would increase cell adhesion and produce results more comparable with literature [57], as opposed to the differentiation results observed on PDMS in the previous chapter. A series of experiments was designed and completed to determine any alignment effects imposed by the patterned substrates.

The alignment influence of patterned topographies for the C2C12 muscle cells are of specific interest because of their differentiation abilities. Differentiation shown *in vitro* so far has been randomly oriented by cell fusion and inherent directionality. *In vivo,* muscle tissues group are obviously aligned to combine contraction force along a designated axis. Recreating the tissue structure on artificial substrates is necessary before continuing applications in regenerative medicine and muscle tissue engineering can be considered. Cell morphology on patterned PS and PDMS, before confluence and differentiation, was investigated.

8.1 Methods

The majority of methods featured in this chapter have been previously described in the scope of this thesis. Cell sub-culture and counting techniques used in this chapter were completed using the methods outlined and used in previous chapters. Photo- and soft lithography processes, detailed in chapter 2, were used for pattern design and fabrication. Elastomeric stencils were fabricated by exclusion moulding, as before, and the subsequent sterilisation and cell culture plating protocols were the same as when stencils were used to pattern Ishikawa growth. Patterns were defined and fabricated in the Nanofabrication Laboratory at University of Canterbury. Microscopy and analytical staining techniques were continued using the protocols previously detailed, as well. Cell culture and analysis were completed within the Biological Applications and Technologies Laboratory at University of Canterbury.

8.1.1 Polystyrene substrate fabrication

Methods were adapted from literature to transfer photolithographic patterns and bioimprint features into polystyrene substrates. Two general method categories were investigated. The first method attempted was solvent casting; the second was hot embossing.

8.1.1.1 Solvent casting methods

Solvent casting consists, fundamentally, of dissolving a polymer product into a solvent solution. The solvent solution, loaded with a polymer volume, is poured over a mould surface. As the solvent is driven out of solution by evaporation, which can be encouraged by heating, the remaining polymer content, conformed to the mould features, hardens to solid form. Two different solvent casting methods were investigated in this work. The first variation had been previously used in the Nanofabrication Laboratory by Dr. Volker Nock and was modified to produce patterned substrates [108]. The second was investigated much later in the project and was modified from the publication of Wang, et. al in 2011 [109].

Polystyrene pellets [MW avg ~35,000, Sigma Aldrich, St. Louis, MO] were dissolved in toluene [Sigma Aldrich, St. Louis, MO] at a known weight to volume concentration. The concentration was varied to affect viscosity of polymer mixture, but the most commonly used ratio was 8% polystyrene to toluene [w/v] [110]. The solution was left overnight for the polystyrene beads to fully and homogeneously dissolve into solution. The resulting solution was stored at room temperature in a protective fume cabinet until further use. SU-8 defined master patterns were used as moulding casts for this first solvent casting protocol. The mould area was surrounded by a well-sealed border before pouring, as liquid solvent, especially at lower polymer concentrations, could leak through conformal or resting seals. Metal rings were sealed to wafer either by a weight placed on top of the ring, not in contact with liquid polymer solution, or permanently affixed around the pattern area with superglue. The polystyrene/toluene solution was then poured over the cast area and allowed to cure for at least 48 hours before removal. The patterned polystyrene was carefully removed by cutting inside the metal boundary with a scalpel and slowly peeling the polystyrene sheet apart from the mould wafer.

The second solvent casting method was implemented much later in the project timeline. Following the methods published by [109], tissue culture grade polystyrene plates were broken into small pieces and dissolved in gamma-butyrolactone [GBL]. Samples were produced by Croydon Dennis, a third professional year undergraduate student at University of Canterbury, as completion of an undergraduate research requirement. Patterns were produced using AZ1518 photoresist on silicon wafers, instead of SU-8, and etching the pattern into the wafer by reactive ion etching. TMCS vapour was allowed to adsorb onto the wafer surface to minimise PDMS adhesion at the surface interface. Soft lithography was used to produce a PDMS mould from the etched wafer features. An outer PDMS ring was conformally sealed to the PDMS mould to prevent leaking and dewetting of the curing PS sheet. A 25% PS to GBL [w/w] solution was combined and mixed on a stir plate overnight to speed up complete solubility. The polystyrene/GBL solution was degassed before pouring into the PDMS mould. Two separate baking steps were done to ensure maximum solvent evaporation. The substrate assembly was first baked at 95°C, just below the boiling point of GBL, for 12 hours to drive the majority out of the solvent to evaporate from the cast assembly. A second baking step of 150°C for an additional 12 hours to cause remaining GBL to evaporate away and allow polystyrene to mould and reflow. After complete curing, the patterned PS sheet was separated from the PDMS mould and UV sterilised for cell culture.

8.1.1.2 Polystyrene embossing methods

Two different hot embossing methods were investigated concurrently with the solvent casting development. The first method relied on a stacked assembly on a hot plate [33]; the second method was adapted from Goral, et. al [111]. Both methods replicated patterns from PDMS moulds, created by soft lithography. Optical microscopy and AFM were used to characterise the pattern resolution and surface roughness. Polystyrene samples were sterilised by UV before use as cell culture substrates. For experimental cell cultures, pre-cut PDMS borders were either conformally sealed to polystyrene substrates or sealed using 45 seconds of Corona oxygen plasma.

The stacking method consisted of a sandwich assembly, weighted down and heated from below by a hot plate [Figure 8.1].

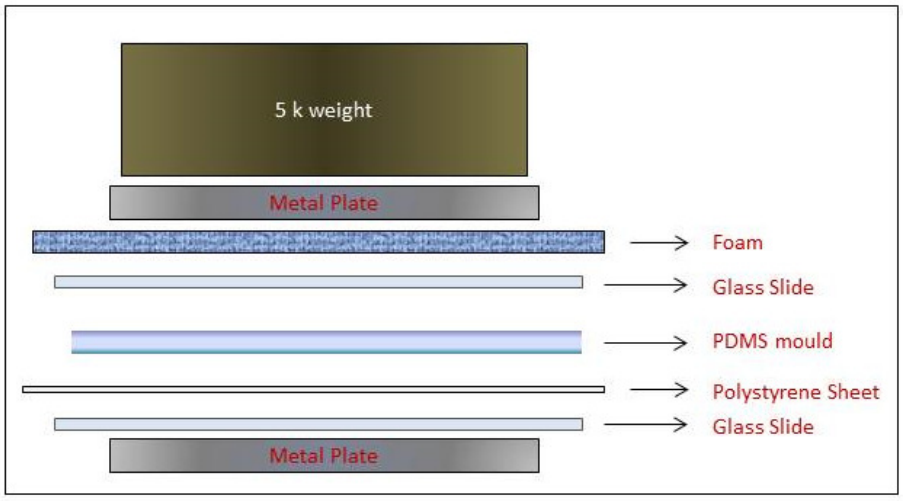

Figure 8.1 - Stacking assembly for hot embossing using a hot plate. The lower metal plate is placed directly onto the hotplate (not shown). Glass slides bracket the polystyrene to be patterned and the PDMS mould in contact. A foam layer, made of dense sponge material ensures equivalent distribution of the pressure generated by the metal plate and 5 kg weight stacked above it.

Styrene sheets were cut to approximately the size of a microscope slide and placed in contact with the PDMS pattern to be replicated. A sponge layer was placed on top of the PDMS mould in order to ensure the weight was distributed evenly across mould interface. Glass microscope slides and flat metal plates were placed on each side of the assembly; one beneath the polystyrene and one on top of the sponge layer. The lower metal plate was placed directly in

contact with the hotplate. A 5kg weight was placed directly on top of the assembly stack to add pressure to the heated system. The hot plate was set at 250°C. Time of heat application was varied to maximise melting and resolution. The entire assembly was removed from the hot plate and allowed to cool to room temperature before mould separation. Substrates were covered immediately to keep clean and only removed for imaging.

The second emboss method was adopted from Goral, et al. [111]. Polystyrene microscope slides were ordered from Nunc-Nalgene [Thermo Fisher Scientific, Scoresby, Australia]. PDMS moulds were created from photo- and soft lithography. Patterned PDMS moulds were conformally sealed in contact with a polystyrene slide. Glass microscope slides were placed on either side of the sealed mould and polystyrene slide. Four medium sized, ¾ in. binder bulldog clips were applied around the slide assembly, two on each side. The focal point of the pressure generated was placed directly over patterned regions of the PDMS. Multiple assemblies were constructed and placed in glass petri dishes for handling. The glass dishes, containing constructs for patterning, were placed in an oven set to 185°C for 10-15 minutes. Upon removal, assemblies were allowed to cool to room temperature before separation.

8.1.2 Cell culture methods

C2C12 sub-culture and seeding techniques used in this work followed the same protocols as sub-culture and counting for Ishikawa cells and previous C2C12 experiments. Myoblasts were seeded consistently throughout these experiments at an initial density of 5.0×10^4 cells/cm^2. Cells were cultured in DMEM-GM for general growth experiments and up to confluence in differentiation experiments. Differentiation was initiated by switching to DMEM-DM, the same as detailed in the previous chapter. For endpoint analysis, culture media was aspirated and cells were fixed for endpoint staining. Immunofluorescent methods, contained in chapter 7, were used to highlight myofibril differentiation.

8.1.3 Bioimprint protocol modifications

Bioimprint protocols were modified in order to produce a PDMS-based mould for polystyrene substrate patterning. Initial cell cultures were seeded and maintained within PDMS chamber borders in accordance with previously described methods. After endpoint media aspiration and

cell fixation, cells were washed to remove traces of fixative and buffer salts and left to dry in the fridge before bioimprinting. Concurrently, liquid PDMS was combined at a 10:1 ratio of elastomer to crosslinker, thoroughly mixed, and desiccated for at least 20 minutes before use. The initial cultures were removed from refrigeration and allowed to reach room temperature before bioimprinting. Liquid PDMS was poured into each of the three cell culture chambers, filled to approximately level with the top. Slides containing the conformally sealed PDMS chamber borders filled with liquid PMDS were placed on hotplates set at 80°C for 2 hours for PDMS curing. Similar to a solvent welding technique, the liquid PDMS was incorporated and inseparable from the pre-existing PDMS chamber borders, combining upon curing to a singular PDMS block. The resulting block was removed from contact and cleaned before future use as a mould within the polystyrene patterning protocols outlined in previously in this chapter.

8.2 Results

Polystyrene substrate fabrication methods produced substrates with varying resolution, thickness, and roughness properties. Characterisation of the surface features was done using bright field and AFM imaging analysis. C2C12 muscle cells cultured on the resulting polystyrene substrates and the inverted PDMS original moulds showed different extents of influence over the growth and organisation of cell adhesion and alignment. Grating patterns had the largest effect on muscle cell growth directionality on both PDMS and polystyrene substrates. Cells in differentiation experiments showed an alignment effect on differentiated myofibrils, this time on all patterned substrates instead of only grated pattern features. Positive bioimprint features were replicated into polystyrene and used as the first positive bioimprint substrate. C2C12 culture shows little alignment to the positive, random bioimprinted cell features.

8.2.1 Polystyrene substrate fabrication

Polystyrene fabrication undertaken early in the project was done using solvent casting from an 8% polystyrene to toluene [w/v] solution directly onto SU-8 defined master patterns. The resulting PS casts showed feature incorporation from the original mould, but not at the expected resolution. As seen by the profile data shown in Figure 8.2, both the intended flat and hole

regions developed a rounded profile. The peak-to-pit depth was about 1.5 µm. Feature width was consistently 5 µm from slope-to-slope. Periodic replication was consistent over 10 µm sections [blue markers in Figure 8.2]. In spite of accurate spacing, a wave pattern featured within the flat regions of the designed pattern [red markers in Figure 8.2]. Whether the pattern faults were transferred from the developed SU-8 patterns or an artefact of the solvent casting process was unknown.

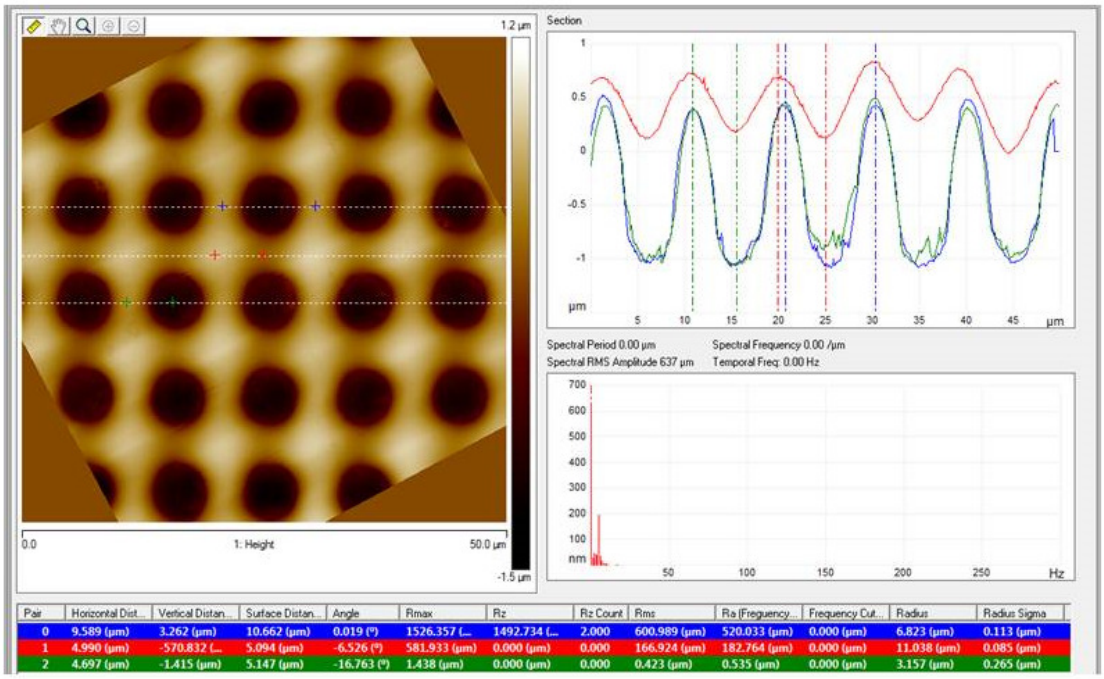

Figure 8.2 - AFM analysis from solvent cast polystyrene patterns moulded directly from SU-8.

Replication from PDMS using the 8% PS/toluene solution provided a thin PS replication once completely cured. The thickness of solvent cast patterns were inconsistent and depended heavily on the weight to volume of the polymer solution and the thickness of the bounding barrier. Increasing the poured volume increased the thickness of the resulting substrate and was easier to handle; but increased pouring volume also led to longer baking times, necessary to drive out all remaining solvent. Higher weight-to-volume polystyrene ratios showed no increase in pattern resolution from PDMS moulds.

Upon imaging, the solvent cast, patterned polystyrene layer showed noticeable microfractures at surface regions of high stress [Figure 8.3], namely around pattern features intended for replication. In the case of Figure 8.3, microfractures developed around this plus-sign alignment mark feature.

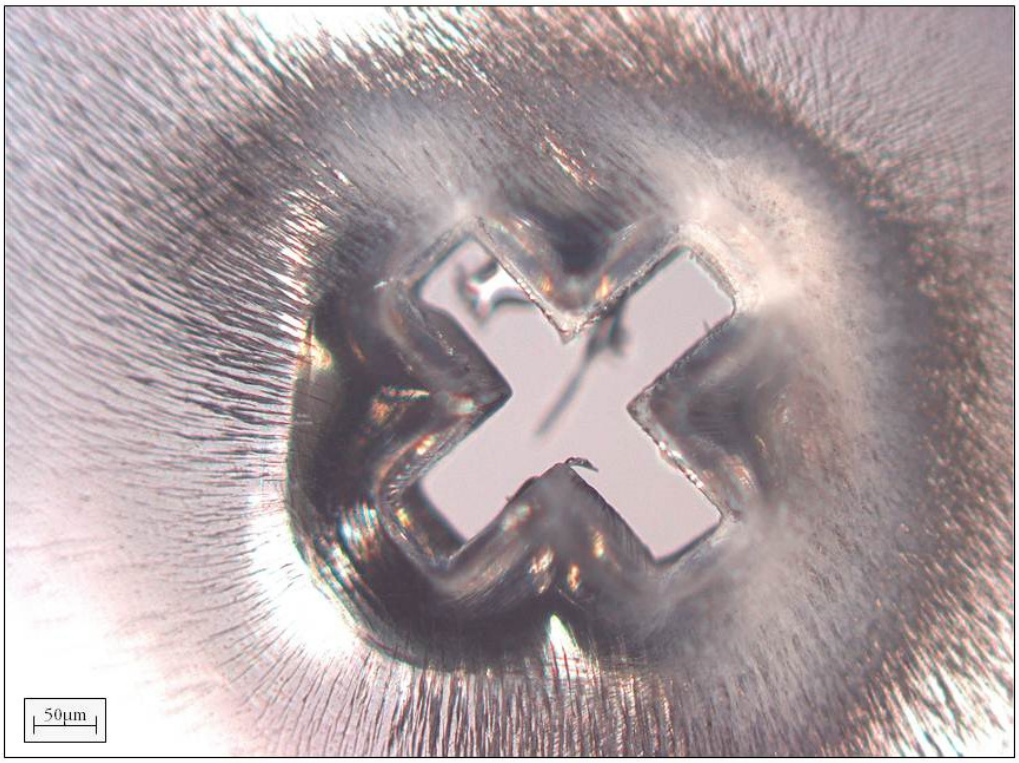

Figure 8.3 – Micro-fractures emanating from the larger alignment features of an SU-8 master used for solvent casting. The thinness of the solvent cast layer also leads to holes through the polymer layer instead of only indentions in the substrate surface.

Whether microfracturing occurred during curing or later during mould separation was unknown. Higher weight-to-volume ratios of polystyrene to toluene showed no significant improvement in cracking and led to adhesive removal of SU-8 as well. Similarly, the evaporation of solvent volume left this mould with insufficient polymer to effectively coat the entirety of the pattern, resulting in holes where pattern indentations were expected. Again in the instance of the cast plus-sign feature in Figure 8.3, the thinness of the substrate caused a through-hole exclusion of the original feature instead of a moulded replica.

At this point, the investigation of polystyrene patterning methods shifted to embossing methods. Embossing methods rely on heat and pressure to apply contact between the mould and a thermoplastic transfer material. The glass transition temperature for polystyrene is 95°C [112]; while this allowed for high-throughput and practical bench top embossing methods, the low transition temperature prevented the polystyrene substrates from being autoclaved for sterilisation. Opaque, sheet styrene was purchased [Evergreen Scale Models, Woodinville, WA]. Stacked assembly pieces were assembled on a laboratory hotplate prior to

the addition of heat. Incomplete melting of the polystyrene layer occurred for heat applications of 250°C for ten minutes [Figure 8.4].

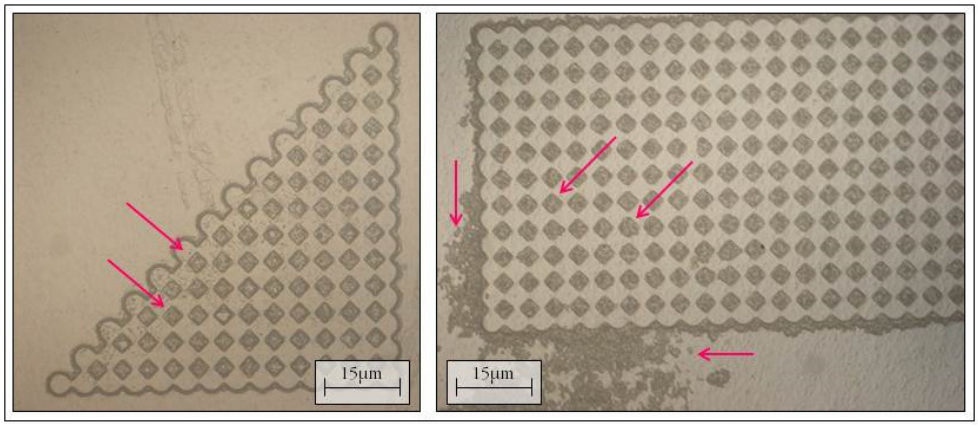

Figure 8.4 - Incomplete melting of polystyrene patterned using the stack-emboss method. Areas of incomplete curing are indicated by magenta arrows.

Incomplete melting of the polystyrene was characterised by the block formation of crystal-like inconsistencies within the moulded surface. AFM analysis showed that the flat areas of the substrate which showed complete melting were significantly flatter, but the overall roughness of the incompletely melted samples was higher than for that of the raw material [Figure 8.5]. Average experimental roughness [RMS = R_q and Average = R_a] for raw material was R_q = 217.67nm and R_a = 107.33nm. For the comparable AFM data on incompletely melted, embossed material the corresponding R_q and R_a values were 496.5nm and 363.5nm, respectively.

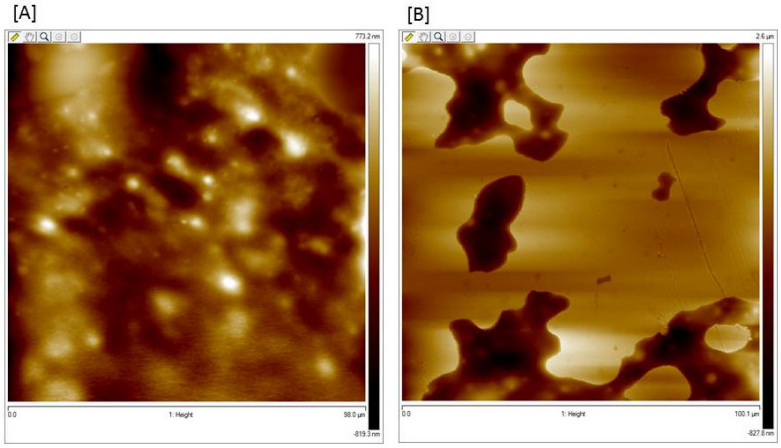

Figure 8.5 – AFM images of polystyrene prior to patterning [A] and melted after incomplete patterning [B].

The background roughness of the styrene substrates was higher than the comparable areas of poly(MA). It is unclear, however, if this is because of the innate roughness of annealed styrene, replicated roughness from the PDMS mould, or just overly exaggerated by the differential contrast microscopy methods required for imaging opaque polymer substrates. Polystyrene moulded from PDMS patterns contained a wave pattern in the substrate surface that was not present in polystyrene never contacted by PDMS [Figure 8.6].

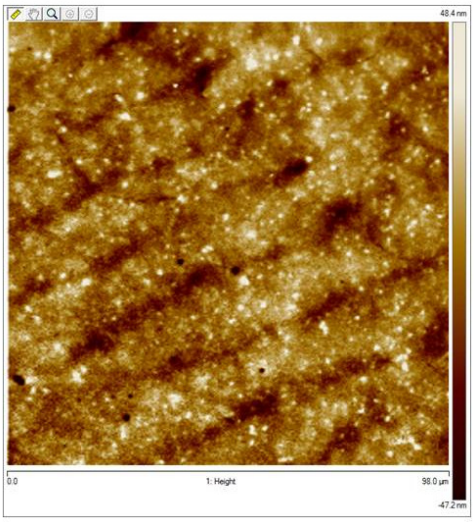

Figure 8.6 - Polystyrene moulded from PDMS containing a wave pattern in the polymer surface.

When time spent at 250°C was increased to 15 minutes, replication efficiency was increased as well. Lower instance of incomplete melting was seen and patterns down to 5 µm were successfully and accurately replicated [Figure 8.7]. Replication resolution was higher for larger pattern features.

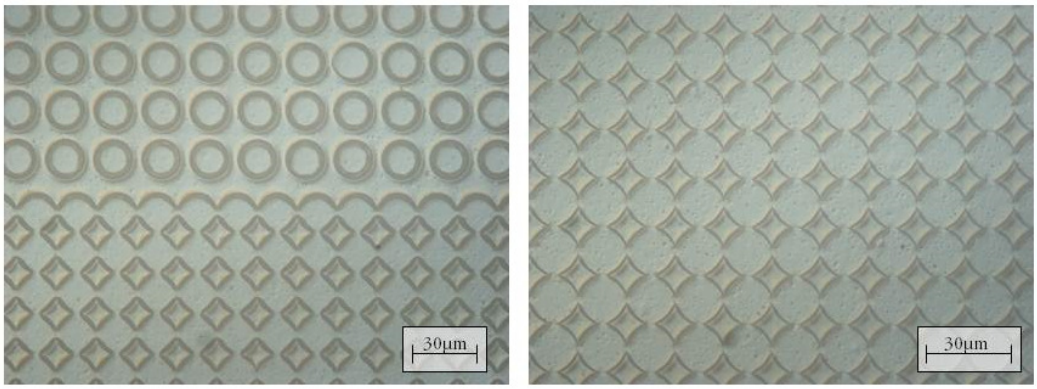

Figure 8.7 - Polystyrene patterned by stack assembly hot embossing.

Polystyrene microscope slides [purchased from Nunc] were placed in contact with the PDMS patterns and sandwiched between two glass microscope slides and bound with ¾" binder clips. The glass slides provided a more even pressure distribution across the polystyrene slide width. Clipped mould constructs were placed in the 185°C oven for 12 minutes. Samples were allowed to cool for an hour before disassembly and separation were attempted. Using the binder clip method, the achievable resolution was similar to that of the stacking emboss method, reliable down to at least 5 μm pattern features. Patterning with pre-fabricated polystyrene microscope slides had the additional benefit of maintaining its translucent property throughout the patterning process, which allowed for easier fluorescent imaging of cells.

Feature resolution using the weighted method depended heavily on the mould-to-styrene contact during the temperature dependent steps. Features transferred with high resolution, but consistently replicated only half of the desired pattern. Grating features on the Nunc slides replicated with no artefacts. Square and circular pillar patterns, however, were resolved completely in only one direction. Using Figure 8.8 as a reference, and imposing a two-dimensional x-y Cartesian coordinate system over the image, accurate replication was achieved in the y-direction, but was incomplete in the x-direction. Patterned substrates intended to contain a square or circular pillar pattern instead contained an undefined uniaxial component to the substrate topography.

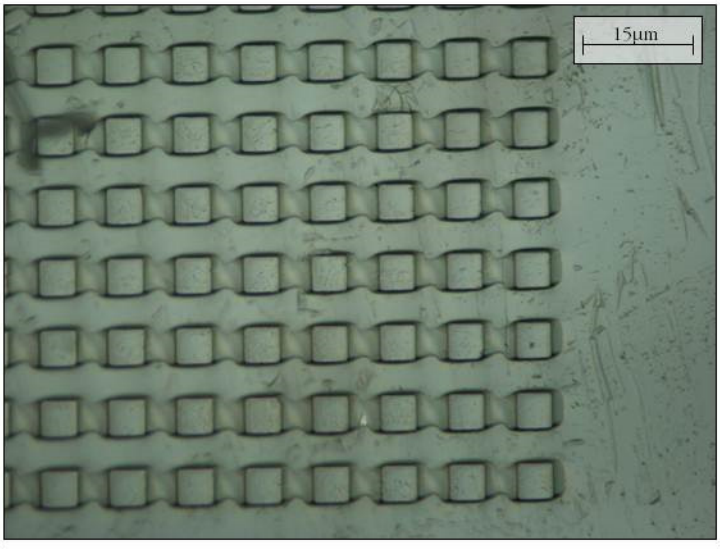

Figure 8.8 - Polystyrene patterned using the bulldog clip embossing method. The directionality of the replicated patterns showed some inherent directionality in the Nunc polystyrene polymer.

Solvent casting using 25% polystyrene dissolved in gamma-butyrolactone [GBL] produced high resolution pattern features; however, the resolution of these features was found to depend on the pattern resolution of the PDMS mould. Island features down to 1 μm side length or diameter were fabricated into a silicon master wafer and transferred to PDMS with soft lithography. When the PDMS mould was imaged, however, the collapse of small scale features, particularly thin grating patterns with high aspect ratios, was visible. It was unknown whether this collapse existed prior to PDMS moulding or not, but the collapsed features were further replicated using the GBL solvent casting method. Figure 8.9 shows the high resolution for the 5 μm circular island features [left image, top half] and the comparatively inconsistent resolution of the 1 μm features in the bottom half of the same image.

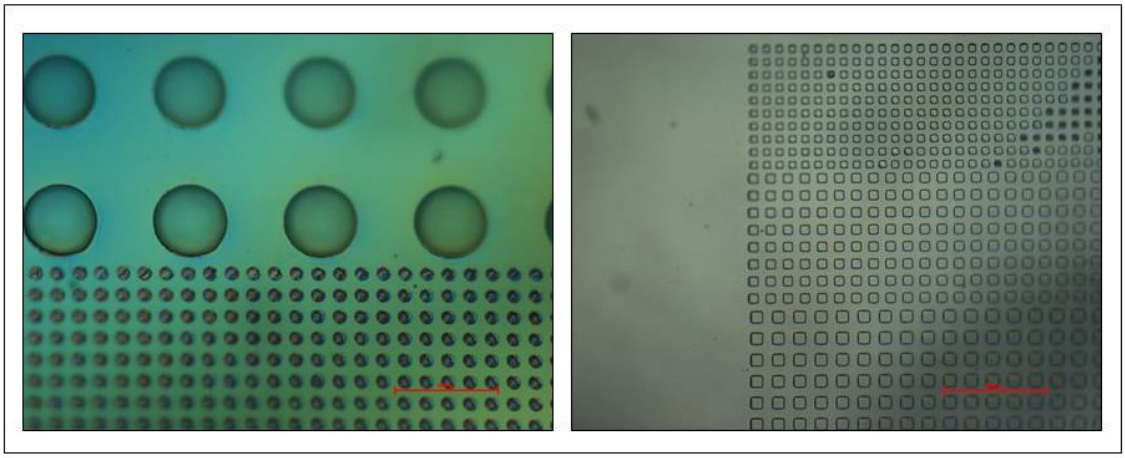

Figure 8.9 - Patterns replicated in polystyrene cast using the GBL solvent casting method. Note the high resolution for the larger features, but the decreased resolution for the features smaller than 3 μm.

The right image of Figure 8.9 shows a gradient of square island patterns cast in polystyrene. The 5 and 3 μm features [bottom and middle size gradients] replicate with consistent resolution; the 1 μm features at the top of the image show lower replication fidelity, evident by the darker, black features predominantly on right edge of the image. These substrates were sterilised and used as cell culture substrates in spite of the variable resolution of the smallest defined features.

8.2.2 C2C12 growth and differentiation on patterned substrates

To determine the effect of patterned features on C2C12 growth and alignment, experiments were conducted on both polystyrene and PDMS substrates. Similarly, two experimental sets were conducted to investigate morphology and phenotype manifestations prior to confluence and after differentiation. Fabricated substrates for the different polystyrene and PDMS substrates were plated at a consistent density to normalise for different substrate surface area. Polystyrene substrates generated using embossing methods were the size of a microscope slide, so PDMS chamber borders were used to define the culture bounds, the same as on glass substrates in previous chapters. Solvent cast polystyrene and PDMS substrates were both broader than the traditional 14 mm PDMS chamber outline. GBL cast polystyrene substrates were too thin to be handled extensively. Therefore, solvent cast substrates and PDMS moulds for culture were, adhered to the bottom of a 100 mm petri dish for cell culture.

C2C12 cells cultured on embossed polystyrene substrates, containing the same patterns used previously for the Ishikawa experiments, showed no noticeable effect on selective cell adhesion or directional growth. Cells grown on the patterns showed no overall preference for either the patterned or flat regions of the polystyrene substrates. Instead greater influence was imposed by a cell's position along the radius of the culture chamber. C2C12 cells near the middle grew to confluence on the pattern or off, while cells toward the border were rarer and less confluent. There was no noticeable distribution effect on localised cell adhesion specifically linked to the pattern features, as appeared to occur with Ishikawa cells on bioimprinted substrates. Myoblast nuclei almost never grew over the raised diamond features and, instead, fell within the 20μm holes. Similarly, connections between diamond features consisted of thin lamellipod extensions and any larger body growth was limited to the constraints of the holes. Endpoint staining analysis for the C2C12 cells above was done with CBB and fluorescent staining and showed that the location of confluence was the most relevant factor to cell growth distribution [left image of Figure 8.10]. Corresponding fluorescent cell staining showed minimal influence of island patterns on cell distribution and lamellipod extension direction and spreading, but did show the effect topographical patterning had on the location of the nucleus [right image of Figure 8.10]. Nuclei were rarely found over the positive diamond pattern features and were instead confined to the circular hole features.

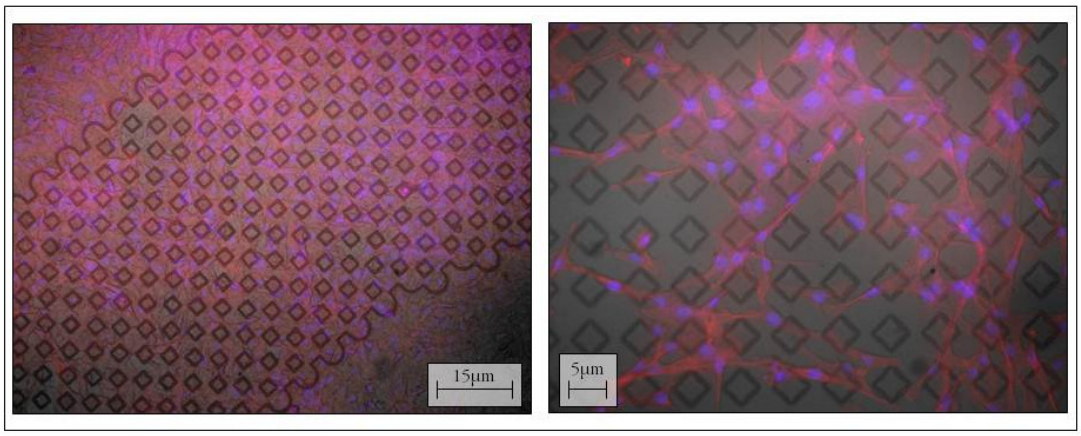

Figure 8.10 - C2C12 cells grown on embossed polystyrene substrates for 24 hours. Confluence [left] appeared to have more effect than the pattern features. Nuclei were almost completely confined to circular hole features instead of climbing or adhering to the diamond island features.

On solvent cast polystyrene substrates which contained grated patterns, developed using a different defined photomask for photolithography, C2C12 cells showed a notable tendency toward alignment and orientation along the grated features. As shown in Figure 8.11, cells aligned along the linear pattern features. Cells growing beyond the patterned region maintained the normal, fibroblastic morphology of non-confluent C2C12 cells and happily grew in cluster up until the border of the patterned region. Grated line patterns were not incorporated in previous mask designs. The morphology variation on the grated features also appeared to either lower the speed of cell proliferation or discourage adhesion, as confluence at this region was reached later than that across the surrounding flat regions.

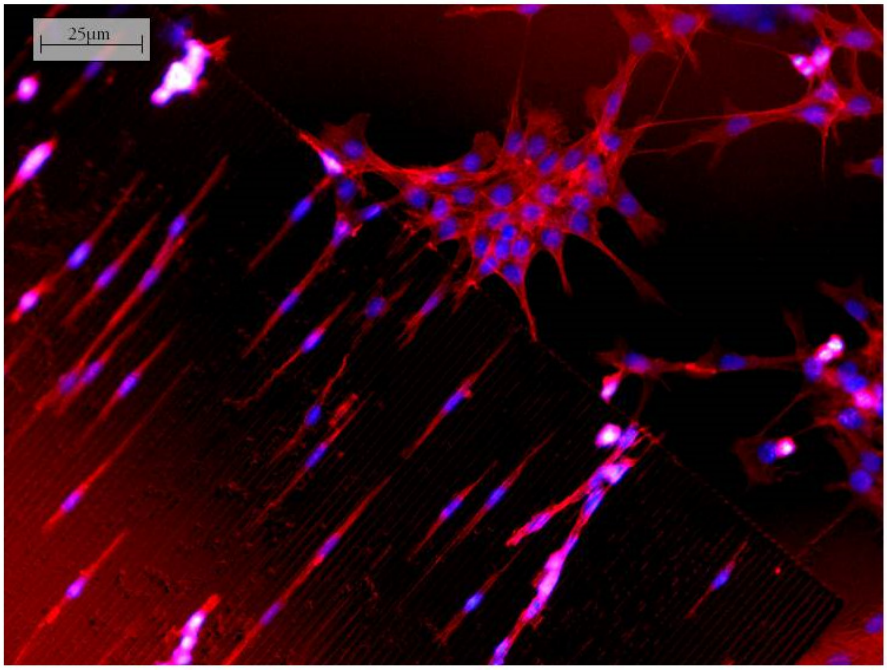

Figure 8.11 - Delineation of C2C12 cells grown on polystyrene grating patterns. Note the drastically different cell morphology on the grating pattern and outside the pattern features.

Morphology variation across patterned substrate topography was observed to depend greatly on the particular topographical feature in question. Pillar pattern showed little influence on size, extension, and cell numbers when compared to the flat areas of the same substrates. In contrast, grated patterns showed highly ordered alignment effects on adhered myoblasts prior to differentiation. Figure 8.12 shows two phase contrast micrographs taken on the same PDMS substrate after 48 of cell growth in culture. The figure on the left shows a region of the PDMS substrate patterned with various sizes and densities of pillar features. C2C12 cells grown on this region of PDMS show the expected 'network' morphology, as characterised in the previous chapter. In the comparable region of the PDMS substrate patterned, in this case, with 5 µm periodic gratings, cells align specifically along the grated features. Contrast between the bilateral linear morphology and the network morphology was documented by the inclusion of the non-patterned flat region within the same capture frame. Morphology direction along the grated patterns was a direct influence of the grated pattern features.

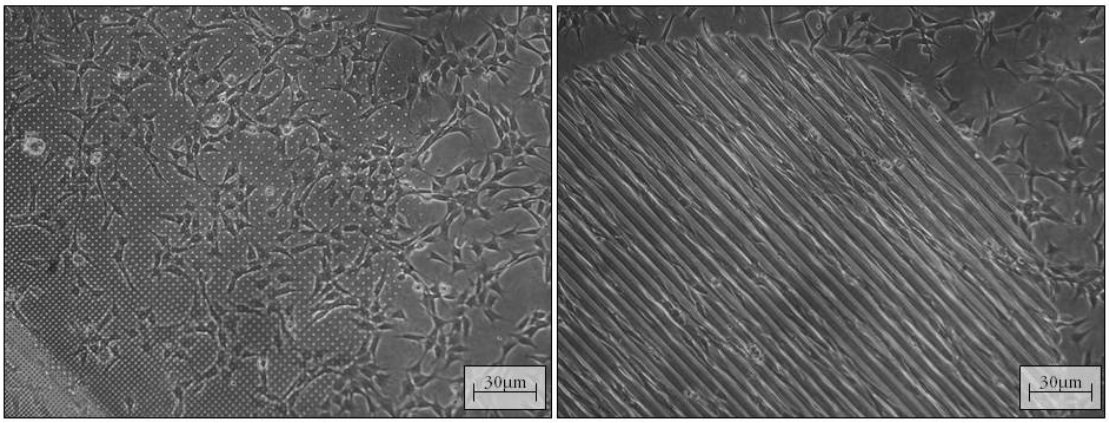

Figure 8.12 - Phase contrast micrographs of C2C12 cells grown on PDMS varied pillar patterns [left] and 5 µm periodic grating patterns [right] for 48 hours. Cells show a distinct morphology difference when aligned with grated pattern features than on flat and island features.

Patterning-induced alignment effects were seen on polystyrene and PDMS before the cells grew confluent. A separate experiment was conducted to determine the effect of the patterned substrates on C2C12 cells intentionally grown beyond confluence and induced toward myotubule differentiation. A new imaging method was utilised to identify cell growth on patterns. Bright field images were taken instead of the third fluorescent channel. The fluorescent channel images were then combined and overlaid on a grayscale copy of the bright field channel image of the same location. The bright field overlay approach worked well because the patterns were easily discernable from the cell features.

Cells were grown to confluence for 5 days before being transferred to DMEM-DM for differentiation. Cultures were maintained for 6 days in DMEM-DM, replenished every 48 hours, before removal for fixation and endpoint analysis. Fluorescent staining, using the bright field background to show the pattern borders, showed extremely delineated myofibrils on the patterned regions. While significant differentiation occurred away from the patterned areas, the directionality of the differentiation was only influenced on the patterned regions and within a 50 µm border region. Differentiation shown in Figure 8.13 shows the lateral alignment of the myofibrils on to the pillar pattern on the lower half of the image. Actin and myosin are co-localised in the structure of myofibrils as part of the acto-myosin contraction complex. Therefore, based on the increase in actin density, myofibrils can be identified without the inclusion of the MF20 immunofluorescent FITC emission. FITC emission was difficult to document due to the brightness of the bright field background layer.

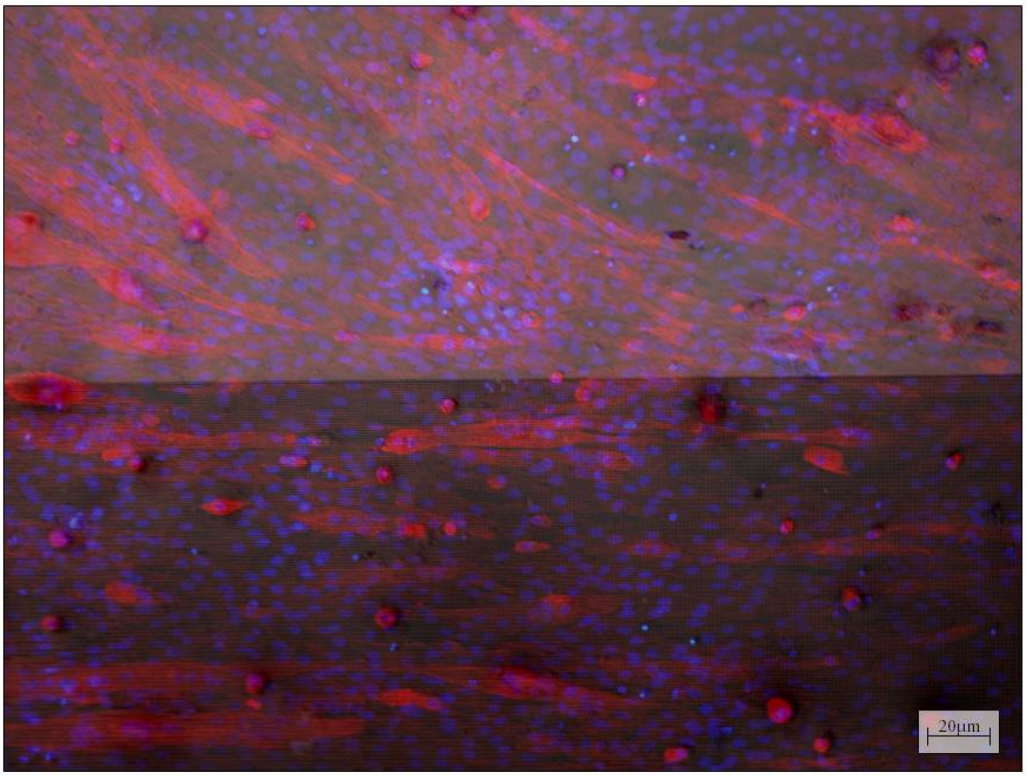

Figure 8.13 - Fluorescent microscopy capture of myofibril differentiation on a patterned polystyrene substrate. Co-localisation of actin [red] and myosin [not shown] led to identification of differentiated myofibrils based on the structure and density of the Atto 594 staining. The top half of the image shows unpatterned polystyrene while the bottom half contains embossed grated patterns.

When the FITC channel was used, pattern regions were defined using secondary software additions, as seen by the dotted white line added after the acquisition of the fluorescent micrograph in Figure 8.14. The 10x magnification images shown in Figure 8.13 and Figure 8.14 accurately indicate the delineation of the differentiation of myofibrils on the patterned regions. No quantitative analysis was done to compare the lengths and/or maturity of the myofibrils on the patterned areas in comparison with the surrounding flat areas due to the overlap and disorganization of the differentiated myofibrils off the patterned area. The fluorescence imaging summed the fluorescent output, obstructing analysis of overlapping fibrils. This effect was seen to a greater extent beyond the patterned regions due to the higher level of differentiation. Similarly, the pattern features interrupted the homogenous FITC emission seen in the substrate-dependent differentiation experiments, causing the fibrils to appear more yellow/orange instead of the strong green emission associated with the myosin expression on control images.

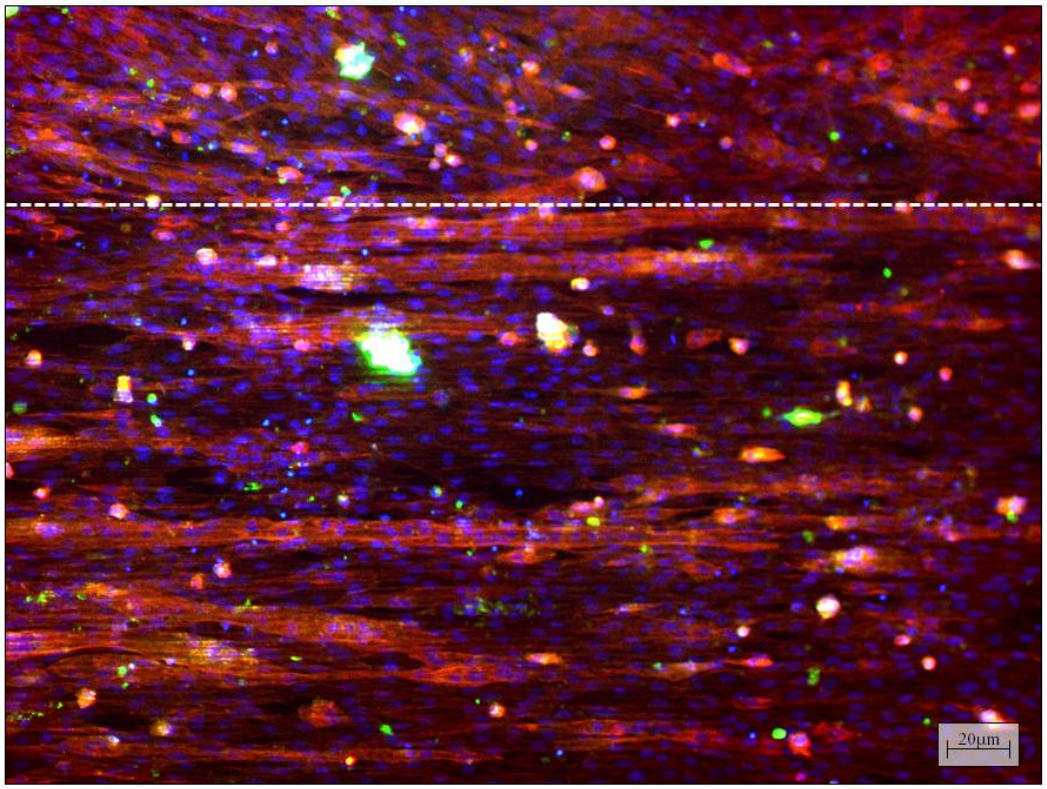

Figure 8.14 - Fluorescent microscopy capture of differentiated myofibrils along a grated pattern on polystyrene. The yellow colour indicates co-localisation of actin [red] and myosin [green], found in differentiated myofibrils. The dashed white line indicates the pattern border with grated features located below the line in this image.

Figure 8.14 shows longer or combined myofibrils on grated patterns, but also shows lower overall differentiation in comparison with the un-patterned substrate area above the white line. Throughout the experiments examining the effects of patterned features on the overall differentiation extent and organisation, cells aligned and differentiated on the patterned features but did not differentiate to the same extent as the cells adhered off the patterned substrate regions. Figure 8.15 captured cells cultured to confluence for 5 days before being shifted to DMEM-DM and driven toward differentiation for 6 days [11 days overall in culture]. The cells were cultured on polystyrene substrates fabricated using the oven embossing method, which resulted, as before, in uniaxial resolution. Some areas of incomplete pattern transfer are also visible in the bright field background of Figure 8.15.

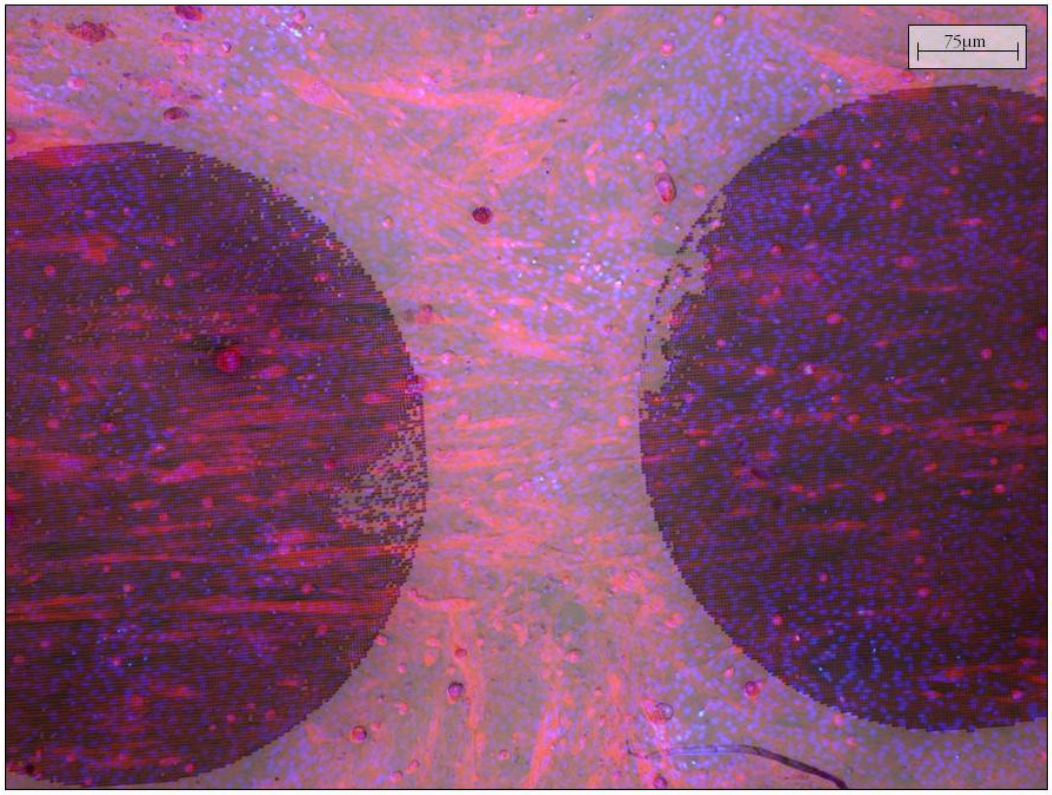

Figure 8.15 - Differentiated myoblasts on patterned polystyrene after 11 days in culture. While highly aligned over the patterned area, differentiation was less complete than off the patterned area. Myofibril differentiation was identified by the density of actin staining due to the co-localization of actin and myosin.

Before confluence, cells demonstrated the alignment organisation associated with the grated pattern features. The incomplete resolution of the island pattern along the length of the substrate created, in effect, a 5 µm grated pattern, which affected cell adhesion and morphology. As the cells grew to confluence, the cells adhered to the pattern grew more slowly than cells proliferating and spreading across the flat areas between the patterned regions. Myoblasts proliferating across the pattern regions took all 5 days in DMEM-GM to reach confluence and dictated the time to DMEM-DM medium replacement. Throughout the duration of differentiation, cells growing on the patterned regions, though well aligned, showed slower myofibril development than the confluent networks grown beyond the patterned areas. Figure 8.16 shows only the Texas Red filter capture for the same field of vision combined for Figure 8.15. The patterned regions are almost discernible from the actin-only image for two reasons: the alignment of the cells and myofibrils and the relative darkness over the patterned areas indicative of lower actin levels in these regions. If left indefinitely, the extent of differentiation

would likely level out across all substrates, though only maintain the grated alignment over the patterned regions.

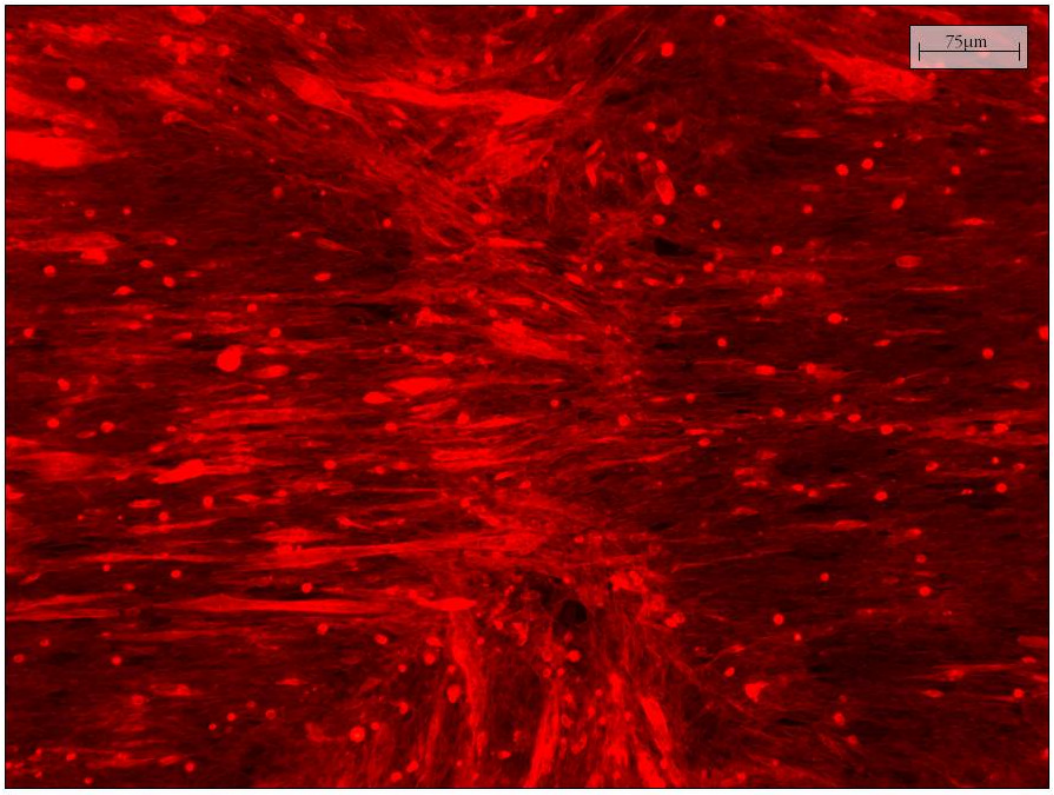

Figure 8.16 - Texas Red filter capture of the same field of vision shown in the overlay image [Figure 8.15] showing on the actin emission of the phalloidin-conjugated Atto 594. The higher emission density in the central region corresponds to more actin present in the central region.

Whether the higher actin fluorescence seen in the central region was due to increased cell density of the background network or indicated increased differentiation for the local region was difficult to determine. Based entirely on observation, the number of fully matured myofibrils, containing five or more nuclei pre-myofibril, was higher for un-patterned regions not containing the orienting effects of the pattern topographies [as seen in Figure 8.16]. Because of the apparent randomness of differentiation orientation in this region it was difficult to isolate overlapping individual myofibrils. The addition of the myosin II immunofluorescence staining was not successful due to the high background, a result of both ineffective washing after staining and the almost continuous differentiation across the substrate highlighted in green. Therefore, specific quantitative data was not obtained to statistically verify these observations.

For comparison with the polystyrene substrates, which showed successful delineation of myofibrils along grated patterns, experiments were reproduced on PDMS substrates. C2C12 cells were seeded on sterile PDMS substrates, fabricated using soft lithography protocols. Importantly, the pattern polarity was inverted by using the PDMS moulds directly cast from the master wafer as substrates. Positive island features on the SU-8 master, which would appear as positive features on polystyrene replication as well, were negative hole features on PDMS substrates. This was less important for grated features than for square and circular island features. As well as the pattern inversion, collapse of small scale features in PDMS was noted on the fabricated substrates.

Myoblast cell cultures on patterned PDMS substrates showed the same overall reaction to the PDMS substrate as demonstrated in the substrate-dependent morphology comparison. Cells were cultured for 5 days in DMEM-GM before the shift to differentiation medium. When the medium was changed to be replaced with DMEM-DM on day 5, large sections of densely packed confluent cells peeled away from the substrate surface and into the medium [indicated by yellow arrows in Figure 8.17]. The cell clusters were carefully removed and placed on a glass microscope slide where they were fixed and stained.

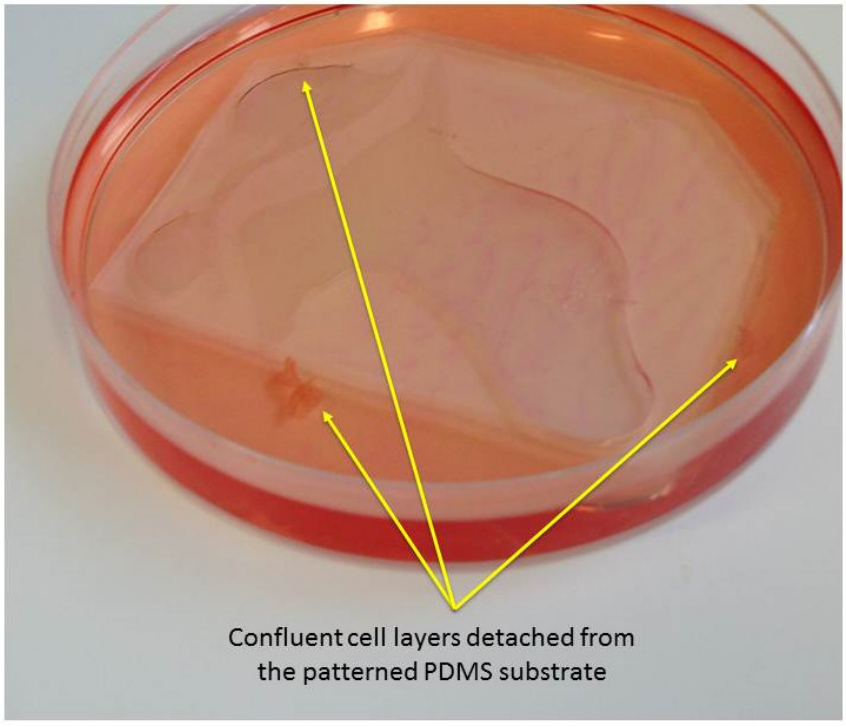

Figure 8.17 - Patterned PDMS after 5 days in DMEM-GM culture. Yellow arrows indicate the large monolayer chunks peeled away from the substrate surface.

Using the confocal microscope, the tissue-like culture sections were imaged by taking single image slices at every 1 μm. Image number varied based on the height of the sample at the imaged regions, but the resulting image stack was summed together to create a three dimensional representation of the cell coagulations and sum images suggestive of the overall three dimensional nature [Figure 8.18]. The cell nuclei are labelled in cyan by the confocal software and indicate the overall size of the confluent cultures which peeled up from the PDMS substrate interface.

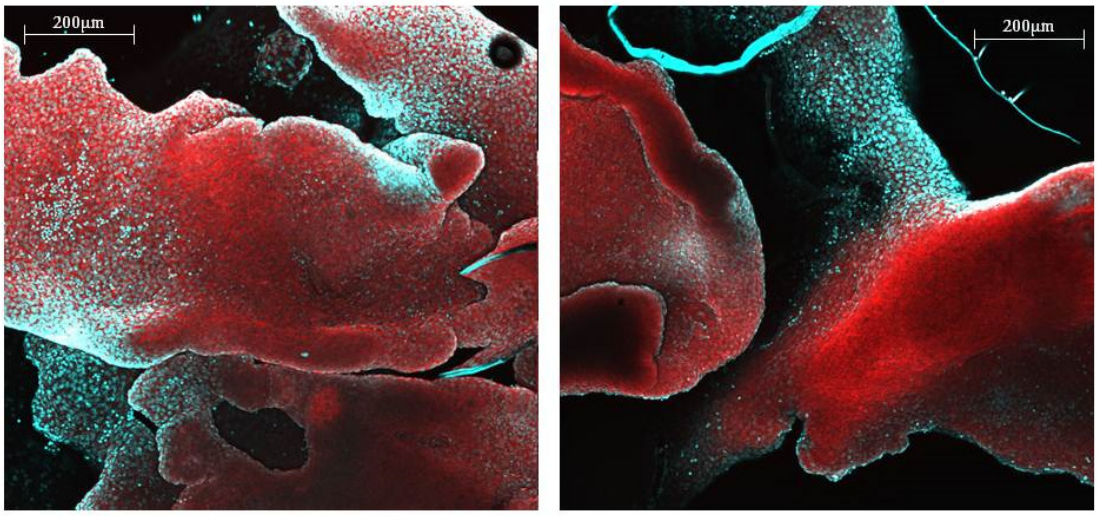

Figure 8.18 - Large chunks of monolayer culture peeled off the patterned PDMS substrates and stained for actin (red) and DNA (cyan).

Concurrently with analysis and imaging of the massive clusters removed from culture, the remaining cells in culture were directed toward differentiation and incubated in DMEM-DM for an additional 5 days. After 120 hours in differentiation medium, cells were removed, fixed and fluorescently stained for analysis. Upon analysis the low confluence was the most immediately observable difference between the PDMS substrates and the previously used polystyrene substrates [Figure 8.19]. The adhered cells were not confluent on either the patterns or the adjacent flat regions. Grated pattern features, some of which showed obvious collapse, caused an alignment effect similar to the cell growth documented prior to confluence on grated polystyrene substrates. Similarly, both on and off the patterned regions, cells grew into tight clusters, evident by areas of dense, bright nuclear staining. The three dimensional aggregates visible in Figure 8.19 were all located over patterned regions, though this observation was not consistent across the entire substrate face.

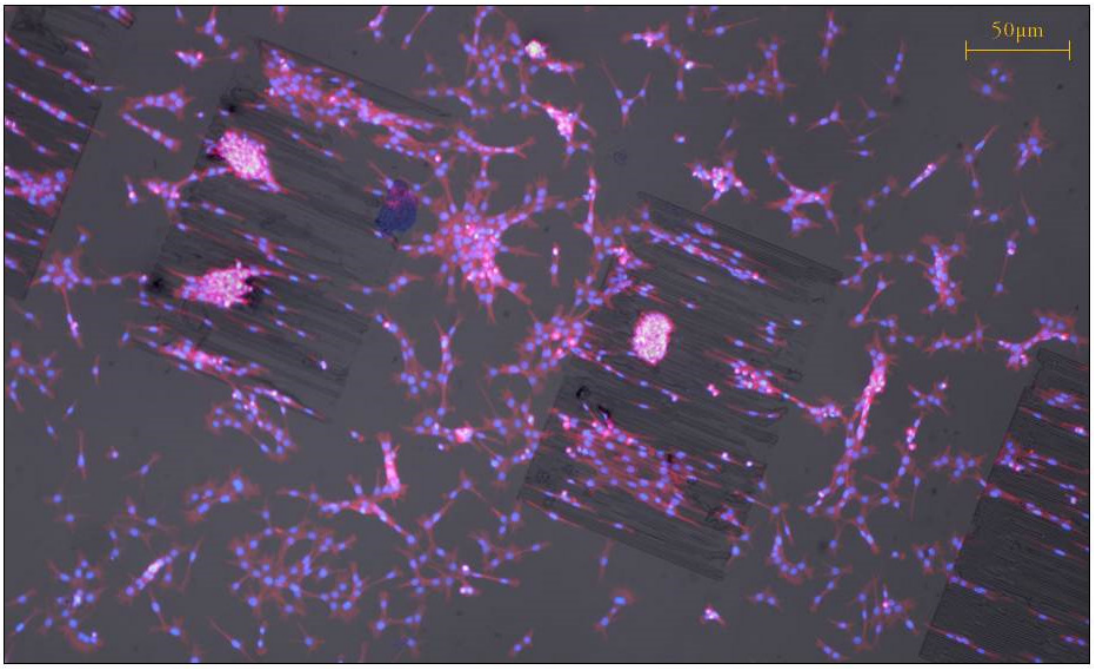

Figure 8.19 - C2C12 cells grown and stained on PDMS after 10 days in culture. Cells are stained for actin (red) and DNA (blue) and overlaid on the bright field image of the patterned PDMS.

In contrast to the C2C12 response to island patterns on the initial embossed polystyrene substrates the positive island features in PDMS directed the growth and direction of lamellipodia extrusion fibres. Actin staining in Figure 8.20 and Figure 8.21 clearly shows the cell extensions growing within the channel sections created by the positive pattern features. Additionally, the nuclear deformation that was induced by the pattern features [Figure 8.21] had never been documented in previous experiments conducted for this thesis, but had been documented in literature [113]. Neither an alignment to the patterned features nor an overall preference for adhesion location was observed in spite of the obvious influence of the pattern features. Island features 5-10 µm had the highest observed cell adhesion. It is important to note that the cells captured in Figure 8.19, Figure 8.20, and Figure 8.21 were all cultured for 10 days total, including 5 days in differentiation medium. Cells were non-confluent at endpoint analysis and showed none of the hallmarks of myofibril differentiation.

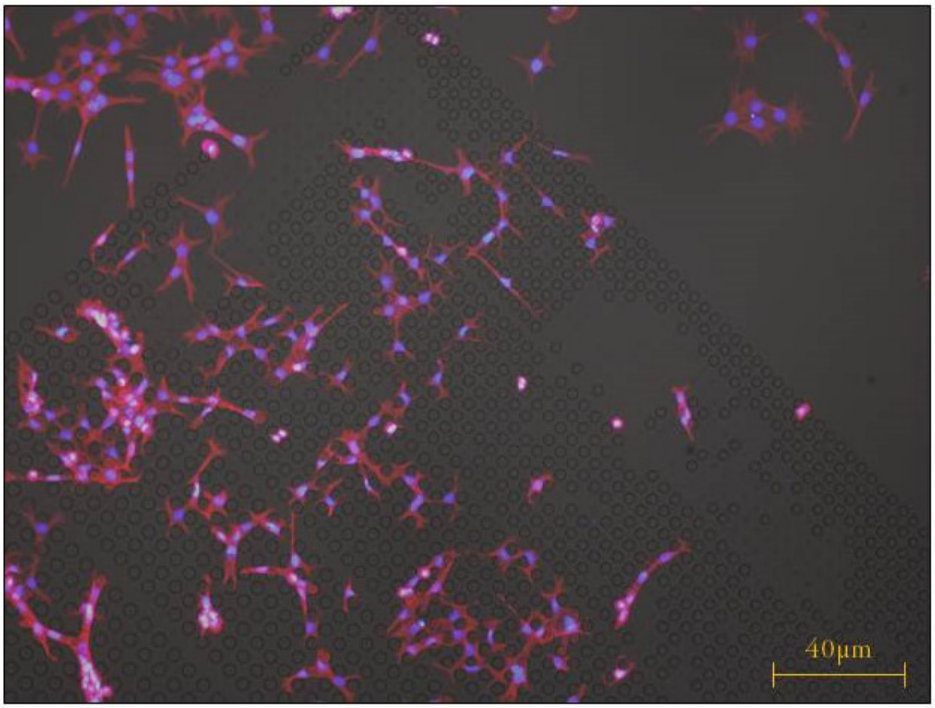

Figure 8.20 - C2C12 myoblasts differentiated on patterned PDMS after a total 10 days in culture. The patterns are graded in size and positive relative to the flat of the substrate.

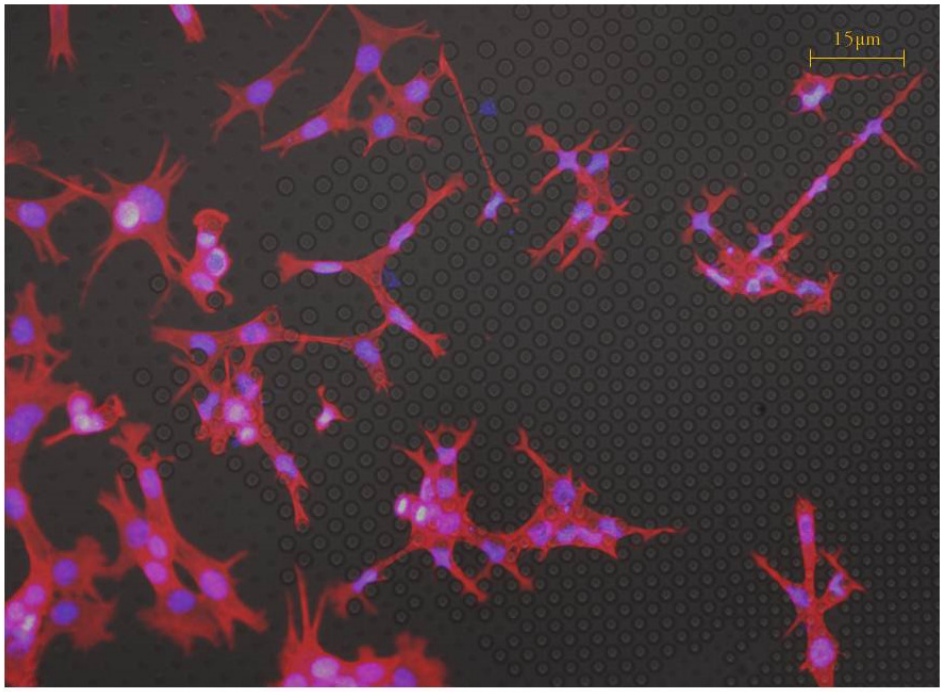

Figure 8.21 - C2C12 myoblasts grown on graded PDMS patterns for 10 days in culture.

8.2.3 Bioimprint protocol modifications

Bioimprint characterization of the C2C12 cell line was initially done using poly(MA) as the imprint medium. Undertaken in Hamilton at Plant and Food Research facilities, microscopy imaging of bioimprinted C2C12 myoblasts showed some interesting organization tendencies across the control substrate surface. As with the Ishikawa cultures, cell confluence varied greatly across the substrate.

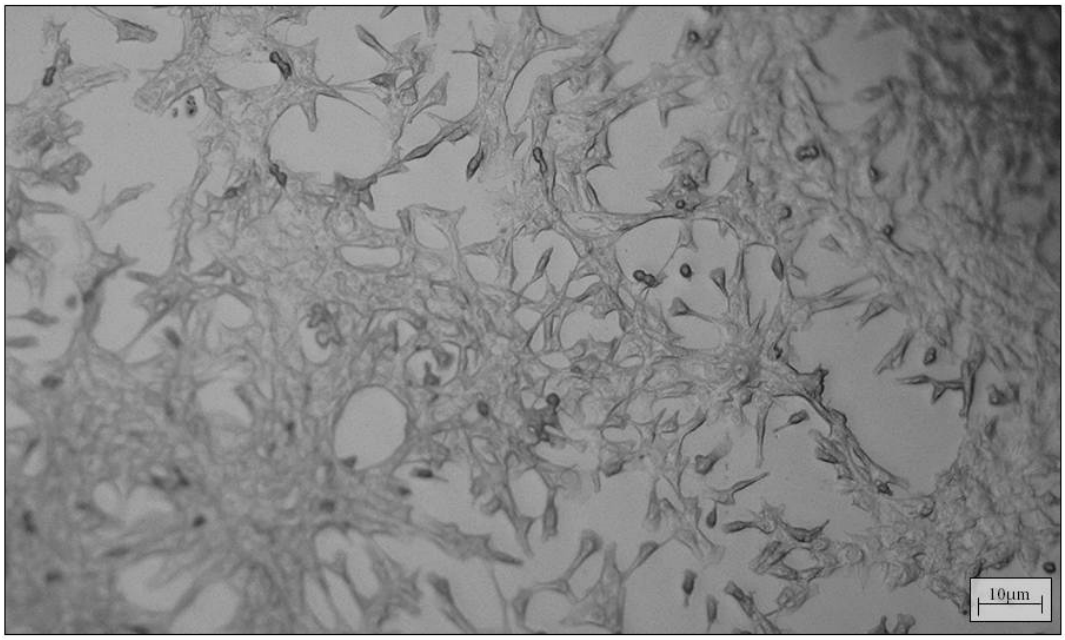

Figure 8.22 - DIC capture of a C2C12 control bioimprint in methacrylate polymer taken at Plant and Food Research in Hamilton, NZ.

The cells consistently grew to higher confluence in the central region. However, in some samples, the highly confluent central regions actually peeled back in the washes before imprinting. These samples show large areas of flat, un-imprinted areas.

The pre-patterning method of using PDMS stencils to define the bioimprinted substrate regions was used with the C2C12 cultures. In accordance with the methods outlined in section 4.1.5, PDMS stencils, 100µm in height, were placed concentrically within larger PDMS borders and sterilised for cell culture use. The stencils had been 'double-baked' to limit any chemical leaching effects that may occur due to uncured PDMS. The myoblasts were plated at 5.0×10^3 cells/cm^2. Cells were incubated in FBS-supplemented DMEM growth medium for 48 hours.

Imaging at 24 hours showed extremely low adhesion, but spreading amongst adhered cells. A high percentage of cells existed in solution, but it was unknown whether these cells were viable or not. Medium was changed at 24 hours to remove cell debris in solution and encourage growth. Notably, none of these unusual growth patterns were seen in the expansion flasks being grown in the same medium simultaneously. At 48 hours, extreme cell death was noted in both chambers containing PDMS stencils and the glass-only controls. Very few cells remained adhered, especially within the stencil regions. A significant number of black dots were also seen at the substrate surface. At first, these black dots were assumed to be a bacterial contamination. However, there was no cloudy or acidic media indication of bacterial presence. Medium was incubated at 37°C overnight to expand any bacterial presence to no effect. Bacterial contamination was thus eliminated as a possible cause of the increased cell death. Lower cell viability was limited to the PDMS-bound chambers and was not found in the concurrent PS expansion flasks.

The experiment was repeated with higher initial cell seeding density, $1.5x10^4$ cells/cm^2. At 24 hours, the experimental stencil samples showed normal, happy cell growth. Dark spots were noted, all of a relatively consistent size, in both the control chambers and on the stencils but with lower prevalence than the lower density experiment. Spots were commonly co-located with cell membrane adhesion points. At 48 hours, some cell death was noted, but not to the same extent as the previous iteration. Stencil patterns were almost completely confluent and cells were successfully contained within the PDMS boundaries, as shown by the fluorescently stained stencilled C2C12s in Figure 8.23.

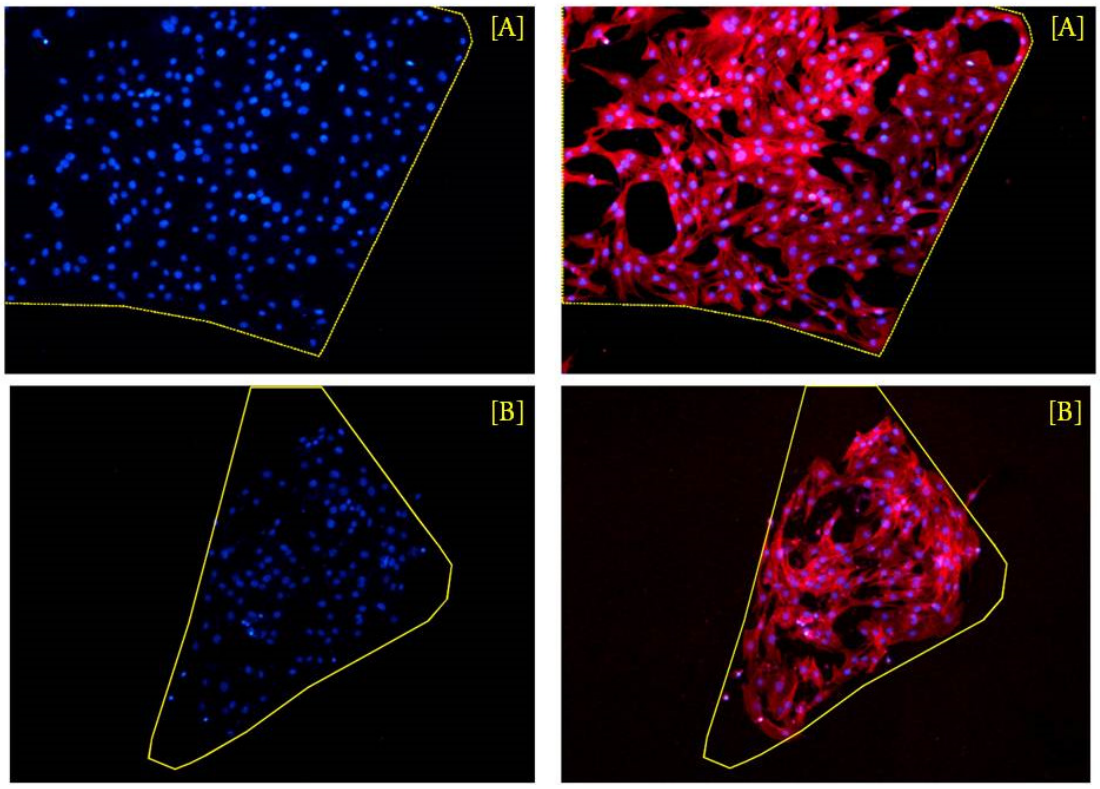

Figure 8.23 - Two examples [A and B] of fluorescently stained C2C12 cells after culture within elastomeric stencils prior to imprinting. Images are taken at 100x total magnification.

While cell death was still higher than expected, the appearance and confluence of the adhered cells was more 'normal' than the withering dissociation seen in the previous experiment. The medium was aspirated and adhered cells were washed repeatedly in PBS to remove cell debris before fixing. Cells were fixed before the PDMS stencils were carefully removed from the chambers. Fixed cells were refrigerated at 4°C while they were dried for bioimprinting. In both trials the cells grew comfortably on the PDMS surface of the stencils as on the exposed glass areas within the stencils. The morphology variation of cells adhered to the PDMS versus cells adhered to the exposed glass was obvious and corresponded to the morphology variation documented in chapter 7.

A fundamental characteristic of the bioimprint technique up to this point has been that it presented negative surface features, i.e. depressions of cell apical membranes rather than positive three dimensional cell representations. Using the polystyrene hot emboss method outlined in the substrate fabrication methods and for the patterned substrates in the previous section, positive bioimprinted substrates were created from PDMS moulds. Figure 8.24 shows

the stencilled C2C12 culture bioimprinted directly into PDMS [left] and transferred into polystyrene [right] via the stacking emboss method.

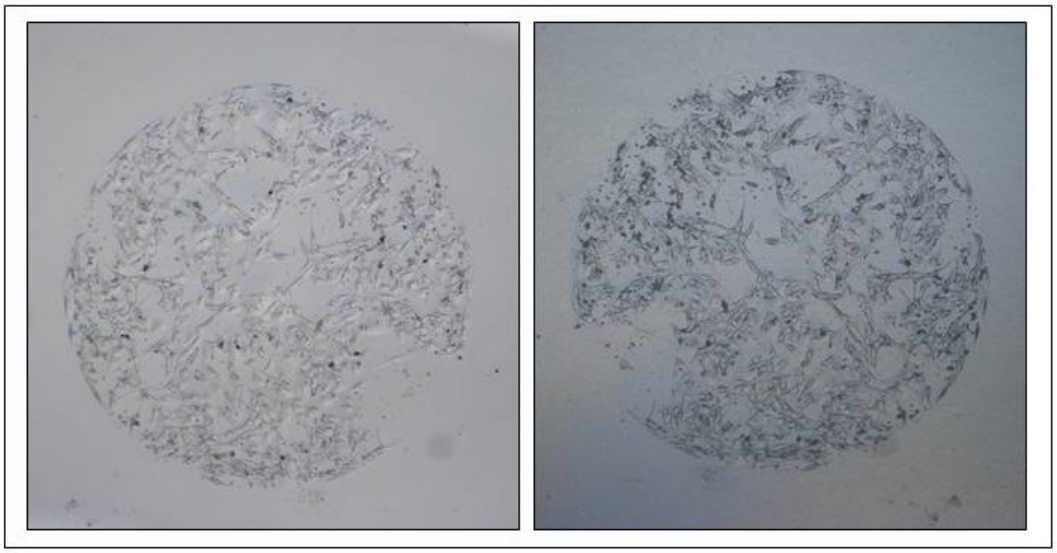

Figure 8.24 - Bioimprinted replicas of stencilled C2C12 myoblasts. The PDMS mould [left] was directly templated from the fixed cells. The stack assembly emboss method was used to transfer the bioimprint features into a polystyrene substrate [right] to be used for cell culture.

Resolution of both the PDMS bioimprinting technique and the embossing to polystyrene was high enough to discern actin stress fibres and was limited by the resolution of the upright microscope instead of the replication resolution. Bright field imaging on both substrates was found to be difficult for high magnifications due to light refraction and substrate thickness. The small black spots, smaller than an individual cell nucleus and more visible in the PDMS image on the left in Figure 8.24, were visible in all replications of the bioimprint. The suspected contaminants were present in the stencil cultures and were replicated through to the polystyrene substrates.

Cells were seeded on the positive polystyrene substrates containing bioimprinted myoblast topography. As shown in Figure 8.25 and Figure 8.26, the CBB stained C2C12 cells grew over and around the positive bioimprint with apparently little awareness [red arrows in Figure 8.26], but also tended to anchor lamellipodia to adjacent features. Adhered cells grew multi-directionally, an observation rarely seen in control culture and never seen on grated pattern features [red arrows in Figure 8.25]. Spreading cells showed no local preference for adhering to the positive features and were, in fact, more often found to be grown on flat areas bounded by the positive bioimprint topography [blue arrows in Figure 8.26]. The same imaging

difficulties present for imaging Ishikawa cells grown on bioimprinted substrates were found for imaging myoblasts grown on polystyrene substrates, namely that bioimprinted features were difficult to visualise beneath stained secondary cells..

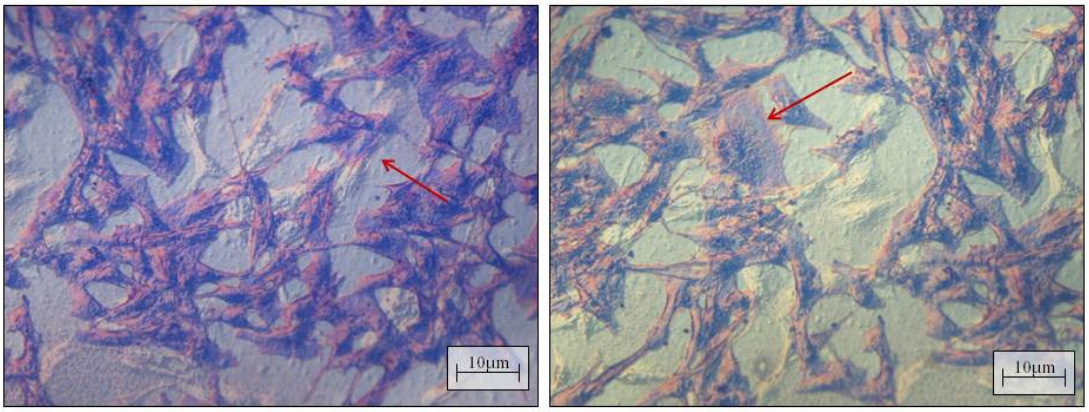

Figure 8.25 - CBB stained C2C12 myoblasts grown on positive myoblast bioimprints in polystyrene. Red arrows indicate areas of increased omnidirectional spreading rarely seen on un-patterned substrates.

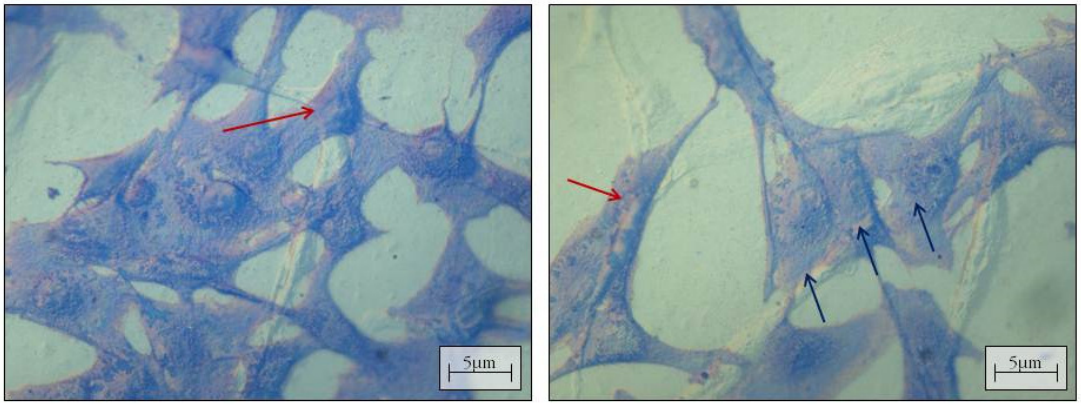

Figure 8.26 - CBB stained C2C12 cells grown on positive myoblast cell features, which had been bioimprinted and transferred into polystyrene. Red arrows indicate regions of cell growth over the three dimensional bioimprint features. Blue arrows indicate cells grown between positive topography features.

8.3 Discussion

8.3.1 Polystyrene substrate fabrication

Fabrication of polystyrene substrates was a positive accomplishment for the development and application of bioimprinting technology. By the time pattern morphology comparison became feasible, poly(MA) had been realised as a non-adhesive, undesirable substrate. Over the course of the experimental work presented in previous chapters the requirement for chemically consistent and cell-friendly substrates became increasingly apparent. Tissue culture polystyrene controls were maintained for comparison in almost all experimental designs. Due to the pervasiveness of polystyrene in cell culture work, locating and replicating fabrication techniques for pattern transfer into polystyrene became a high priority goal after the deficiencies of the poly(MA) were identified. Methacrylate substrates were not investigated in experimental work involving the alignment and differentiation of C2C12 cells.

Solvent casting methods were experimentally attempted prior to investigating embossing methods. Polystyrene in toluene solvent casting had been previously used in the Nanofabrication Laboratory at University of Canterbury and was, therefore, the first polystyrene replication method applied. Patterns were accurately replicated to the minimum feature size, 5 μm, but did not produce the expected vertical side walls for square and circular pillar pattern features. This was evident by AFM scanning and surface analysis. Suggested causes of the low fidelity replication of the bounding features were curing stress at the feature edges and PDMS swelling and alteration due to toluene adsorption.

Local stress of curing a thin layer of PS had an effect on the local deformation and likely contributed to the underlying wave artefact seen in Figure 8.2. Thickness consistency was found to be difficult to predict because of the volume of solvent lost during overnight evaporation. As the polystyrene formed to the pattern features, adhesion force between the polystyrene and PDMS layers was equilibrated by local stress patterns. The attempted separation of the cast from the PDMS mould commonly resulted in fracturing, as seen in Figure 8.3. Whether these defects developed during curing or exist only as a result of sample removal is unknown. If the solid cast was too thin, the substrate rolled up immediately upon separation

from the PDMS mould. In the event of either micro-fracturing or curling of the thin cast, the substrate was no longer viable as an experimental cell culture substrate.

Toluene and other organic solvents can cause swelling in PDMS, so the accuracy of a solvent-based casting protocol for replications from PDMS was questionable. Different solvents cause different swelling of the PDMS mould. While no swelling effects were detected for toluene, examination of the resolution was not undertaken due to the exclusion of this method due to induced stress. The later selection of gamma-butyrolactone [GBL] as solvent was based on the work of Wang et. al [109], which asserts no swelling for GBL replication from PDMS. Indeed, no mould swelling was observed for GBL solvent casting either.

Embossing methods provided a higher throughput protocol for substrate production, but with inconsistent reproducibility of features below 5 μm. One observable artefact and possible explanation for this was incomplete melting of the substrate. Though 185°C, the lowest temperature used for embossing, is well beyond the glass transition temperature of polystyrene, the heat distribution through the entire assembly was not necessarily even and could have varied across the substrate width. Artefacts indicating areas of incomplete melting showed higher overall surface roughness. This effect was most commonly observed at small-scale features and border areas, all with a texture inconsistent with the fully melted and set regions seen in Figure 8.5.

Stack embossing on the hotplate was found to have a higher resolution than the bulldog clip method; however the heating inconsistencies and variability throughout the stacked assembly led to difficulty in defining the temperature at the substrate surface. Optimization determined that 12-15 minutes on heat was sufficient for melting, but the total time at temperature was unknown. In contrast, the exact time and temperature of the oven and clip complex were known throughout the embossing procedure when using the binder clip method.

The directionality associated with island pattern features embossed using the binder clip method was likely due to a property of the polystyrene slide manufacturing process. No effect was seen for grated patterns, in which topography varies along only one axis which corresponded to the polystyrene directionality. Because a large local pressure gradient was highly unlikely across uniaxial 5 μm distances, the effect was attributed to an inherent directionality within the polystyrene substrate. The working theory suggests that the microscope slides were roll extruded during fabrication to ensure homogeneous thickness.

Similar to the effect of a rolling pin on dough, roll extrusion thins a bulk material to a desired thickness before further processing. In this case, semi-amorphous polystyrene being roll extruded would adopt the directionality of the roller and may maintain that inherent directionality after further processing. This effect was not documented in the original paper [111]; however, feature sizes in the original paper were comparatively large.

Grating patterns were first added to experimental patterns in this section. While the patterned substrates had little effect on the cancerous Ishikawa cells, the literature describes a distinct alignment effect for C2C12 cells on grated patterns; grated patterns between 5-25 μm seem to have the largest effect on C2C12 morphology on substrates of any material [99, 107, 114-116]. Alignment experiments in literature had been completed on polystyrene only once previously, therefore, replication and verification was required before behaviour characteristics for cells grown on polystyrene bioimprint samples could be generalised. These findings were verified by the experiments conducted in which cells were removed prior to driven differentiation. [Interactions between Ishikawa cells and topographically modified substrates had not been studies before this work. Ishikawa cell culture on grated patterns could be included in future work to determine whether the effects seen on dewetting artefacts were in fact due to the linear features.]

For periodic grating patterns, defining the substrate as positive or negative was less important than previously discussed with pit and pillar patterns. As shown in Figure 8.27, due to the square wave appearance of the pattern cross-section, the features could locally be simultaneously defined as both positive and negative relative to the immediately adjacent feature over the patterned expanse. For Island patterns, all features were surrounded by a relative change in height resulting in local extremes [Figure 8.27 image 2], which do not exist in the uniaxial variation of grated features. At the boundaries of the grated areas, the definitions applied for pillar and hole patterns were used.

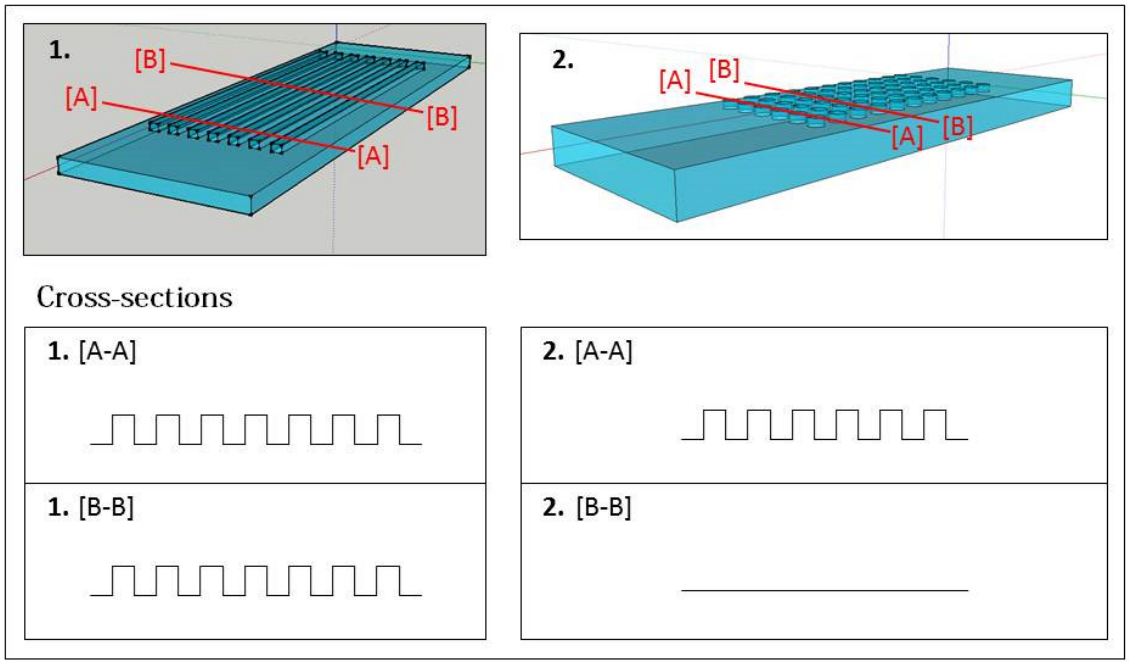

Figure 8.27 - Comparative cross-sections of positive grated and positive, circular pillar patterns. While the periodic gratings are consistent along the length of the pattern the cross-section varies along the length of the pillar-patterned region. This emphasises the importance of defining the topography for non-periodic patterns.

8.3.2 C2C12 growth and morphology on patterned polystyrene

Because of their fusion and delineation, C2C12 cells are commonly used to investigate the effects of surface patterns on cell growth, organization, and differentiation. From delineation and alignment on patterned surfaces to single myotubule formation, C2C12 cells have well-defined and well documented morphologies [117, 118]. Unpatterned surface roughness was found to cause cell alignment along the direction of scratch features on PDMS substrates after only 24 hours but caused no significant increase in myofibril differentiation [60]. Similarly, Charest, et. al. and Huang, et. al. found no significant increase in C2C12 myofibril differentiation on linear micropatterned substrates, though myofibrils aligned to the pattern features [99, 106]. These findings are contradicted for stem cells differentiated into other endpoint cell types [100]. Results suggest alterations in vertical depth are more effective in aligning myoblast cultures. The morphology variation observed and documented in the previous chapter had not been previously reported in literature concerning C2C12 growth on patterned PDMS and polystyrene substrates. To determine the influence that the topography would have patterned polystyrene and PDMS were used in cell culture for morphology and differentiation experiments.

Results showed the most observable and pronounced organisational variation on grated patterns. This agrees with the existing literature on the subject [106]. Similarly, while grated patterns of all sizes influenced the directionality of the alignment, 5-10 μm periodic gratings had increased cell adhesion before confluence. This also concurs with existing literature. We posit that this is due to the width of the grating features being large enough to accommodate the cell nucleus without too much deformation.

The positive, diamond-shaped island features used for the first morphology tests on polystyrene showed no alignment effects and little influence over the cell organization in general. Confluence was found to be the largest contributing factor to cell organisation at any given frame of vision across the substrate. Because these substrates were fabricated by embossing, the depth of the features is not as well defined as for cast substrates and may have provided a faster route for cell expansion across pattern features than deeper, more isolated features would have provided. Myoblasts grew just as well to areas of incomplete melting as all other exposed polystyrene surfaces. Embossing into Nunc polystyrene microscope slides, the grating patterns resolved completely and exactly, however, square and circular pillar patterns only resolved across the width of the substrate. In effect, this created a semi-resolved grated pattern along the length of the substrate. Myoblasts differentiated on polystyrene substrates fabricated by this method show the increased alignment associated with grating patterns even on the areas intended to contain pillar features.

Morphology variation on PDMS substrates was consistent with the combination of morphology characteristics seen by the C2C12 cells in other experiments. Cells grown off the patterned region on PDMS showed the network morphology discussed extensively in the previous chapter. Cells grown on grated patterns conformed to the same alignment influence observed on polystyrene substrates. The only divergence away from expectations of cell behaviour on PDMS substrates occurred on island patterns after the differentiation duration. Cells showed an inability to climb the pattern side walls and, thus, grew around and to the pattern features. While conformation to the pattern was not seen on any other substrate, it is not entirely unexpected. The resolution for PDMS patterns is likely to be higher than for any of the polystyrene substrates because of one less replication phase. In combination with the inherent hydrophobicity of PDMS the increased side wall resolution may be incompatible with cells going over the top of the side walls of the pattern features.

Differentiation on patterned polystyrene substrates showed the directionality of cell growth continued through the membrane fusion and was maintained for complete myofibril differentiation. Aligned myofibrils were observed predominantly on grated patterns, but were also seen on substrates fabricated from polystyrene microscope slides containing the semi-resolved pillar patterns. Interestingly, myofibril differentiation did not occur to the same extent on patterned areas as in the adjacent flat regions. There are two theories to account for the lowered instance of mature differentiation, both of which assume the requirement of a confluent background support structure, posited in the previous chapter as a requirement of the differentiation mechanism.

The first theory suggests that the increased surface area provided by the patterned substrates increases the surface energy in those regions enough to increase the local hydrophobicity [17, 21, 66]. Seeded cells would then locally preferentially adhere and grow confluent faster at un-patterned areas. Confluence achieved on patterned regions was observed as occurring more slowly, though just as completely, as cells adhered to the flat regions. In this case, the confluent cells on the flat substrates would be more tightly packed than cells grown over the patterned areas, possibly inducing faster and more complete membrane fusion after the shift to differentiation media. No experimental analysis included investigation on the differentiation at different densities of confluence.

An alternative or additional theory suggests, more directly, that due to the imposition of directionality on the patterned areas, the opportunities for membrane fusion are fewer and, thus, not as extensive as the compact, chaotic organisation of unpatterned differentiation. Bilaterally aligned cells growing along grated patterns would only have the opportunity to fuse with the cells on each of the elongated ends in order to maintain the alignment observed in mature myofibril formation. Even accepting a completely confluent, though grated, supporting background network, the limited options for membrane fusion combination would lead to both lower instance of completely differentiated mature myofibrils and lower extent of differentiation overall. Additionally, no work has been done to determine the optimal cell morphology for differentiation. It is possible the consistently-sized confluent cells with no imposed morphology differentiate more readily, as well.

The same aligned differentiation was not observed on PDMS substrates. The complete peeling of confluent, connected, tissue-like sheets from PDMS substrates after 5 days in growth media was both unexpected and unprecedented. Smaller, spheroid-like aggregates were observed in

the substrate-dependent morphology experiments detailed in chapter 7, however, nothing comparable to the sizes seen on the patterned PDMS substrates. Similarly, nothing has been reported in literature to validate the consistency in which cells grown on PDMS aggregate into multi-cellular clusters. In the previous chapter, trypan exclusion staining suggested that the majority of cells in the spheroid remained viable, even though they were no longer adhered to the substrate. In this case, no viability staining was attempted, but confocal imaging showed reliable nuclear staining and intact actin networks.

As suggested by the non-adhesive properties of the methacrylate polymer used in earlier works, it is probable that the intracellular adhesion forces are stronger than the adhesion to the culture substrate. PDMS is hydrophobic without treatment. Therefore, the most probable cause for the large scale removal of the confluent cell monolayer was the application of a shear force from the shift to driven differentiation and the subsequent inability of the individual cells to preferentially maintain adhesion to the culture substrate instead of neighbouring cells. For this hypothesis, barring membrane damage during the separation process, there is no reason to assume cell death in the removed tissue-like cluster containing thousands of undifferentiated muscle cells. This result suggests a range of potential applications for tissue engineering research not previously associated with PDMS substrate patterning studies.

The increased presence of non-adhered cells in suspension was most likely due to an unidentified chemical effect from the PDMS. Cytotoxic effects of PDMS were documented by [89] previously, but was not reported in the literature supporting stencil applications [84, 85]. While there was no obvious indication of chemical contamination in the Ishikawa cultures reported on in previous chapters, it is possible that the cancer cells were simply more robust and were not affected to the same extent. Bacterial contamination was considered as another possible cause of the high cell numbers in suspension. While contamination does not always lead to cell death, the suspicious, consistently-sized dark spots in suspension appeared with morphology similar to known cocci bacterial contaminants. Fluorescent staining with Hoechst 33342 stained DNA co-localised to the debris locations, suggesting a bacterial contamination; however, this result could have been the result of over-staining and high background. Testing of unused culture media showed no bacterial contamination after 24 hours in incubation, which would have caused an exponential increase in bacteria numbers to create obvious indicators of bacterial presence. No indicators, such as pH change or optical density increase, were observed. PDMS stencils and polystyrene substrates were sterilised before use, but were the only

fabricated portion of the cell culture assembly and, therefore, the most probable contamination source.

The dark spots seen in culture, initially thought to be bacteria, were tentatively identified as abandoned lamellipodia. Known mechanisms exist for the breakage of lamellipodia used for motility; therefore, it is likely abandoned extrusion fibres account for some of the high biological debris present. C2C12 cells are highly communicative and send long, spindly lamellipodia and microfilaments in all directions. The 'band-snapping' mechanism for the breakage of the unsupported lamellipod extensions was suggested as a plausible non-contamination based theory to explain the presence of the small, dark organic material. As the cells move and divide, these tenuous extrusions can no longer be maintained and are severed, either intentionally or inadvertently [3]. The expanding lamellipodia is adhered to the substrate at intervals, not continuously, along the substrate. Therefore, when the extending region is broken, the two halves 'roll up' in opposite directions toward the nearest adhesion point. The result is dark masses of concentrated cell debris predominantly located at the membrane boundary. The localisation of Hoechst 33342 staining must be attributed to high background or over-staining for this explanation to account for all results.

In more confluent cultures, these extensions are fewer and shorter, possibly due to breaking and abandonment. Higher seeding density minimised lengthy membrane extrusions, hypothetically the cause of the adhered cell debris in the previous experimental cultures. Similarly, a higher starting density grew to higher confluence within the same culture period and provided more complete coverage in bioimprinted stencilled areas, even accounting for the loss of coverage due to non-adhered cells in suspension.

8.3.3 Bioimprint fabrication and analysis

Bioimprint features were replicated into polystyrene using PDMS as the bioimprinting mould instead of the methacrylate polymer. In the most initial phases of the bioimprinting technology, PDMS was tested as the imprinting medium, but was rejected due to the effects of dehydration on the cells during the 2 hour baking step. At the time, the bioimprint was being used exclusively for high resolution imaging of cell features, so accurate replication resolution was more critical. The most commonly observed dehydration artefact was a ring formation around the nucleus, probably suggestive of the collapse of the nuclear envelope due to dehydration.

For substrate patterning, continued pattern replication caused decreased resolution and, thus, the artefacts caused during curing were both less critical to the end function of the bioimprint and were less likely to be propagated through the replication protocol. To minimise the effect of dehydration during curing, cells were fixed prior to imprinting.

PDMS stencils were used to dictate bioimprinted regions in the final substrate. Difficulties achieving 100% confluence are visible in Figure 8.23 and Figure 8.24, and failed to provide complete borders of bioimprinted regions next to the flat expanses of the remainder of the substrate. Increasing cell death after 24 and 48 hours in culture prevented improvement on bioimprint border definition. Resolution of both PDMS and polystyrene substrates containing bioimprinted information accurately replicated actin stress fibres, visible at 1000x magnification with the upright Nikon 80i microscope. Maximum resolution of the Nikon is approximately 740 nm, according to the specifications for the aperture and objective settings. Therefore, resolution was assumed to be accurate to 1 μm, though probably accurate beyond that point. As seen in Figure 8.24, pattern replication could be imaged in both the mould and resulting substrate. Polarity inversion of the bioimprint features led to the first positive bioimprinted substrate.

Though growth on positive bioimprint substrates showed some adherence effects, C2C12 cells did not localise to the positive bioimprinted cell features. Non-differentiation culture on positive polystyrene substrates showed high numbers of branching lamellipodia which contacted and often adhered to positive cell features. C2C12 cells grew over and across the bioimprinted features, but showed a tendency to adhere and develop until contact with positive 'barrier' features. Similarly, consistent examples of cells growing in a more 'endothelial' morphology, more polygonal and less bilateral, were observed and documented. In effect, the area between two positive bioimprint features could be viewed as a relative negative feature. It is unknown whether the C2C12 cells adhering within the relatively negative space between positive bioimprinted features is intentionally selecting that position due to recognition of the features on either side or not. The tendency of the C2C12 myoblasts to locate and spread in these regions could be correlated to the effects seen on the Ishikawa cells showing selective adhesion and variable morphology across slightly negative regions. Myoblasts grown on positive bioimprint substrates showed no specific selectivity for localised adhesion to topographical cell features, but consistently used the positive features as anchors for

outstretched extrusion fibres and grew within the valleys created by the mountainous positive cell topographies.

Though the experimental results remain in the preliminary stages, the consistency of the cell size and morphology variation between positive and negative bioimprinted surface features suggests that the microenvironment experienced by the cells in each of these instances is not as different as initially expected. In contrast to the vertical side wall features of lithographically patterned substrates, both positive and negative bioimprint cell membrane features consist of a sloping gradient. The slope, which is defined by the contact angle of adhering cells [Figure 8.28], would have the same scalar magnitude for both positive and negative substrate features because the positive is replicated directly from the negative mould. Therefore, the effect of positive bioimprinted substrates, in comparison specifically with their corresponding negative inversion, might have been overestimated. Additional experimental testing is required to verify this result.

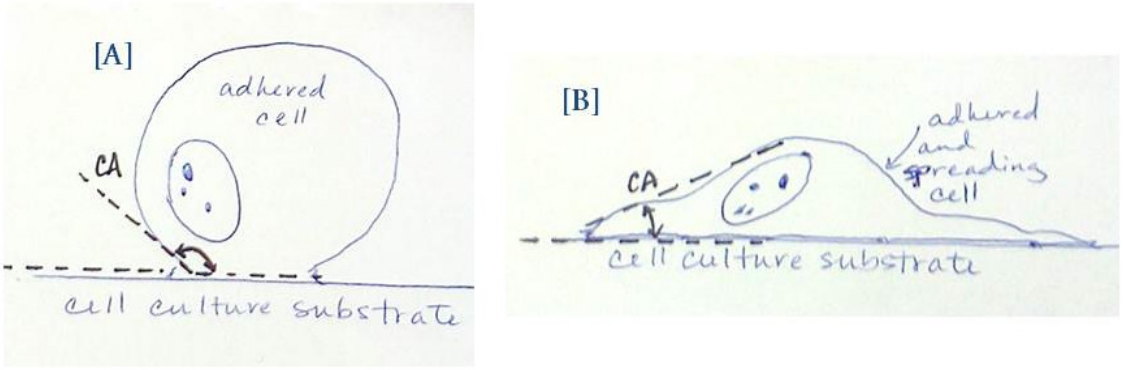

Figure 8.28 - Comparative contact angle measurements for newly or loosely adhered cells [A] in comparison with fully adhered and spreading cells [B]. The slope, relative to the flat topography of the cell culture substrate, is replicated into methacrylate polymer by bioimprinting. This affects the topography experienced by the secondary cell cultures grown on positive and negative bioimprinted substrates.

Experimental investigation into the effect of bioimprint influence on C2C12 morphology and differentiation was curtailed for two reasons; the first more practical, the second more theoretical.

First, questionable contamination status of the C2C12 line, as suggested by images such as Figure 8.24, complicated the imaging and analysis methods and results. As suggested in the previous section, the visible debris seen in the C2C12 cultures could be snapped extension

fibres. Although, no decisive indicators of bacterial contamination were found, the increased cell death seen throughout the PDMS stencilling experiments as well as the presence of similarly-sized, unidentified debris in culture combined to undermine the confidence of inferences and observations for these cultures.

The second reason cell organisation on bioimprinted substrates was not further investigated in this work was due to the success of the previous results of alignment on patterned polystyrene substrates. In order to determine the alignment effects on a bioimprint of aligned myofibrils, a primary alignment method was required. Patterned polystyrene accurately and extensively aligned the myofibrils. The extent to which myofibrils organised along the pattern features called into question what increased expectation of alignment could be achieved by bioimprinted substrates. Because the primary patterning method was so effective, additional observable influence, specifically for myofibril alignment, was unlikely.

Bioimprinted substrates, specifically negative-feature bioimprints, are likely to affect the adhesion and growth of myoblasts, predominantly through time to differentiation and protein expression. The investigation of these aspects required additional methods never previously considered in this work [i.e. fusion index, mature myofibril quantification, and genetic analysis methods]; and was, therefore, considered beyond the time frame required for the submission of this thesis and will be further outlined in suggested future work in the next chapter.

9 Conclusions and Future Work

9.1 Summary and conclusions

Literature and experimental background for this work provide a strong basis for the importance of substrate topography on cell adhesion and growth. Surface modification, both chemical and topographical, has been developed to alter substrate adhesive properties specific to the intended application. At the outset of this work, bioimprinting existed specifically as a transfer medium for detailed imaging analysis of nanoscale cell surface features. Characterisation of resolution and cell artefact was completed previously by Dr. Muys and Dr. Samsuri, but in the isolated context of an imaging technology. In response to the assertion that accurate replications of the cell culture monolayer were faithfully replicated into a permanent polymer substrate Associate Professor Maan Alkaisi suggested that the indicated topography may influence cell organisation, adhesion, and growth when used as a cell culture substrate. Comparison of bioimprint substrates to fabricated patterns was necessary as a control for net overall topographical influence. Throughout the work documented in this thesis, interesting observations and hypotheses were made regarding the growth of both Ishikawa endometrial cancer cells and C2C12 mouse myoblasts on modified substrate surfaces.

Cell sub-culture, counting, and seeding methods followed the same protocol for both cell lines. Control morphology for Ishikawa cancer cells was determined to be dependent on cell adhesion to the substrate. Adhered cells developed a polygonal morphology, typical of endothelial cells, but with less consistency of cell size than the C2C12 cells. High proliferation rates and three dimensional growths beyond confluence were also characteristic of Ishikawa control cultures. C2C12 controls developed distinguishable lamellipodia, characteristic of a ‘fibroblastic’ morphology. Myoblasts tended to align in a swirling pattern in control culture, an organisational characteristic not observed in random adhesion and spreading of Ishikawa cultures.

Because the predominant method of characterisation and analysis was qualitative observation, several staining protocols were used with several microscopy techniques to provide a more complete context for observation. Coomassie brilliant blue, a general protein stain, was found

to provide useful information about cell location relative to topographical features. Fluorescent staining with Hoechst 33342 and phalloidin-conjugated Atto 594 highlighted the location of the nucleus in relation to the cytoskeletal constructs and cell boundaries. Phase contrast and differential interference contrast [DIC] variations of bright field microscopy were used for cell culture monitoring and support as well as substrate surface characterisation. Atomic force microscopy [AFM] provided high resolution imaging to determine surface characteristics and replication resolution. Fluorescent and confocal microscopy were used to highlight fluorescently stained cell features and images were often overlaid onto bright field images to determine a relative relationship with the substrate topography.

The bioimprint protocol, as it existed at the outset of this undertaking, resulted in methacrylate-based polymer substrates which had not been previously tested for compatibility with cell culture. Modification of the protocol to exclude the thickening agent, triglyme, necessitated complete re-characterisation of the polymer ratios and curing process. Inherent stress within the cured polymer was found to be caused by both the ratio of ethylene glycol dimethacrylate [EGDMA] included in the liquid mixture and the high curing speed required by the bioimprinting protocol. The concavity and artefacts associated with curing stress did not preclude the use of samples for cell culture, but caused more difficulties for imaging and analysis than flat substrate samples.

Biocompatibility testing was completed in this work to determine the practicalities of using the methacrylate polymer as a cell culture substrate. Initial results showed high numbers of cells in suspension and three dimensional adhered aggregates as opposed to the expected monolayer spreading. Upon bioimprint immersion in media, with no cells present, the media immediately developed a light orange appearance indicating an acidic pH shift. The addition of a long water soak to remove any water-soluble, unreacted methacrylic acid monomers from the polymer proved to eliminate the pH shift when media was added for culture. To address the accidental incorporation of cell material into the bioimprinted polymer, ultrasonic lysing and trypsin soaking steps were added to denature and/or remove biological material before secondary cell culture.

The resulting working protocol for the bioimprinting technique was developed and is completely outlined in chapter 3. Liquid polymer was mixed at a consistent ratio of six parts EGDMA to three parts methacrylic acid [MAA] with the addition of one part IRGAcure as the photoinitiating ingredient. Importantly, the liquid polymer was found to dissolve polystyrene

consumable labware due to the relative similarity of the solubility constants. This explains the permanent adhesion during attempted bioimprinting protocols from polystyrene. From this point, all initial and control cultures were cultured on glass substrates. Curing was completed using the Omnicure UV source and waveguide on 40% iris opening for 240 seconds. Cycled curing was found to have a negative effect in comparison with the longer continuous exposure. The presence of a remaining liquid layer was combatted with either another 240 second curing cycle or immediate immersion in the first of the biocompatibility washes. The resulting polymer sample had a moulded surface containing both the overall monolayer organisation of the template cell culture and high resolution replications of individual cell membrane features. The biomimetic topography of the bioimprinted methacrylate substrate has the potential to affect cell growth properties when used as a cell culture substrate.

Ishikawa cells grown on bioimprinted substrates immediately showed a preferential adhesion to the template region, but failed to spread across the substrate, instead growing upward in three dimensional spheroids. The second iteration showed the cells spreading across the bioimprinted areas in a confluent monolayer, but also showed significant peeling up of that monolayer at the interface between the bioimprinted and flat topography regions. Though these tentatively proved a preferential affinity for cell adhesion to the bioimprinted area, they also showed the low adhesiveness of the methacrylate polymer as a cell culture substrate. It is unclear what, if any, effect biological material incorporated into the bioimprint features had on the secondary Ishikawa cell cultures. Overgrowth experiments, where cells were cultured for longer than the initial culture had been prior to imprinting, were the first to show distinct alterations of the Ishikawa cell's size and morphology on the flat regions. These observations were strong indications that the fabricated underlying topography altered cell morphology and validated the initial assumptions that the microenvironment is an important contributor to the success and extent of cell adhesion and spreading.

To be able to accurately determine which substrate regions contained bioimprinted features, and to be able to differentiate the bioimprint features from the secondary cells growing on top of the negative bioimprint topography, three methods were applied: biomapping, fluorescein incorporation into the liquid methacrylate polymer, and stencilling of the initial cell culture prior to imprinting. These methods provided the most information about cell culture and organization when used in combination with each other. Biomapping illustrated the concept of 'graded confluence' across the substrate diameter. Fluorescein incorporation into the polymer

allowed for four channel fluorescent and confocal imaging, which provided results showing exact alignment of Ishikawa cells to bioimprinted features. Stencilling provided a designed map of which areas contained bioimprint topographies and which areas were flat. In combination with fluorescein, cells cultured on stencilled bioimprint substrates showed different average cell sizes when compared across the bioimprint-flat interface.

In order to determine whether the arrangement and morphology effects found on bioimprinted substrates were, in fact, only a result of the negative substrate topography and gravity, geometric patterns were designed and fabricated using photolithography. Replication into PDMS using soft lithography techniques allowed for the transfer of the pattern features into a variety of other polymeric materials, including the methacrylate polymer used for bioimprinting. A consistent concern throughout the replication work was the effect of the inversion of the pattern features. Planning was required throughout the process to ensure that pillar features in the photomask were going to come out as pillar features as many as three replications down the line.

During the patterning process several of the artefacts previously insinuated by bioimprinted features were easier to observe and define. 'Double vision' artefacts were difficult to confidently distinguish on bioimprinted substrates due to the irregular nature of the cell growth. For regular, defined pattern geometries, 'double vision', 'dewetting' and 'bubbling' artefacts were easily identifiable and sometimes required the rejection of a sample substrate.

Pattern features were selected to be 5-60 μm. This range was chosen for two reasons; the assertion that cells 'prefer' topographical features on the same order of magnitude as the adhered cell size [5, 63] and to determine the effect of micro-scale pattern features for subtraction from the net effect of bioimprinted topographies on cell growth. Bioimprinted substrates contain accurate cell information from the full cell size down to 5-20 nm. Cells probe their surrounding environment with nanoscale surface proteins [3]. Therefore, by identifying cell growth effects contributed by only the micron-scale features, by using artificial, fabricated polymer substrates, it was possible to subtract the effect from the combined overall effect of bioimprint topographies on Ishikawa morphology and growth.

Ishikawa cells grown on patterned substrates showed the importance of the 'graded confluence' theory. The reaction of the Ishikawa cells to the local topography was directly related to local confluence, which varied across the radius of the circular culture substrates. In the confluent

central locations, the cells overgrew the pattern features with little acknowledgment in less than 24 hours of cell culture. In contrast, at the edges of the patterned region, more alignment to the pattern was observed. The patterns were most effective at influencing Ishikawa cell growth in two unexpected regions: the interface between patterned regions and the surrounding flat regions and at dewetting artefacts across the substrate face. In both cases, cells were found to be localised around, though not directly 'along', the border regions. The working theory suggests that seeded cells initially adhere at these interfaces and then proliferate from there, causing the local culture which is not so much aligned as just local. The mechanism for the initial adherence is not yet defined. Nevertheless, it does suggest that macroscopic features of a substrate influence the response to the micro- and perhaps even nanoscale features. These responses may have important implications in areas of cancer development and tissue repair where the relationship of a cell to the topography of the overall tissue may be critical.

Micro-scale patterning determined the organisational effects observed on bioimprinted patterns were not limited to gravitational reaction to negative 'hole' features. The lack of acknowledgement of the pattern features and the obvious influence of interfacial and dewetting boundaries suggests that at least a combination of factors was involved in Ishikawa cell organisation to the bioimprinted regions. The patterns did highlight the importance of actin as a cytoskeletal protein, however. Density of actin staining was used as an indicator of adhesion and emitted heavily at the vertical side walls of pattern features. Whether the increase in actin was due to a climbing effect or due to the cumulative nature top-down bulk fluorescence, the increased presence of actin at the exact interface with vertical features showed the protein's importance for spreading and adhesion.

The switch to C2C12 murine myoblast cell line was driven by the hypothesis that hallmark properties of cancerous cells were enough to obscure adhesion and proliferation results on patterned and bioimprinted substrates. Adhesion properties of cancer cells are more complex than non-cancerous cells, specifically metastatic and invasive tumour cells. Variable adhesion and unmitigated proliferation are two key characteristics of cancer which may have contributed to the organisation and selective adhesion seen in previous experiments. C2C12 cells had been previously bioimprinted and could be driven to further differentiation into myocytes, myofibrils, or, with supplementation of BMP-2, osteoblasts.

Prior to investigation on patterned and bioimprinted substrates, the morphology was characterised across four widely used cell culture substrates. [Substrate-dependent morphology

was not completed for Ishikawa cancer cells based on the wealth of morphology characterisation already available within the current research group and the assumption that the robustness of cancer cells would likely overwhelm any effect of substrate chemistry on flat substrates.] Almost accidentally, this experiment meant as a quality control across possible cell culture substrates provided examples of the variability of cell morphology based on surface chemistry and properties. The extreme morphology difference between C2C12 cells grown on PDMS and tissue culture polystyrene [TCPS] substrates has not been previously reported in literature. In the literature, no substantial cell morphology variation, from that on TCPS, was observed when PDMS was used as a substrate [99, 100]. The literature also contains significant support for various PDMS surface treatments used to decrease the hydrophobicity of PDMS-fabricated substrates [reported un-treated contact angle of ~110-115°] [97]. Though no surface treatments were mentioned in the only publication differentiating C2C12 cells on PDMS substrates, the mounting evidence in the literature regarding PDMS surface modification suggests PDMS pre-culture treatment might shift the extreme morphology observed in this work back toward a more traditional fibroblastic morphology.

The obvious difference between C2C12 growth on TCPS and PDMS was just as apparent for experiments continuing beyond non-confluent to supplemented differentiation. Differentiation was encouraged by the switching of media from DMEM supplemented with 10% FBS to low serum DMEM supplemented with 2% horse serum. On un-patterned, flat representative samples of each of the four trial substrates, the differentiation was most complete on TCPS and glass. Cultures on Permanox were slower to reach confluence and would likely differentiate completely given enough time in culture. Cultures on PDMS showed no inclination toward differentiation and instead pulled away from the substrate completely and aggregated into three dimensional cell clusters, reminiscent of the spheroids produced by Ishikawa cultures on non-adhesive substrates, discussed previously in chapters 1, 2, and 4.

Unintentionally, substrate-dependent C2C12 differentiation culture provided several useful insights which were combined into a proposed mechanism for muscle cell differentiation. A confluent background support network was determined to be necessary for differentiation. Nucleation sites for the initiation of differentiation were always obviously three dimensional and beginning to grow above the underlying support network. As the myoblast membranes fuse together to form myofibrils the pulling force between the cells was possibly the cause of the cells pulling up from the less adhesive PDMS substrate and into the three dimensional clusters.

Lower contact angle measurements for TCPS and glass [experimentally determined to be between 50-70° for each] suggest they would be more adhesive substrates and, therefore, not prone to the same phenomena. While some minor differences were seen in the 'time to differentiation' on glass and Permanox substrates, for which the background confluence remained intact, the most extreme variation was seen between the TCPS control and PDMS. Any differentiation within the three dimensional cell clusters adhered on PDMS was obscured by the three dimensional nature of the cluster and the limitations of bulk fluorescence microscopy.

Because it was quite obvious from the previous results that substrate chemistry and/or the substrate surface properties [i.e. surface roughness, surface energy] affected the morphology and differentiation routines of C2C12 myoblasts, the effect of fabricated patterned substrates was investigated. In contrast to the previously fabricated patterned substrates, the substrate samples produced for this work were fabricated into polystyrene using either solvent casting or hot embossing methods. Pattern feature size was decreased to account for the smaller C2C12 cell type and periodic grating patterns were included based on literature recommendation. Solvent casting methods produced higher resolution, but had lower throughput and higher inherent stress which could cause micro-fractures at the surface. Hot embossing had lower resolution, but high throughput and the additional benefit of being sterilised by the embossing process.

Early results showed no effect of positive diamond island pillars having any specific effect on C2C12 growth beyond the dictation of nuclear location. Coomassie brilliant blue and fluorescently stained samples showed the nuclear envelope almost always located in the lower, hole regions of the patterned regions and seldom seen on the top surface of the pillars. Later replications of the experiment included substrates containing grated pattern features, which drastically and obviously altered C2C12 morphology and organisation.

Grated patterns between 5-10 μm had a pronounced effect on C2C12 directional alignment before and during differentiation. Prior to differentiation, cells grew to the pattern features, but appeared to prefer patterns of sizes greater than the width of the nucleus in order to minimise nuclear deformation. Cells grown on patterns took up to 5 days to reach confluence; this was often longer than time to confluence for cells grown on the adjacent flat regions. Whether due to the lower density of the confluent network or due to the lower number of adjacent cells in a delineated organization, C2C12 cells adhered and aligned to patterned areas were found to

differentiate to a lower extent than cells randomly adhered to the flat polystyrene regions. Differentiation, however, was aligned to the orientation of the patterned substrate and, thus, obviously influenced either by the pattern directly or by the initial cell organisation.

On patterned PDMS substrates, cell culture results were parallel to the results on patterned polystyrene prior to the switch to low serum differentiation medium. While cells expressed the varied morphology observed in the previous substrate-dependent experiments, undifferentiated myoblasts aligned to the grated pattern features and showed little acknowledgement of the square and circular island features. At the point of media change, large sheets of the confluent monolayer peeled away from the PDMS substrate and into solution. Though peeling had been observed from the non-adhesive methacrylate previously, the magnitude of the tissue-like chunks removed from the PDMS substrates was unprecedented. Similarly, this effect has not been previously reported for PDMS in literature. This result has interesting implications for patterned PDMS substrates as biomaterials for potential *ex vivo* tissue development models and regenerative wound healing applications which require an adhesive construct during growth but need to be easily separated from the substrate for patient application.

Successful replication of bioimprint topography into polystyrene substrates was also demonstrated in this work. Instead of attempting to cure from the methacrylate polymer into PDMS for future moulding, PDMS was used directly as the bioimprinting medium. No significant artefacts of this curing technique were noticed within the range of the bright field microscope resolution. The bioimprint topography was transferred into polystyrene using hot embossing techniques. In contrast with previous methacrylate bioimprint substrates, bioimprinted polystyrene features were built up from the surface and represented positive substrate features. The influences of positive bioimprint substrates on cell growth properties was briefly addressed but left largely unstudied in this thesis due to the time constraints on final submission but could present an important experimental comparison for traditional, negative bioimprint substrates and control cultures. Development of bioimprinted polystyrene substrates was a tangible engineering advance demonstrated in this work. By either embossing or solvent casting methods, fabricated polystyrene substrates had consistent chemistry across each substrate and between substrates produced by the same method. Production of consistent, high resolution bioimprint substrates in a widely accepted cell culture material is an important advance for continuing bioimprint applications.

Though studies were limited, cell culture experiments on positive bioimprinted polystyrene substrates showed the primary effect was anchoring of networking lamellipod contacts. Cells showed no preference for adhesion to the stencilled bioimprint regions over the expanses of flat polystyrene. Cultured myoblasts showed no particular alignment to the bioimprinted topographies, but did show morphology variation when grown in the flat valleys immediately bounded by bioimprinted cell features. C2C12 cells showed cell spreading similar to the Ishikawa spreading on flat regions bounded by, in that case negative, bioimprint features. As discussed in chapter 8, this suggests that positive and negative bioimprinted substrate topographies may not have as different effects as initially assumed. For anchorage-dependent cell types, identification of positive bioimprinted apical cell membrane features might enhance the organisation effects of secondary cell cultures with minimal disruption of the observed preferential adhesion. However, more experimental data is required to verify this hypothesis.

Experimental work investigating the effects of the bioimprint on muscle cell differentiation was not completed due to the magnitude of the undertaking and the success of primary alignment. Successfully characterising bioimprinted myoblasts at different percentages of confluence and before and after differentiation represented a significant undertaking. Further determining the influence of the underlying bioimprinted substrate on secondary cell growth and differentiation was similarly substantial. However, the timeline for submission of this thesis prevented continued experimental lab work due to the magnitude and preliminary nature of the current results at that time.

In addition to the time constraints, the necessity for bioimprinted substrates for secondary cell culture alignment was lessened by the alignment effectiveness of geometrically patterned substrates. Though secondary cell culture on aligned, bioimprinted myofibrils would be interesting and would possibly influence the speed and extent of differentiation, it is unlikely that the effect would be as substantial as the influence observed using geometric patterns and would, therefore, be of less interest for clinical applications. To investigate the effect an aligned, differentiated bioimprint substrate would have on growing C2C12 cells in culture, an alignment method for the initial cell culture, prior to bioimprinting, was necessary. Geometric patterning proved effective in myofibril differentiation alignment; bioimprinting and secondary cell culture on the bioimprinted substrates was therefore unnecessary for myofibril alignment.

Geometric patterning proved effective in myofibril differentiation alignment; bioimprinting and secondary cell culture on the bioimprinted substrates was unnecessary for alignment. The

bioimprinted background topography containing the nanoscale features of a confluent myoblast monolayer, a necessary component of myoblast differentiation toward myofibrils, may encourage faster cell growth and differentiation for secondary cells relative to TCPS and glass controls. Important characterisation projects, such as time to differentiation and variation of the pheno- and genotypes, as well as additional applications and extensions to other relevant cell types are important but beyond the limited timeframe of this thesis submission. The discussion of some immediately identifiable future projects generated from the scope of work completed in this thesis are outlined and discussed in the following section.

9.2 Future work

As with most experimental research, additional observations regarding cell interactions with fabricated substrates produced more questions than answers. While many of these questions were addressed within the scope of the presented thesis, many questions remain and provide interesting research and potential applications for the theories generated in this work.

9.2.1 Additional experimental methods

The most obvious assertion for future work for the bioimprinting technology and the effects of substrate topography on cell growth is additional characterisation of the substrates and cell culture based on existing techniques and methods. Contact has been made with a group in Luxembourg to examine the bioimprint topography with combination AFM-SIMS testing. This method of analysis would produce an accurate representation of the topography using the AFM, but would also provide information regarding the surface chemistry of the methacrylate polymer. None of the polymer ingredients contain nitrogen side groups; therefore, a detected presence of nitrogen would be due to either cell debris contamination or from atmospheric conditions, which could be determined by comparison with control substrates. From the resulting data, we would be able to draw conclusions regarding the quantity of cell debris incorporated onto the bioimprinted substrates and the effectiveness of the cleaning protocols as well as hypothesise the impact the presence of cellular debris has on cell adhesion and growth.

Some biological analysis methods could similarly be used with existing experimental techniques to provide a more complete representation of cell survival in culture. Adhesion and proliferation assays could be run to determine the number of cells adhering and the relative proliferation rates across different substrates and control samples. The complexity of the tests ranges from optical density measurements of stained protein lysate [MTT or CBB assay] to incorporation of a nucleotide analogue into cellular DNA to monitor proliferation [BrdU assay]. Similarly, incorporation of viability testing and analysis of cell death pathways could provide useful information regarding the status of adhered and non-adhered cells. Fluorescence-activated cell sorting [FACS] could be a useful tool for determining the viability status of a sample cell population and for comparison of 'cause of death' of non-viable cells. Apoptotic pathways, self-destruct, suicide pathways for cells, initiate a cell death response detectably different from necrotic cells, which were killed in response to external, environmental factors. Analysing the relative viability and 'cause of death' would determine the effect the surface topographies and substrates have on cell death pathways before and after confluence.

9.2.2 Positive versus negative topographies

While the identification of positive and negative topographies was critical to the analysis of pattern features throughout the work discussed in this thesis, the direct comparison of positive and negative versions of the same features, either patterned or bioimprinted, was never undertaken. Given the strength of the results shown in the last chapter of C2C12 reacting to positive pillar patterns in PDMS and the morphology correlations between C2C12 growths on positive polystyrene bioimprints with Ishikawa cells on negative bioimprints suggests an influential effect worthy of further investigation. Methods for cell culture and substrate fabrication reported in this thesis could easily be utilised and expanded to create a decisive set of experimental substrates, with the same polymer chemistry, containing positive and negative substrates. Quantitative or qualitative analysis could be performed using a combination of adhesion and proliferation analysis and the microscopy techniques discussed in this thesis.

9.2.3 Substrate properties and cell behaviour

The most relevant versions of this experiment were conducted within the scope of this thesis as a quality control experiment to guarantee the consistency of cell morphology and proliferation across the substrates tested. Specifically for the C2C12 cells, substrate chemistry and wettability was found to have a drastic effect on the spreading morphology of the cells. Basic surface properties were determinable with AFM and product specification information. Continuing this work with substrates directly relevant to tissue engineering and regenerative medicine applications would be beneficial to both the profile of the bioimprinting work and the relevance of the work toward commercialisation applications.

Throughout this thesis, cell culture substrates were consistently commercial or fabricated polymers. The focus on polymers was critical to the characterisation and consistency of cell culture for this work, and polymer application for medical devices has advanced beyond polystyrene. Methacrylate polymers are used in artificial teeth and contact lenses specifically because of their anti-adhesive properties. Conducting polymers are of particular interest in combination with the alignment and differentiation of fully formed myofibrils. Aligned muscle fibres formed along conductive polymer designs could contract to a provided electronic stimulus and provide an artificial model for molecular and mechanistic research. Similarly, most osteo-implants are currently produced in titanium alloy. Investigating and adapting the bioimprinting technology to metallic materials would open a new avenue of applications. Determining the effect of substrate modulus at directing C2C12 myoblast differentiation toward the less common differentiation product, osteoblasts, and comparing that to the modulus of *ex vivo* bone samples and current implantable scaffold materials in literature would provide a relevant, clinically applicable research goal for bioimprint technology.

9.2.4 Selective cell adhesion

Surface modification had an obvious, if not always quantifiable, effect on the morphology of the cultured cells. Further investigation into the selective nature of adhesion and the influence of the topography across cell types would provide interesting details into the actual selectivity of the bioimprinted topography. An experiment is proposed where two cell lines of different morphologies, A and B, are simultaneously cultured separately and in co-culture. Bioimprints

are taken in triplicate of each control population: A, B, and A + B. Secondary application of each of the potential cell culture solutions would result in nine experimental permutations [e.g. cells of A grown on bioimprinted A + B]. Results of the experimental sets would provide valuable information about cell morphology and substrate selectivity. Would cells grown on co-cultured substrates adhere to selected regions of the same cell type? Would cells of type A conform to the substrate morphology of a cell-type B bioimprint?

Molecularly imprinted polymers [MIPs] have had some success when used as protein-specific sensor devices [6]. Selective cell adhesion of bioimprinted substrates could provide a similar sensory system on a larger scale. Though a lock-and-key system on the cellular level is not supported by the results of the experimental data collected and presented throughout this thesis, local cell selectivity was seen to an extent. Hence a substrate may provide an increased affinity for a specific cell type from suspension. Essentially working as a chromatography column, bioimprinted substrates may be able to pull a selected cell population out of suspension with limited effect on the other cells in suspension. For example, primary anterior pituitary tissue is composed of six different cell types [119]. Researchers working specifically with gonadotrophs need to separate that specific cell type away from the rest of the heterogeneous cell population. The current low yield methods could be used initially to fabricate a bioimprinted substrate, which could then be used as a highly specific chromatography column, selectively removing the desired cell type from solution.

9.2.5 Stem cell differentiation

Using the methods and techniques, based on underlying topographical cues, developed for differentiating C2C12 myoblasts toward directed cells lines for experimental analysis of differentiation of more complex stem cell progenitor cells, such as mesenchymal stem cells [MSCs], would provide a host of biomaterial engineering and regenerative medicine applications for bioimprint technologies. Material properties, such as elastic modulus and porosity [120, 121], and topographical substrate patterning [65] have been shown to affect the fully differentiated phenotype of MSCs. The ability to replicate positive and negative bioimprinted features into a variety of polymeric materials provides a range of possible materials for potential use as cell culture substrates or scaffolds. Topographically-specific,

biocompatible scaffolds with the potential to encourage and direct differentiation of adult MSCs would be an exciting contribution to current regenerative medical research.

9.2.6 Genetic expression

Though not discussed to any extent in this thesis, the morphology and phenotype of a cell are specific indicators of genetic expression. Increased adhesion requirements lead to over-expression of adhesion complex proteins [FAK, cdc42, cadherin, etc.]. Similarly, the effect of adhesion on cancer proliferation and metabolism can be monitored in the same way. No genetic expression analysis, either directly using PCR or large scale arrays, or quantitative protein analysis were conducted on the cell sample used in this work. Though immunofluorescent [IF] staining for myosin heavy chain [MHC] was used in the final chapters, this technique could also be used to identify specific adhesion sites. With high resolution confocal scanning and a bit of luck, the IF stained adhesion proteins could be co-located to specific topographical features.

9.3 Concluding remarks

Throughout the work encompassed in this thesis several consistent phenomena were observed which led to the proposition of several continuing applications. The three dimensional growth of the Ishikawa cancer cells both helped and hindered the analysis of cell culture on bioimprinted substrates. The inadvertent fabrication of a non-adhesive substrate provided a construct for tethered spheroid growth which can be further developed for three dimensional microtumour studies. Selective adhesion to the bioimprinted regions was shown with Ishikawa endometrial cancer cells, in combination with a cell size variation for cells grown beyond the bioimprinted regions. The discussion of the 'cancerousness' of single, representative cells could provide enough debate to fill a philosophy thesis, but the alteration of the phenotypic expression of cells across topographically modified substrates are indicative of a shift in genetic expression, plausibly related to a decrease in invasive and metastatic tendencies. The results of C2C12 mouse myoblasts suggest a similar substrate-dependent phenotype, both for growth and differentiation. The patterning results on polystyrene verified the observations found in literature regarding cell growth to grated patterns. In contrast, the obvious morphology shift and the tissue-like chunks resulting from C2C12 culture on PDMS were not observed in published literature and have not been previously reported. The confluent growth of cell monolayers without permanent adhesion to the underlying substrate could prove applicable for the generation of wound healing biomaterials that form a 'skin'. Defining the time to differentiation and the effect of a bioimprinted substrate on the speed and extent of stimulated differentiation may further solidify the validity of the generated myofibril alignment model. Continued investigation of bioimprinting technology for fabrication and production of cell culture substrates, in combination with new and innovative analysis methods, is likely to provide a host of strategies for research and clinical application.

10 References

[1] H. Lodish, A. Berk, P. Matsudaira*, et al.*, *Molecular Cell Biology*, 6 ed. New York: W.H. Freeman, 2008.

[2] B. D. Ratner, A. S. Hoffman, F. J. Schoen*, et al.*, Eds., *Biomaterials Science*, 2 ed. Elsevier Inc., 2004.

[3] A. Wells, Ed., *Cell Motility in Cancer Invasion and Metastasis.* Springer, 2006.

[4] H. G. Craighead, C. D. James, and A. M. P. Turner, "Chemical and topographical patterning for directed cell attachment," *Current Opinion in Solid State and Materials Science,* vol. 5, pp. 177-184, 2001.

[5] R. G. Flemming, C. J. Murphy, G. A. Abrams*, et al.*, "Effects of synthetic micro- and nano-structured surfaces on cell behavior," *Biomaterials,* vol. 20, pp. 573-588, 1999.

[6] E. Verheyen, J. P. Schillemans, M. van Wijk*, et al.*, "Challenges for the effective molecular imprinting of proteins," *Biomaterials,* vol. 32, pp. 3008-3020, 2011.

[7] S. Y. Chou, P. R. Krauss, and J. R. Preston, "Imprint Lithography with 25-Nanometer Resolution," *Science,* vol. 272, pp. 85-87, 1996.

[8] J. J. Muys, M. M. Alkaisi, and J. J. Evans, "Bioimprint: Nanoscale Analysis by Replication of Cellular Topography Using Soft Lithography," *Journal of Biomedical Nanotechnology,* vol. 2, pp. 11-15, Apr 2006.

[9] B. Alberts, A. Johnson, J. Lewis*, et al.*, *Molecular Biology of the Cell*, 4 ed. New York: Garland Science, 2002.

[10] J. Pardee, *The Actin Cytoskeleton in Cell Motility, Cancer, and Infection*: Morgan & Claypool Life Sciences, 2009.

[11] J. Folkman and A. Moscona, "Role of cell shape in growth control," *Nature,* vol. 273, pp. 345-349, 1978.

[12] K. von der Mark, J. Park, S. Bauer*, et al.*, "Nanoscale engineering of biomimetic surfaces: cues from the extracellular matrix," *Cell and Tissue Research,* vol. 339, pp. 131-153, 2010.

[13] M. J. Lydon, T. W. Minett, and B. J. Tighe, "Cellular interactions with synthetic polymer surfaces in culture," *Biomaterials,* vol. 6, pp. 396-402, 1985.

[14] M. Kato and M. Mrksich, "Rewiring Cell Adhesion," *Journal of the American Chemical Society,* vol. 126, pp. 6504-6505, 2004.

[15] F. L. Yap and Y. Zhang, "Protein and cell micropatterning and its integration with micro/nanoparticles assembly," *Biosensors and Bioelectronics,* vol. 22, pp. 775-788, 2007.

[16] D. R. Jung, R. Kapur, T. Adams*, et al.*, "Topographical and Physicochemical Modification of Material Surface to Enable Patterning of Living Cells," *Critical Reviews in Biotechnology,* vol. 21, pp. 111 - 154, 2001.

[17] A. S. Curtis, J. V. Forrester, C. McInnes*, et al.*, "Adhesion of cells to polystyrene surfaces," *The Journal of Cell Biology,* vol. 97, pp. 1500-1506, 1983.

[18] I. Beaulieu, M. Geissler, and J. Mauzeroll, "Oxygen Plasma Treatment of Polystyrene and Zeonor: Substrates for Adhesion of Patterned Cells," *Langmuir,* vol. 25, pp. 7169-7176, 2009.

[19] T. B. F. Woodfield, S. Miot, I. Martin*, et al.*, "The regulation of expanded human nasal chondrocyte re-differentiation capacity by substrate composition and gas plasma surface modification," *Biomaterials,* vol. 27, pp. 1043-1053, 2006.

[20] A. Nandakumar, Z. T. Birgani, D. Santos*, et al.*, "Surface modification of electrospun fibre meshes by oxygen plasma for bone regeneration," *Biofabrication,* vol. 5, pp. 015006, 2013.

[21] A. Carre and V. Lacarrire, "How Substrate Properties Control Cell Adhesion. A Physical-Chemical Approach," *Journal of Adhesion Science and Technology,* vol. 24, pp. 815-830, 2010.

[22] N. G. Maroudas, "Chemical and Mechanical Requirements for Fibroblast Adhesion," *Nature,* vol. 244, pp. 353-354, 1973.

[23] Y. Wang, G. Wang, X. Luo*, et al.*, "Substrate stiffness regulates the proliferation, migration, and differentiation of epidermal cells," *Burns,* vol. 38, pp. 414-420, 2012.

[24] S. Hussein and S. M. Mukhopadhyay, "Cell Growth in a Porous Microcellular Structure: Influence of Surface Modification and Nanostructures," *Nanoscience and nanotechnology letters,* vol. 3, pp. 110-113, 2011.

[25] J. Nakanishi, T. Takarada, K. Yamaguchi*, et al.*, "Recent advances in cell micropatterning techniques for bioanalytical and biomedical sciences," *Analytical sciences,* vol. 24, pp. 67-72, 2008.

[26] C. S. Chen, M. Mrksich, S. Huang*, et al.*, "Geometric Control of Cell Life and Death," *Science,* vol. 276, pp. 1425-1428, 1997.

[27] G. S. May and S. M. Sze, *Fundamentals of semiconductor fabrication*, Wiley international ed. New York: Wiley, 2004.

[28] A. N. Broers, A. C. F. Hoole, and J. M. Ryan, "Electron beam lithography—Resolution limits," *Microelectronic Engineering,* vol. 32, pp. 131-142, 1996.

[29] D. Qin, G. M. Whitesides, and Y. Xi, "Soft lithography for micro- and nanoscale patterning," *Nature Protocols,* vol. 5, pp. 491, 2010.

[30] H. Shi, W.-B. Tsai, M. D. Garrison*, et al.*, "Template-imprinted nanostructured surfaces for protein recognition," *Nature,* vol. 398, pp. 593-597, 1999.

[31] R. C. Schmidt and K. E. Healy, "Controlling biological interfaces on the nanometer length scale," *Journal of Biomedical Materials Research Part A,* vol. 90A, pp. 1252-1261, 2009.

[32] J. A. Liddle, G. M. Gallatin, and L. E. Ocola, "Resist requirements and limitations for nanoscale electron-beam patterning," in *Symposium on Three-Dimensional Nanoengineered Assemblies*, Boston, MA, pp. 19-30, 2002.

[33] W. Hu, E. K. F. Yim, R. M. Reano*, et al.*, "Effects of nanoimprinted patterns in tissue-culture polystyrene on cell behavior," *Journal of Vacuum Science Technology A,* vol. 23, pp. 2984-2989, 2005.

[34] J. J. Shi, A. R. Votruba, O. C. Farokhzad*, et al.*, "Nanotechnology in Drug Delivery and Tissue Engineering: From Discovery to Applications," *Nano Letters,* vol. 10, pp. 3223-3230, 2010.

[35] S. Lee, *Materials in Biology and Medicine*, 1 ed. Boca Raton: CRC Press, 2012.

[36] Z. X. Xu, H. J. Gao, L. M. Zhang*, et al.*, "The Biomimetic Immunoassay Based on Molecularly Imprinted Polymer: A Comprehensive Review of Recent Progress and Future Prospects," *Journal of Food Science,* vol. 76, pp. R69-R75, 2011.

[37] S. A. Piletsky, E. V. Piletskaya, A. V. El'skaya*, et al.*, "Optical Detection System for Triazine Based on Molecularly-Imprinted Polymers," *Analytical Letters,* vol. 30, pp. 445-455, 1997.

[38] G. Vlatakis, L. I. Andersson, R. Muller*, et al.*, "Drug assay using antibody mimics made by molecular imprinting," *Nature,* vol. 361, pp. 645-647, 1993.

[39] B. D. Ratner and H. Shi, "Recognition templates for biomaterials with engineered bioreactivity," *Current Opinion in Solid State and Materials Science,* vol. 4, pp. 395-402, 1999.

[40] D. A. Spivak and K. J. Shea, "Investigation into the scope and limitations of molecular imprinting with DNA molecules," *Analytica Chimica Acta,* vol. 435, pp. 65-74, 2001.

[41] L. D. Bolisay, J. N. Culver, and P. Kofinas, "Molecularly imprinted polymers for tobacco mosaic virus recognition," *Biomaterials,* vol. 27, pp. 4165-4168, 2006.

[42] O. Käppeli, P. Walther, M. Mueller*, et al.*, "Structure of the cell surface of the yeast Candida tropicalis and its relation to hydrocarbon transport," *Archives of Microbiology,* vol. 138, pp. 279-282, 1984.

[43] F. Braet, R. de Zanger, C. Seynaeve*, et al.*, "A comparative atomic force microscopy study on living skin fibroblasts and liver endothelial cells," *Journal of Electron Microscopy,* vol. 50, pp. 283-290, 2001.

[44] J. Muys, "Cellular Analysis by Atomic Force Microscopy," Doctor of Philisophy, Electrical and Computer Engineering, University of Canterbury, Christchurch, 2006.

[45] F. Samsuri, M. M. Alkaisi, J. J. Evans*, et al.*, "Detection of changes in cell membrane structures using the Bioimprint technique," *Microelectronic Engineering,* vol. 88, pp. 1871-1874, 2011.

[46] F. B. Samsuri, "Single cell analysis using atomic force microscopy [AFM]," Doctor of Philosophy, Electrical and Computer Engineering, University of Canterbury, Christchurch, 2010.

[47] X. Zhou, J. Shi, F. Zhang*, et al.*, "Reversed cell imprinting, AFM imaging and adhesion analyses of cells on patterned surfaces," *Lab on a Chip,* vol. 10, pp. 1182-1188, 2010.

[48] X. T. Zhou, F. Zhang, J. Hu*, et al.*, "Cell imprinting and AFM imaging of cells cultured on nanoline patterns," *Microelectronic Engineering,* vol. 87, pp. 1439-1443, 2010.

[49] M. Karlsson, F. Johansson, and M. Kanje, "Polystyrene replicas of neuronal basal lamina act as excellent guides for regenerating neurites," *Acta Biomaterialia,* vol. 7, pp. 2910-2918, 2011.

[50] "Cancer's epicentre: New understanding of how cancers work is yeilding new treatments," *The Economist* (Apr 7, 2012).

[51] D. W. Hutmacher, D. Loessner, S. Rizzi*, et al.*, "Can tissue engineering concepts advance tumor biology research?," *Cell,* vol. 28, pp. 125-133, 2009.

[52] D. E. Ingber, "Can cancer be reversed by engineering the tumor microenvironment?," *Seminars in Cancer Biology,* vol. 18, pp. 356-364, 2008.

[53] D. Hanahan and Robert A. Weinberg, "Hallmarks of Cancer: The Next Generation," *Cell,* vol. 144, pp. 646-674, 2011.

[54] M. Nishida, "The Ishikawa cells from birth to the present," *Human Cell,* vol. 15, pp. 104-117, 2002.

[55] H. Beug, S. Grunert, and M. Jechlinger, "Diverse cellular and molecular mechanisms contribute to epithelial plasticity and metastasis," *Nature Reviews Molecular Cell Biology,* vol. 4, pp. 657, 2003.

[56] N. B. Nardi and L. Meirelles, "Mesenchymal Stem Cells: Isolation, In Vitro Expansion and Characterization," in *Stem Cells*. vol. 174, pp. 249-282. A. Wobus and K. Boheler, Eds., Heidelberg: Springer, 2006,.

[57] B. J. Papenburg, E. D. Rodrigues, M. Wessling*, et al.*, "Insights into the role of material surface topography and wettability on cell-material interactions," *Soft Matter,* vol. 6, pp. 4377-4388, 2010.

[58] A. J. Engler, S. Sen, H. L. Sweeney*, et al.*, "Matrix Elasticity Directs Stem Cell Lineage Specification," *Cell,* vol. 126, pp. 677-689, 2006.

[59] E. Prosecká, M. Rampichová, L. Vojtová, *et al.*, "Optimized conditions for mesenchymal stem cells to differentiate into osteoblasts on a collagen/hydroxyapatite matrix," *Journal of Biomedical Materials Research Part A,* vol. 99A, pp. 307-315, 2011.

[60] K. Shimizu, H. Fujita, and E. Nagamori, "Alignment of skeletal muscle myoblasts and myotubes using linear micropatterned surfaces ground with abrasives," *Biotechnology and Bioengineering,* vol. 103, pp. 631-638, 2009.

[61] L. E. McNamara, R. J. McMurray, M. J. P. Biggs, *et al.*, "Nanotopographical Control of Stem Cell Differentiation," *Journal of Tissue Engineering,* vol. 1, 2010.

[62] C. Galli, G. Passeri, F. Ravanetti, *et al.*, "Rough surface topography enhances the activation of Wnt/β-catenin signaling in mesenchymal cells," *Journal of Biomedical Materials Research Part A,* vol. 95A, pp. 682-690, 2010.

[63] E. Martinez, A. Lagunas, C. A. Mills, *et al.*, "Stem cell differentiation by functionalized micro- and nanostructured surfaces," *Nanomedicine (London, England),* vol. 4, pp. 65-82, 2009.

[64] A. Béduer, C. Vieu, F. Arnauduc, *et al.*, "Engineering of adult human neural stem cells differentiation through surface micropatterning," *Biomaterials,* vol. 33, pp. 504-514, 2012.

[65] M. J. Dalby, N. Gadegaard, R. Tare, *et al.*, "The control of human mesenchymal cell differentiation using nanoscale symmetry and disorder," *Nat Mater,* vol. 6, pp. 997-1003, 2007.

[66] E. Engel, E. Martínez, C. A. Mills, *et al.*, "Mesenchymal stem cell differentiation on microstructured poly (methyl methacrylate) substrates," *Annals of Anatomy - Anatomischer Anzeiger,* vol. 191, pp. 136-144, 2009.

[67] D. Yaffe and O. R. A. Saxel, "Serial passaging and differentiation of myogenic cells isolated from dystrophic mouse muscle," *Nature,* vol. 270, pp. 725-727, 1977.

[68] T. Katagiri, A. Yamaguchi, M. Komaki, *et al.*, "Bone morphogenetic protein-2 converts the differentiation pathway of C2C12 myoblasts into the osteoblast lineage," *The Journal of Cell Biology,* vol. 127, pp. 1755-1766, 1994.

[69] P. Veliça and C. M. Bunce, "A quick, simple and unbiased method to quantify C2C12 myogenic differentiation," *Muscle & Nerve,* vol. 44, pp. 366-370, 2011.

[70] J. S. Bonifacino, M. Dasso, J. B. Harford*, et al.*, Eds., *Short Protocols in Cell Biology*. Hoboken, N.J.: John Wiley, 2004.

[71] "Hoechst 33342: Instructions," ed: Thermo Scientific.

[72] A.-T. GmbH. “Atto 590,” 2010.

[73] P. Bajaj, B. Reddy, L. Millet*, et al.*, "Patterning the differentiation of C2C12 skeletal myoblasts," *Integrative Biology,* vol. 3, pp. 897-909, 2011.

[74] G. Cox. *Optical Imaging Techniques in Cell Biology*. 2 ed. Boca Raton: CRC Press, 2012.

[75] Nikon, "Eclipse 80i Microscope Instructions."

[76] B. P. Jena, J. K. H. Hörber, ed., *Force microscopy: applications in biology and medicine*. Hoboken, N.J.: Wiley-Liss, 2006.

[77] L. W. Francis, P. D. Lewis, C. J. Wright*, et al.*, "Atomic force microscopy comes of age," *Biology of the Cell,* vol. 102, pp. 133-143, 2009.

[78] G. Binnig, C. F. Quate, and C. Gerber, "Atomic Force Microscope," *Physical Review Letters,* vol. 56, p. 930, 1986.

[79] C. A. Schneider, W. S. Rasband, and K. W. Eliceire, "NIH inage to ImageJ: 25 years of image analysis," *Nature Methods,* vol. 9, 2012.

[80] Ciba Specialty Chemicals, Inc., "Ciba IRGACURE 2022," ed, 2003.

[81] D. Wlodkowic, S. Faley, J. Skommer*, et al.*, "Biological Implications of Polymeric Microdevices for Live Cell Assays," *Analytical chemistry,* vol. 81, pp. 9828-9833, 2009.

[82] M. Moloney, L. McDonnell, and H. O’Shea, "Atomic force microscopy of BHK-21 cells: an investigation of cell fixation techniques," *Ultramicroscopy,* vol. 100, pp. 153-161, 2004.

[83] E. Yoshii, "Cytotoxic effects of acrylates and methacrylates: Relationships of monomer structures and cytotoxicity," *Journal of Biomedical Materials Research,* vol. 37, pp. 517-524, 1997.

[84] E. Ostuni, R. Kane, C. S. Chen*, et al.*, "Patterning Mammalian Cells Using Elastomeric Membranes," *Langmuir,* vol. 16, pp. 7811-7819, 2000.

[85] A. Folch, B.-H. Jo, O. Hurtado*, et al.*, "Microfabricated elastomeric stencils for micropatterning cell cultures," *Journal of Biomedical Materials Research,* vol. 52, pp. 346-353, 2000.

[86] MicroChem, "NANO SU-8," ed, 2010.

[87] R.-Z. Lin and H.-Y. Chang, "Recent advances in three-dimensional multicellular spheroid culture for biomedical research," *Biotechnology Journal,* vol. 3, pp. 1285-1285, 2008.

[88] Y. Mei, T. Wu, C. Xu*, et al.*, "Tuning Cell Adhesion on Gradient Poly(2-hydroxyethyl methacrylate)-Grafted Surfaces," *Langmuir,* vol. 21, pp. 12309-12314, 2005.

[89] K. J. Regehr, M. Domenech, J. T. Koepsel*, et al.*, "Biological implications of polydimethylsiloxane-based microfluidic cell culture," *Lab on a Chip,* vol. 9, pp. 2132-2139, 2009.

[90] K. Roy, Ed., "Biomaterials as Stem Cell Niche" in *Studies in Mechanobiology, Tissue Engineering, and Biomaterials*. vol. 2, pp. 1-309. A. Gefen, Ed., Heidelberg: Springer 2010.

[91] G. Mahmud, S. Huda, W. Yang*, et al.*, "Carboxybetaine Methacrylate Polymers Offer Robust, Long-Term Protection against Cell Adhesion," *Langmuir,* vol. 27, pp. 10800-10804, 2011.

[92] S. Patel, R. G. Thakar, J. Wong*, et al.*, "Control of cell adhesion on poly(methyl methacrylate)," *Biomaterials,* vol. 27, pp. 2890-2897, 2006.

[93] "Lithography," in *Encyclopedia Britannica: Encyclopedia Britannica Online Academic Edition*, Encyclopedia Britannica Inc., 2012.

[94] Y. Xia and G. M. Whitesides, "Soft Lithography," *Annual Review of Materials Science,* vol. 28, pp. 153-184, 1998.

[95] S. P. Desai, D. M. Freeman, and J. Voldman, "Plastic masters-rigid templates for soft lithography," *Lab on a chip,* vol. 9, pp. 1631-1637, 2009.

[96] L. Gitlin, P. Schulze, and D. Belder, "Rapid replication of master structures by double casting with PDMS," *Lab on a chip,* vol. 9, pp. 3000-3002, 2009.

[97] A. Mata, A. Fleischman, and S. Roy, "Characterization of Polydimethylsiloxane (PDMS) Properties for Biomedical Micro/Nanosystems," *Biomedical Microdevices,* vol. 7, pp. 281-293, 2005.

[98] I. Johnson and M. T. Z. Spence, Eds., *The Molecular Probes Handbook,* 11 ed. Life Technologies, 2010.

[99] J. L. Charest, A. J. García, and W. P. King, "Myoblast alignment and differentiation on cell culture substrates with microscale topography and model chemistries," *Biomaterials,* vol. 28, pp. 2202-2210, 2007.

[100] K. Shimizu, H. Fujita, and E. Nagamori, "Micropatterning of single myotubes on a thermoresponsive culture surface using elastic stencil membranes for single-cell analysis," *Journal of Bioscience and Bioengineering,* vol. 109, pp. 174-178, 2010.

[101] D. Lahiri, A. P. Benaduce, L. Kos*, et al.*, "Quantification of carbon nanotube induced adhesion of osteoblast on hydroxyapatite using nano-scratch technique," *Nanotechnology,* vol. 22, p. 355703, 2011.

[102] L. M. Pakstis, J. P. Dunkers, A. Zheng*, et al.*, "Evaluation of polydimethylsiloxane modification methods for cell response," *Journal of Biomedical Materials Research Part A,* vol. 92A, pp. 604-614, Feb 2010.

[103] E. Berthier, E. W. K. Young, and D. Beebe, "Engineers are from PDMS-land, Biologists are from Polystyrenia," *Lab on a Chip,* vol. 12, pp. 1224-1237, 2012.

[104] B. N. Lourenco, G. Marchioli, W. L. Song*, et al.*, "Wettability Influences Cell Behavior on Superhydrophobic Surfaces with Different Topographies," *Biointerphases,* vol. 7, 2012.

[105] A. Tropmann, L. Tanguy, P. Koltay*, et al.*, "Completely Superhydrophobic PDMS Surfaces for Microfluidics," *Langmuir,* vol. 28, pp. 8292-8295, Jun 2012.

[106] N. F. Huang, S. Patel, R. G. Thakar*, et al.*, "Myotube Assembly on Nanofibrous and Micropatterned Polymers," *Nano Letters,* vol. 6, pp. 537-542, 2006.

[107] P.-Y. Wang, H.-T. Yu, and W.-B. Tsai, "Modulation of alignment and differentiation of skeletal myoblasts by submicron ridges/grooves surface structure," *Biotechnology and Bioengineering,* vol. 106, pp. 285-294, 2010.

[108] J. B. Recknor, J. C. Recknor, D. S. Sakaguchi*, et al.*, "Oriented astroglial cell growth on micropatterned polystyrene substrates," *Biomaterials,* vol. 25, pp. 2753-2767, 2004.

[109] Y. Wang, J. Balowski, C. Phillips*, et al.*, "Benchtop micromolding of polystyrene by soft lithography," *Lab on a Chip,* vol. 11, pp. 3089-3097, 2011.

[110] J. B. Recknor, D. S. Sakaguchi, and S. K. Mallapragada, "Directed growth and selective differentiation of neural progenitor cells on micropatterned polymer substrates," *Biomaterials,* vol. 27, pp. 4098-4108, 2006.

[111] V. N. Goral, Y.-C. Hsieh, O. N. Petzold*, et al.*, "Hot embossing of plastic microfluidic devices using poly(dimethylsiloxane) molds," *Journal of Micromechanics and Microengineering,* vol. 21, p. 017002, 2011.

[112] T. A. Osswald, E. Baur, S. Brinkmann*, et al.*, *International Plastics Handbook*. Cincinnati: Hanser Gardner Publications, 2006.

[113] P. M. Davidson, H. Özçelik, V. Hasirci*, et al.*, "Microstructured Surfaces Cause Severe but Non-Detrimental Deformation of the Cell Nucleus," *Advanced Materials,* vol. 21, pp. 3586-3590, 2009.

[114] D. J. R. Evans, S. Britland, and P. M. Wigmore, "Differential response of fetal and neonatal myoblasts to topographical guidance cues in vitro," *Development Genes and Evolution,* vol. 209, pp. 438-442, 1999.

[115] Y. Zhao, H. S. Zeng, J. Nam*, et al.*, "Fabrication of Skeletal Muscle Constructs by Topographic Activation of Cell Alignment," *Biotechnology and Bioengineering,* vol. 102, pp. 624-631, 2009.

[116] M. T. Lam, S. Sim, X. Y. Zhu*, et al.*, "The effect of continuous wavy micropatterns on silicone substrates on the alignment of skeletal muscle myoblasts and myotubes," *Biomaterials,* vol. 27, pp. 4340-4347, 2006.

[117] L. Ricotti, S. Taccola, I. Bernardeschi*, et al.*, "Quantification of growth and differentiation of C2C12 skeletal muscle cells on PSS-PAH-based polyelectrolyte layer-by-layer nanofilms," *Biomedical Materials,* vol. 6, 2011.

[118] S. Burattini, P. Ferri, M. Battistelli*, et al.*, "C2C12 murine myoblasts as a model of skeletal muscle development: morpho-functional characterization," *European Journal of Histochemistry,* vol. 48, pp. 223-233, 2004.

[119] E. N. Marieb, *Human Anatomy & Physiology*, 4 ed. Benjamin/Cummings Science Publishing, 1998.

[120] S. Miot, T. Woodfield, A. U. Daniels*, et al.*, "Effects of scaffold composition and architecture on human nasal chondrocyte redifferentiation and cartilaginous matrix deposition," *Biomaterials,* vol. 26, pp. 2479-2489, 2005.

[121] D. E. Discher, P. Janmey, and W. Yu-li, "Tissue Cells Feel and Respond to the Stiffness of Their Substrate," *Science,* vol. 310, pp. 1139-43, 2005.